Curtin University of Technology
School of Applied Chemistry

The Mechanism of Bayer Residue Flocculation

Franca Jones

"This thesis is presented as part of the requirements for
the award of the Degree of Doctor of Philosophy
of the
Curtin University of Technology"

May, 1998

Dedicated to my parents, Linda and
Michele Smiriglia, and to my
husband, Anthony.

"Discovery consists of seeing what everybody has seen but thinking what nobody has thought"

Albert Szent-Györgyi from The Scientist Speculates, 1962

Acknowledgments

I would like to thank Professor Jeff Dunn, head of the Curtin University of Technology School of Applied Chemistry, for the opportunity to undertake the PhD. I gratefully acknowledge the assistance and guidance of my supervisors Assoc. Professor Bill van Bronswijk and Dr. John Farrow. They have shown remarkable patience and perseverance and I thank them for all their efforts.

Special mention must also go to Dr. Andrew Rohl (whose expertise guided me through the molecular modelling work) and to Dr. Craig Klauber (who generously gave his time to conduct the XPS experiments and process the data). I particularly appreciate the interest and time that was devoted by them.

To Dr. Peter Austin and the Particle Analysis Facility, many thanks for the various analysis undertaken on my behalf. Similarly, thanks to Dr. Peter Choo's Analytical Group at CSIRO Division of Minerals.

I would like to thank my colleagues, fellow PhD students, of whom there are too many to name but who made my time at Curtin pleasurable and stimulating. I wish to thank Dr. Phillip Fawell, Ms. Jean Swift and the flocculation group from CSIRO Division of Minerals for their kind assistance on a daily basis. To Dr. Phillip Fawell a special acknowledgment for his assistance with the MALLS and FBRM work.

I gratefully acknowledge the CSIRO's contribution which made it possible for me to work in their laboratories at Waterford.

In particular, I would like to thank the AJ Parker CRC for Hydrometallurgy and the Australian Research Council (and Australian taxpayers) who supported me financially with scholarships during this period.

Many thanks and appreciation to Gerald Roach, Alcoa of Australia, for his interest in this work and refinery experience input, MSI of San Diego for the use of the InsightII software which is the source of the molecular modelling pictures, and Peter Chapman for his help and the Vibrational Spectroscopy Facility at Curtin for use of the FTIR equipment.

Abstract

The aim of this study was to determine the mechanism of Bayer residue flocculation. Hematite was chosen as the test substrate as it is a common Bayer residue mineral. Batch settling tests were used to gain an understanding of the aggregation mechanism and to compare the effect of different parameters on flocculation performance. Flocculant adsorption isotherm measurements were related to changes in flocculation performance. Infrared spectroscopy was used to ascertain the configuration of adsorbed flocculant on the hematite surface.

Batch settling tests showed that under strong caustic conditions hematite is naturally coagulated and that flocculation occurs via a bridging mechanism. This was confirmed by results which showed that factors which affect the bridging efficiency of the flocculant had an impact on aggregation. In particular, temperature and caustic concentration were found to greatly influence flocculation performance. This is due mainly to changes in the viscosity of the liquor, but may also be linked to the kinetics of particle-particle and particle-flocculant collisions resulting in a less efficient aggregation process. Ionic strength did not impact on performance as the flocculant was at a limiting size for synthetic liquors containing TC $\geq$ 50 and TA $\geq$ 10.

Increasing ionic strength did not increase the adsorption density of the flocculant on hematite nor did altering the salt cation species from Na^+ to Ca^{2+}. It can be concluded, therefore, that the flocculant is chemisorbed through surface complexation, since if it were electrostatically bound an increase in flocculant adsorption should have been observed with increasing ionic strength or cation charge. The surface complexation mechanism was supported by infrared results which showed that the flocculant vibrational bands were shifted on adsorption. The magnitude and direction of the shift suggests a bridging bidentate structure at pHs $\geq$ 11, while a monodentate structure exists at pH 7. In the presence of calcium there is also some electrostatically adsorbed flocculant at pH 7, with the calcium being in a bidentate chelating structure, but this is not observed at much higher pHs.

The flocculant had an adsorption isotherm best described by a Langmuir-Freundlich expression with a monolayer coverage of ~164 $\mu g\ m^{-2}$ of hematite. The adsorption density was lowered by the presence of carbonate and silicate and the action of both is

thought to be due to their adsorption on active sites blocking polymer adsorption. Carbonate has an impact on flocculant adsorption at concentrations >10 mg g^{-1} while in the case of silicate ~0.2 mg g^{-1} is required for the adsorption density of the flocculant to be affected. While it has been confirmed that silicate does adsorb on hematite, it was not possible to determine whether this was adsorption of a silicate species or an aluminosilicate species.

X-ray photoelectron spectroscopy (XPS) showed conclusively that sodium is not involved in the adsorption of the carboxylate to the hematite surface. The lower peak shift between the backbone carbon and the carboxylate carbon suggests that the carboxylate is bonded directly to iron which has a low effective charge.

Flocculant adsorption was atomistically modelled using decanoate and decandioate molecules. Modelling supported the results from XPS and infrared analysis and showed the carboxylate oxygen atoms in both organic molecules bonded directly to the surface iron atoms. Adsorption was preferred on near unhydrated surfaces with the most stable adsorption configuration being a non-symmetrical bridging bidentate structure as inferred from the infrared results.

TABLE OF CONTENTS

1. INTRODUCTION 1

1.1 The Bayer Process 2

1.1.1 The unit operations 2

1.1.2 Bayer liquor composition 7

1.1.3 Bayer residue solids 7

1.2 Aggregation in Solid/Liquid Separation 10

1.2.1 Coagulation 11

1.2.2 Flocculation 13

1.3 Flocculation of Bayer Residue 26

1.3.1 Thickener operation 26

1.3.2 Bayer residue flocculants 28

1.3.3 Factors which affect Bayer flocculation 33

1.4 Summary of Chapter and Scope of This Study 38

2. MATERIALS AND METHODS 41

2.1 Materials 41

2.2 Methods for Sample Characterisation 44

2.2.1 Hematite 44

2.2.2 Flocculants 45

2.3 Synthetic Bayer Liquors 47

2.3.1 Synthetic Bayer liquor make-up 47

2.3.2 Analysis of liquors 47

2.4 Flocculation State Determination 48

2.4.1 Dispersion of solids 48

2.4.2 Settling rate 48

2.4.3 Turbidity 49

2.4.4 Stability of hematite under high caustic conditions 50

2.4.5 Focused beam reflectance measurements 50

2.4.6 Concentrating refinery waste solids 51

2.4.7 Precipitation of desilication products (DSPs) onto hematite 51

2.5 Flocculants in Synthetic Bayer Liquors 51

2.5.1 Flocculant preparation 51

2.5.2 Measurement of flocculant concentration in synthetic Bayer liquors - the Hyamine method 53

2.6 Spectroscopy **54**

2.6.1 Fourier transform infrared (FTIR) 54

2.6.2 X-ray photoelectron spectroscopy (XPS) method for determining the mode of flocculant adsorption 57

2.7 Molecular Modelling **59**

2.7.1 Potentials used to describe hematite 60

2.7.2 Hydrating the hematite surface 61

2.7.3 Adsorbing the flocculant onto hydrated hematite 62

2.8 Summary **63**

3. SAMPLE CHARACTERISATION AND METHOD EVALUATION **65**

3.1 Sample Characterisation **65**

3.1.1 Hematite samples 65

3.1.2 Flocculant characterisation 67

3.1.3 Refinery materials characterisation 70

3.2 Hyamine Method for Determination of Flocculant Concentration in Synthetic Bayer Liquors **74**

3.2.1 Addition of gluconate 74

3.2.2 Effect of time and temperature 74

3.2.3 Caustic strength 75

3.2.4 Dissolved salts 75

3.2.5 Flocculant acrylate content and molecular weight 77

3.2.6 Sensitivity, reproducibility and error analysis 77

3.3 Aggregation State Method **79**

3.3.1 Reproducibility and error analysis 80

3.3.2 Limitations of settling curves 80

3.3.3 Relationship between turbidity and solids content 81

3.3.4 Refinery measurements 83

3.4 Infrared Spectroscopic Determination of the Adsorption Mechanism **84**

3.5 Summary **86**

4. THE FLOCCULATION BEHAVIOUR OF HEMATITE **88**

4.1 Sensitivity of Flocculation Performance to Process **88**

4.1.1 Flocculant ageing 89

4.1.2 Conditioning of hematite solids with caustic solution 91

4.1.3 Supersaturation of the liquor 94

4.1.4 Effect of solids 96

4.1.5 Temperature 98
4.1.6 Summary 101

4.2 Mechanism of Hematite Aggregation 101
4.2.1 Stability of hematite suspensions in caustic liquor 101
4.2.2 Flocculation of hematite in caustic liquor 103

4.3 Adsorption of Polyacrylate 104
4.3.1 Effect of flocculant dosage 104

4.4 The Effect of Caustic Concentration on Flocculation Performance 110
4.4.1 Settling characteristics 110
4.4.2 Polymer conformation 113

4.5 Infrared Spectra of Adsorbed Flocculant 116
4.5.1 Adsorption conformation 119

4.6 X-ray Photoelectron Spectroscopy (XPS) Results 123
4.6.1 Flocculant 123
4.6.2 Adsorbed flocculant on hematite 124

4.7 Proposed Adsorption Mechanism 127

4.8 Summary 128

5. THE EFFECT OF IMPURITIES ON HEMATITE FLOCCULATION 130

5.1 Solution Impurities 130
5.1.1 Sulphate, chloride and phosphate 130
5.1.2 Carbonate 133
5.1.3 Calcium 137
5.1.4 Silicate 143

5.2 Solid Impurities 148
5.2.1 The effect of a homogenous surface contaminant 148
5.2.2 Precipitation of a DSP on hematite 156
5.2.3 Changing the particle size distribution of refinery solids 158

5.3 Summary 160

6. MOLECULAR MODELLING OF FLOCCULANT ADSORPTION ON HEMATITE 162

6.1 Introduction 162

6.2 Potentials 164

6.3 Surface Hydration of Hematite **164**

6.3.1 {011} and {210} surfaces 169

6.3.2 {111} Fe-terminated surface at monolayer coverage 171

6.3.3 {111} Fe-terminated surface at less than monolayer coverage 174

6.3.4 {111} O-terminated surface 174

6.4 Adsorption of Carboxylate Groups onto Hydrated Hematite **176**

6.5 Summary **181**

7. SUMMARY AND CONCLUSIONS **183**

7.1 Hematite **183**

7.1.1 The hematite surface 183

7.1.2 The flocculation mechanism of hematite in synthetic Bayer liquors 184

7.1.3 The adsorption mechanism 185

7.1.4 Process parameters' impact on hematite flocculation 185

7.2 Impurities **186**

7.2.1 Solution impurities 186

7.2.2 Solid Impurities 187

7.3 Refinery Solids **188**

7.4 Future Work **189**

BIBLIOGRAPHY **191**

APPENDIX: PUBLICATIONS FROM THIS THESIS **208**

1. INTRODUCTION

The Bayer process (patented by Karl Bayer in 1888) is the most common method of refining bauxite into alumina. In 1996, 48 million tonnes of alumina were produced worldwide, mainly as feed for aluminium production. Australia is one of the world's largest producers, accounting for an estimated 25 % of the total world alumina output. There are six Australian refineries and Western Australia dominates national output, producing approximately 60 % of Australia's alumina. Excluding agriculture, the alumina industry was the fourth largest exporter from Western Australia in 1996 - 1997, just behind gold, petroleum and iron ore (Department of Resources Development, 1997).

In Western Australia bauxite is obtained from the Darling Range and although inexpensive to mine the bauxite is low in quality, producing approximately 2.5 tonnes of residue solids for each tonne of alumina (Glenister and Thornber, 1985). In 1992 Australia generated approximately 30 % (20.1 million tonnes) of the residue solids produced from the Bayer process worldwide (Glenister, 1992).

The handling of Bayer residue solids by the process of flocculation, thickening, clarification and filtration is a major issue for all refineries as it impacts on both the environment (due to caustic entrained in the liquor) and on the cost of production (caustic losses cost tens of millions of dollars per annum). To date there is little fundamental knowledge of the aggregation mechanism of Bayer residue, what is known about the factors affecting the aggregation of waste solids is of an empirical nature.

This study has sought to produce a mechanistic understanding of the factors which affect aggregation of residue solids in Bayer liquors.

1.1 THE BAYER PROCESS

Bauxite is refined to alumina using what is essentially a dissolution-recrystallisation process. It involves four main stages; digestion, clarification, precipitation and calcination (Figure 1.1). The Bayer process is successful because aluminium bearing minerals dissolve in strong caustic while most other minerals do not. The bauxite ore is crushed to an appropriate size range (normally 100 % under 30 mm) before treatment with caustic. Once the gangue material has been separated, recrystallisation produces pure aluminium trihydroxide, $Al(OH)_3$, which is calcined to Al_2O_3.

1.1.1 THE UNIT OPERATIONS

1.1.1.1 Digestion

Bauxite contains aluminium bearing minerals of which gibbsite, $Al(OH)_3$, and boehmite, AlO(OH), are the most important. The proportion of these minerals in the bauxite determines the processing temperature; ~150 °C for gibbsite and ~250 °C for boehmite. Both reactions are carried out under high pressure (up to 240 kPa).

Gibbsite is the dominant aluminium mineral in Darling Range (Western Australia) bauxite and dissolves according to the reaction:

$$Al(OH)_3 + NaOH \rightarrow Na^+ + Al(OH)_4^- \qquad \text{(Eqn. 1.1)}$$

The solution obtained from digestion is supersaturated with respect to aluminium and is termed a 'pregnant liquor'. After digestion the temperature and pressure are lowered in a series of flash vessels to ~100 °C and atmospheric pressure.

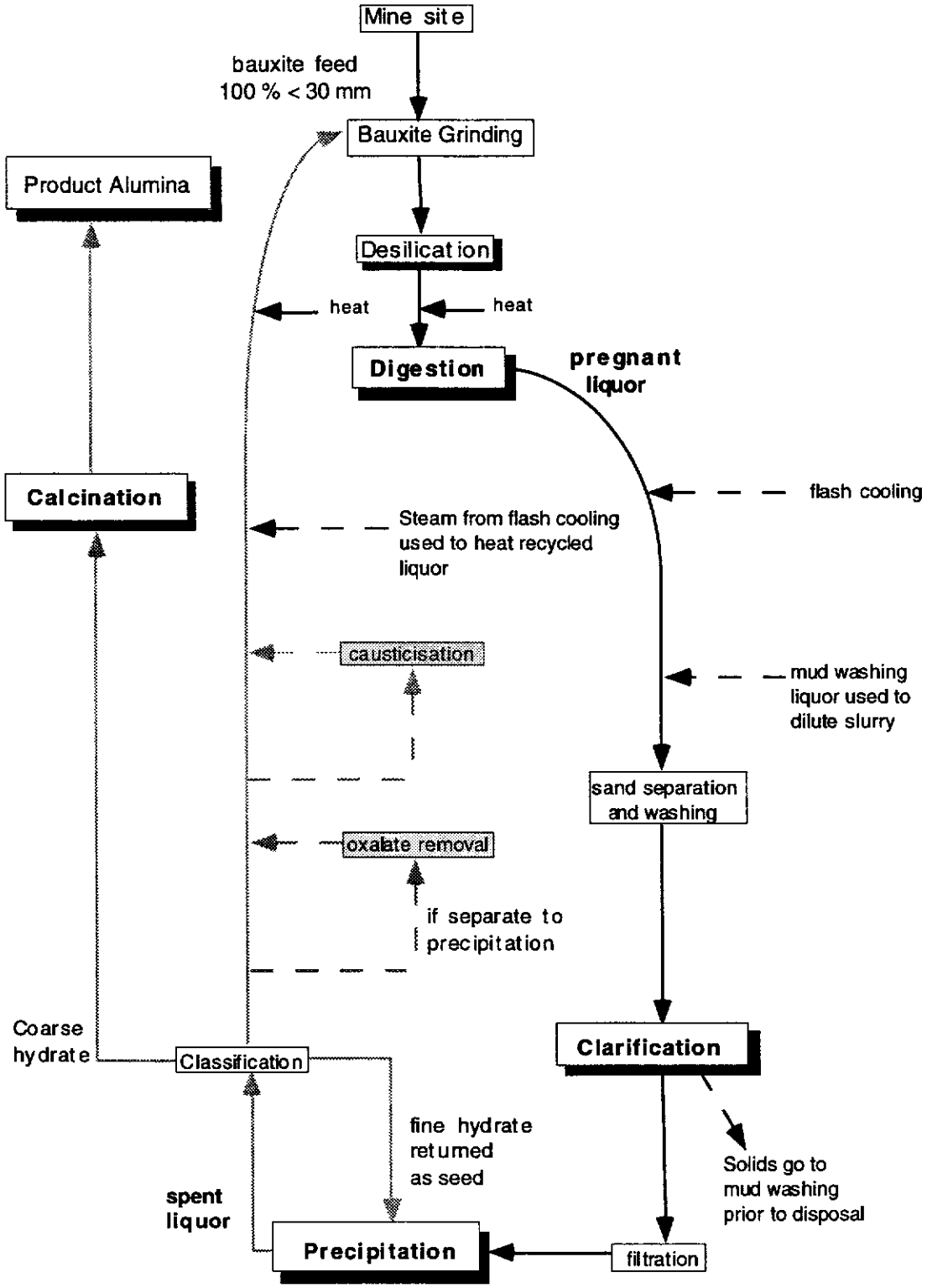

Figure 1.1 Schematic representation of the Bayer process for refining bauxite to alumina.

1.1.1.2 Clarification

The residual solids need to be separated from the pregnant liquor prior to precipitation. The waste residue is split, using sand traps, between the coarse 'sand fraction' (larger than about 150 μm) and the fines (under 150 μm) which are often referred to as 'red mud' (Glenister and Thornber, 1985) or 'Bayer residue'. The sand is washed to re-coup as much caustic as possible before disposal.

The fine residue is separated from the pregnant liquor by the addition of a water soluble, macromolecular polymer (flocculant) to aggregate the waste. The polymer acts by adsorbing onto several particles causing the fine suspended particles to form into larger structures which settle faster. The flocculated solids are settled in a large tank called a 'thickener' to produce a dense sediment. A more detailed description of a thickener is given in Section 1.3.1 .

The *overflow* (the clarified supernatant liquor removed from the top of the thickener) is passed through filters to remove any solids and the pregnant liquor is cooled (~80 °C) before entering the precipitation stage.

The separation of solids and liquor must be conducted quickly or aluminium trihydrate will precipitate during clarification. This is known as autoprecipitation and results in loss of product. It is vital to alumina production that clarification be effective. Poor flocculation can lead to excessive fines in the overflow which can clog the filters and lower production rates. Additionally, any solids which pass through the filter can contaminate the product. Ineffective flocculation may also lead to higher loss of caustic by entrainment within the residue.

1.1.1.3 Precipitation

Precipitation is a very slow process that is carried out in stages and is the reverse of the dissolution reaction (Equation 1.1). Firstly, fine gibbsite seed crystals are added to the cooled pregnant liquor in the primary precipitators. Agglomeration of the fine crystals occurs forming larger particles. Newly nucleated particles are incorporated into the agglomerated structures. In the subsequent stages further precipitation fills the interstitial voids within the agglomerates thereby strengthening the growing particles.

By the end of precipitation the temperature of the liquor is ~60 °C, the liquor is no longer supersaturated with aluminium and is called a 'spent liquor'. The aluminium trihydrate (known simply as hydrate) is classified using hydrocyclones to obtain the desired size. Coarse particles are filtered and calcined while fines are returned to precipitation as seed crystals.

1.1.1.4 Calcination

Conversion of hydrate to anhydrous alumina involves calcining it in a fluid-bed or rotary calciner at about 1000 °C. The heat flows against the solids and is applied in stages. The product normally contains less than 1 % moisture. The reaction is:

$$2Al(OH)_3 \xrightarrow{\Delta} Al_2O_3 + 3H_2O \qquad \text{(Eqn. 1.2)}$$

1.1.1.5 Side stream processes

The major unit operations essentially define the Bayer process. Nevertheless, there are other operations which are significant to alumina production such as residue washing, mud disposal, oxalate removal and causticisation. These are described briefly below.

Residue Washing

The dense sediment from the thickener (underflow) is washed free of caustic in a separate unit operation. This involves a series of thickeners (washer train) set up so that water flows against the flow of solids in a counter-current operation. The counter-current process ensures that fresh water is used to desorb the lowest caustic residue (enabling the highest extraction) and involves several flocculation steps at a continuously decreasing caustic strength (Kahane, 1992).

Mud Disposal

The coarse sand and flocculated fine residue are pumped to a disposal area where the two are sometimes recombined and further concentrated to about 50 wt % solids in 'super thickeners'. Super thickeners operate in the same manner as conventional

thickeners except that the rakes and dimensions are designed to produce higher underflow solids. The super thickener residue is pumped into purpose built drying fields which have been lined with an impermeable clay to avoid caustic seepage into the soil. The solids are spread into 1 m deep stacks and allowed to dry naturally. Run-off passes into drainage channels and is collected in lakes. The process results in a high level of caustic recycle. The residue and sand are completely dewatered and can be used to rehabilitate the lake area.

Oxalate Removal

Western Australian Bayer process liquors can contain up to 30 g L^{-1} Total Organic Carbon (TOC). The organics are continually recycled with the liquor and eventually oxidise to sodium oxalate or carbonate. All Western Australian refineries remove sodium oxalate from the process stream (as it causes problems with the precipitation of hydrate) by one of two means:

1. Allowing oxalate to precipitate with hydrate and washing with hot water which dissolves the oxalate. Coprecipitation, the cheaper of the two removal methods, can lead to product contamination if undissolved oxalate remains within the structure.

2. Separate crystallisation at the lower temperature of approximately 60 °C after hydrate precipitation. The spent liquor is seeded with oxalate, the product is flocculated in a thickener and removed. Separate removal requires another thickener and is more expensive than coprecipitation but ensures product purity.

Causticisation

Carbonate can be formed by the Bayer liquor adsorbing carbon dioxide from the atmosphere and by the degradation of dissolved organics. It is undesirable to lose caustic strength due to carbonate formation as this affects the efficiency of extracting aluminium from the bauxite. The liquor is therefore re-causticised by treating it with lime. The less soluble calcium carbonate precipitates and the hydroxide is reformed according to the equation:

$$CO_3^{2-} + Ca(OH)_2 \rightarrow CaCO_3 + 2OH^- \qquad \text{(Eqn. 1.3)}$$

1.1.2 BAYER LIQUOR COMPOSITION

The liquor composition differs at various stages of the Bayer process. After digestion the liquor will be supersaturated with aluminium, whereas it is close to saturation after precipitation (spent liquor). Similarly, the TOC level changes before and after oxalate removal. Other solution species can also vary and while some are low in Bayer liquors (for example, calcium: <20 mg L^{-1}) they are still thought to have an important effect. As a reference point, a typical Western Australian spent liquor would have the approximate composition given in Table 1.1.

Table 1.1 Approximate composition of a Western Australian spent liquor.

TA	240 g L^{-1}	**Calcium**	≤20 mg L^{-1}
TC	210 g L^{-1}	**Carbonate**	30 g L^{-1}
A/TC	0.3	**Chloride**	20 g L^{-1}
TOC	30 g L^{-1}	**Sulphate**	30 g L^{-1}
Oxalate	2 g L^{-1}		

The following definitions apply:

TA Total Alkalinity (see glossary).

TC Total Caustic (see glossary).

A/TC The alumina (A) in solution, divided by the TC (see glossary).

1.1.3 BAYER RESIDUE SOLIDS

Bauxites from different sources will differ in their mineralogy and physical properties and after digestion the residue will have been altered as the waste solids comprise not only undissolved minerals but also freshly precipitated material. Reactions between solution species leads to the precipitation of apatite-like compounds, due to the presence of calcium and phosphate (Sankey and Schwarz, 1984; O'Donnell and Martin, 1976), and of zeolite-like compounds, due to the presence of silicates in the liquor (Cardile, 1992).

1.1.3.1 Physical properties

Parekh and Goldberger (1976) found that 50 % of the residue passing through clarification was less than *ca.* 10 μm. Yong and Ludwig (1986) found the Kirkvine (Jamaica) waste was 75 % under 1 μm but the Arvida (Quebec) residue only had 25 % under 1 μm. Glenister and Thornber (1985) found Kwinana waste had 40 % under 2 μm. The residue solids had specific gravities of 3.3 (Kirkvine), 2.8 (Arvida) and 3.02 g cm^{-3} (Kwinana) respectively. Li and Rutherford (1996) found residue solids from various sources had specific gravities between 3.6 - 4.0 g cm^{-3} with specific surface areas of 30 - 50 m^2 g^{-1}. The surface area for the waste solids investigated by Yong and Ludwig (1986) were 50.5 and 14.5 m^2 g^{-1} for the Kirkvine and Arvida samples respectively. The common features are that residue solids are fine with a high surface area and hence flocculants are required to achieve their efficient and effective removal.

1.1.3.2 Composition

The aggregation of solids by flocculants is very sensitive to the solids' surface properties and different minerals do not interact with a flocculant in the same way or to the same degree. It is vital, therefore, not only to know the composition of the residue but to also have an indication of its mineralogy and its surface structure. A summary of composition data on bauxites and Bayer residue solids is presented in Table 1.2.

The dominant minerals found in Bayer waste solids are hematite, goethite and quartz but significant levels of anatase, boehmite, calcite, sodalite and tricalcium aluminate have also been reported (Yamada *et al.*, 1980; Li and Rutherford, 1996).

It should be noted that not all of the aluminium is recovered from the bauxite. There are several reasons for this; aluminium is lost in reactions with other solution species, it may be present as boehmite which requires higher temperatures to dissolve than gibbsite, or the aluminium may be incorporated into the goethite/hematite structure in which case it is difficult to extract (Roach, 1992).

Table 1.2 General composition of bauxites and Bayer residue solids.

Compound	Bauxites (%)	Residue Solids (%)
Al_2O_3	29 - 84	12 - 27
total SiO_2	0.5 - 24	0.5 - 30
Fe_2O_3	1 - 30	31 - 63
TiO_2	1 - 4	1 - 23
CaO	0.1 - 2	1 - 11
Na_2O	N/A	3 - 10
Ga	0.003 - 0.008	N/A
Loss On Ignition	9 - 31	5 - 17

This information was compiled from; Yamada *et al.* (1980), Pawlek (1995), Yong and Ludwig (1986) and Glenister and Thornber (1985).

Hematite

Hematite is an iron oxide with the formula Fe_2O_3. As shown in Table 1.2, iron oxide comprises 30 - 60 % of all residue solids and can be 0 - 100 % hematite depending on the source (Li and Rutherford, 1996; Yamada *et al.*, 1980). Hematite has a density of 5.26 g cm^{-3} and its structure is essentially the same as that of corundum (Schwertmann and Cornell, 1991). Aluminium can isomorphously substitute for iron up to 15 % (Schwertmann and Cornell, 1991) and this can cause reduced aluminium extraction.

Goethite

Goethite can be the dominant mineral in residue solids referred to as 'yellow' muds and can be 0 - 100 % of the iron oxide present (Li and Rutherford, 1996; Yamada *et al.*, 1980). It has the formula FeOOH, a density of 4.26 g cm^{-3} (Schwertmann and Cornell, 1991) and consists of octahedra extensively hydrogen bonded to each other. Aluminium can isomorphously substitute for iron to *ca.* 30 %, thus high goethitic

bauxites can mean even lower aluminium extraction if aluminium is bound in the goethite lattice.

Quartz

Quartz, SiO_2, can be the major constituent of Bayer residue (Li and Rutherford, 1996; Yamada *et al.*, 1980), has a density of 2.65 g cm^{-3} and dominates other forms of silicates in the bauxite feed. The silicon in quartz is tetrahedrally coordinated and the tetrahedra are edge connected forming a hexagonal spiral structure (Drees *et al.*, 1989). Silica, in bauxites, is referred to as reactive or unreactive. Quartz is essentially unreactive in low temperature digestion processes (<200 °C).

Desilication Products (DSPs)

Kaolinite and halloysite are typical reactive silicas. They will dissolve in Bayer liquor and subsequently react with solution species (such as Al, Cl, and Ca) to produce what are known as desilication products (DSPs). The most common forms of desilication products are cancrinite and sodalite (Cardile, 1992). Precipitation of the silica causes scale which can clog pipes and reaction vessels, and it can coprecipitate with hydrate contaminating the product. For this reason, prior to digestion many refineries operate a 'desilication' step which precipitates the dissolved silica as DSPs in a controlled manner.

1.2 AGGREGATION IN SOLID/LIQUID SEPARATION

Many mineral processes require the production of a clear liquid effluent with minimal suspended solids and/or a dense solid product containing minimal liquid (Hogg *et al.*, 1987); alumina refining requires both.

The settling of a solid particle in a fluid can be described by Stokes' equation:

$$U = \frac{d^2(\rho_p - \rho_l)g}{18\eta} \qquad \text{(Eqn. 1.4)}$$

where U is the settling rate of the particle, d is its diameter, ρ_p is the density of the particle, ρ_l and η are the density and the viscosity of the liquid, respectively. Richardson and Zaki (1954) showed that this relationship also holds for aggregates. As the settling rate is proportional to the square of the particle/aggregate diameter, small increases in size result in large increases in settling rate. This is especially useful for very fine particles which would otherwise take excessively long times to settle of their own accord. By creating larger structures, settling can be made significantly faster.

Aggregation is essential in the separation of Bayer residue solids from liquor, however, in the process the density of the aggregates decreases (due to entrained liquor). As can be seen from Stokes' equation, if the density of the aggregate decreases towards that of the fluid the settling rate is reduced. Thus, increased settling due to size can be offset by a decrease in density.

La Mer (1964) was the first to distinguish between aggregation by adjustment of the electrical double layer (by addition of inorganic salts or adjustment of pH to change the surface charge) and aggregation by addition of organic polymeric substances. The former was termed coagulation while the latter was termed flocculation. This distinction is adopted here to differentiate between the two mechanisms.

1.2.1 COAGULATION

Goüy (1910) and Chapman (1913) independently showed that when there are charges on the surface of a sphere, counter-ions will accumulate and form a double layer with a thickness equivalent to the Debye length. The counter ions are not static but move due to thermal energy, thus, these ions form a 'diffuse double layer'. Away from the surface all ions approach bulk concentrations and the potential decreases exponentially. Stern (1924) developed the model further to incorporate adsorbed ions on the surface (Figure 1.2).

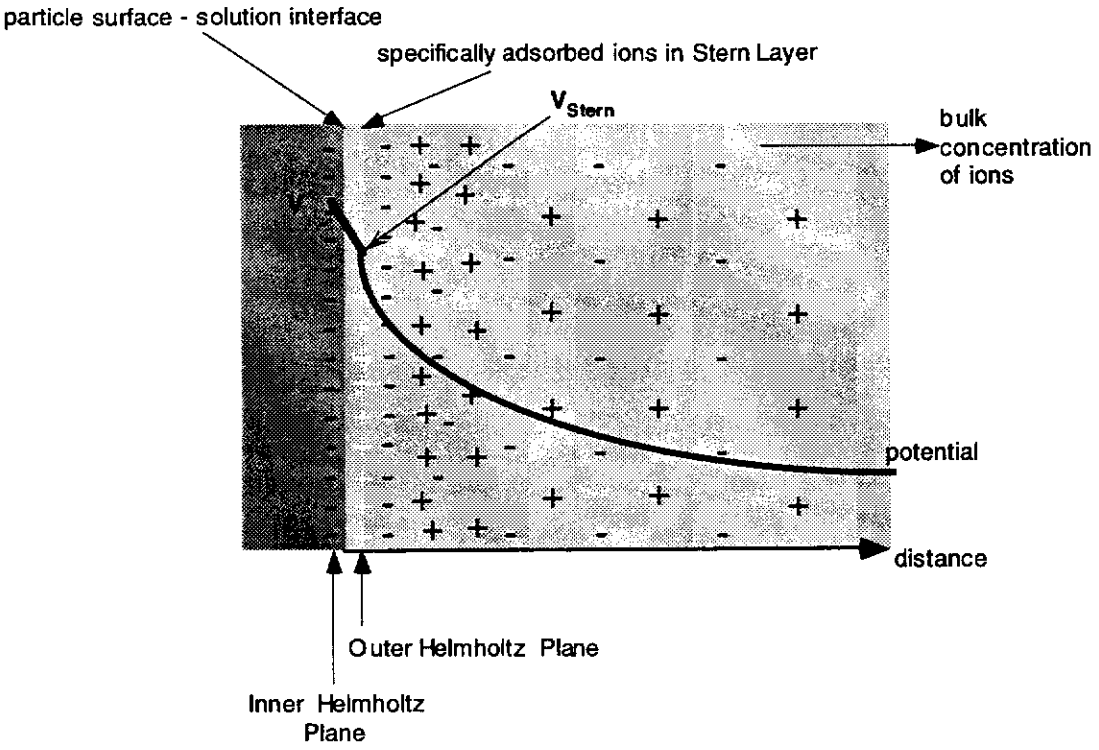

Figure 1.2 Representation of the electrical double layer on a flat surface.

Ions which do not adsorb on the surface are known as 'indifferent ions'. They form a diffuse double layer and screen the surface charge but do not penetrate as far as the Stern layer. Ions which do adsorb are known as 'specifically adsorbing counter-ions' (Gregory, 1989). Gregory (1989) estimated that the Stern layer (or Outer Helmholtz Plane) is 0.3 - 0.5 nm from the particle surface. Ions in solution which control the surface charge by adsorption or desorption are known as 'potential determining ions'. H^+ and OH^- are potential determining ions for most metal oxides.

Since solid particles in aqueous solution invariably obtain a surface charge, Derejaguin and Landau (1941) and Verwey and Overbeek (1948) were able to use double layer theory to predict the stability of colloidal particles. This has become known as DLVO theory and has proved successful in explaining the stability of colloidal suspensions under many conditions. A colloidal sol is considered unstable if the particles aggregate and grow to form larger particles when collisions occur.

In solution, a particle can experience:

i) van der Waals forces (always attractive)
ii) Electrostatic forces and (attractive or repulsive)
iii) Structural forces (attractive or repulsive)

The total potential experienced by a particle will be given by:

$$V_T = V_A + V_R + V_S \qquad \text{(Eqn. 1.5)}$$

where V_T is the total potential, V_A is the attractive potential, V_R is the repulsive potential and V_S is the solvent-structural potential. The stability of the particle is determined by the balance of these forces. The attractive potential is of the London/van der Waals type and becomes dominant at short distances. The repulsive potential is electrostatic in nature and the solvent-structural forces can be either repulsive or attractive depending on the solvent mediated forces which are significant up to 5 nm from the surface. Solvent interactions resulting in a positive V_S are known as 'hydration forces' while those resulting in a negative V_S are known as 'hydrophobic interactions'. At room temperature the thermal energy of particles should be enough to coagulate a system unless repulsive forces dominate.

Techniques have been developed which measure the potential at the 'surface of shear' which is the surface of the particle including any specifically adsorbed ions. This potential is known as the zeta potential, ζ. Experimental evidence has shown that the onset of rapid coagulation is correlated to the absolute value of ζ being less than approximately 30 mV.

The high ionic strength nature of Bayer liquors will cause shielding on mineral surfaces which double layer theory predicts should result in all minerals being coagulated. In reality, Bayer residue solids prior to flocculation are reasonably stable taking hours to settle appreciably. This is probably due to steric stabilisation induced by the adsorption of organics on the mineral surfaces.

1.2.2 FLOCCULATION

1.2.2.1 Flocculants

Flocculants are water soluble, organic polymer molecules of high molecular weight that are used in many industrial processes to control the aggregation state of suspensions; such as stabilising ceramic slurries prior to dye casting (Armstrong *et al.*, 1994; Hashiba *et al.*, 1993; Bergström *et al.*, 1992) and flocculating mineral suspensions (Smellie Jnr. and La Mer, 1958; Hsu and Lin, 1996; Pugh and Lundström, 1987; Kretzschmar *et al.*, 1993). The important features of a flocculant molecule are:

i) Chemical composition.

The functional groups on the flocculant determine the interaction with the mineral surface. Polymers, therefore, can consist of various functional groups; for example, carboxylate, amide, sulphonate, quaternary ammonium salt, and ether linkages. Many flocculants contain more than one functionality and are referred to as copolymers.

ii) Tacticity (sequence of monomer units).

Changes in tacticity can give a polymer quite distinct properties (Panzer and Halverson, 1989). That is, if monomers A and B are used to make up the polymer, the tacticity can be random (ABBABAABAB), alternating (ABABAB) or in 'blocks' (AAABBB) each of which will result in different properties.

iii) Molecular weight distribution.

The size distribution of the polymer and its polydispersity can affect its performance as a flocculant since long chain polymers can preferentially adsorb over short chains (Lyklema, 1995).

iv) Extent of branching.

While most flocculants are designed to minimise branching and provide a linear chain, this is not always achieved. If the polymer molecule is not linear but is extensively branched this may limit its flocculation ability.

1.2.2.2 Mechanisms of flocculation

Flocculation by the addition of an organic polymer is a rapid and efficient means of achieving solid-liquid separation. The adsorption of the polymer on the surface is a critical step in any flocculation process and is normally very fast. Flocculation is, therefore, often dominated by the kinetics of the reaction rather than the thermodynamics. Furthermore, desorption of flocculant requires all adsorbed polymer segments to desorb simultaneously. Thus, flocculation is often found to be a non-equilibrium and effectively irreversible process (Lyklema, 1989).

Flocculation differs from coagulation in that van der Waals attraction is not the dominant force which determines instability. Long chain polymeric organic molecules are effective flocculants at very low concentrations because they can penetrate several 'double layer thicknesses' into the solution and particles do not necessarily need to approach each other closely for aggregation to occur (Hunter, 1987). Adsorption of a flocculant (Figure 1.3) is achieved by adsorption of the individual segments and can occur in various modes; 'tails' are attached to the particle at one end only, 'trains' are consecutive segments of polymer adsorbed on the surface and 'loops' are attached to the particle at two points but free from the particle otherwise (Lyklema, 1995).

Flocculants can act as destabilising agents via different mechanisms; bridging flocculation, surface modification and electrostatic patch effects.

Bridging Flocculation

Bridging flocculation is the most common mechanism of flocculation encountered. The term 'bridging' was first introduced by Ruehrwein and Ward (1952) and describes a process where segments of a polymeric flocculant create a 'bridge' between two or more particles (Figure 1.3). Aggregation is hindered, therefore, when the flocculant adsorbs on one particle alone.

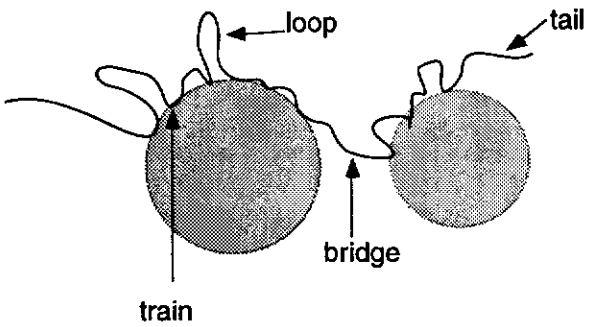

Figure 1.3 Bridging flocculation of two particles by a flocculant molecule.

Bridging flocculation can occur both on charged and uncharged surfaces with neutral polymers or with polyelectrolytes. Flocculation is entropically unfavourable as the randomness of the polymer in solution is lost on adsorption. However, due to the multiple adsorption sites only a small favourable enthalpy of adsorption is required per segment to overcome this and for adsorption to occur (Lyklema, 1995).

Fleer and Scheutgens (1993) and Koopal (1992) demonstrated that while tails may make up only a small fraction of the total segment profile of the adsorbed layer thickness, they have a large impact on the flocculation action of the polymer.

Increasing the ionic strength will lead a polyelectrolyte to approximate the behaviour of an uncharged polymer in solution and thereby increases the amount adsorbed (Fleer and Scheutgens, 1993). This is due to the decreasing electrostatic repulsion between adsorbed and solution polyelectrolyte with increasing concentration of screening ions. The change in ionic strength will also alter the conformation of the polyelectrolyte in solution which may in turn alter the conformation on adsorption.

The conformation of the flocculant in solution determines how effective a polymer molecule is at forming bridges (Figure 1.4). If the flocculant is in the 'stretched' conformation then adsorption onto other particles is more likely since the probability of a polymer-particle collision is higher.

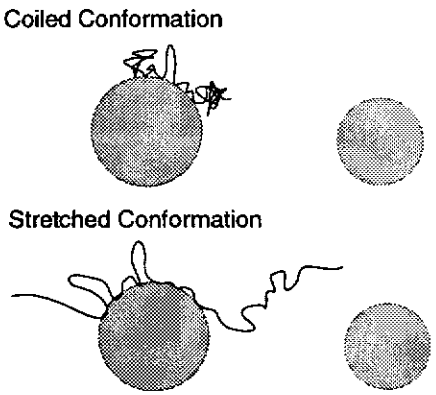

Figure 1.4 The conformation of the flocculant in solution and adsorbed on the particle determines the bridging efficiency.

The conformation of the flocculant after adsorption is also important. While flat adsorption implies a strong affinity between flocculant and surface, it is not beneficial for bridging flocculation which relies on loops and tails extending into the solution to bridge between particles. The amount of polymer adsorbed on the surface is sometimes a function of its molecular weight. When the adsorption is strong and a 'flatter' conformation is adopted, the amount of flocculant adsorbed is less sensitive to molecular weight. In this situation, once the surface has been covered to a monolayer, the mass of flocculant per unit surface area is fixed. At higher molecular weight fewer polymer molecules will be needed to form the monolayer but the mass will be essentially the same. When the polymer adsorbs with many loops and tails, as the molecular weight increases, approximately the same numbers of molecules will be

required to achieve a monolayer. As these molecules become larger the mass of flocculant required per unit surface area will be seen to increase (Fleer and Scheutgens, 1993).

It is predicted from bridging flocculation theory that at low flocculant dosage only a limited number of aggregates will form and these will not be much larger than the primary particles (Figure 1.5). A significant proportion of the solids will remain as discrete particles (Hunter, 1987) and hence the mean settling rate is expected to be low.

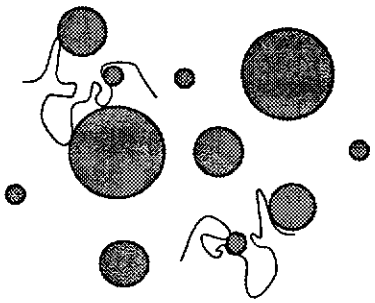

Figure 1.5 Bridging at low flocculant concentrations.

As the flocculant dosage is increased the number of particles bridged increases (Figure 1.6) and the mean settling rate increases. Higher flocculant dosages increase the extent of bridging until a maximum settling rate is observed.

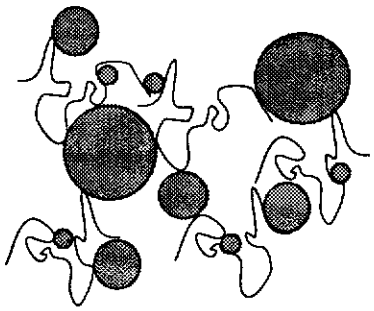

Figure 1.6 Bridging at close to the optimal flocculant concentration.

If the flocculant dosage is further increased some particles will be completely covered with flocculant (Figure 1.7) which will prevent them from bridging to other particles because there is no free surface area to do so. The mean settling rate decreases as the number of discrete particles begins to rise, this is referred to as 'steric stabilisation'. Thus bridging flocculation theory predicts that there will be an optimum flocculant dosage, beyond which re-dispersion will occur (Hogg, 1984).

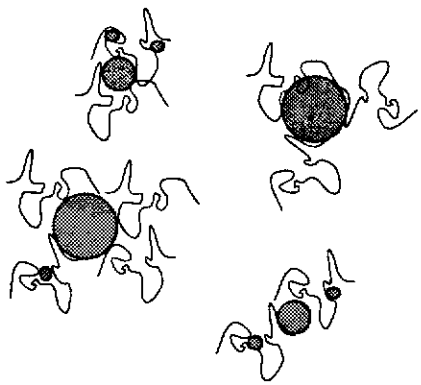

Figure 1.7 Bridging flocculation decreases beyond the optimal flocculant concentration.

Surface Modification

Flocculation by surface modification is an extension of bridging theory for the case where the interaction of the flocculant with the solvent is poor. In normal bridging flocculation it is assumed that the polymer has a strong affinity to both the surface and solvent. When all particles are completely covered with flocculant they are sterically stabilised as no bridging can occur. When the interaction between polymer segments is greater than the interaction of these segments with the solvent, aggregation can occur. This aggregation is not due to bridges formed across particles, it is purely due to the interaction of the flocculant molecules alone (Figure 1.8).

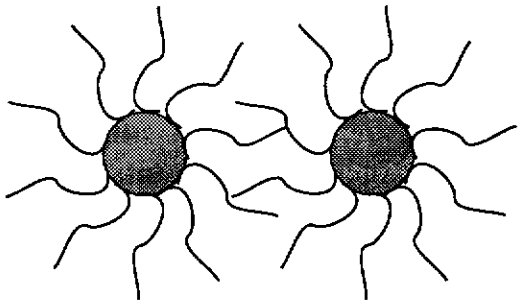

Figure 1.8 Aggregation due to surface modification.

In bridging flocculation as the polymer dosage is increased re-stabilisation will often occur. In the case of surface modification increasing polymer dosage increases flocculation as more and more polymer is adsorbed and available to interact.

Electrostatic Patch Mechanism

The electrostatic patch mechanism is very similar to the charge neutralisation concept in standard DLVO theory. The difference here lies in the charge neutralisation being localised to small, specific regions. Electrostatic attraction will cause a negatively charged polymer to adsorb on a positive surface. In those places that have polymer adsorbed the surface charge will have been neutralised and if polymer adsorption continues, an excess charge due to the polymer can occur. This enables other particles to be electrostatically attracted to the oppositely charged regions (Figure 1.9). This localised electrostatic attraction has given rise to its description as 'electrostatic patch' flocculation (Gregory, 1989).

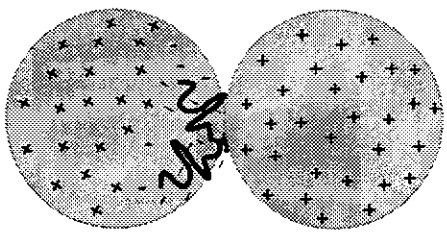

Figure 1.9 Electrostatic patch flocculation of two particles.

As the concentration of the flocculant increases the number of flocculant molecules adsorbed increases also. Thus, a point is reached where the particles have reversed charge due to adsorbed flocculant. Electrostatic repulsion then causes the slurry to stabilise.

1.2.2.3 Adsorption

For flocculation to occur adsorption on the mineral surface is essential. Many studies have been conducted on flocculant adsorption on iron oxides in aqueous systems (Bajpai and Bajpai, 1996; Dryzmala and Fuerstenau, 1987; Khangoankar and Bala Subramani, 1993; Lee and Somasundaran, 1989). All found that as the pH was increased the adsorption of both polyacrylate and/or copolymers of polyacrylamide (see Section 1.3.2.2 for structural details) and polyacrylate decreased. This effect was attributed to the increasing negative charge on the surface, diminishing the ability of the flocculant to interact with the surface by hydrogen-bonding (for polyacrylamide

copolymers) or electrostatic interactions (polyacrylate). All studies showed Langmuir type behaviour in that a plateau was reached, but theoretical curves were not fitted to the results.

Adsorption theory

Adsorption can occur by two mechanisms, *Chemisorption*, a process which involves the formation of chemical bonds between surface and adsorbing molecules and *Physisorption*, which involves forces of attraction (such as van der Waals) between a surface and adsorbing molecule but in which no chemical bonds are created or broken. Adsorption may be modelled via a number of theoretically derived isotherms which relate the amount of adsorbate in solution to the amount adsorbed onto the surface at a given temperature:

$$q = f(c) \qquad \text{(Eqn. 1.6)}$$

where q is the amount of adsorbate on the surface, and c is its equilibrium solution concentration.

Thermodynamically, while the Gibbs free energy of adsorption is equal to zero (equilibrium conditions), the standard Gibbs free energy is not (Lyklema, 1995). It is given by:

$$\Delta G^{\circ}_{ads,i} = -RT \ln K_{ads,i} \qquad \text{(Eqn. 1.7)}$$

In solution, adsorption is an exchange process whereby solvent molecules on the surface are exchanged for adsorbate molecules. The thermodynamic properties must be calculated for all the interactions taking place between all species (adsorbing molecule, substrate, and solvent). Thus, in adsorption from solution it is not the interfacial properties of the adsorbate which determines the affinity for the surface but the properties of the whole system (Lyklema, 1995). The exchange process can be written chemically as:

$$I_{soln} + nW_{surf} \Leftrightarrow I_{surf} + nW_{soln} \qquad \text{(Eqn. 1.8)}$$

where I is the adsorbing species and W is the solvent molecule. If it is assumed that the number of solvent molecules displaced by the adsorbing species is equal to 1, then (Lyklema, 1995):

$$\frac{\theta}{1-\theta} = K\frac{x}{1-x} \qquad \text{(Eqn. 1.9)}$$

where K is a constant, θ is the fraction of surface covered and x is the mole fraction. If the mole fraction of the adsorbing species is x, then 1-x represents the mole fraction of the solvent. In essence, x/1-x is, therefore, a concentration referenced to the amount of solvent. If c* is used for x/1-x the equation becomes equivalent to the Langmuir adsorption equation, that is;

$$\theta = \frac{Kc^*}{1 + Kc^*} \qquad \text{(Eqn. 1.10)}$$

Irving Langmuir, who was the first to describe adsorption of gases onto solid surfaces in 1916, used a kinetic argument to derive this isotherm. He made the following assumptions in developing his theory:

- There are a fixed number of adsorption sites
- Each site can adsorb only one molecule (no multilayers were permitted)
- The enthalpy of adsorption is the same for all sites (the surface is homogenous) and does not alter with the fraction of surface covered, θ.

In reality, however, surfaces are known to be non-uniform and the enthalpy of adsorption will decrease with increasing θ as the most energetically favourable sites will be occupied first. Other isotherms developed to account for this include the Freundlich isotherm;

$$q = Ac^x \qquad \text{(Eqn. 1.11)}$$

and the Langmuir-Freundlich equation

$$q = A\{Bc^x / (1 + Bc^x)\} \qquad \text{(Eqn. 1.12)}$$

where c is the equilibrium concentration, A is the 'monolayer' coverage and B and x are constants representing the equilibrium of the adsorption equation and the homogeneity of the surface respectively. All the interactions that determine the overall adsorbate-surface relationship cannot be separated and hence care should be taken in placing any physical significance to the parameters obtained from isotherms for adsorption from solution. However, the value of obtaining isotherms is the ability to determine the variation of the adsorbed species under different conditions.

The high molecular weight fraction (or longer chain lengths) of flocculants have been found to adsorb preferentially over the lower molecular weight fraction. This is not due to the additional enthalpy of adsorption gained from more segments being attached (on the longer chains) but is caused by the lower entropy decrease when longer chains

adsorb (Lyklema, 1995). The energy on adsorption of a segment can be represented by χ^s which is equal to:

$$\chi^s = (\Delta U_{ads,W} - \Delta U_{ads,I}) / kT \qquad \text{(Eqn. 1.13)}$$

where kT have their usual meaning (Boltzman's constant and temperature), U is the internal energy and W and I are defined as the solvent molecule and polymer segment respectively. The critical value where adsorption of a polymer is favourable is χ^s = ~0.29 (Lyklema, 1995) which means that the difference in internal energy between the solution flocculant and adsorbed flocculant need only be of the order of ~0.3 kT per segment.

1.2.2.4 Flocculation kinetics

There are two modes of aggregation; perikinetic aggregation where particles collide due to diffusion and orthokinetic aggregation where particles collide because of the fluid motion. Von Smoluchowski (1916, 1917) first determined the kinetics of aggregation for irreversible aggregation, that is, no aggregate rupture.

For perikinetic aggregation the rate constant, k_{ij}, is given by;

$$k_{ij} = \frac{2kT}{3\eta} \frac{(r_i + r_j)^2}{r_i r_j} \qquad \text{(Eqn. 1.14)}$$

where k is Boltzman's constant, T is temperature, η is viscosity of the liquid and r is the radii for particle i and j respectively (Gregory, 1989). For orthokinetic aggregation von Smoluchowski introduced a shear rate, γ, term to describe the laminar flow. The rate constant then becomes;

$$k_{ij} = (4/3)\,\gamma\,(r_i + r_j)^3 \qquad \text{(Eqn. 1.15)}$$

Clearly, orthokinetic aggregation is very sensitive to aggregate size.

However, the kinetics of flocculation are not simply those of aggregation. Flocculation is a complex system and encompasses several processes which have yet to be fully investigated. Flocculation involves:

- mixing of slurry and flocculant solution
- adsorption of polymer onto particle surfaces

- conformational adjustment of the polymer after adsorption
- collisions with other particles
- growth of aggregates
- rupture of aggregates

Many of these subprocesses occur simultaneously throughout an aggregating system (Figure 1.10).

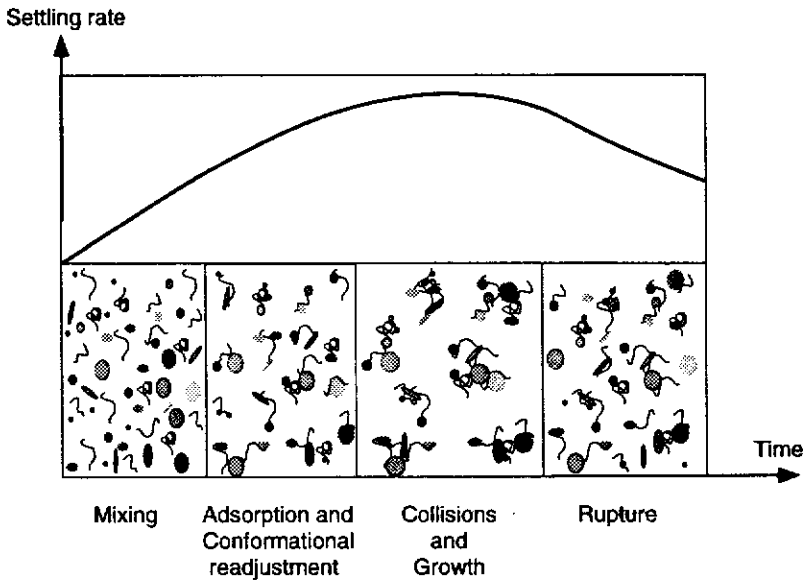

Figure 1.10 Schematic of the processes involved in flocculation and the effect on settling rate (diagram courtesy of Dr. John Farrow, CSIRO Division of Minerals).

By far the most studied section of flocculation kinetics has been collisions with other particles which can be modelled by orthokinetic aggregation (Gregory, 1989; Hsu *et al.*, 1995). Adsorption is assumed to be very fast and therefore does not dominate the kinetics. Only recently has conformational adjustment after adsorption been studied (Yu and Somasundaran, 1996), and found to take several minutes. However, this investigation was conducted by altering the solution composition.

In systems with fluid shear, particularly turbulent flow, aggregates 'grow' to a critical size depending on the conditions and strength of the aggregate (Gregory, 1989). The flocculated aggregate can be ruptured by the shear conditions stripping the polymer molecule from one or more particles. A favourable collision with another particle must occur soon after otherwise the flocculant will adsorb onto the surface already containing segments of polymer, thus breaking the bridge irreversibly. The irreversibility of bridging flocculation is often used to differentiate it from coagulation where aggregates reform after the shear has been removed.

Bremer *et al.* (1995) have found that the forces leading to rupture are approximately proportional to $\gamma\eta r^2$. That is, rupture of an aggregate is dependent on the shear rate, the viscosity of the fluid and the square of the aggregate radius. From this it can be concluded that the larger the aggregate the more likely it is to be ruptured under given conditions.

1.2.2.5 Settling theory

The settling of solids depends not only on the properties of the individual particles and aggregates but also on the fluid dynamics of the system. By increasing the solids, the hydrodynamic interactions of the system are altered and different regimes of settling or sedimentation are encountered. A description of these different regimes is given below.

A particle at infinite dilution experiences three forces (Hogg *et al.*, 1993); gravitational, hydrodynamic and Brownian/stochastic forces. The force of gravity acting on a particle is offset by the buoyancy and drag forces. The drag experienced is dependent on the velocity of the particle and by equating all of these forces the Stokes' equation is derived (Equation 1.4). Stokes' equation is only valid when the solids concentration is low and there are no long range interactions between particles.

Beyond the Stokes' region is the hindered settling zone. In this regime the solids concentration is higher and particles 'jostle' each other. The presence of other particles in the path of the falling solids causes hindered settling to be slower than Stokes' settling for the same sized particle. Richardson and Zaki (1954) found that hindered settling obeys:

$$U = U_{ST} (1 - \phi)^{4.65} \qquad \text{(Eqn. 1.16)}$$

where U is the hindered settling velocity, U_{ST} is the Stokes' velocity and ϕ is the volume fraction of solids. They also concluded that this equation could be used for aggregates.

On occasion, an induction period may be encountered prior to the onset of visible settling, this induction period is not properly understood and may be due to the kinetics of aggregation (Witten and Sander, 1981; Kolb *et al.*, 1983; Meakin, 1983; Gregory, 1989).

As the solids concentration increases further 'networked settling occurs'. This is similar to hindered settling but results in continuous rather than transient hydrodynamic interactions between particles. The slower, networked settling is often accompanied by the presence of a mudline (a distinct demarcation between settling solids and supernatant liquor) which allows settling to be followed visually, however, Hogg *et al.* (1993) found that the presence of a mudline is also determined by the physical properties of the particle (such as particle size).

If the solids concentration is increased further the gel region is encountered. Settling no longer occurs as the solids concentration is so high that all particles are networked to form one large aggregate. The solids concentration at which the gel region is formed is dependent on the size, morphology, and density of the particles and the extent of particle interactions (Zrinyi *et al.*, 1988).

Settling measurements conducted in batch mode eventually show compression of the solids (Figure 1.11). As the particles reach the bottom of the container, other solids settle above them which causes a pressure to be exerted, thereby compacting the sediment. At equilibrium, this force equates to the compressive yield stress of the sediment.

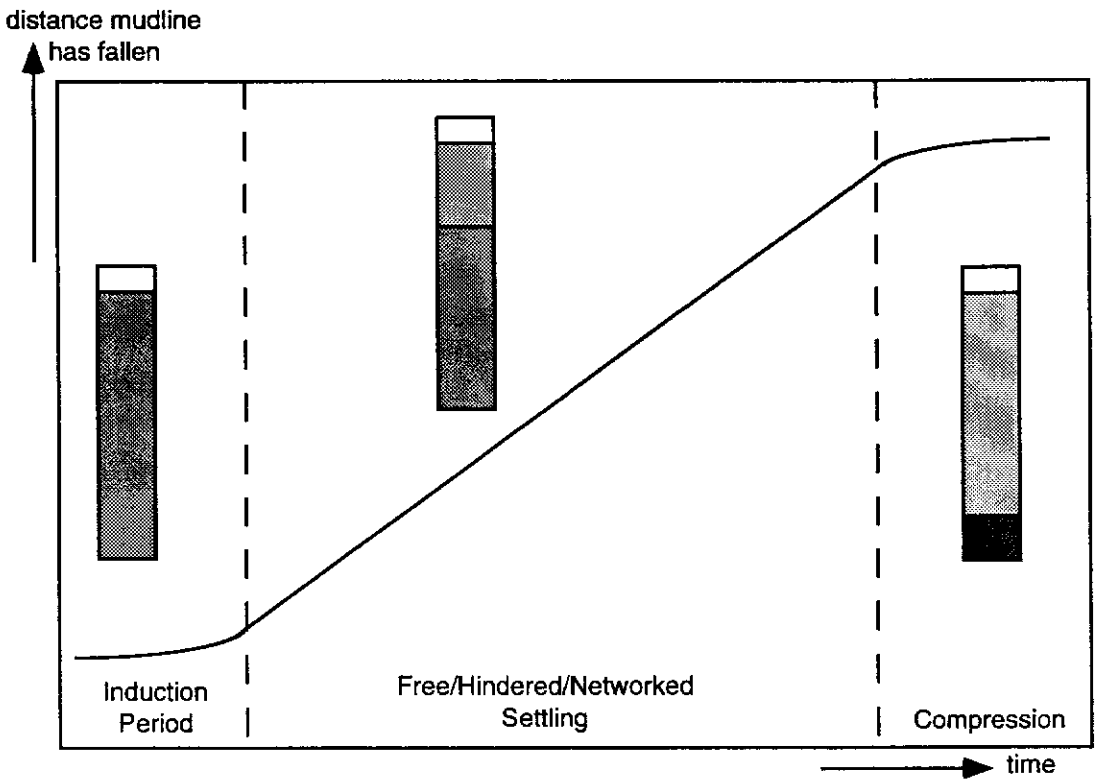

Figure 1.11 A typical curve of the distance the mudline has fallen versus time.

Many authors have attempted to describe mathematically the settling characteristics of particles over the entire region shown in Figure 1.11 (for example: Hogg *et al.*, 1993; Buscall and White, 1987; Sarmiento and Uhlherr, 1979). However, for the purposes of determining comparative aggregation states, the linear settling rate and residual turbidity are sufficient (Song *et al.*, 1992; Bhatty *et al.*, 1982; Michaels and Bolger, 1962).

1.3 FLOCCULATION OF BAYER RESIDUE

Very little information on the flocculation of Bayer residue is available in the public arena. Due to its commercial importance there may be work covered by confidentiality clauses in alumina producers' and flocculant manufacturer's research reports. In this section what is publicly available about Bayer residue flocculation is reviewed.

1.3.1 THICKENER OPERATION

Thickeners (Figure 1.12) are used extensively in mineral processing as the most cost effective unit operation for solid/liquid separation. Thickener performance, as relating to clarification in the Bayer process (waste residue separation in the primary thickeners) is described in some detail below.

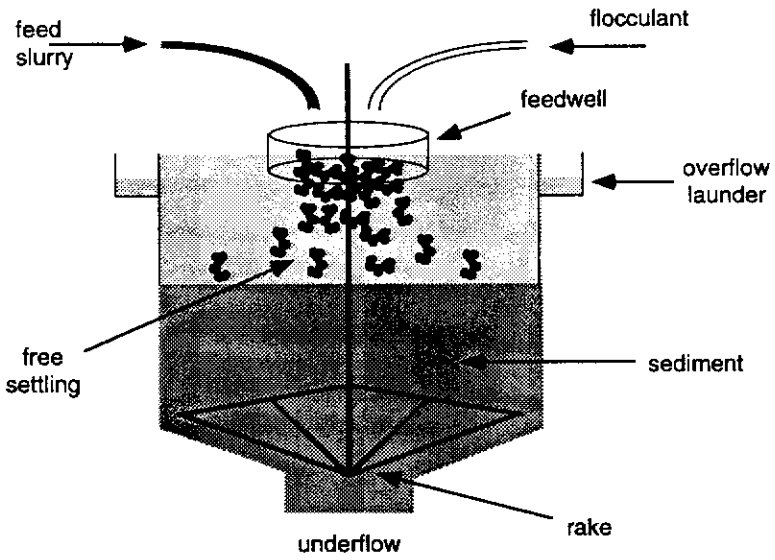

Figure 1.12 Schematic of a thickener.

Initially, the slurry feed (~70 g L^{-1}) is contacted with a dilute flocculant stream in the feedwell. Feedwells are characterised by turbulent flow which ensures reasonable mixing. The residence time in the feedwell is important as aggregate rupture will eventually dominate (Section 1.2.2.4). The solids concentration and the flocculant concentration coming into the feedwell are key parameters in optimum thickener performance. This is because if flocculant is not homogenously distributed throughout the slurry local overdosing can occur. The newly formed aggregates, which settle much faster than discrete particles against the upflow of liquor, result in a clarified solution at the top of the thickener. The clarified supernatant spills over the edge into a launder surrounding the thickener - this is termed the overflow. The velocity of the liquor flowing to the top of the thickener is called its 'rise velocity'. The aggregates must settle faster than the rise velocity or they will report to the overflow.

After the aggregates have been formed in the feedwell quiescent conditions are required so as not to break any aggregate structures. In alumina refining, it is important that the solids have a short residence time in the thickener to avoid autoprecipitation of hydrate. However, the residence time has to be long enough to produce a small 'bed' so that entrainment of liquor in the thickened solids is minimised. This bed consists of aggregated solids which have previously settled. The pressure exerted by the weight of the bed aids in dewatering the aggregates as the burden of freshly settled solids forces liquor out and compresses the solids even further.

The dewatered, thickened solids (underflow) are constantly raked within the thickener so that they move towards a central discharge point. Centrifugal pumps are commonly used to remove the solids from the thickener.

Indicators of efficient thickener performance in the production of alumina are:

i) Low overflow solids (clarity)
ii) High underflow solids (densification)
iii) Fast settling rates (and thus high throughput)
iv) Low flocculant consumption
v) Stability of operation.

Evans (1992) correctly points out that fast settling aggregates do not necessarily form a dense underflow. Flocculants which produce large aggregates contain much entrained liquor and as such can result in a lower density underflow than if no polymer were used (Figure 1.13). Both for settling and for dewatering purposes, large, dense aggregates are usually the most desirable.

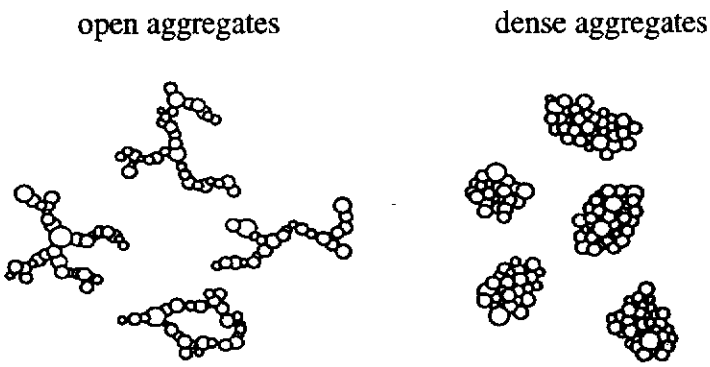

Figure 1.13 Aggregate structures (after Farrow and Warren, 1989).

1.3.2 BAYER RESIDUE FLOCCULANTS

Three groups of flocculants are used in the Bayer process. They are:

i) starch
ii) polyacrylate and polyacrylamide/polyacrylate copolymers
iii) polyhydroxamate copolymers

1.3.2.1 Starch

Starch is a natural product which contains amylose and amylopectin, with material from different sources containing different ratios of these components. Figure 1.14 and Figure 1.15 show the structure of these components in the chair conformation.

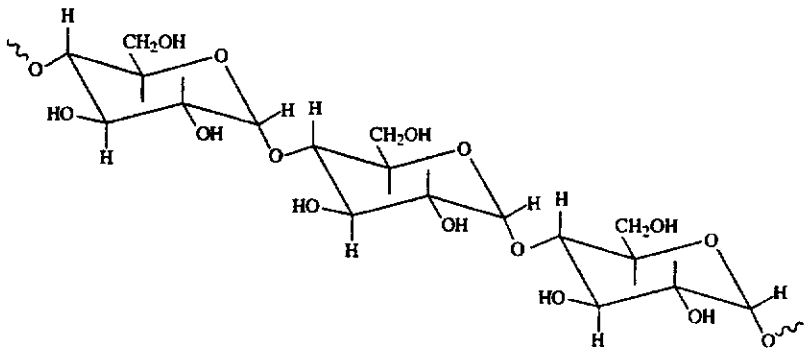

Figure 1.14 Amylose in the chair conformation after Morrison and Boyd (1977).

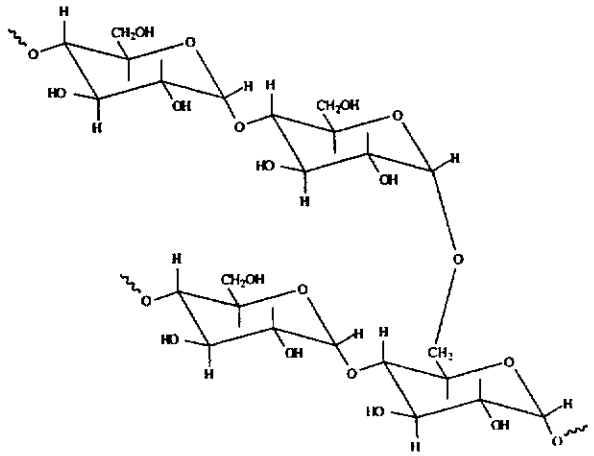

Figure 1.15 Amylopectin in the chair conformation after Morrison and Boyd (1977).

Flocculation of Bayer residue to aid the separation of fine solids from the liquor was first patented in 1942 (Brown, 1942) and involved the use of starch as the flocculating agent. Starch produces very good overflow clarity (Ryles and Avotins, 1996) but requires large dosages (typically kg t^{-1}) to achieve good settling rates (Tóth and Zoldi, 1982; Pearse and Sartowski, 1984; Kahane, 1992; Basu *et al.*, 1986).

Starch has been found to be mostly irreversibly adsorbed on Bayer residue solids (Bell, 1986). Radioactive starch was used to determine its adsorption and it was found that only 20 % of the starch could be desorbed by washing or by long holding times in the thickener. The amount of starch adsorbed by the residue solids was not affected by the presence of other organics and the DSP impurity phases were found not to adsorb starch. The monolayer coverage for starch adsorption on residue solids was 300 - 400 mg m^{-2}.

The low desorption of starch found by Bell (1976) implies that it is a reversible process to some degree. It could be concluded that either starch desorption is limited to certain minerals or all of the minerals desorb starch to a small extent. As Bell (1976) found that DSPs did not adsorb starch and Weissenborn (1993) has shown that starch is irreversibly adsorbed onto hematite at pH 10, the view that starch may be more strongly adsorbed onto some minerals compared to others under Bayer conditions is most likely the correct one.

While today synthetic polymers are standard, starch is still used at times in the Bayer process in conjunction with synthetic polyelectrolytes for controlling clarity (Ryles and Avotins, 1996).

1.3.2.2 Polyacrylate and polyacrylamide copolymers

High molecular weight synthetic polymers were suggested as possible alternatives to starch in the 1960s, (for example Sibert, 1968). However, their use did not gain wide spread acceptance until the 1970s (Connelly *et al.*, 1986).

Polyacrylamide is a neutral flocculant while a pure polyacrylate polymer is 100 % anionic. Less anionic flocculants are produced by incorporating acrylate units within the polyacrylamide structure to produce the desired charge. This type of copolymer is commonly used in many mineral processes (for example, cane sugar mud flocculation - Crees *et al.*, 1991; iron oxide flocculation - Dryzmala and Fuerstenau, 1987; quartz flocculation - Healy, 1961; oxide flocculation - Lee and Somasundaran, 1989). The structures of polyacrylate and polyacrylamide are shown in Figure 1.16.

Figure 1.16 Structures of polyacrylamide and polyacrylate.

The main advantage of using synthetic polymers is their lower dosage requirements. While the addition of starch requires kilogram per tonne quantities to produce good

settling rates, only gram per tonne quantities are required for the synthetic polymers (Pearse and Sartowski, 1984; Tóth and Zoldi, 1982; Kahane, 1992; Basu *et al.*, 1986). However, the use of synthetic flocculants can present problems. Chandler (1976) found that the main difficulties were;

i) preparing a truly homogenous flocculant solution
ii) the stability of the synthetic flocculant solution
iii) the fragility of the aggregates produced by synthetic flocculants.

As an example of the instability of the flocculant solution, Chandler (1976) described how ten seconds in a blender can totally de-activate the flocculant. The fragility of the aggregates produced was demonstrated by different mixing conditions. Gentle plunger mixing of the flocculating slurry produced a settling rate of 2.37 m h^{-1} (quoted as 7.78 ft h^{-1}) while inverting a cylinder ten times gave 0.24 m h^{-1} (quoted as 0.78 ft h^{-1}). In comparison, residue solids which were flocculated using starch maintained the same settling rate even after ten inversions. Despite the importance that the flocculant make-up procedure can have on performance it is not often discussed in the literature.

Synthetic polymers come in both dry powder and emulsion form and cover a large range of molecular weights. While increasing the molecular weight should increase the probability of a 'bridge' being formed, proper dispersion of the flocculant becomes more difficult due to the increased viscosity. Connelly *et al.* (1986) found, for this reason, that often an optimum molecular weight exists which gives optimal performance. This was supported by work conducted by Basu *et al.* (1986) who found a 'medium' molecular weight flocculant produced better settling rates than a 'high' molecular weight flocculant.

The conformation of the polymer in solution is believed to be an important factor in Bayer residue settling. Due to the high ionic strength of Bayer liquors and the shielding of the flocculant charge by the abundance of counter ions present, the polymer is expected to be in the coiled configuration.

When copolymers are used, the anionic content of the flocculant determines its charge and, therefore, its conformation. It has been found that in high soda liquors (Basu *et al.*, 1986; Kontopoulos *et al.*, 1981; Leontaridis and Marinos-Kouris, 1992), due to screening effects, a 95 % anionic copolymer of acrylamide/acrylate gave better settling rates than a 100 % homopolymer of acrylate. Basu *et al.* (1986) suggested that the 100 % polyacrylate was in the coiled configuration while the 95 % copolymer was more stretched. Lower anionic polymers may be found in the extended conformation

provided that hydrolysis does not readily occur (Sankey and Schwarz, 1984). A stretched polymer will have a higher probability of forming a bridge between particles, thus these results suggest that a bridging flocculation mechanism occurs in Bayer liquors. This is further supported by the work of Pearse and Sartowski (1986) who prepared flocculants in low soda liquors because they were found to give superior results, undoubtedly due to the polymer conformation being more stretched at the lower ionic strengths.

1.3.2.3 Polyhydroxamate

Polyhydroxamates are a recent flocculant innovation designed especially for the Bayer system (Rothenberg *et al.*, 1989). The structure is shown below (Figure 1.17) and is based on ethanolamine compounds which are known to complex with iron in basic solution. This flocculant type is normally produced as a copolymer of acrylamide, acrylate and hydroxamate. It has been shown to improve clarity to the same levels as starch (Rothenberg *et al.*, 1989) but at much lower dosages.

The results of Rothenberg *et al.* (1989) show that refinery Bayer residues do not always display high settling rates when polyhydroxamates are used. It was found that polyhydroxamates generally require higher dosages to achieve the same settling rates as polyacrylates/polyacrylamides, however, better overflow clarities are always achieved.

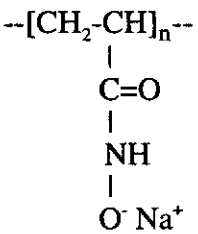

Figure 1.17 Chemical structure of polyhydroxamate.

Ringenbach *et al.* (1993) and Han *et al.* (1973) found that polyhydroxamic acid was irreversibly adsorbed onto hematite. Spitzer *et al.* (1991) found the structures formed by polyacrylates were more sensitive to shear and produced weaker aggregates than those formed by the addition of the polyhydroxamate.

1.3.3 FACTORS WHICH AFFECT BAYER FLOCCULATION

Reports on Bayer residue flocculation are dominated by the factors which affect it. The studies are mainly of an empirical nature and invariably do not offer mechanistic evidence to support the hypotheses.

1.3.3.1 Physical properties of residue solids

Particle size is well known to affect settling rate whether flocculant is present or not. Buravlev *et al.* (1972) investigated Bayer residue from both Yugoslav and Greek bauxite sources. Their results are not applicable to Bayer liquors as the samples were washed prior to experimentation, but they did find that the Yugoslav residue which had a finer size distribution had a slower settling rate. Parekh and Goldberger (1976) have shown that most waste solids have particle size distributions with 50 % less than 10 μm and that the finer solids settled more slowly (in the absence of flocculant).

Solids concentration has a dominant effect on settling. As the solids content increases the settling rate decreases (Basu *et al.*, 1986; Parekh and Goldberger, 1976; Farrow *et al.*, 1985; Kontopoulos *et al.*, 1981; Blecic and Adzic, 1990). These observations are explained by the increased hindered settling that occurs as solids concentration is increased. Also, higher solids concentration benefits clarity as fine particles are trapped within aggregates. Orban *et al.* (1973) found that settling of residue solids was correlated to total surface area, which is both a function of particle size and solids content.

1.3.3.2 Mineralogy

The flocculant functional groups will not interact in the same way with different minerals and this is supported by literature reporting the effects of mineralogy on the settling of Bayer residue. The minerals most investigated are goethite, hematite, and anatase. Along with phosphates, these are discussed below.

It is well established that residue solids high in goethite do not settle as well as those high in hematite (Basu *et al.*, 1986; Buravlev *et al.*, 1972; Yamada *et al.*, 1980). There

are three possible reasons for the different settling characteristics of goethite compared to hematite: surface properties, density and morphology. Hematite settles faster than goethite (10 mL min^{-1} compared to 2 mL min^{-1} according to Basu, 1983) even in the absence of flocculant due to its higher density (Section 1.1.3.2) and morphology. The morphology of goethite is acicular while that of hematite is rhombohedral. Morphology is known to affect settling (Allen, 1990) and an acicular crystal does not settle as quickly as a rhombohedral particle due to hydrodynamic factors. However, as found for starch (Weissenborn, 1993; Bell, 1976), the difference in surface composition may mean that more flocculant is adsorbed on hematite than goethite. This highlights the interplay between physical factors and mineralogy - is it the different surface compositions of hematite and goethite which affect settling or is it purely the physical density/morphology which causes the difference? As yet, no one has fully addressed this issue.

In an attempt to improve goethitic residue settling in Bayer liquors, much work has been conducted on the transformation of goethite to hematite. Goethite was found to be more soluble than hematite in sodium aluminate solutions and the solubility increased with increasing temperature and free caustic. Basu (1983) concluded that goethite could, therefore, reprecipitate as either goethite or hematite during both thickening and precipitation. As a result, in the refinery situation a fresh iron oxide surface (as either goethite or hematite) could be depositing onto the solids. However, Ni *et al.* (1968) claim that if iron were to precipitate after digestion the most likely product would be an iron hydrogarnet.

Buravlev *et al.* (1972) attempted to show that calcination of the Bayer residue, to convert goethite to hematite, improved the settling rate. They performed experiments in glass vessels at temperatures varying from 200 - 700 °C but did not take into consideration sintering, density or morphology effects. In this temperature range, silica from the glassware would undoubtedly be extracted. Thus, their results cannot be unambiguously attributed to the conversion of hematite to goethite.

A more thorough investigation on the effect of transforming goethite to hematite was conducted by Basu (1983). This was performed in two ways; by heating the goethite in air which leaves the morphology of the original goethite unaltered, and by dissolving the goethite and reprecipitating it as hematite which does not. It was shown that while the particle size was essentially the same as that of the reprecipitated hematite, the hematite derived from heating had a lower settling rate due to its morphology. Comparison of the goethite and hematite with the same morphology did show an improvement in settling on transformation. However, density differences

will contribute to this result. It is thus still unclear whether the flocculant does indeed interact with goethite in a different way to hematite and thereby produces aggregate structures which settle more slowly.

Anatase (TiO_2) is found in many residue solids but it is not normally a major component. Yamada *et al.* (1980) generated waste solids by digesting various bauxites from world sources in high pressure bombs. They found that flocculation for the individual minerals was 'good' for anatase (78 m h^{-1}), boehmite (26 m h^{-1}) and hematite (10 m h^{-1}) while it was 'bad' (but did not quantify) for goethite, gibbsite, quartz and kaolinite. Differences in particle size, morphology or densities were not considered. They found that residues high in goethite were not flocculated well by polyacrylates and that conversion of the goethite to hematite had limited benefit. The settling rate of the highly goethitic residue was most dramatically improved when both the hematite and anatase content was increased. It was found that higher settling rates were observed with greater than 7 % anatase content. In effect, Yamada *et al.* (1980) appear to suggest some synergistic relationship between the minerals.

In contrast, the addition of anatase was found to decrease the settling rate of the waste solids according to Prakash and Horváth (1981) and this correlated with the increase in surface area present. However, they did not adjust the starch dosage to compensate for the increase in total surface area. As the flocculant adsorbs onto the mineral surface, and this is dependent on the active sites available for adsorption, flocculant consumption expressed as g t^{-1} can be misleading. A better measure of flocculant consumption is often in terms of mass of flocculant per unit surface area. Yamada *et al.* (1980), using a polyacrylate flocculant, accounted for the increased surface area and so these two investigations may not be as contradictory as they might first appear.

Phosphate minerals are thought to inhibit residue flocculation (Grubbs *et al.*, 1980; O'Donnell and Martin, 1976). While phosphate compounds are well known as electrostatic dispersants, this mechanism of action in high ionic strength conditions appears unlikely. Grubbs *et al.* (1980) found a correlation between phosphate content and settling rates even though it is ≤ 0.2 % for most bauxites. O'Donnell and Martin (1976) stated that phosphate itself did not inhibit residue flocculation but that phosphate precipitates calcium as apatite-like compounds and removes lime which would otherwise benefit the settling of residue solids.

1.3.3.3 Inorganic impurities

The main inorganic impurity effects reported in the literature have been for calcium and carbonate. Calcium has been suggested as being beneficial to settling while carbonate is not.

Calcium has been proposed to act in a number of ways. Basu *et al.* (1986) have shown that calcium ions will decrease the solubility of iron in aluminate solutions. Therefore, calcium could induce precipitation of fresh iron oxide surfaces onto which the flocculant might adsorb. Calcium also aids the transformation of goethite to hematite which is known to flocculate better with polyacrylates (Yamada *et al.*, 1980; Spitzer *et al.*, 1991; O'Donnell and Martin, 1976; Basu *et al.*, 1986). Calcium can remove phosphate as apatite-like compounds (Sankey and Schwarz, 1984; O'Donnell and Martin, 1976) or it may form calcium bridges on the surface for flocculant adsorption (Rothenberg *et al.*, 1989). The calcium can also precipitate as either tricalcium aluminate, calcium carbonate or calcium hydroxide, again forming a fresh surface for the flocculant to attach (The and Sivakumar, 1985; Whittington, 1996).

Yamada *et al.* (1980) found that settling of residue solids was enhanced by the presence of all Group II cations in the order $Mg^{2+} < Ca^{2+} < Sr^{2+} < Ba^{2+}$. This series suggests a cation size or polarisability effect. It does not seem feasible that the size would be inherently important, thus, it may be due to stronger interactions when more polarisable metals are present. Whether this is the result of stronger surface-metal or metal-flocculant interactions is unclear. Their data show a decreasing enhancement with increasing caustic strength. Perhaps, for the case of calcium, several of these mechanisms occur simultaneously.

Carbonate is ubiquitous in all Bayer liquors; refineries often re-causticise with lime before digestion to remove carbonate as it is not active in the extraction of aluminium from bauxite. Hunter *et al.* (1990) found lime was beneficial to residue settling and this was believed to be due to the re-causticisation of the liquor, as shown by Equation 1.3 (see page 6). They also claim that carbonate in Bayer liquors adsorbs on mineral surfaces and interferes with flocculant adsorption. No evidence was presented for this claim.

Basu *et al.* (1986), found sodium sulphate increased the settling rate, however, no other data on sulphate effects on residue settling is available. No reasons why sulphate should be beneficial, when phosphate is harmful, were given.

1.3.3.4 Organic impurities

Dissolved organics are considered undesirable in the Bayer process as they increase the possibility of product contamination and/or poisoning of the seed surface during precipitation. The level of organics can be high (up to 30 g L^{-1} TOC) and little is known about their specific chemical structure. What is known is that the organics are predominantly humic in origin (and therefore are soluble in caustic) and contain carboxylate and other negatively charged functional groups.

Organics, such as humics and oxalate, were shown to decrease the settling rate of goethite (Basu *et al.*, 1986) and residue solids (Yamada *et al.*, 1980), and Sankey and Schwarz (1984) found that Jamaican bauxites settled much faster in synthetic liquors than in refinery liquors containing a high concentration of soluble organics.

Flocculants can also contribute to the level of dissolved organics. Pearse and Sartowski (1984) found that, at a Hungarian plant, 40 - 50 % of the liquor organics could be attributed to starch as it degraded in the high caustic environment. They found that most of the organics extracted from the bauxite was subsequently removed from the process by adsorption onto residue solids. They also showed that synthetic polymers did not significantly contribute to the organic content of the liquor which they attributed to the flocculant being completely adsorbed by the waste solids.

1.3.3.5 Other factors

While most studies have concentrated on solution or mineralogical effects, the use of multi-flocculant addition and the effects of temperature on settling have also been investigated.

Multi-point addition of flocculant to the feed was regarded as beneficial by Pearse and Sartowski (1984) and Connelly *et al.* (1986). Pearse and Sartowski (1984) used a two point flocculant addition method to flocculate residue solids from a Hungarian bauxite source. In the first addition, 50 - 80 % of the flocculant dosage was added and the slurry pumped through a centrifugal pump which ruptured most of the macro-aggregate structure. The remaining flocculant dosage was then added and the reformed aggregates allowed to settle. They claimed that this produced faster settling aggregates but presented no data to substantiate the claim. Connelly *et al.* (1986) stated (but no experimental details were given) that multi-addition of polymer results in better settling rates compared to single stage addition. However, Spitzer *et al.* (1991) observed dual stage flocculant addition to be superior to single stage addition for polyhydroxamate but not for polyacrylate flocculants.

Since flocculation is dependent on the kinetic conditions, temperature should be an important factor in the settling of residue solids. It has been found (Basu *et al.*, 1986; Blecic and Adzic, 1990) that as temperature increased the settling rate increased, as would be expected from the (i) increased collision frequency at higher temperature, (ii) the possible increased polymer adsorption due to its uncoiling and (iii) the lower viscosity of the slurry at higher temperatures.

1.4 Summary of Chapter and Scope of This Study

In summary, limited fundamental knowledge is available about the flocculation of residue solids in Bayer liquors. Although many studies have been conducted on the adsorption of carboxylic acids or polymers in aqueous solutions (Gong *et al.*, 1991; Pavez *et al.*, 1996, Allara and Nuzzo, 1985; Lee *et al.*, 1996) it is not known whether their conclusions are also relevant to high caustic environments such as the Bayer system. Direct information on the adsorption of polyacrylate onto residue minerals under Bayer conditions was, therefore, considered important and hematite was chosen

for investigation as it is one of the dominant minerals found in all Bayer residue solids and has a less variable composition than the often similarly abundant goethite. Synthetic Bayer liquors were used so that the impact of the different parameters could be assessed individually. Experiments in refinery liquors would have caused difficulties in interpretation due to existing solution species and possible interference from organics.

The specific aims of this project were to:

i) Investigate the parameters which affect hematite flocculation in synthetic Bayer liquors.

ii) Determine the mechanism of interaction between the surface groups on hematite and the functional groups of the flocculant.

To achieve these aims the following strategy was used:

- Empirical information on settling rates, and how they were affected by impurities, was obtained. The mode of flocculation (bridging, surface modification, or electrostatic patch) was determined. Impurities investigated covered both solution species and surface species. The solution species of interest were the sodium salts of carbonate, sulphate, phosphate, chloride and silicate known to be present in Bayer liquors. Additionally, calcium chloride (to observe the effect of calcium) and operational parameters (such as solids concentration, caustic strength, temperature, aluminium supersaturation) were studied. Two types of surface contaminants on hematite were investigated; one was an amorphous silicate that can occur naturally on hematite and the other was freshly precipitated DSP on hematite. These surface contaminant experiments were designed to shed light on the effect desilication products have on residue settling.
- Adsorption density measurements to determine whether changes in settling rate are due to changes in adsorbed flocculant were undertaken. This is essential information as flocculation performance can be determined by factors other than flocculant adsorption.
- X-ray Photoelectron Spectroscopy (XPS) was utilised to investigate the interaction between the flocculant and hematite. Configuration of the flocculant molecule on the surface was studied by Fourier Transform Infrared (FTIR) techniques. This information highlighted the nature of the flocculant bonding mechanism with the surface.

- Theoretical modelling was undertaken to obtain independent information which would support (or negate) the mechanism of adsorption determined from spectroscopy. It is also a powerful tool for investigating the adsorption process at an atomic level.
- Refinery samples (solids and liquor) were investigated to compare them with laboratory results for hematite. Although it was recognised that real residue solids are of a highly variable nature, it was deemed necessary to investigate the possible use of refinery materials or at least compare them with the pure hematite results.

By integrating this information, a mechanistic understanding of polyacrylate adsorption on hematite in synthetic Bayer liquors was obtained.

2. MATERIALS AND METHODS

An integrated approach was required to obtain the necessary data for determining the mechanism of flocculation in the Bayer system. This required the use of the following:

- a method to assess the aggregation state of flocculated suspensions
- a method to determine the residual flocculant concentration in synthetic Bayer liquors
- surface analytical methods to probe the surface structure of the adsorbed flocculant.

This chapter outlines the samples used and describes the techniques developed for this purpose.

2.1 MATERIALS

- Hematite Sample A was a natural sample from Mt. Newman, Western Australia. It was crushed and ground and stored in deionised water prior to use.

- Hematite Sample B was a Kanto chemicals product.

- Hematite Sample C was a Bayer Australia product. A proportion of Sample C was purified by dialysis against caustic and water; this will be referred to as 'Cleaned Sample C'.

- Bayer residue solids were obtained from a refinery thickener. Feed slurry (10 L) was collected from a primary thickener pipe via a sample port. The feed solids concentration was 60 g L^{-1} and the thickener temperature was 102 °C. After collection, the feed was mixed in a thermostatted stainless steel tank. For settling tests, samples of the feed slurry (250 mL) were added to plastic measuring cylinders via a discharge tap in the tank.

- Refinery sand samples. A sample of waste sand (20 kg) from the sand traps was obtained. It was washed with deionised water by decantation over several weeks to remove most ions in solution and to redisperse any coagulated material. After washing, the sand was wet screened into size fractions, of which three were used. The size fractions were 38-185, 185-315, and 400-800 μm with a d_{50} of 148, 214 and 402 μm respectively.

- H199-B, a Nalco Chemicals Ltd. proprietary product, (Batch number 6501053) was an emulsion polymer used for flocculating refinery residue solids.

- Other flocculants were obtained as dry powders from SNF Floerger. These were polyacrylates or a copolymer with polyacrylamide (Table 2.1).

Table 2.1 Manufacturer's specifications for SNF Floerger flocculants.

flocculant	**batch number**	**anionic content (% by number)**	**molecular weight ($g\ mol^{-1}$)**
AN995SH	K1556	100%	17 million
AN970SH	K772	70%	17 million
AN970BPM	J1695	70%	10 million
AN970VHM	K1562	70%	20 million
HP1	1015	100%	10,000
AN910SH	J1518	10%	17 million

- Sodium hydroxide (AR grade) from Crown Scientific.

- Aluminium trihydrate (known as C31) from Alcoa Chemicals, Arkansas.

- Sodium gluconate (Technical grade) from Rowe Scientific.

- Potassium fluoride (RdH grade) from Rowe Scientific.

- Hydrochloric acid (AR grade) 1 M convol solution from BDH Merck.

- Nitrogen gas of ultra high purity, from BOC Gases, was used with an in-line filter without further purification.

- Sodium silicate ($Na_2SiO_3.5H_2O$, AR grade) from Ajax Chemicals.

- Sodium chloride (AR grade) from BDH Merck.

- Sodium carbonate (AR grade) from BDH Merck.

- Anhydrous sodium sulphate (AR grade) from Ajax Chemicals.

- Sodium phosphate ($Na_3PO_4.12H_2O$, AR grade) from Rowe Scientific.

- Sodium nitrate (AR grade) from Ajax Chemicals.

- Calcium chloride (Technical grade) from BDH Merck.

- Calcium oxide (Technical grade) from Ajax Chemicals.

- Calcium carbonate (AR grade) from Ajax Chemicals.

- Calcium hydroxide (AR grade) from Univar.

- Hyamine 1622 (diisobutylphenoxyethoxyethyldimethylbenzylammonium chloride, >99% purity) was from BDH Merck.

- Potassium bromide (spectroscopic grade) from BDH Merck.

- Polyethylene glycol (PEG) 400 USP was an APS Chemicals Distributors product, batch number: 72A96.

- Dextran T10, was obtained from Pharmacia.

2.2 METHODS FOR SAMPLE CHARACTERISATION

2.2.1 HEMATITE

The solid samples were characterised using the following techniques:

- Surface areas were determined using a Quantachrome Autosorb I which utilises a standard BET isotherm with nitrogen as the adsorbent.

- Particle size distribution results were obtained on a Malvern Mastersizer using a laser light scattering technique.

- FTIR spectra of the solids were obtained by diffuse reflectance after dilution to 2 %w/w in KBr, as discussed in Section 2.6.1.

- Elemental analyses were obtained by inductively coupled plasma (ICP) spectrometry using a Varian Liberty 220 emission spectrophotometer. The samples were acidified using 2 M HCl prior to analysis.

- Differentiation between crystalline and amorphous silica was determined by slurrying 1 g of the dry solids in 200 mL of 4 M NaOH at 60 °C for 24 hours. The solids were removed by filtration and the filtrate analysed by ICP.

- X-ray diffraction (XRD) spectra were obtained on a Philips X-pert diffractometer. Copper K_α radiation was used for all samples using the conditions specified in Table 2.2. Refinery waste solids were characterised by XRD after drying the washed samples from several batches and gently grinding them prior to analysis.

Table 2.2 XRD conditions.

monochromator: graphite	divergent slits: 1 °
detector: proportional counter	receiving slits: 0.45 mm.
primary slits: söller	2θ angle range: 5 - 65
step size: 0.025 °	step time: 0.5 s

- Scanning Electron Microscopy (SEM) images were obtained on a JOEL JSM-5800LV Scanning Microscope in order to view morphology.

2.2.2 FLOCCULANTS

Flocculants were characterised using the following techniques:

- FTIR spectroscopy. FTIR spectra were obtained using either a KBr disc transmission method or a diffuse reflectance technique as discussed in Section 2.6.1. The emulsion flocculant was precipitated in acetone and dried prior to analysis. FTIR results were used to determine the functional groups present in the flocculant.

- Nuclear magnetic resonance (NMR). ^{13}C NMR was used to measure anionic content (Zurimendi *et al.*, 1984; Kulicke *et al.*, 1993) which involved preparing a highly concentrated but viscous polymer solution in water (~5 %w/w). Sonication (Heat Systems Ultrasonics XL2000, 20 kHz, 5 s pulse, 15 s delay for 4 - 6 hours) was used to reduce the polymer molecular weight and thereby lower the viscosity, which improves the resolution of the NMR spectrum (Kulicke *et al.*, 1993). Metal fines from the sonication were removed by centrifugation (13,000 rpm for 3 hours). Flocculant sample (2 mL), D_2O (1 mL) and dioxane (as the standard) were mixed in a NMR tube and the spectrum collected with a Varian Gemini 200 MHz instrument. The chemical shifts from the NMR spectrum identified functional groups and from the peak areas the ratio of acrylate to acrylamide (% anionic character) was calculated.

- Multi angled laser light scattering (MALLS) was used to obtain flocculant molecular weights. MALLS measures the light scattering behaviour of particles simultaneously at various angles (θ). The proportion of scattered light versus angle is directly related to the molecular weight. A Wyatt Technology Corp. DAWN DSP instrument fitted with a helium-neon laser (632.8 nm) was used (Figure 2.1). Normalisation of the detectors was carried out with Dextran solution. In evaluating molecular weights, samples were prepared as 2 %w/w solutions in MilliQ water then diluted in NaCl (prepared in MilliQ water) to produce a solution that was 0.5 M NaCl. The flocculant was dialysed against 0.5 M NaCl for 48 hours and filtered through a 3 µm pore membrane prior to analysis. Solutions of differing concentrations in 0.5 M NaCl were prepared for

light scattering measurement and the filtered 0.5 M salt solution was utilised as the background. The sample was analysed in a flow through, optically clear cell. A Debye plot (scattered intensity divided by concentration versus $\sin^2\theta$) was used to calculate the molecular weight. A full description of the derivation of molecular weight from light scattering is given by Wyatt (1993).

MALLS was also operated in batch mode to obtain the hydrodynamic size of the flocculant at various salt and caustic concentrations. Solutions were filtered (0.2 μm filter) to minimise particle contamination and placed in a clean, optically clear, vial for measurement. Flocculant was then added (50 $\mu g\ g^{-1}$) and the difference in scattering used to construct a Debye plot from which the hydrodynamic size (root mean squared radius of gyration) was obtained (Wyatt, 1993).

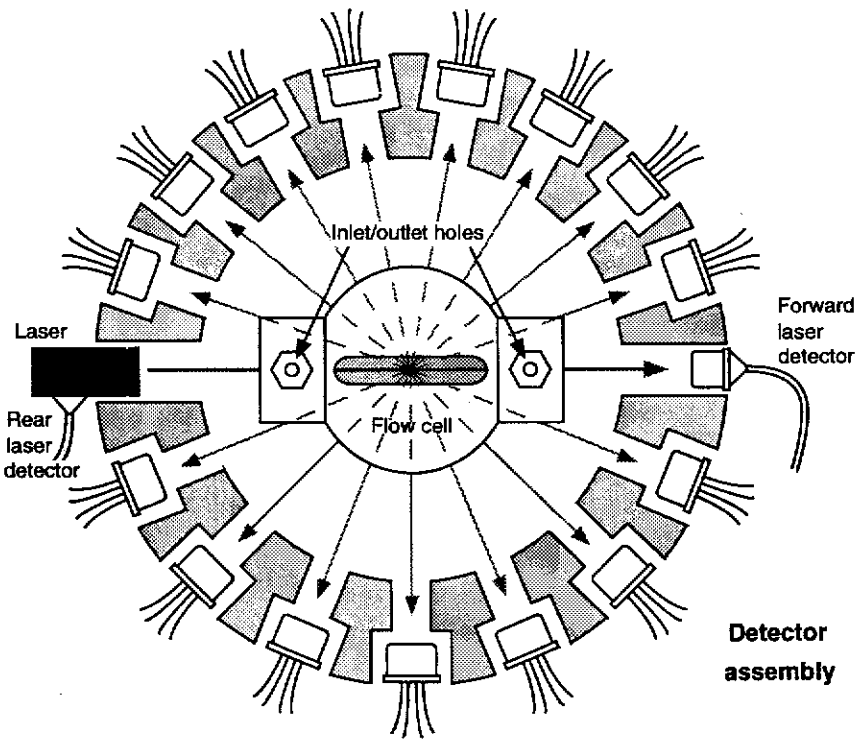

Figure 2.1 Layout for MALLS analysis of flocculant average molecular weight (diagram courtesy of Dr. Phillip Fawell, CSIRO Division of Minerals).

2.3 SYNTHETIC BAYER LIQUORS

2.3.1 SYNTHETIC BAYER LIQUOR MAKE-UP

Synthetic Bayer liquors were prepared under conditions which minimised carbonate contamination so that the level of sodium carbonate could be fixed through controlled addition.

Sodium hydroxide (392 g) was dissolved in boiled deionised water (500 g) and stored for at least 3 days. At this concentration (~16 M), carbonate and other less soluble species salt out. The caustic solution was then filtered (0.45 μm filter) under nitrogen into a stainless steel vessel to which the required amount of aluminium trihydrate was added. The mixture was heated under a nitrogen atmosphere to dissolve the aluminium trihydrate. The hot liquor was filtered under nitrogen then stored in high density polypropylene containers in a refrigerator. This concentrated liquor was diluted with boiled deionised water prior to use and further sodium carbonate or other salts were added at this stage if required.

2.3.2 ANALYSIS OF LIQUORS

The concentration of the liquors used in each experiment was confirmed using a titration method similar to that developed by Watts and Utley (1953), but with addition of gluconate rather than tartrate. Sufficient sodium gluconate (~24 mL, 400 g L^{-1}) was added to a liquor sample to complex the aluminate in solution before titration with HCl (0.5 M). Potassium fluoride (25 mL, 300 g L^{-1}) was then added to release the hydroxide ions associated with aluminium and titrated once again with HCl. The position of the inflection points in the titration curve were used to calculate the amount of alumina, caustic and carbonate present in the liquor.

No ageing effects were observed for the stored concentrated liquors.

2.4 FLOCCULATION STATE DETERMINATION

2.4.1 DISPERSION OF SOLIDS

To obtain information on settling rates and flocculation states, it is important that the solid to be investigated is fully dispersed. The settling rate is very sensitive to particle size and agglomerated solids will settle at very different rates to discrete particles.

A Heat Systems Ultrasonics XL2000, 20 kHz machine with a horn tip was used to disperse the suspension. Experiments were conducted in caustic (TC = 200) to determine the power setting and time required to fully disperse the solids, as assessed by particle size distribution measurements. It was found that 2 minutes sonication at a power setting of 6 (settings range from 1 - 10) was sufficient to fully disperse the solids for all hematite samples.

2.4.2 SETTLING RATE

The clarification stage in alumina plants is normally conducted above 90 °C. To conduct settling tests at these temperatures, a bath was constructed which utilised polyethylene glycol (PEG) as the heating fluid enabling temperatures of >90 °C to be obtained without boiling the bath fluid. A pneumatic plunger system (Figure 2.2) was designed to give reproducible mixing that did not involve electrical or water sensitive equipment.

The number of strokes and the rate at which the strokes were delivered was adjustable. It was found that a stroke period of ~2.7 seconds (or one complete cycle ~5.4 s) was sufficient to uniformly distribute the particles throughout the entire volume. The speed of the plunger movement was 0.098 m s^{-1} through the suspension. This was kept constant throughout the study.

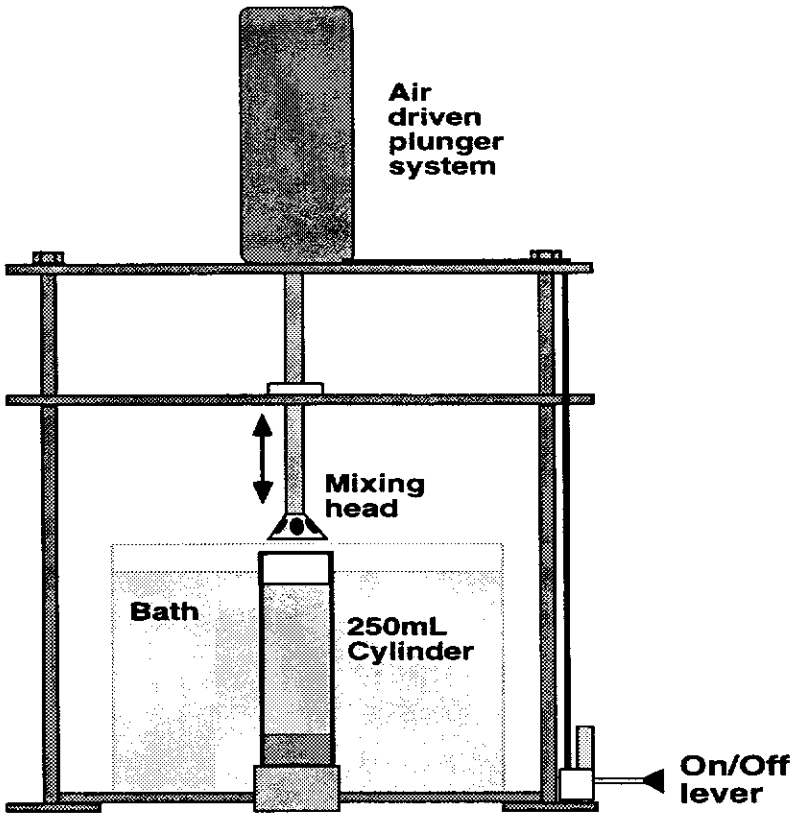

Figure 2.2 Bath and plunger set-up for batch settling tests.

Slurries were predispersed using a hand operated plunger and then placed in the cylinder holder. Four automated strokes re-dispersed the slurry, then the flocculant was added. Once fully mixed (3 cycles), the plunger was removed and the settling of the mudline timed with a stop watch. The results from settling were plotted as a graph of distance fallen (mm) versus time (min). The settling rate was then converted to m h^{-1} (accepted industry units for settling rate) by taking the slope of the first linear region of the plot, after any induction period (Farrow and Warren, 1993).

It was found that, for the refinery samples, twelve strokes (six cycles) of the plunger were required to thoroughly mix the flocculant solution into the feed slurry.

2.4.3 TURBIDITY

After settling, the sample was left for one hour untouched in the bath. The supernatant liquor was then sampled 75 mm below the meniscus with a syringe and placed in a turbidity meter vial. Turbidity was measured using a Hach Turbidimeter which was calibrated regularly (approximately once a fortnight) and had a working range of

0 - 2000 NTU (Normalised Turbidity Units). The turbidity value fluctuated quite markedly so the average of the three highest readings was taken to counter this. All material remaining in suspension had a settling rate of < 0.08 m h^{-1}.

No evidence was found for gibbsite precipitation during the one hour standing period.

2.4.4 STABILITY OF HEMATITE UNDER HIGH CAUSTIC CONDITIONS

Measurements were conducted to determine the natural aggregation state of hematite in very high caustic solutions. In addition, flocculants were added to this system to evaluate the mode of aggregation. Hematite Sample B and pure concentrated caustic solution (16 M) were used in all experiments. The settling rate was measured by timing the mudline in 100 mL Pyrex cylinders at room temperature at varying caustic concentration (10^{-8} - 6 M NaOH) with a stop watch. The flocculants AN995SH and HP1 were used.

2.4.5 FOCUSED BEAM REFLECTANCE MEASUREMENTS

Focused beam reflectance measurements (FBRM) involve a probe in which a laser beam is constantly rotating. This beam is focussed into the slurry and the particles reflect the light. The probe measures a chord length based on the reflected light and this results in an *in situ* determination of chord length distribution (Fawell *et al.*, 1997). The difference between MALLS and FBRM is that FBRM relies on refractive index differences between the solution and the 'particle' of interest. FBRM measures reflected light rather than scattered light and the minimum size detectable is much larger than MALLS. Hematite Sample C in pure caustic and in synthetic Bayer liquors was flocculated using AN995SH at 35 g L^{-1} solids concentration at room temperature to obtain direct information on flocculation (and aggregate rupture). The FBRM probe was a Lasentec® instrument.

2.4.6 CONCENTRATING REFINERY WASTE SOLIDS

The concentration of solids in the refinery thickener feed suspensions was found to be ~60 g L^{-1}. These fine solids were very stable (did not aggregate) in Bayer liquor over the time scale of hours despite the high ionic strength. It was impossible, therefore, to settle the solids and decant the supernatant liquor to create higher solids concentrations. Solids were therefore filtered off and a known quantity of the wet cake reintroduced into the samples to create higher solids concentrations. Filtration may have altered the particle size distributions from that in the refinery stream.

2.4.7 PRECIPITATION OF DESILICATION PRODUCTS (DSPS) ONTO HEMATITE

Hematite Sample A (60 g) was digested at 150 °C in TC = 180 (500 mL) liquor with kaolin (4.5 g) for 30 minutes. During this time the kaolin dissolves and reprecipitates as DSP. The hematite digestion was repeated without kaolin present under the same conditions as a reference. The formation of DSP was verified by SEM, FTIR and XRD.

2.5 FLOCCULANTS IN SYNTHETIC BAYER LIQUORS

2.5.1 FLOCCULANT PREPARATION

2.5.1.1 Stock solutions

Stock solutions were prepared from the powder flocculants by adding deionised water to an accurately weighed flocculant sample (~1.0 g) which had been pre-wetted with 1 g of ethanol. The container was capped and the mixture gently shaken by hand for 1 minute. More water was added and the mixture gently swirled by hand for a further minute. This was repeated until sufficient water was added to produce a 0.5 %w/w solution of flocculant. The stock solution was gently agitated on a shaking table for 3 hours to fully dissolve the polymer then stored in a refrigerator for 3 days prior to use.

2.5.1.2 Dilute solutions

Dilute solutions of the powder flocculants (~0.1 %w/w) were made by adding a known quantity of the stock solution to caustic, synthetic liquor or water depending on the experimental conditions. The dilute solution was equilibrated for an hour prior to use. Flocculant was added on a dry flocculant per gram of hematite basis. Flocculant AN995SH was used for all experiments unless otherwise stated.

Dilute emulsion polymer flocculant solutions (H-199B, 0.13 %w/w) were prepared by adding the flocculant dropwise into spent liquor at 75 °C which was being vigorously mixed using a magnetic stirrer. The solution was mixed for a further 5 minutes to ensure complete dissolution and stored in a thermos flask to maintain temperature prior to use. Flocculant was added on a gram of 'active' flocculant per weight of dry residue solids basis.

2.5.1.3 Activity of flocculants

Because flocculants are ultra long chain organic molecules they are susceptible to entanglement or rupture depending on shear and other conditions during preparation. Uniform preparation of the flocculant solution is not straight forward, thus, it was necessary to monitor the 'activity' of the flocculant and assess whether there was any discrepancy in flocculant performance between different stock solutions.

A dilute flocculant solution was prepared in deionised water and equilibrated overnight. Kaolin (0.5 %w/w) was dispersed, by ultrasonication, in 0.2 M NaCl solution. Flocculant was added to the slurry and thoroughly mixed using end over end inversion (Figure 2.3). This was repeated at several flocculant dosages and a curve of settling rate versus flocculant dosage plotted from the results. Similarly 'active' flocculant solutions result in superimposable settling rate versus dosage curves (see Figure 3.3).

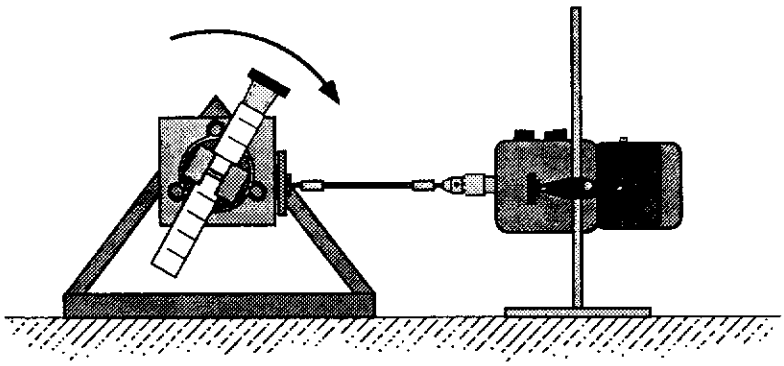

Figure 2.3 Cylinder rotator implemented for flocculant activity test (after Scott *et al.*, 1996).

2.5.2 MEASUREMENT OF FLOCCULANT CONCENTRATION IN SYNTHETIC BAYER LIQUORS - THE HYAMINE METHOD

The method developed for flocculant determination in synthetic liquors was adapted from a turbidimetric technique originally proposed for determining flocculant concentrations in wastewater (Crummett and Hummel, 1963; Michaels and Morelos, 1955). It involves precipitating the flocculant with a cationic surfactant (Hyamine 1622) as a fine colloid, with the turbidity of the suspension being proportional to the concentration of flocculant present. Allison *et al.* (1987) found this technique to be more sensitive for pure polyacrylate than for copolymers of acrylamide and acrylate. This reflects the number of negative charges on the flocculant molecule available to interact with the positive charges of the surfactant.

It was found that the turbidity could be followed both by transmittance at a fixed wavelength or by a nephelometer. The nephelometer had the benefit of a short analysis time, 10 minutes. The method was very sensitive to other contaminants present and solution composition information was required to adequately construct a calibration curve. In wastewater treatment this was found to be difficult.

The increased sensitivity for pure acrylate has been exploited to allow the determination of residual flocculant in well characterised liquors. Investigation of the possible parameters which may affect the flocculant determination method was undertaken and is presented in Section 3.2.

2.5.2.1 Method description

Solutions

Sodium gluconate was dissolved in pre-boiled (to minimise carbonate) deionised water to make a 400 g L^{-1} solution and filtered (0.45 μm filter) prior to use. Hyamine 1622 was dissolved in pre-boiled deionised water to make a 4 g L^{-1} solution and filtered (0.45 μm filter) prior to use.

Determination of adsorbed flocculant

After 1 hour, 30 mL of the supernatant (from a batch settling test) was pipetted into a centrifuge vial containing 10 mL of gluconate solution. Once cooled to room temperature, the sample was centrifuged at 2000 rpm overnight (this was shown not to affect the measured flocculant concentration) to settle any particulates (especially suspended hematite). 20 mL was then pipetted into a turbidity vial containing 5 mL of the Hyamine 1622 stock solution. The vial was inverted once, the turbidity measured after 9, 9.5 and 10 minutes and the values averaged.

The flocculant concentration was determined from the averaged turbidity by reference to a calibration curve, obtained in the same manner but with known amounts of flocculant added to a pure synthetic Bayer liquor sample. The flocculant concentration in solution was determined in μg g^{-1}.

The flocculant adsorption density (i.e. the surface excess, μg m^{-2}) was calculated from the difference between the flocculant concentration before and after contact with the hematite, and the total surface area of the solids (determined prior by BET).

2.6 SPECTROSCOPY

2.6.1 FOURIER TRANSFORM INFRARED (FTIR)

Vibrational spectroscopy (infrared and Raman) involves exciting molecules to higher vibrational energy states. While infrared requires dipole changes during the vibration, Raman requires polarisability changes. The spectrum of a molecule is altered by its symmetry group and so both infrared and Raman can provide valuable information on the conformation of a molecule. Infrared spectra were obtained of the hematite and the

flocculant as well as the flocculated samples so that an assessment of the adsorbed flocculant configuration could be made. All FTIR spectra were obtained on a Bruker IFS 66 instrument using the conditions listed in Table 2.3. Attempts to use Raman were unsuccessful, using both FT or dispersive instrumentation, as the technique was not sensitive enough to enable adsorbed flocculant to be detected.

Table 2.3 FTIR conditions.

	KBr disc	DRIFT
resolution (cm^{-1})	4	4
detector	DTGS*	MCT*
aperture (mm)	12	8
scans	32	256

* DTGS - deuterated triglycine sulphite, MCT - mercury-cadmium-telluride

2.6.1.1 Infrared method

Flocculant adsorption

Diffuse Reflectance Infrared Fourier Transform (DRIFT) is a convenient and widely applied technique for the determination of surface specific information (for example, Lee *et al.*, 1996; Weissenborn, 1993; Gong *et al.*, 1991). The method used was modified from that developed by Weissenborn (1993). Hematite Sample B was considered the most suitable for studying adsorption conformation due to its higher surface area. Samples were prepared at various pHs ranging from 7 to 14, using AN995SH (100 % polyacrylate) as the flocculant.

Particular care was taken to exclude CO_2 from the atmosphere and carbonate from the solutions by contacting the solution with hematite for 24 hours. The supernatant was then decanted (under a nitrogen atmosphere) onto fresh, carbonate free hematite, placed in an airtight container and sonicated. Under a nitrogen atmosphere flocculant was added, the slurry capped and sonicated once more. This was left to equilibrate for a further 24 hours.

Slurry pH was confirmed with a pH meter, except for the pH 14 sample which was titrated. An Orion model SA520 pH meter with an Orion pH electrode, capable of measuring pH to two decimal places and calibrated using certified standards, was used.

Solids were separated by centrifugation (overnight at 2000 rpm), the supernatant then being decanted under nitrogen and the solids dried under vacuum. The samples were not washed to minimise the loss of flocculant from the surface.

Hematite samples without flocculant present were prepared in the same manner.

Spectroscopy

All samples (0.024 ± 0.001 g) were intimately mixed with previously dried KBr (1.176 ± 0.001 g) by gentle grinding so as not to break up particles. To maximise reflectance and minimise spectral distortion, the mineral-KBr mixtures were passed through a 150 μm stainless steel sieve (Childers *et al.*; 1986) and the <150 μm fraction used. This mixture was then used to make either a KBr disc or was placed in the DRIFT sample cup for analysis. The cup of the DRIFT accessory (12 mm diameter and 2 mm depth) was loosely filled (0.30 ± 0.05 g) with the sieved solids and levelled with a spatula. The sample chamber was purged with clean, filtered nitrogen prior to spectra being obtained. Spectra were obtained against a similarly sized KBr background.

Spectra of the adsorbed flocculant were obtained by subtracting the appropriate hematite spectra. Carbon dioxide exclusion was successful for $pH \leq 13$ but not above. The high pH adsorbed flocculant spectra, therefore, also have carbonate subtracted from them. Subtraction was considered acceptable when the 1780 cm^{-1} carbonate peak had been eliminated. The accuracy of band positions in the 1600 - 1300 cm^{-1} region is thus reduced due to the uncertainty in the subtraction of the broad carbonate band found in this region.

Some polymer samples produced 'rubbery' solids on drying which could not be sieved and were used 'as is'. Their DRIFT spectra showed comparable peak positions to their transmission spectra.

2.6.2 X-RAY PHOTOELECTRON SPECTROSCOPY (XPS) METHOD FOR DETERMINING THE MODE OF FLOCCULANT ADSORPTION

X-ray photoelectron spectroscopy (XPS) is one of many Electron Spectroscopy for Chemical Analysis (ESCA) techniques. It involves exposing the sample to X-rays and detecting the energy of radiation emanating from the sample. The adsorption of the X-rays by the sample results in emission of electrons from the inner core of the atom's orbitals. The kinetic energy of the emitted electron is lowered by the energy required to remove it from the atom, known as the binding energy. Since the incident radiation energy is known and the energy of the emitted electron is detected, the binding energy can be calculated directly from the data. In this way all but hydrogen atoms can be distinguished unambiguously. Also, as only the electrons emitted from the top few layers of the sample surface make it to the detector, XPS is a surface analysis technique. The sampling depth depends on the material and can be 30 - 100 Å (Swingle and Riggs, 1975).

2.6.2.1 Method

XPS spectra were obtained on an upgraded VG ESCALAB Mk II (base pressure $<10^{-10}$ mbar) with 5-channeltron electron detection, conventional Mg/Al twin anode source and a monochromated Al source. Only the twin anode source (VG type XR2E2) was required and it was modified with a 0.8 μm thick aluminium foil window. The Mg and Al K_α anodes were run at 300 W (15 kV at 20 mA emission). The analyser is a concentric hemisphere with a 150° spherical sector and a 150 mm mean radius of curvature. Constant analyser pass energies (constant resolution) of 5, 20 and 50 eV were used with the entrance analyser slits and five similar parallel exit slits (type A1) in a rectangular (6 x 15 mm) configuration. The analyser viewed a ~6 mm diameter area of sample. Spectra were collected normal to the specimen's surface with an X-ray incidence angle of 50° off normal. The spectrometer was calibrated using the Ag $3d_{5/2}$ line at a binding energy of 368.29 eV and the Au $4f_{7/2}$ line at 84.00 eV (Anthony and Seah, 1984) with a negligible measured deviation from linearity over this range.

Both wide scan spectra over 1100 eV, at an instrumental resolution of 50 eV pass energy, and narrow scan spectra for the C 1s and O 1s peaks at the higher resolution of

20 eV pass energy were acquired. It is generally impractical to go to pass energies lower than 20 eV although data was acquired down to 5 eV for the AN995SH polymer standard. The presence of sodium caused interference in the spectra; the Na KLL interfered with the C 1s when using Mg K_α radiation and with the O 1s using Al K_α radiation. Thus, it was necessary to examine the C 1s with Al K_α and the O 1s with Mg K_α. This caused some inconvenience as quantitative analysis must take into account both cross-section and incident flux variation in the spectra.

The AN995SH flocculant standard was 'cast' from a sample swollen by MilliQ water and allowed to dry. The hematite samples (with and without flocculant, pH 7) were prepared both by pressing previously dried powders into indium foil to improve electrical conductivity and by drying aqueous slurries in powder stubs to form a thin film. With flocculant on the hematite the films had a tendency to crack on 'curing'. While this method was preferred for preparation, the samples did suffer from time dependent static charge shifts. As the photoelectrons escape from an electrical insulator they leave behind a positively charged surface. This causes the energy levels to be shifted. For the hematite sample the shift was up to several eV over the normal time period for acquisition in some cases. Normally a steady state is reached whereby the sample reaches a maximum charged state, however, for these samples no such steady state was observed.

To overcome the static charging difficulty, the C 1s and O 1s spectra were acquired by accumulating individual 40 second scans, 30 to 60 scans were taken but kept separate for initial processing. The peak shifts were then determined by a non-linear least squares fit, shifted to a common point on the energy scale and then summed.

All samples were maintained at ~150 K during analysis so as to minimise any possible radiation damage from induced thermal effects. Radiation damage would be evident as peak shape changes with time during acquisition.

2.6.2.2 Data analysis

Data analysis was conducted using both VG Eclipse 2 software and custom software for the Fourier transform deconvolution. After charge alignment of the multiplexed spectra the sequence of data analysis involved:

- removal of a Shirley background (Shirley, 1972) over a wide region, including all the higher energy X-ray satellites.
- removal of the X-ray lineshape via fast Fourier transform arithmetic for the O 1s, Na 1s and C 1s components of the flocculant standard spectra (Klauber, 1993). The only smoothing applied in this process is the choice of the frequency cut-off (generally 100).
- background and peak fit. For simplicity this was done separately rather than simultaneously.

For adsorbed flocculant the signal to noise ratio of the raw data was not considered sufficiently good to deconvolute the X-ray source line function, hence the only data treatment for this sample is the subtraction of a limited width Shirley background. On either side of the background limits a binomial smoothing routine has been passed through the data. This effectively 'zeroes' the satellite features. This approach does slightly artificially reduce the intensity of the backbone carbon C 1s but would only have a minor influence on the determined shift. As the X-ray line function (which would have normally been removed) is purely Lorentzian the best approach to the final state peak fit was to use Voigt profiles.

Static charge correction for the flocculant standard was achieved by alignment of the principal C 1s component, representing the backbone $-(CH_2-CH-)_n$, to 285.0 eV (Beamson and Briggs, 1992). All the spectra shown are displayed in terms of count rate (counts per second).

2.7 MOLECULAR MODELLING

There are aspects of adsorption in solution which cannot be readily observed via experiment. One in particular is the surface structure of the hydrated hematite sample prior to adsorption. Using techniques such as FTIR and XPS it is impossible to tell whether adsorption is preferred on a particular face (unless single crystals are used) and hence much valuable information is unobtainable. Molecular modelling was, therefore, a novel aid for interpreting experimental results and probing the surface structure and interactions not accessible via experimental methods.

The simulations reported in this study employ the atomistic potential technique. The method involves deriving accurate potentials which describe the interactions between

the atoms of a system and then use the MARVIN (Gay and Rohl, 1995) code to simulate and minimise surface configurations. The MARVIN program describes a surface using a simulation cell split into two regions; Region I contains the atoms near the surface while Region 2 reproduces the effect of the bulk lattice on these atoms. The structural units (ions, atoms or molecules) in Region I are allowed to relax to a minimum energy configuration while those in Region II remain fixed. The thickness of the bulk region (II) is determined such that the interaction of the lowest bulk atoms with the lowest surface atoms is negligible, while the surface region (I) is sufficiently thick for the surface energy to converge.

2.7.1 POTENTIALS USED TO DESCRIBE HEMATITE

In modelling any system atomistically, reliable potentials which describe it are necessary. The model should include both long range Coulombic interactions and shorter-range van der Waals attractive and Pauli repulsion interactions. The last two are commonly described by a Buckingham potential (Bush *et al.*, 1994);

$$V_{ij}^{short} = A_{ij}\exp\left(\frac{-r_{ij}}{\rho}\right) - c_{ij}r_{ij}^{-6} \qquad \text{(Eqn. 2.1)}$$

where r_{ij} is the distance between atoms i and j and A_{ij}, ρ and c_{ij} are fitted parameters. The shell model of Dick and Overhauser (1958) is introduced to describe the polarisability of the atom. This involves separating the atom into a core (where the entire mass of the atom is centred) and a shell (where the 'valence' electrons are situated). A spring (or harmonic) potential;

$$V_{ij}^{spring} = (1/2)kr_{ij}^2 \qquad \text{(Eqn. 2.2)}$$

is used to keep the core and shell attached to each other.

Additionally, a Morse potential was included to describe the OH bond in the OH^- ion:

$$V_M = D_e\left(\left[1-\exp\left\{-\alpha\left(r_{ij}-r_0\right)\right\}\right]^2 - 1.0\right) \qquad \text{(Eqn. 2.3)}$$

where D_e is the dissociation energy, r_o is the equilibrium bond length and α is the force constant of the bond.

To obtain reliable values for the parameters of the potential functions used to describe chemisorption of water on hematite (Fe_2O_3), the potentials were simultaneously fitted to goethite (α-FeOOH) and lepidocrocite (γ-FeOOH) as well as hematite using relaxed fitting (Gale, 1996).

Wherever possible, existing potentials in the literature (Schröder *et al.*, 1992; Lewis and Catlow, 1985) were used unchanged, reducing the number of parameters in the fit. The inclusion of the iron-oxyhydroxide structures allowed the derivation of iron-hydroxide and oxide-hydroxide potentials, which are vital for an investigation of the hydrated hematite surfaces.

2.7.2 HYDRATING THE HEMATITE SURFACE

For the energy of a surface to be finite the cell must be cleaved such that no dipole exists in the z-direction (Fripiat, 1977). This greatly reduces the number of possible configurations for a surface. To determine the surface structure of several hematite crystal planes in vacuum, the unrelaxed surface and attachment energies were calculated for the three most commonly observed faces in natural hematite specimens (Hartman, 1989). The equilibrium growth model states that of all the possible surface configurations on a given face, the one with the lowest surface energy will be present. The attachment energy model predicts that the one with the lowest absolute attachment energy will be present (Gay and Rohl, 1995). For the three faces studies here, both models yield the same surface configurations.

Once the most stable cut of each face was determined, water molecules were dissociated onto them. This was achieved by attaching an OH ion to a iron atom which was less than fully coordinated. A hydrogen atom was then bonded to a neighbouring surface oxygen to obtain charge neutrality. This was repeated until each surface iron was fully 6 coordinated (100 % coverage). Less than full coordination of iron was also investigated by bridging OH ions between them, but maintaining charge neutrality.

After trialing several different starting positions of the added hydroxide and proton moieties for each minimisation, that with the lowest energy was used to calculate the surface energy (Nygren *et al.*, 1997):

$$E_{surf} = \frac{E_{reg1} - mE_{bulk} + 0.5nE_{corr}}{A} \qquad \text{(Eqn. 2.4)}$$

where E_{surf} is the surface energy, E_{reg1} is the energy of Region I from MARVIN, E_{bulk} is the bulk energy of the unit cell, m is the number of unit cells in Region I, A is the area of the simulation cell, n is the number of hydroxide ions present on the surface and E_{corr} is the correction energy. The correction energy must be included as the surface contains atoms not found in the bulk. Thus, an additional energy component arises due to the energy required to dissociate the water molecule to form the hydroxide on the surface.

The three planes investigated in this study were the {111}, {011} and {210} faces (in rhombohedral coordinates). These planes vary in surface area, so to try and keep them as close to each other as possible and to exclude any edge effects a 2x2, 2x1 and 1x1 simulation cell was used for the {111}, {011} and {210} planes respectively.

2.7.3 ADSORBING THE FLOCCULANT ONTO HYDRATED HEMATITE

The decanoate and decandioate ions were used as models for the flocculant since a flocculant molecule is too large (~20 million g mol^{-1}) to model properly. The charged ions, rather than the acid forms, were chosen since polyacrylate is deprotonated even at pH 7 (Bloys van Treslong and Staverman, 1974) and the dioate was included to investigate the effect of multiple adsorption sites. The potassium decanoate unit cell coordinates were obtained from the Cambridge Crystallographic Database and using the consistent valence augmented forcefield (CVFF aug) from Molecular Simulations Incorporated (MSI), the potentials describing the interactions operating within the decanoate and decandioate structure were used such that the unit cell of the decanoate was reproduced. Additionally, the potentials between the carboxylates and hematite were obtained using the extensible systematic forcefield (ESF) from MSI.

An additional potential required to describe the organic molecules was a four body potential of the form:

$$V = k*(1 + S*\cos\{P*\theta\}) \qquad \text{(Eqn. 2.5)}$$

where k, S and P are constants. This potential maintains the geometry of the organic.

A (9-6) Lennard-Jones potential of the form:

$$V = (A/r^9) - (C/r^6) \quad \text{(Eqn. 2.6)}$$

where A and C are constants, was found to be sufficient (rather than a Buckingham type potential) to describe the organic-hematite interactions.

The potentials were used to adsorb organic on the surface on the most stable hydrated plane, and on a less energetically favourable plane, by removing an hydroxide ion per carboxylate unit. The hydroxide was removed from several different positions and many different starting configurations were trialed to ensure the minimum energy configuration was obtained. For the decandioate, the distance between carboxylate units (~12.6 Å) meant that only the two farthest hydroxides (10.5 Å apart) on the {111} plane could be removed to give a structure which then minimised. This was due to the steric energy of the organic molecule in trying to adsorb in such a strained configuration.

The replacement energy of the organic for hydroxide on this surface was calculated according to Rohl *et al.* (1996):

$$\Delta E_{rep} = (E_{surf+org} + nE_{OH}) - (E_{surf} + E_{org}) \quad \text{(Eqn. 2.7)}$$

where $E_{surf+org}$ and E_{surf} is the energy of the hydrated surface with and without organic respectively from MARVIN, E_{org} is the internal energy of the isolated organic which was calculated using GULP (Gale, 1992-1996), E_{OH} is the energy of the OH ion (equal to 7.0525 eV) and n is the number of hydroxides removed.

2.8 SUMMARY

Settling rate and turbidity methods have been developed to measure the aggregation state of hematite in Bayer conditions. These tests were also used to determine the impact of various parameters on flocculation performance. However, aggregation state measurements do not elucidate whether these changes are due to the mode or amount of flocculant adsorbed.

For the first time a relatively simple technique has been adapted to assess the residual flocculant concentration in synthetic Bayer liquors. Thus, differences in settling characteristics can be correlated to adsorption density. Also, an adsorption isotherm can be constructed which gives information on the monolayer coverage (and subsequently on the adsorbed area occupied by the flocculant).

Specialised surface analytical techniques (FTIR and XPS) were developed to probe the chemical configuration of the flocculant adsorbed on the hematite surface while molecular modelling was used to further reveal aspects which experiments could not.

In combination, these methods enabled an in-depth understanding of the polyacrylate interaction with the hematite surface in synthetic Bayer liquors to be obtained.

3. SAMPLE CHARACTERISATION AND METHOD EVALUATION

This chapter outlines the characterisation of the solids and flocculants used in this study. It also presents the important features and limitations of the methods described in the previous chapter. The properties of refinery materials, which demonstrate the difficulty in working with such real samples, are also presented.

3.1 SAMPLE CHARACTERISATION

3.1.1 HEMATITE SAMPLES

The chemical analysis results obtained for hematite Samples A, B and C are shown in Table 3.1.

SEM images showed Sample A comprised non regular particles with sharp edges which is not unusual for a sample which has been crushed and ground. Hematite samples B and C were fairly uniform spherical particles.

All samples showed hematite as the only crystalline phase in their respective XRD spectrum (JCPDS #33,664). Hematite Sample C (which had a relatively high SiO_2 content) did not show any other XRD patterns other than hematite suggesting the silicon was present as an amorphous compound.

Table 3.1 Physical properties of hematite Samples A, B and C.

	Sample A (Mt Newman)	Sample B (Kanto)	Sample C (Bayer)
Surface area ($m^2 g^{-1}$)	2.64	8.25	14.58
Particle size (μm)			
d_{10}	0.43	0.24	0.18
d_{50}	3.80	0.70	0.38
d_{90}	12.48	9.50	5.79
Chemical composition (wt%)			
Fe_2O_3	98.11	98.80	96.52
TiO_2	0.02	1.45	0.03
SiO_2	0.88	0.08	2.73
Total oxides	99.01	100.23	99.32
XRD pattern	hematite*	hematite*	hematite*

*JCPDS = Joint Committee on Powder Diffraction Standards - Powder Diffraction File

As seen from Table 3.1, the Mt Newman and Kanto samples (Samples A and B) were of a similar purity, but differed in their size distribution and surface area. Sample C had a much higher surface area, finer particle size and contained a significant amount of SiO_2.

The DRIFT and FTIR transmission spectra of Sample C are shown in Figure 3.1 and clearly shows that the DRIFT spectrum is superior, as it allows more features to be observed than the transmission spectrum, which has the sloping baseline often found for hematite (Weissenborn, 1993; Gong *et al.*, 1991).

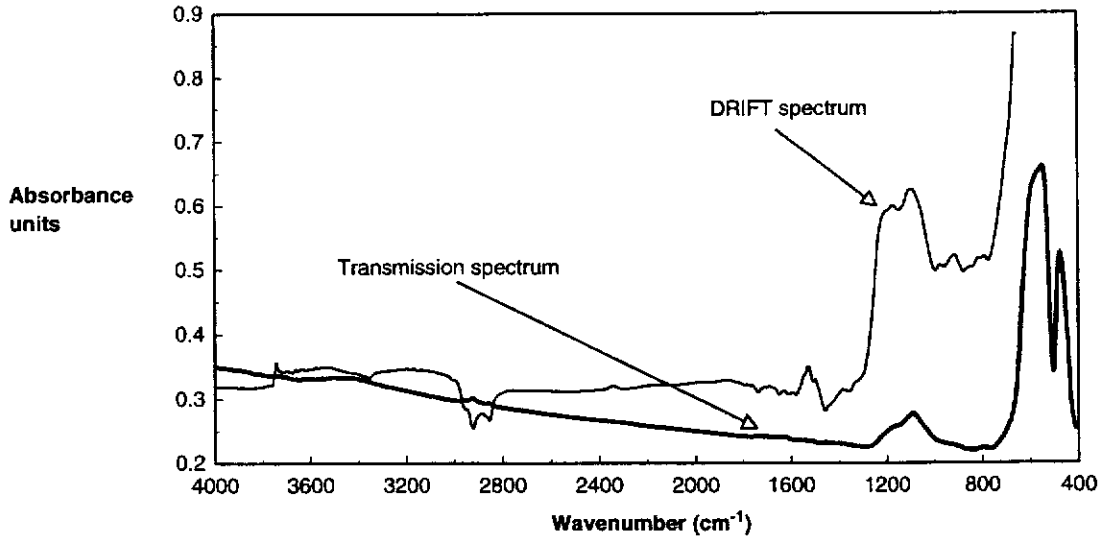

Figure 3.1 KBr transmission and DRIFT spectra of Sample C hematite.

The spectra have broad peaks in the 1000 -1200 cm^{-1} region indicative of Si-O stretching and are similar to those of the pure silicate Opal-A (Drees *et al.*, 1989). However, aluminosilicates also have bands within this region (Wada, 1989). The impurity was considered a surface contaminant due to its variable intensity in the transmission spectra, where it varied from close to 0 to 20 % of the hematite peaks. Elemental analysis (ICP) showed that aluminium could be leached from hematite Sample C but the extent was not consistent from sample to sample (varying between 0 and 3 %). This variation was not due to sampling inconsistency thus suggesting the possible presence of a naturally formed aluminosilicate of variable composition. A distinction between pure silicate and aluminosilicate could not be made for this impurity.

3.1.2 FLOCCULANT CHARACTERISATION

The measured molecular weights and anionic contents of the flocculants used (Section 2.2.2) are given in Table 3.2.

Table 3.2 Molecular weight and anionic content of all polymers used.

flocculant	anionic content (% by number)	molecular weight (g mol^{-1})
AN995SH	100%	$(1.4\pm0.1)\times10^{7}$
AN970SH	61%	$(1.4\pm0.1)\times10^{7}$
AN970BPM	61%	$(1.1\pm0.1)\times10^{7}$
AN970VHM	61%	$(1.8\pm0.2)\times10^{7}$
HP1	100%	$(1.5\pm0.1)\times10^{4}$
AN910SH	12%	$(1.5\pm0.1)\times10^{7}$
H199B	100%	$(1.4\pm0.2)\times10^{7}$

The FTIR transmission spectrum of AN995SH (used to determine the adsorption configuration) is given in Figure 3.2 and shows characteristic polyacrylate peaks at 2930 cm^{-1} (CH stretch), 1550 cm^{-1} (asymmetric COO^- stretch), 1450 cm^{-1} (CH bend) and 1410 cm^{-1} (symmetric COO^- stretch). The 3500 cm^{-1} band is due to associated water, as AN995SH is a 100 % anionic sodium salt.

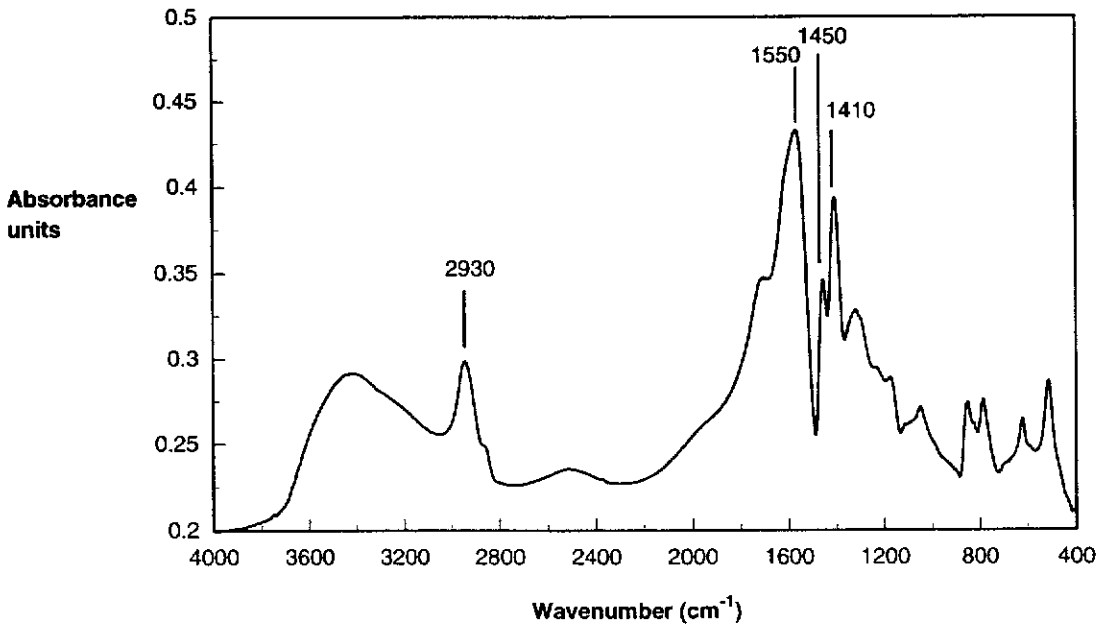

Figure 3.2 FTIR transmission spectrum of AN995SH flocculant.

3.1.2.1 Activity of flocculants

It was found that the preparation procedure for AN995SH flocculant stock solutions (Section 2.5.1) did not result in greatly different activities for different stock solution samples (Figure 3.3). While variations in settling rate were observed these were not significant. The uncertainty in the settling rate measurement accounted for any differences and indicates that the flocculant make-up procedure resulted in consistent flocculant stock solutions. No significant differences in aged samples were observed, obviating the need to use freshly prepared samples. Comparisons between tests could, therefore, be made without the uncertainty of whether the flocculant characteristics were different for different stock solutions.

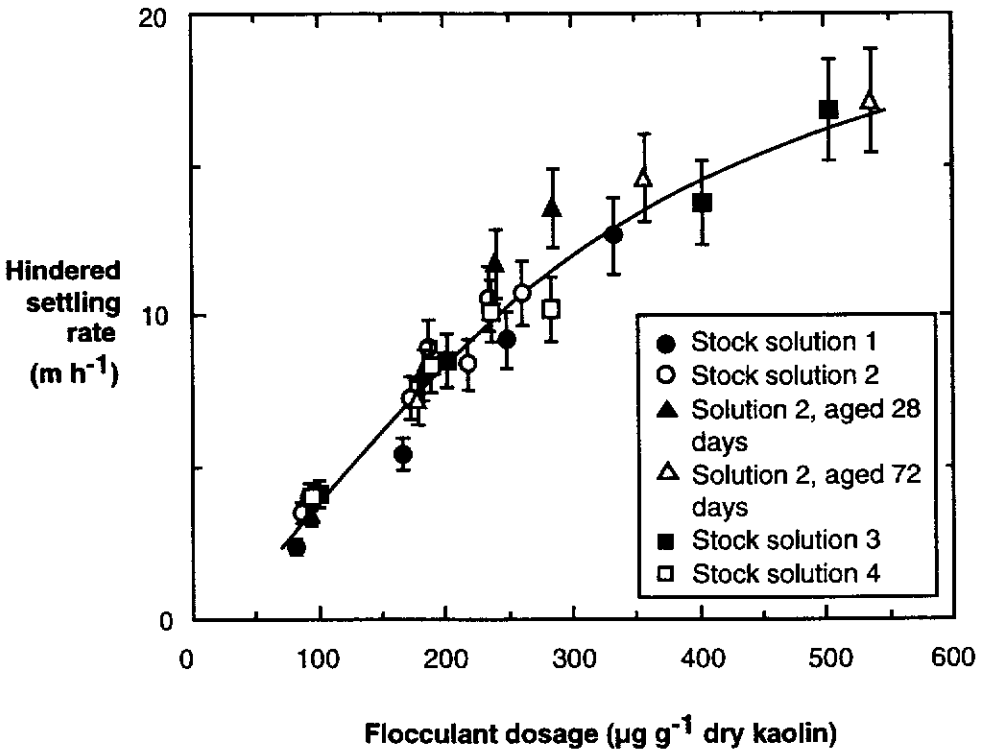

Figure 3.3 The measured settling rate of kaolin versus flocculant dosage added for different flocculant stock solutions and different ages of stock solutions.

3.1.3 REFINERY MATERIALS CHARACTERISATION

Experiments were conducted on refinery samples for comparison with the pure hematite results, therefore, these solids were characterised prior to any evaluation of data. In particular, it was critical to establish whether the different batches of solids investigated were of similar or varying physical and chemical properties.

3.1.3.1 Solids concentration and mineralogy of the thickener feed suspensions

The average solids content of 19 thickener feed samples was 3.8±0.2 %w/w (approximately 58 g L^{-1}), of these 10 were analysed for mineral composition by XRD.

The crystalline phases present were quartz, muscovite, hematite, goethite, boehmite and anatase. Sodium aluminium silicate hydrate was also identified but due to its amorphous nature the small peaks may not have been representative of the actual content. The crystalline phases were compared to quartz (the mineral with the strongest peak intensity) and the results (Figure 3.4) show that muscovite [$KAl_2(Si_3Al)O_{10}(OH)_2$] was the next most abundant mineral while the goethite to hematite peak ratio was always greater than 1. Preferred orientation of some minerals means that the XRD peaks may not be strictly quantitative.

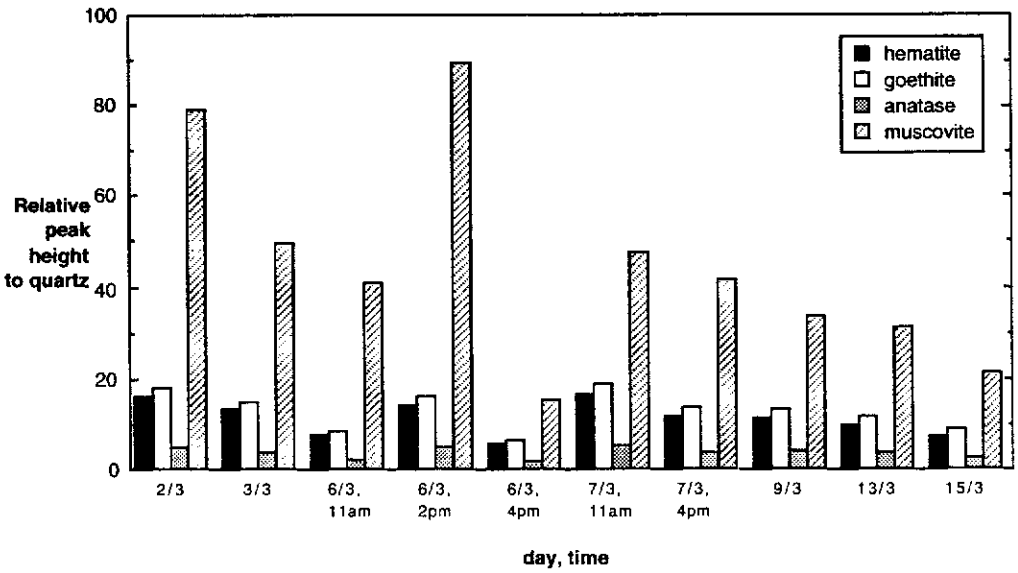

Figure 3.4 Mineralogy as determined from XRD for different batches of refinery sample feed.

The goethite, hematite and anatase content in the thickener feed samples does not vary as significantly as the muscovite between samples. This suggests that perhaps the mineralogy is more stable than implied from this graph and the variation in muscovite is caused by preferred orientation effects. Elemental (ICP) analysis of these samples showed there was 1 - 2 % Al and 0.4 - 1 % Si dissolving into solution. Utilising the XRD and ICP results the *approximate* composition, given the problems associated with XRD quantification, for the dominant minerals was determined for three samples and is given in Table 3.3. As can be seen, the mineralogy was not consistent from batch to batch.

Table 3.3 Approximate composition of Bayer residue from different batches.

Mineral	**Sample 1 (%)**	**Sample 2 (%)**	**Sample 3 (%)**
Quartz	28	35	48
Muscovite	25	18	13
Aluminosilicate	2	3	1
Goethite	17	16	15
Hematite	15	14	12

3.1.3.2 Particle size distribution (PSD) for refinery samples

Analysis of the different refinery feed samples collected over a period of 10 days showed the d_{10} size did not vary significantly (Table 3.4), however, the d_{50} and d_{90} values confirm that the physical properties of the particles within the feed did change with time. Such a variation would be expected to impact on the settling rate of the flocculated suspensions and would need to be taken into consideration when assessing results.

Table 3.4 Particle sizes of different Bayer residue batches.

Sample	d_{10} (μm)	d_{50} (μm)	d_{90} (μm)
1	0.69	10.94	125.8
2	0.83	11.62	121.9
3	0.79	10.07	127.7
4	0.68	7.43	63.4
5	0.81	13.01	168.0

3.1.3.3 Refinery liquor composition

Analysis of 14 liquor samples collected over a 10 day period had an average composition of TC = 201, TA = 241 and A/TC = 0.72 with standard deviations of ≤ 2 %. Other solution species such as TOC, NaCl and Na_2SO_4 were not determined.

3.1.3.4 Correlation of settling with refinery solids characteristics

There was a significant variation in the standard settling rate (see Section 2.4.2) obtained with each batch (Figure 3.5) and attempts were made to correlate this variation with either mineralogy or particle size. Comparison of the settling rate data with the d_{90} values obtained from the PSD results showed a correlation (Figure 3.6) of increasing settling rate with increasing size. Two samples were subsequently wet screened at 75 μm and analysed by XRD. The coarse fraction was dominated by quartz with some muscovite. Minerals such as hematite and goethite were present in trace amounts. The fine fraction showed a similar mineral content to the bulk. A distinction could not be made as to whether the observed correlation was due to the particle size or quartz content.

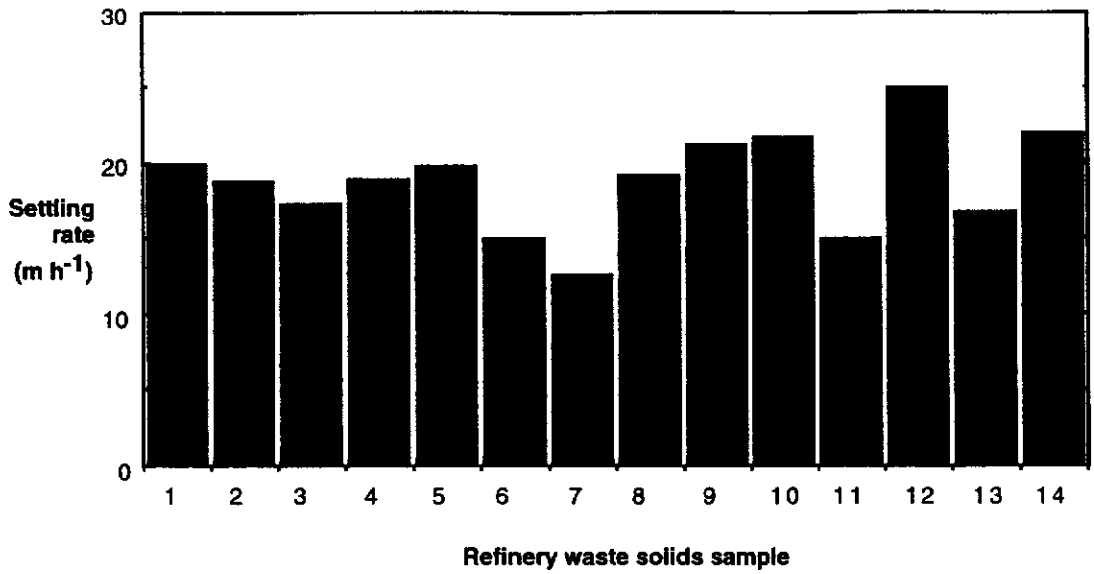

Figure 3.5 Settling rate obtained using standard test conditions for feed samples collected over a period of 10 days.

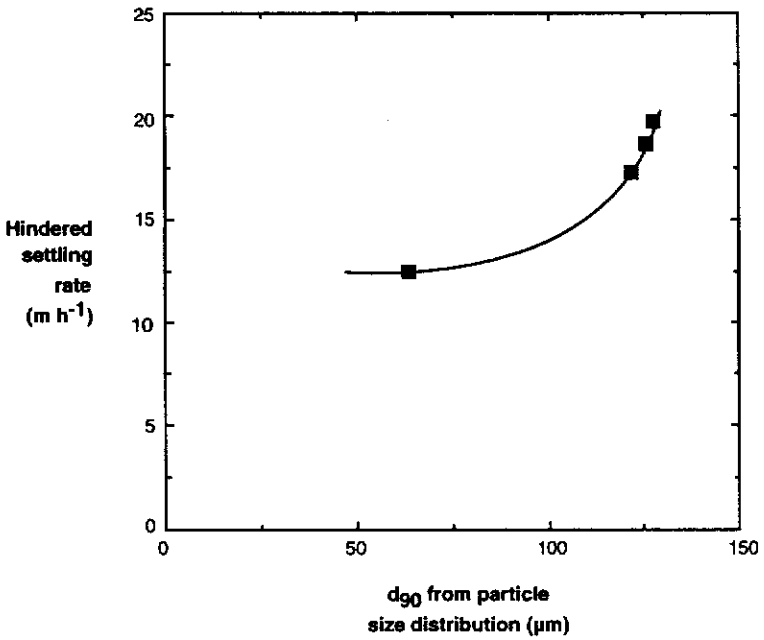

Figure 3.6 Correlation between settling rate observed and d_{90} value obtained from PSD results.

3.2 HYAMINE METHOD FOR DETERMINATION OF FLOCCULANT CONCENTRATION IN SYNTHETIC BAYER LIQUORS

The turbidimetric Hyamine method was developed to measure residual flocculant concentration in liquors and thereby construct an adsorption isotherm. The factors which may affect the accuracy of the flocculant determination were investigated using a synthetic Bayer liquor comprising 1.89 M NaOH, 0.294 M Al_2O_3 and 0.094 M Na_2CO_3, unless otherwise stated.

3.2.1 ADDITION OF GLUCONATE

It was essential to add gluconate to the synthetic liquor solutions to prevent any possible precipitation of aluminium trihydrate during the analysis. The presence of gluconate (80 g L^{-1}) was found to have minimal effect on the measured turbidity (Figure 3.7). The calibration still gave good linearity as a function of the flocculant concentration in the synthetic Bayer liquor. It was concluded that gluconate could be added to prevent aluminium trihydrate precipitation without significant effect on flocculant concentration measurements.

3.2.2 EFFECT OF TIME AND TEMPERATURE

Crummett and Hummel (1963) found that the maximum turbidity (by nephelometry) was recorded after 10 minutes. In this work, each sample recorded a maximum at slightly different times. However, the 10 minute value was very close to the maximum and gave good linearity as a function of the flocculant concentration, it was therefore used in all measurements. No effect with temperature was seen over the range 20 °C to 80 °C.

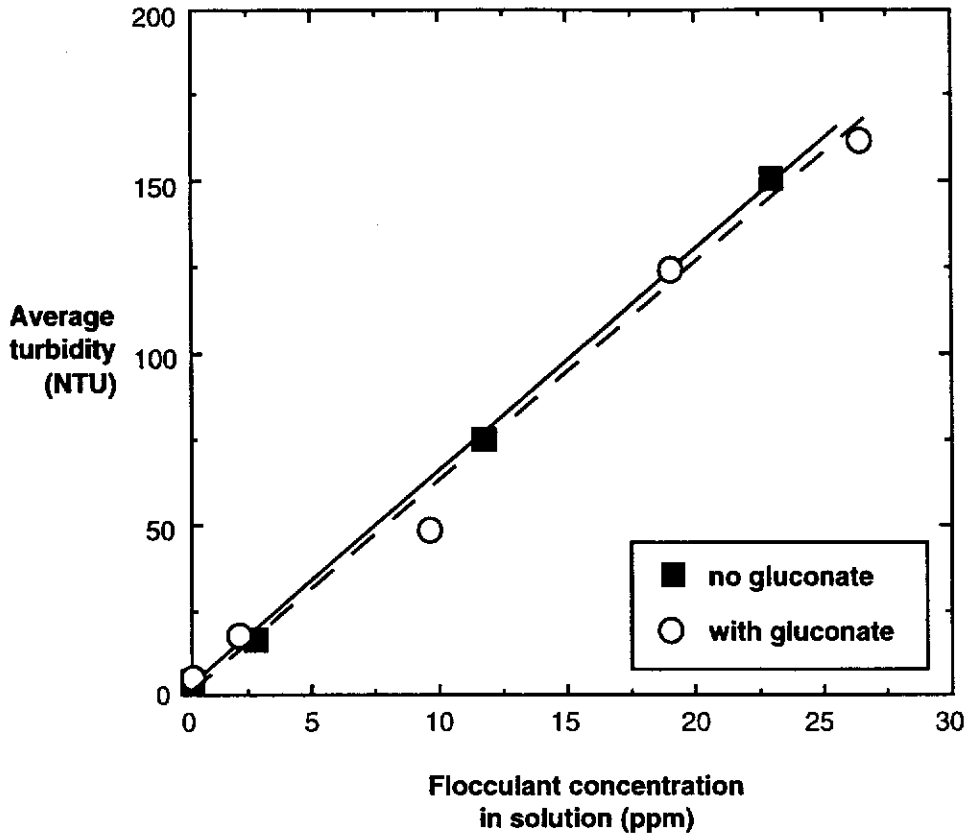

Figure 3.7 Effect of gluconate in synthetic Bayer liquor on the turbidity of the Hyamine-flocculant suspensions.

3.2.3 CAUSTIC STRENGTH

Increasing caustic concentrations up to ~4 M NaOH affected the sensitivity of the turbidimetric technique without altering the linearity, as determined from solutions containing between 1 and 30 $\mu g\ g^{-1}$ flocculant at different caustic strengths (2 to 4 M NaOH). However, above ~6 M NaOH precipitation of the Hyamine occurred with caustic alone and interfered with the flocculant determination. This was overcome by dilution of strong caustic liquors to below ~4 M NaOH prior to analysis. The minimum caustic concentration analysed by this technique was 10^{-7} M (pure water).

3.2.4 DISSOLVED SALTS

Crummett and Hummel (1963) found that there were many interferences which made the technique difficult for waste waters of unknown composition. The major Bayer

inorganic impurities were therefore examined for their effect on the flocculant analysis method.

Carbonate and sulphate were both found to lower the sensitivity of the calibration curve without altering the linearity and must therefore be taken into account. The effect on the recorded turbidity with increasing carbonate concentration is shown in Figure 3.8 for synthetic Bayer liquor solutions containing 25 μg g^{-1} flocculant.

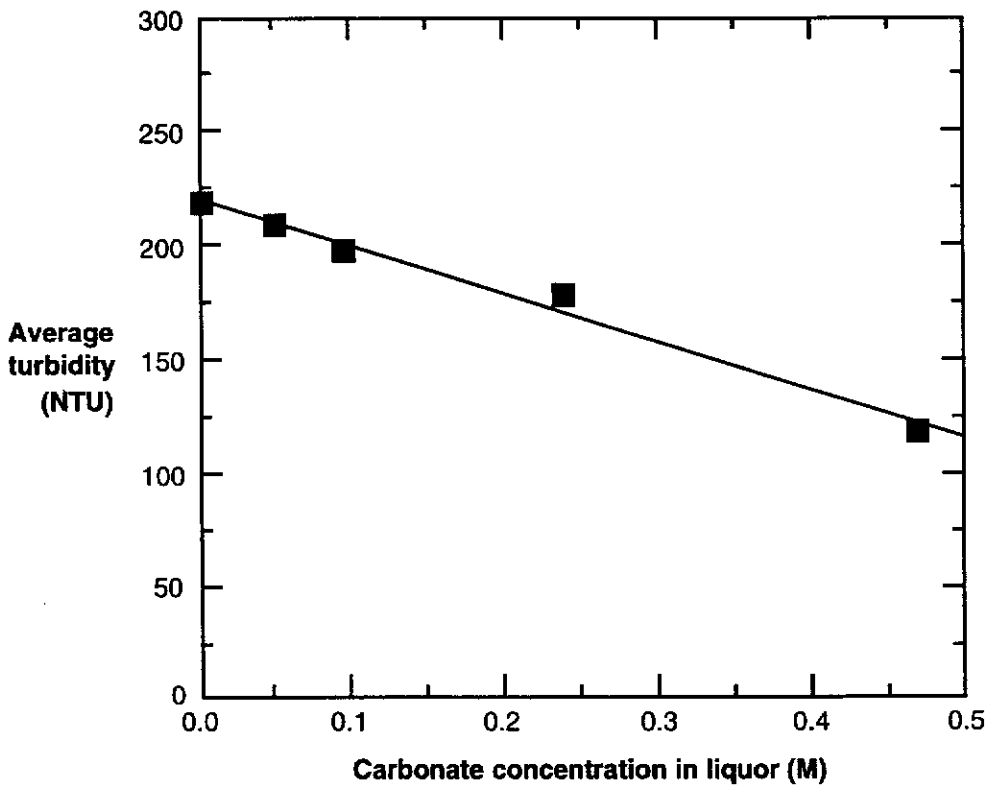

Figure 3.8 Effect of carbonate concentration on the turbidity of Hyamine-flocculant suspensions for synthetic Bayer liquor containing 25 μg g^{-1} flocculant.

The presence of chloride above 0.25 M in the synthetic Bayer liquor caused precipitation of the Hyamine surfactant. Allison *et al.* (1987) found a similar effect in aqueous solutions. However, if the synthetic Bayer liquor was diluted to a chloride level below ~0.125 M prior to analysis, then the effect of chloride was similar to that of carbonate and sulphate and can also be taken into account.

Aluminium concentrations up to ~0.7 M Al_2O_3 were found not to affect the calibration.

3.2.5 FLOCCULANT ACRYLATE CONTENT AND MOLECULAR WEIGHT

A significant loss in sensitivity was observed with a reduction in the acrylate content of the flocculant (Figure 3.9a). The two flocculants used had the same molecular weight (1.4×10^7 g mol^{-1}), but AN995SH was a polyacrylate whereas AN970SH was a copolymer containing 60 % acrylate and 40 % acrylamide. This difference in sensitivity is a consequence of the reduction in the number of acrylate units per unit weight of flocculant which are available to interact with the Hyamine 1622 surfactant.

Flocculant molecular weight appeared to have no effect, as shown by the measurements obtained with three 60% polyacrylate flocculants (AN970SH, BPM and VHM) given in Figure 3.9b. However, the molecular weight range used was quite small (1.1×10^7 to 1.8×10^7 g mol^{-1}) and an effect might be discernible over a wider range.

3.2.6 SENSITIVITY, REPRODUCIBILITY AND ERROR ANALYSIS

As shown in Figure 3.10, the turbidimetric technique gave an excellent linear response between flocculant concentration in the synthetic Bayer liquor and the turbidity of the resultant Hyamine-flocculant precipitate. The technique was very sensitive to flocculant concentration, 0.5 $\mu g\ g^{-1}$ being readily detectable.

The reproducibility of the calibration data was estimated from turbidity measurements resulting from addition of Hyamine to ten aliquots of a synthetic Bayer liquor containing 4.6 $\mu g\ g^{-1}$ flocculant. The uncertainty at the 95 % confidence interval was 4 %. All similar measurements were taken to have this level of uncertainty.

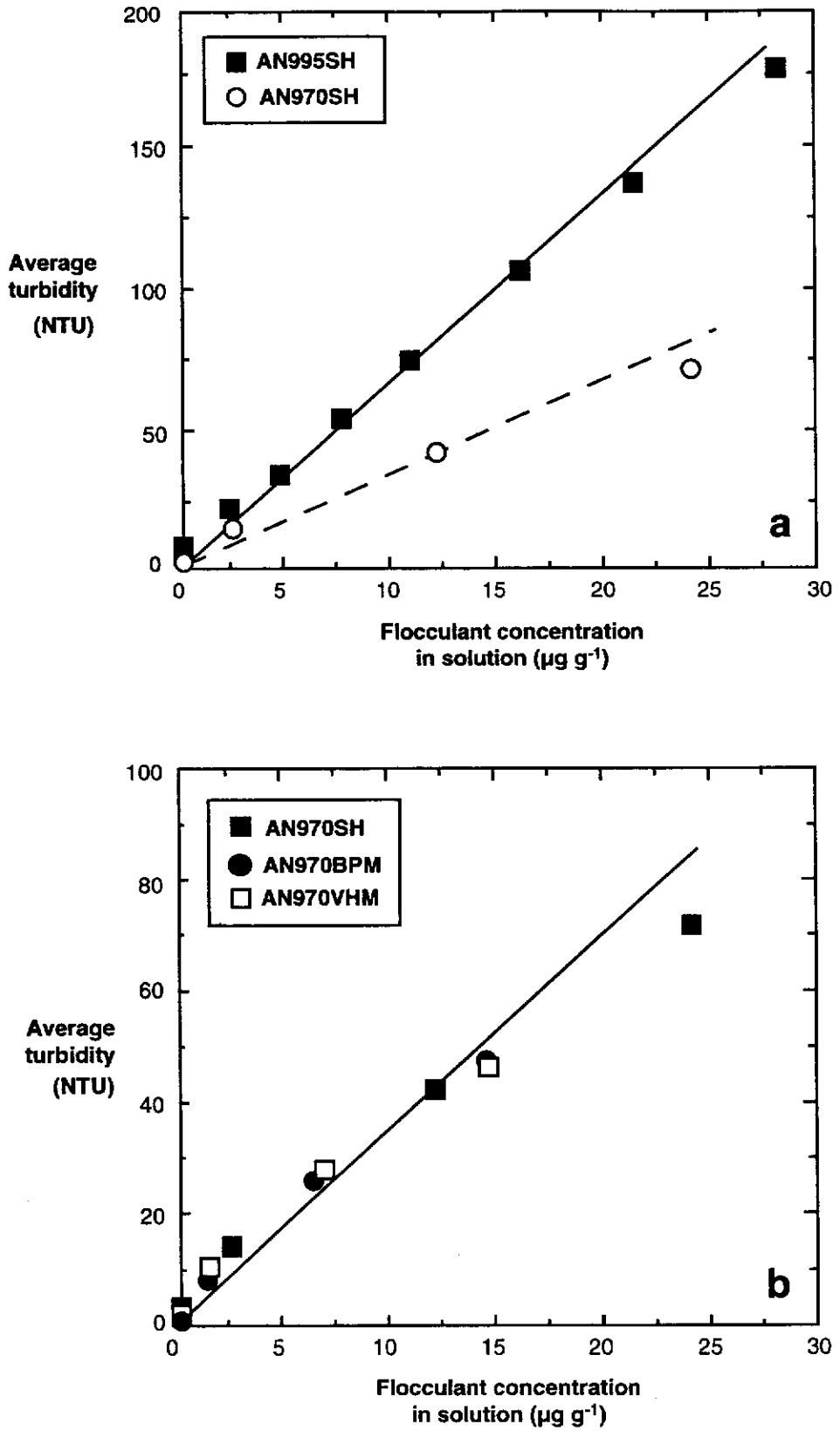

Figure 3.9 Effect of flocculant anionic character (a) AN995SH being 100 % and AN970SH being 60 % polyacrylate, and molecular weight (b) which varies from 1.1 to 1.8 x 10^7 g mol^{-1} on the turbidity of Hyamine-flocculant suspensions for various flocculant concentrations in the synthetic Bayer liquor.

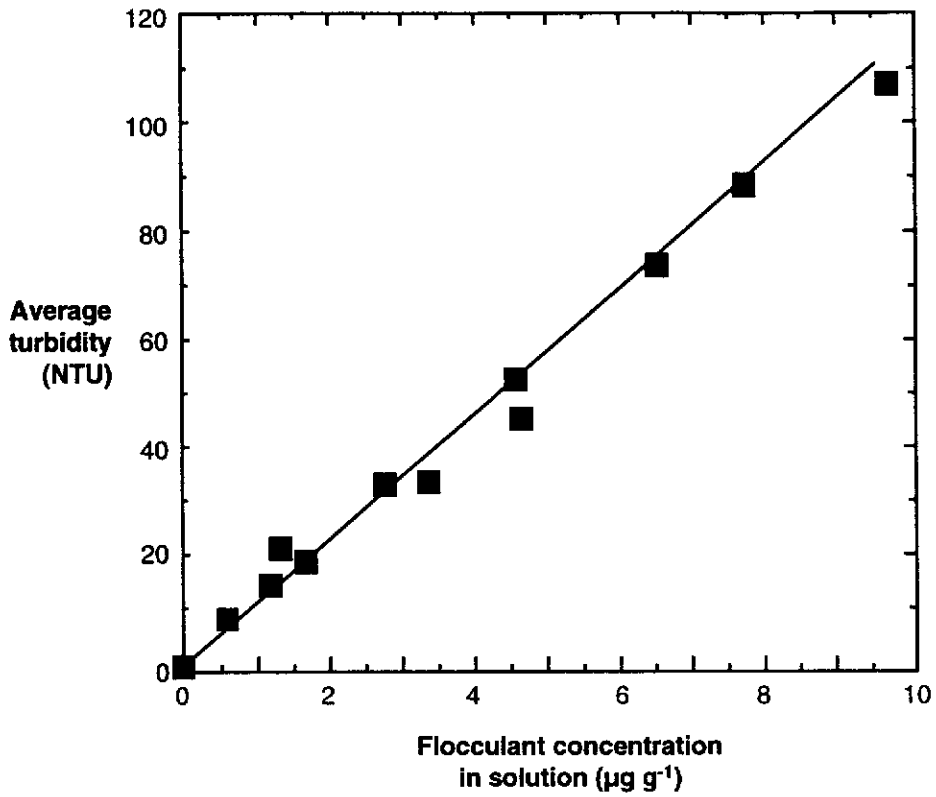

Figure 3.10 Turbidity of Hyamine-flocculant suspensions as a function of flocculant concentration in the synthetic Bayer liquor.

The reproducibility of turbidity measurements made on flocculant solutions after contact with hematite, determined from forty identical adsorption tests, had a 95 % confidence interval of 10 %. This higher spread of values, compared to measurements with flocculant solutions not contacted with hematite, may be due to traces of residual hematite not removed by centrifugation. As it was not possible to determine the extent of this, a 10 % error was assumed for residual flocculant concentrations from adsorption measurements.

3.3 AGGREGATION STATE METHOD

In this work the extent of flocculation was determined by established batch test methods (Song *et al.* , 1992; Bhatty *et al.*, 1982; Michaels and Bolger, 1962), which were first assessed for their reliability.

3.3.1 REPRODUCIBILITY AND ERROR ANALYSIS

The reproducibility of twelve duplicate settling rate tests performed at different times was found to be 20 ± 3 m h^{-1} (Figure 3.11). Analysis of a further 40 duplicate results showed the 95 % confidence interval to be *ca.* 10 % and this value is used for all settling rate data. The reproducibility of turbidity results for the twelve settling tests was found to be 97 ± 33 NTU (Figure 3.11). This was a large error but the 95 % confidence interval for the 40 duplicate results was found to be 10.5 %. It was considered that the turbidity was more variable than 10 % and was conservatively estimated at 15 %. These error values are in agreement with Farrow and Swift (1996) who found up to 10 % error in settling tests and 8 - 20 % in turbidity results.

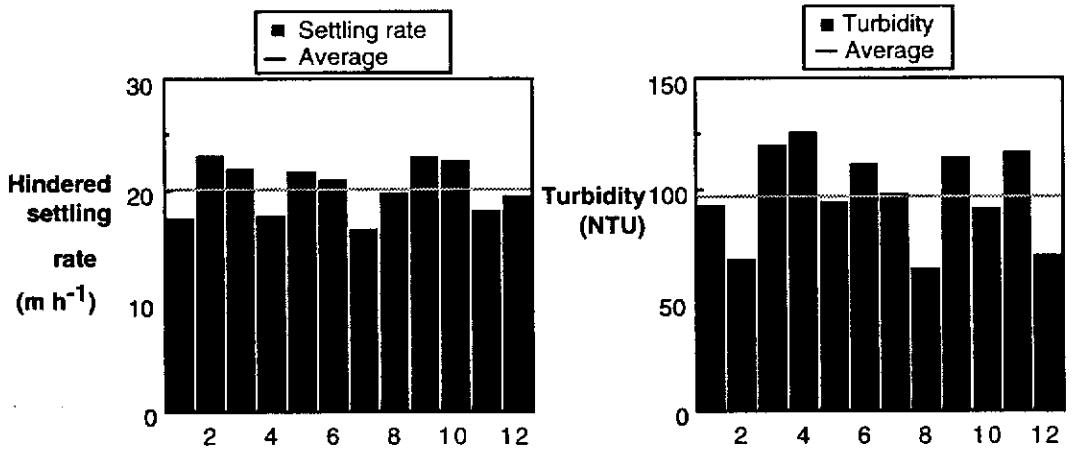

Figure 3.11 Twelve experimental results from equivalent settling tests conducted at different times.

3.3.2 LIMITATIONS OF SETTLING CURVES

The single most important limitation of settling curves is that, alone, they give no information on aggregate structure. Settling is dependent not only on size but also on density (Equation 1.4, page 11); that is, settling curves do not distinguish between small dense aggregates which have the same settling rate as larger, less dense aggregates. Another important consideration is that settling is also morphology dependent, hence, minerals of different morphologies cannot be directly compared.

As mixing conditions influence aggregate size and structure (Farrow and Swift, 1996), reproducible mixing is essential to produce similar aggregates under similar flocculation conditions. The plunger apparatus (Section 2.4.2) has some limitations in

delivering such ideal conditions. The shear conditions induced by the plunger action are not uniform throughout the cylinder and one 250 mL cylinder may not be precisely the same diameter as another, producing shear conditions of a slightly different nature. This accounts for the observation that while most settling rate curves showed good linear settling over a wide range of the distance fallen others fell quickly at the beginning and showed compression earlier under the same conditions. The inclusion of this data has contributed to the uncertainty in the measurements but removed the possibility of subjective bias had they been excluded.

3.3.3 RELATIONSHIP BETWEEN TURBIDITY AND SOLIDS CONTENT

The supernatant liquor turbidity is used as a measure of residual particles which have not settled over the one hour time period. Experiments were conducted to correlate residual solids with observed turbidity.

Figure 3.12 shows that hematite Samples A and C have a good linear correlation between turbidity and solids content for both cold water and caustic solutions. In hot (~80 °C) caustic solutions coagulation is rapid due to the increased kinetics and leads to a negative deviation from linearity at higher solids content. It should also be noted that hematite Sample A, which has a larger d_{50}, has a lower turbidity at the same solids concentration as hematite Sample C, undoubtedly due to the different morphology/particle sizes of the two hematite samples.

Turbidity is determined not only by particle numbers but also by particle size. It is unlikely that the particles which contribute to the turbidity have the same particle size distribution as the bulk flocculated sample. Therefore, with non-homogenous mineral samples it cannot be determined whether a change in the turbidity is due solely to particle number effects. Despite this, it is clear that there is a relationship between increasing solids and increasing turbidity.

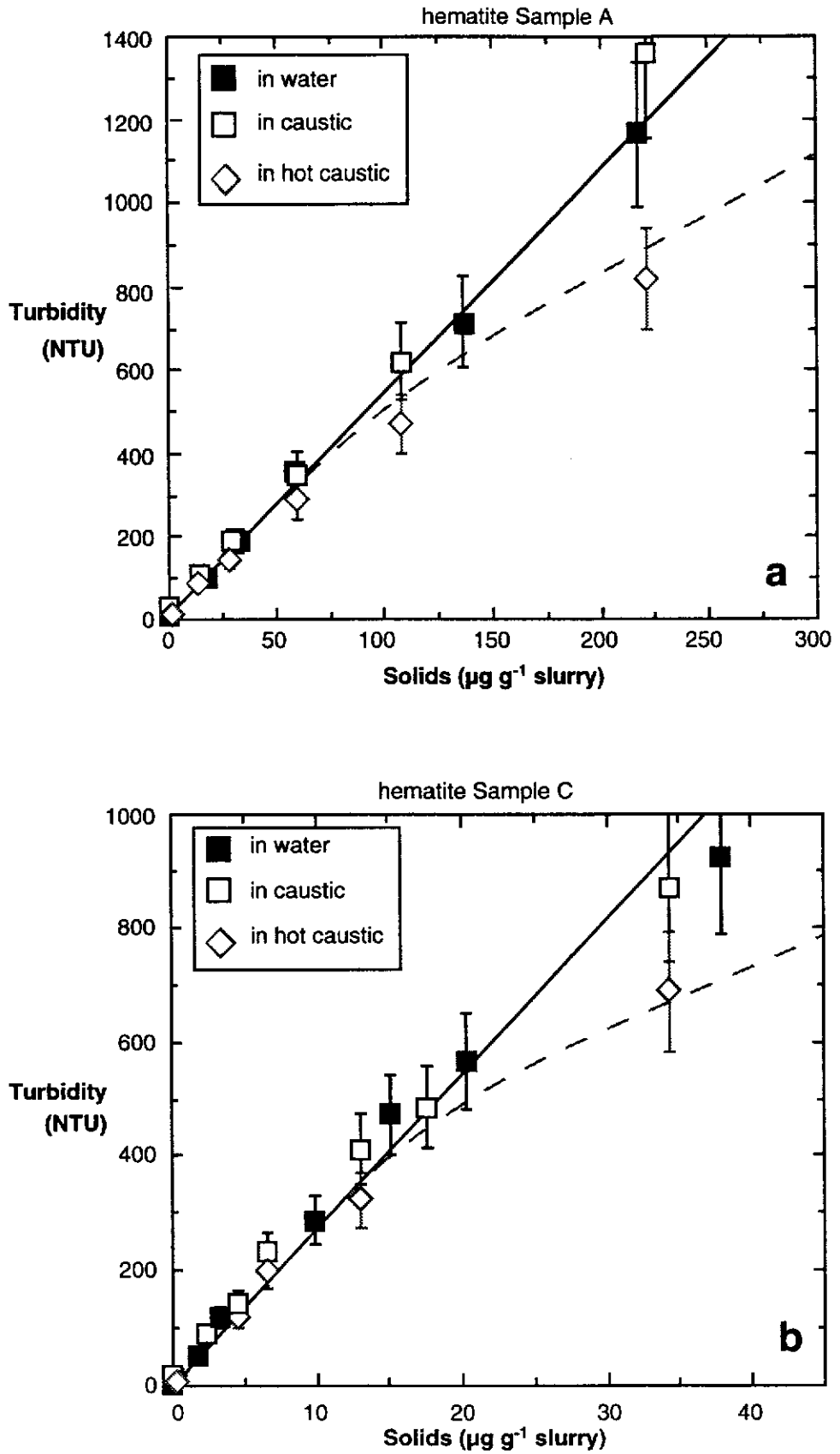

Figure 3.12 Solids present versus turbidity for hematite Sample A (a) and Sample C (b) in water, caustic and hot caustic (~80 °C) solutions (TC = 200).

3.3.4 REFINERY MEASUREMENTS

As discussed in Section 3.1.3, the mineralogy and the particle size of refinery samples was variable from batch to batch. Consequently, settling tests using refinery materials required additional procedures for acquisition and analysis of data. These are outlined below.

3.3.4.1 Autoprecipitation of the liquor

Bayer thickener feed liquors are supersaturated in dissolved aluminium, consequently, after 60 - 90 minutes autoprecipitation occurs. The settling rate was measured at 20 m h^{-1} before the onset of autoprecipitation but was only 12 m h^{-1} after. The difference is believed to be due to a proportion of flocculant adsorbing onto the freshly precipitated aluminium trihydroxide, thereby restricting aggregation of the residue solids.

In an attempt to prevent autoprecipitation, and thereby avoid having to collect fresh feed every 2 hours, the use of sodium gluconate was investigated. Gluconate is well known to stop the precipitation of hydrate (Watts & Utley, 1956). The settling rate was found to change from 20 to 10 m h^{-1} and the turbidity changed from 350 to 678 NTU with addition of 200 g L^{-1} gluconate, showing that its presence altered the settling characteristics and could not be used as an autoprecipitation inhibitor.

Therefore all measurements were conducted using feed solids within 90 minutes of collection from the refinery.

3.3.4.2 Nature of the mudline

Settling tests rely on being able to follow the mudline with time, however, refinery solids did not show a distinct interface between solution and solids, even with the flocculant fully dispersed through the system. To minimise the errors due to this,

settling was timed from the 230 to 90 mL mark of the cylinders and not every 20 mL as was the case for laboratory experiments using pure hematite.

3.3.4.3 Comparison of results

The characteristics of the refinery samples changed from batch to batch due to variation in the nature of the bauxite and the processing conditions. This made comparison between experiments difficult. Added to this was the necessity of using fresh samples to overcome autoprecipitation problems. The comparison of data from different batches of solids was essential, hence, a system of standardisation was established. Settling rates under different conditions were ratioed to a standard test conducted on each batch to give relative information. The standard test was a flocculant dosage of 170 $\mu g\ g^{-1}$ dry solids (using the 24 hours aged flocculant allowed to cool to room temperature).

For most experiments duplicate measurements were averaged and assigned an error bar representing the variation between duplicates. Where a duplicate was not performed a variation of 10 % was assumed (Section 3.3.1).

3.4 INFRARED SPECTROSCOPIC DETERMINATION OF THE ADSORPTION MECHANISM

Fourier Transform Infrared (FTIR) techniques fall into the general categories of reflection and transmission. Information on the bulk is obtained by cold pressing discs with KBr and passing an infrared beam through the sample; this is a transmission spectrum. Attenuated Total Reflection (ATR) and Diffuse Reflectance Infrared Fourier Transform (DRIFT) analyse radiation reflected by the system under investigation and so are more surface sensitive.

ATR involves the infrared beam internally reflecting inside a crystal. The beam interacts with material on the crystal surface via an evanescent wave and the reflected radiation is analysed (Figure 3.13). A detailed description of the use of ATR can be

found in Schrader (1995). For Bayer conditions, a zinc selenide crystal was used as it is alkali resistant.

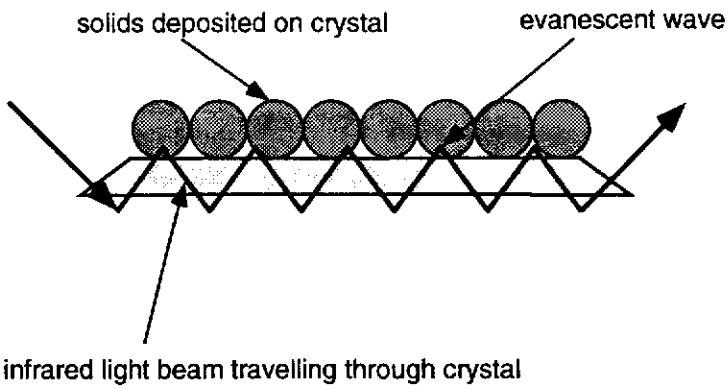

Figure 3.13 Schematic diagram of a horizontal ATR cell.

Horizontal-ATR was extensively evaluated as it allows *in situ* investigations. However, after treating Sample A with flocculant no spectral features which would indicate adsorbed polyacrylate were observed. This was thought to be due to the large particle size which would mean a low surface area in contact with the crystal. Sample B was tried because of its finer particle size (greater surface area) also without success. Finally, the flocculant was replaced with a polyacrylate of much lower molecular weight, ~10,000 g mol^{-1} (HP1). This too did not result in any spectral features indicating adsorbed species, despite the high polyacrylate concentrations used (up to 5000 $\mu g\ g^{-1}$). Horizontal-ATR was thus abandoned as a possible technique for studying adsorbed flocculant on hematite but was still used for solution samples.

DRIFT (as described in Section 2.6.1) involves diluting the sample in KBr and analysing the diffuse (rather than specular) reflected radiation (Figure 3.14). It was found that infrared, in general, is not particularly sensitive to polyacrylate adsorbed on hematite and that monolayer coverage (~2000 $\mu g\ g^{-1}$ added flocculant) was required to obtain a DRIFT spectrum. However, compared to ATR, DRIFT did give spectral features which correlated with flocculant adsorption and was a relatively simple method. DRIFT, however, requires drying of the sample and is, therefore, not an *in situ* technique, as the drying process may subtly and unavoidably change the nature of the adsorbed species.

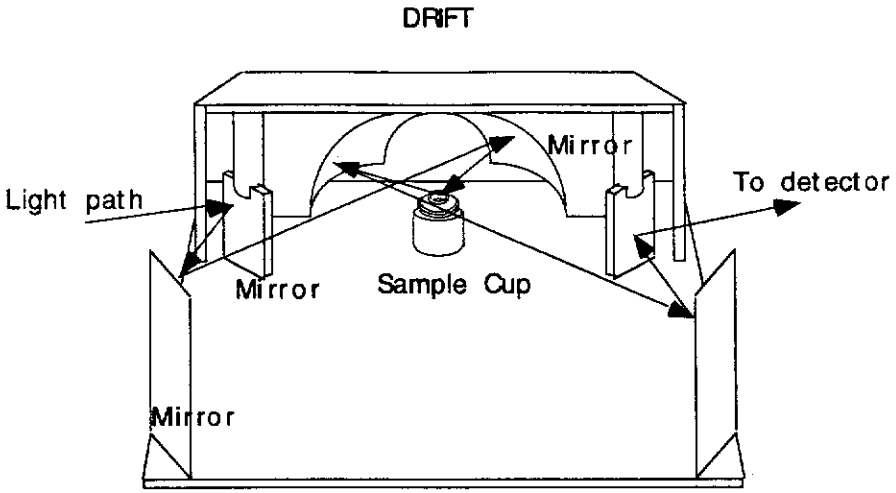

Figure 3.14 Schematic representation of the DRIFT system.

3.5 SUMMARY

Hematite samples and flocculants were fully characterised showing that two samples (A and B) were similar in purity and varied slightly in particle size. Hematite Sample C contained a surface contaminant of silicate or aluminosilicate composition and offered the possibility of investigating the effect of surface impurities on hematite flocculation.

The Hyamine method for residual flocculant determination is a simple and sensitive technique for synthetic liquors (0.5 $\mu g\ g^{-1}$ detection limit). This is an important technique which allowed the adsorption density of the flocculant on hematite to be obtained under Bayer conditions for the first time. Changes in aggregation state determined from settling tests can thus be correlated with changes in adsorption, should they occur. For this technique to be effective the liquor composition must be known as most salt species also interact with the Hyamine.

Settling rate and turbidity results give information on the relative aggregation state of suspensions but such macroscopic techniques cannot give information on the aggregate structures being formed as large, open aggregates may have the same settling as small, dense aggregates.

Infrared results for hematite showed that ATR, while being an *in situ* technique, was not sensitive enough to the adsorbed flocculant and could not be used to determine the

adsorbed configuration. DRIFT is not an *in situ* method and thus may result in subtle and unknown changes to the surface on drying.

Characterisation of the refinery solids showed variability in the mineralogy and physical properties with each batch. Standardisation was thus necessary in order to adequately interpret results.

4. THE FLOCCULATION BEHAVIOUR OF HEMATITE

Hematite Samples A and B were sufficiently pure for use in mechanistic studies. The specific aims were to:

- assess the impact of Bayer process parameters such as supersaturation, and solids concentration on the efficiency of flocculation,
- determine the mode of aggregation,
- determine the adsorption isotherm,
- compare refinery feed slurries and plant flocculant to pure hematite and AN995SH and
- propose a mechanism for polyacrylate adsorption onto hematite.

While it has already been shown that the refinery residue solids were highly variable, their behaviour compared to that of pure hematite should give an indication of the applicability of the hematite data to the Bayer process.

4.1 SENSITIVITY OF FLOCCULATION PERFORMANCE TO PROCESS CONDITIONS

Before conclusions could be reached into the mode of aggregation and the mechanism of adsorption, information was required on whether process variables and other parameters affect the degree of flocculation. The sensitivity of flocculation to flocculant age, solids contact time with caustic, A/TC, solids concentration, and temperature was therefore assessed. All tests were conducted at 93 °C, unless otherwise stated.

4.1.1 FLOCCULANT AGEING

There is no published literature on whether ageing of polyacrylate flocculants in Bayer liquor affects settling performance but there have been a number of investigations on polyacrylamide ageing in aqueous conditions at near neutral pH. Narkis and Rebhun (1966), Shyluk and Stow (1969), Haas and MacDonald (1972) and Chmelir *et. al.* (1980) observed viscosity changes in aqueous polyacrylamide solutions and attributed this change to 'ageing'. Flocculant ageing is often synonymously used to describe flocculant degradation, however, a change in settling performance need not be directly related to the break-up of the flocculant molecule. This is highlighted by the Kulicke and Kniewski (1981) study which attributed ageing to a polymer conformational effect. The only study in Bayer liquors to mention flocculant ageing was that of Chandler (1976) who stated (but presented no evidence) that flocculants are chemically unstable in Bayer liquors.

In this study, ageing refers to any changes in the activity of the flocculant molecule which impacts on its flocculation behaviour. The effect of ageing was determined directly from settling rate and turbidity measurements. Refinery solids and liquors, and H-199B were used as it had already been shown that little ageing occurred for the polyacrylate flocculant (AN995SH) in the activity tests (Section 3.1.2.1). The results are presented as a ratio to the standard test (as given in Section 3.3.4). The liquor had a TC = 201, TA = 241, A/TC = 0.72 and a flocculant dosage of 200 $\mu g\ g^{-1}$ was used.

The results show that the settling rate was changing for 1 - 2 hours after preparation (Figure 4.1). After this time very little effect on settling rate was observed. Notably, the 24 hour flocculant sample which had been allowed to cool to room temperature before use gave the same performance as an equivalent hot sample. It follows that the temperature of the added flocculant solution does not appear to strongly affect performance.

The short period over which settling was affected by the flocculant age does not support a chemical degradation process. Thus, these results do not agree with Chandler's (1976) notion of chemical degradation, at least not on the time scale investigated. The flocculant is not being continually destroyed (which would result in a steady decrease in settling rate) but the conformation could be becoming more coiled leading to a loss in bridging efficiency.

Differences in settling over a 1 to 2 hour period are likely to be caused by conformational changes, as previously suggested for polyacrylamide in aqueous solutions by Kulicke and Kniewski (1981) and for coal flocculation by Henderson and Wheatley (1987).

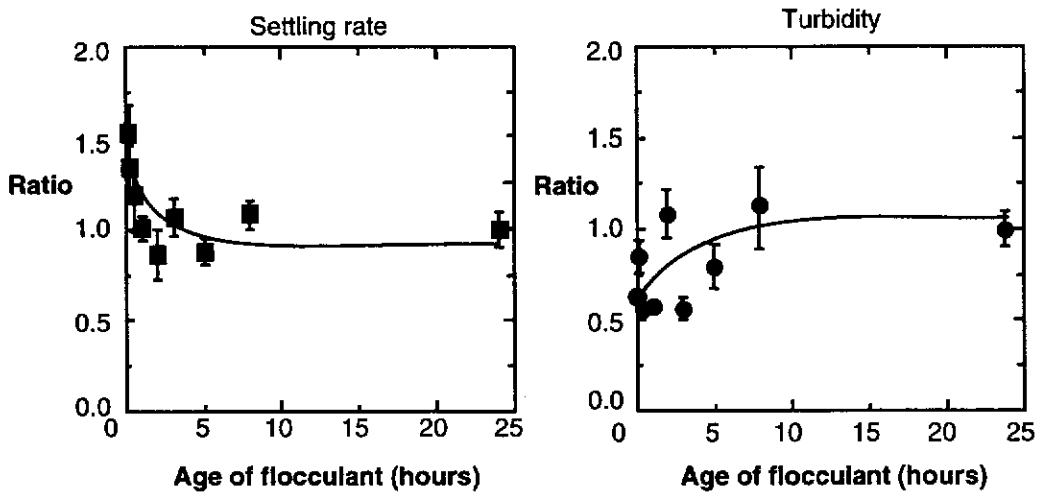

Figure 4.1 Effect of age on flocculation performance of H-199B in refinery Bayer liquors. (Ratio refers to the performance compared to a standard test; see Section 3.3.4)

The refinery flocculant used was an emulsion which can transform from an elongated molecule in the neat phase (100 % polyacrylate in organic phase, no screening) to a coiled structure in Bayer liquor (100 % polyacrylate in high ionic strength Bayer liquors, complete screening). The results presented above are consistent with this view.

Given the hypothesis of a conformational change, turbidity should increase to a steady value, mirroring the settling results. The observed results are less clear, although a similar curve can be fitted to the data, albeit with less confidence. The inhomogeneity of the refinery solids and the greater uncertainty in the turbidity measurements are most likely the major contribution to the increased scatter.

As the polyacrylate was found to be stable after 1 - 2 hours and its temperature was not relevant, all flocculant solutions were allowed to equilibrate for at least one hour prior to use.

4.1.2 CONDITIONING OF HEMATITE SOLIDS WITH CAUSTIC SOLUTION

Flocculation is very sensitive to the surface characteristics of the solids and hence a reproducible surface must be used. Hematite Sample A was crushed and ground in a rod mill and stored as a slurry in deionised water. During the settling test this aqueous slurry is in contact with strong caustic, perhaps altering its flocculation performance.

Figure 4.2 shows the result of ageing the aqueous hematite slurry in TC = 200 caustic solution for different periods and then conducting a settling test at a TC = 100, TA = 110 and A/TC = 0.3 with a flocculant dosage of 15 $\mu g\ g^{-1}$. It was observed that 20 hours were necessary to equilibrate the surface with respect to both settling rate and turbidity. Beyond the 20 hour period only minor changes occur and after 24 hours both settling rate and turbidity are essentially constant.

The results reveal that contact of the hematite slurry with caustic solution leads to surface modification over a ~20 hour period. This is likely to be due to a change in the surface hydration state of hematite between the initial contact with water and the subsequent contact with caustic liquor.

The surface modification mechanism was confirmed by treating an aqueous slurry of hematite Sample A with pure caustic solution such that the pH was raised from 8 to ~11. The slurry was then monitored with a pH meter until equilibration had been reached. Figure 4.3 shows the pH decreases to an equilibrium value after the initial increase on addition of the caustic solution. The slurry appears to reach equilibrium after approximately 3 hours, significantly faster than the ageing effect observed with settling tests.

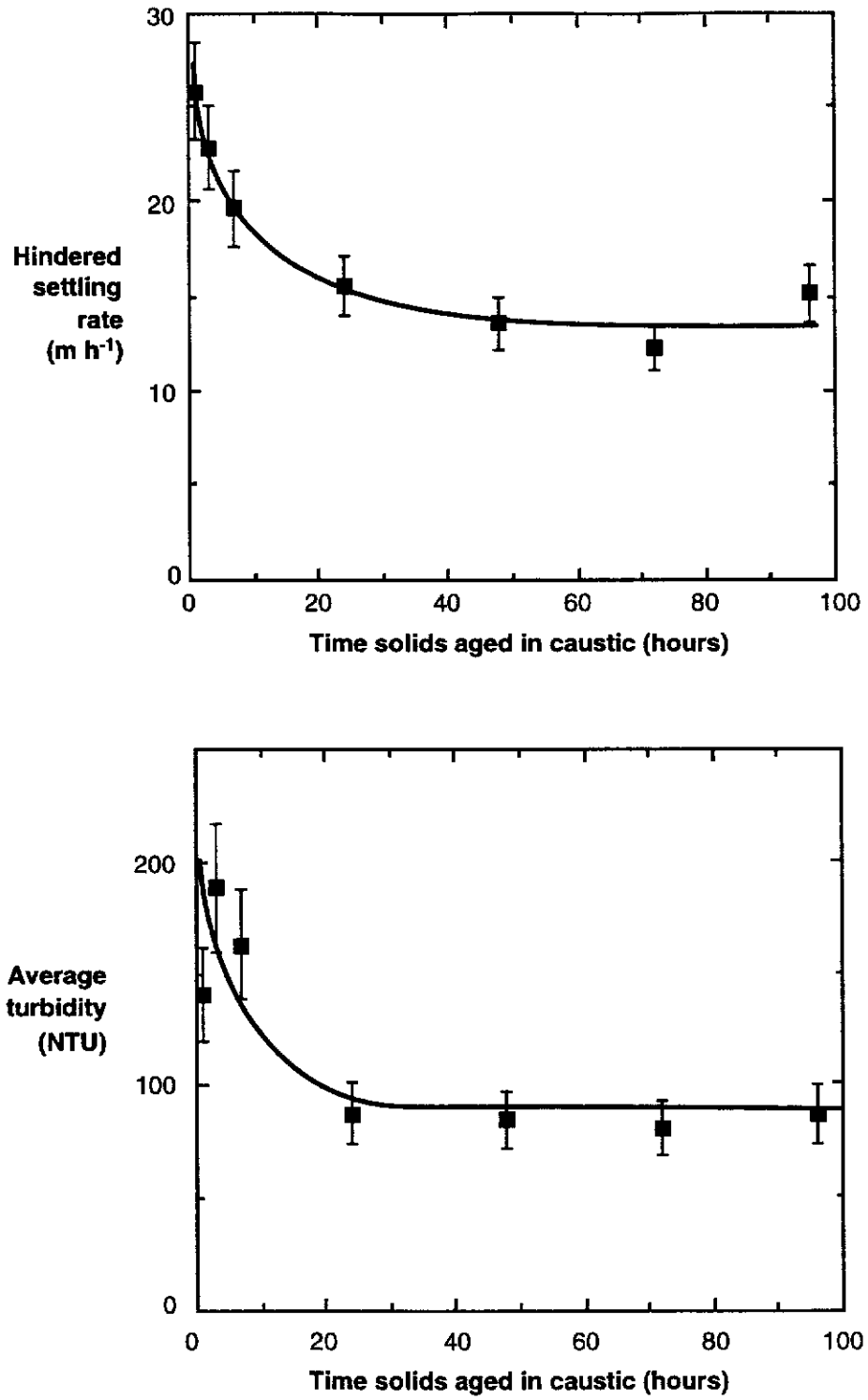

Figure 4.2 The sensitivity of flocculation to conditioning of the hematite with caustic solution.

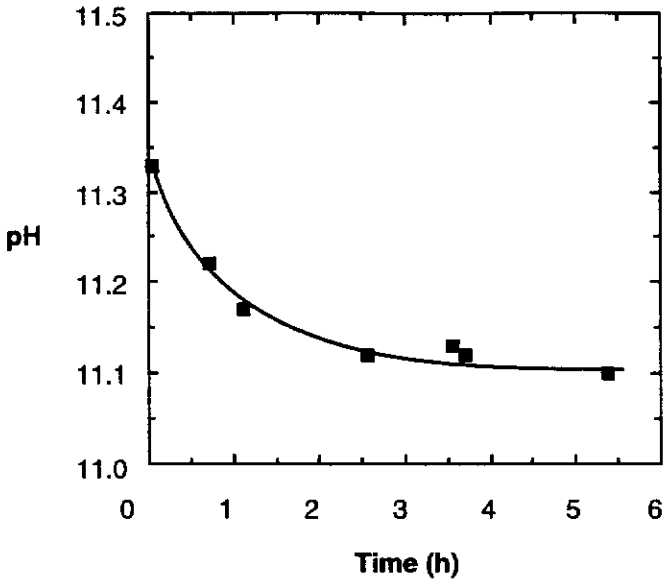

Figure 4.3 Equilibration of the pH of hematite Sample A on addition of pure caustic solution.

The observed removal of OH^- from solution with time is most probably due to surface hydroxides on the hydrated hematite reacting with solution hydroxide to produce water or may be due to the reaction of OH^- directly with Fe to form Fe-OH (Figure 4.4) or both.

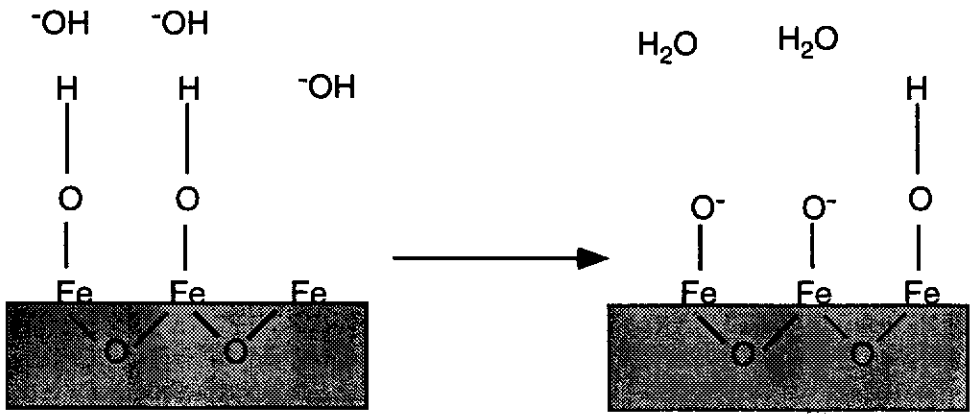

Figure 4.4 Schematic representation of the surface reaction of solution hydroxide ions with hematite surface hydroxides to form water.

The longer equilibration time observed in synthetic liquors could be due to two factors:

- the caustic concentration is much greater and, therefore, more time is required to reach equilibrium or
- the surface modification is still continuing in the above experiment but the changes in pH are too small to be detected.

As equilibration of the surface was achieved after ~20 hours, an ageing period of 24 hours was maintained for all comparative studies.

4.1.3 SUPERSATURATION OF THE LIQUOR

Normal refinery liquors are supersaturated in aluminium (A/TC ~0.7) during the clarification stage. Aluminate ions are, therefore, abundant in solution and may affect settling through either enhanced adsorption on the hematite surface or complexation with the flocculant in solution. The liquors used for these settling tests contained TC = 100, TA = 110 and a flocculant dosage of 15 $\mu g\ g^{-1}$ was used.

The results, for settling rate and turbidity (Figure 4.5), show no discernible trend due to aluminium concentration. That settling rates are not altered by changes in A/TC implies the surface of hematite in Bayer liquors does not interact with aluminate, or if it does it is only weakly interacting (in the compressed double layer).

The lack of an affect with A/TC also suggests that the aluminium is strongly bound to the OH^- ions. If this were not the case, some Al complexation of the polyacrylate would have been expected (McCluskey *et al.*, 1989). This lack of complexation between aluminate ions and simple carboxylates has been confirmed by ^{13}C nuclear magnetic resonance and Raman spectroscopic studies (van Bronswijk, 1997).

The results indicate that the outcomes from settling tests conducted in low A/TC liquors should be applicable to higher A/TC systems. All comparative tests were therefore subsequently conducted in low A/TC liquors which avoided complications due to possible autoprecipitation.

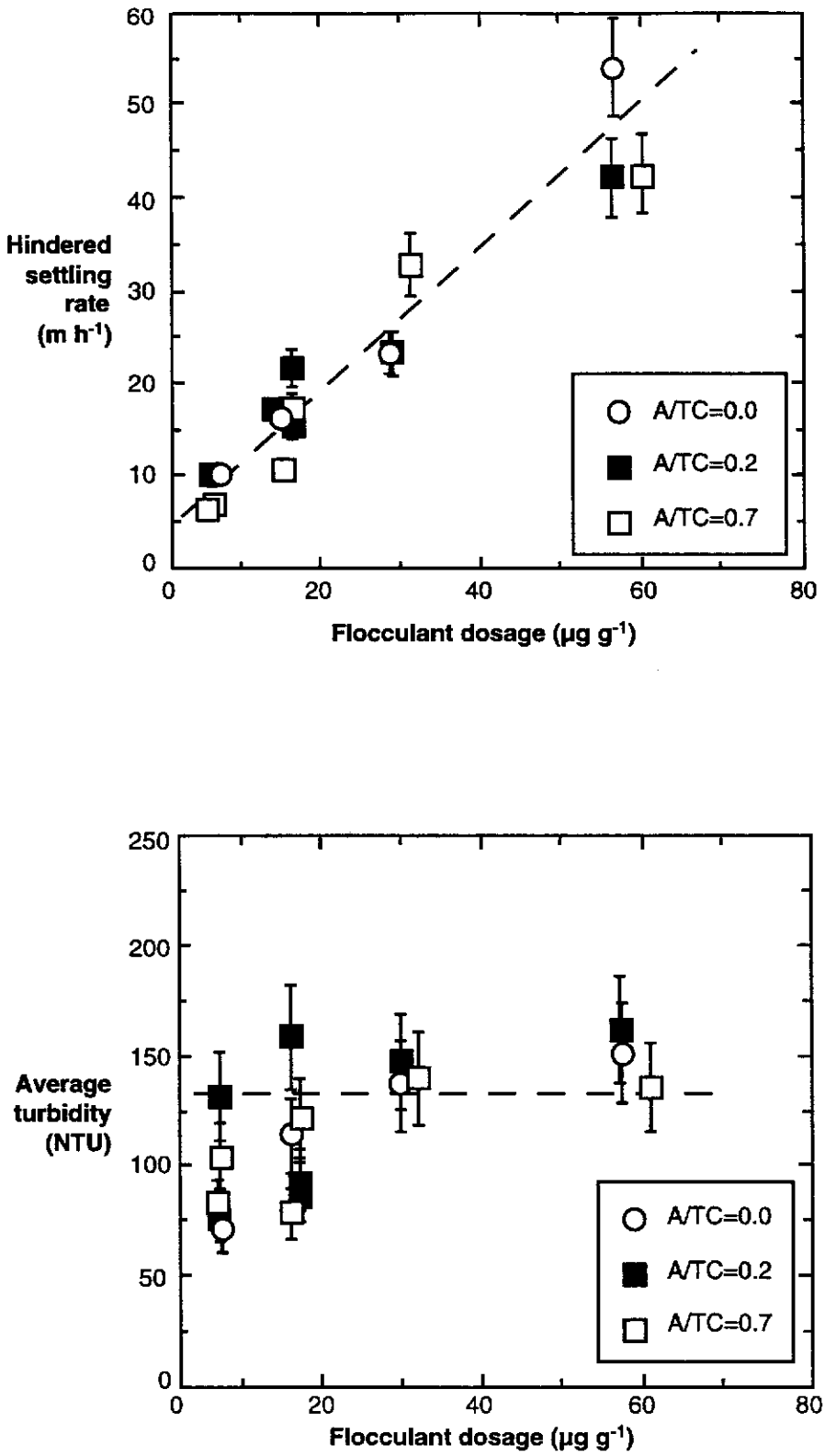

Figure 4.5 The sensitivity of flocculation on the A/TC of the liquor.

4.1.4 EFFECT OF SOLIDS

Much published literature notes that settling in Bayer systems is sensitive to solids concentration (Basu *et al.*, 1986; Parekh and Goldberger, 1976; Farrow *et al.*, 1985; Kontopoulos *et al.*, 1981; Blecic and Adzic, 1990). The effect solids concentration has on flocculation for hematite Sample A was determined using liquors comprising TC = 100, TA = 110, A/TC = 0.3 and a flocculant dosage of 15 $\mu g\ g^{-1}$ was used.

Surprisingly, altering the solids content was found to have no effect on settling rate while turbidity (Figure 4.6) decreased slightly. The turbidity results did not show a linear trend with increasing solids concentration with the values at 120 g L^{-1} falling between those of 60 and 90 g L^{-1}. As solids concentration is increased it would be expected that turbidity should decrease as fine particles are trapped by the sweeping action of the settling solids. However, at higher solids concentration proper dispersion of the flocculant throughout the system becomes more difficult leading to local overdosing and some redispersion of the slurry which is then reflected in the turbidity values. The minimum turbidity values observed at 90 g L^{-1} solids concentration may be due to the balance of these two factors. The observed increasing turbidity with increasing flocculant dosage is also probably a result of more residual fines being present due to local overdosing.

While no correlation was observed between settling rate and solids concentration this could be due to the restricted range of solids concentration investigated. That is, 120 g L^{-1} solids may not be sufficiently concentrated to show an observable hindered settling effect (decreasing settling with increasing solids) given the uncertainty inherent in the values of the settling rate measurements.

4.1.4.1 Refinery solids

Settling experiments conducted with refinery samples were inconclusive as shown by the settling rate ratios in Figure 4.7. The results did not correspond with expected trends from aggregation theory, or with the available literature (Basu *et al.*, 1986; Kontopoulos *et al.*, 1981; Leontaridis and Marinos-Kouris, 1992; Parekh and Goldberger, 1976; Blecic and Adzic, 1990).

The most likely explanation is that the samples were not similar in either mineralogy (caused by process variables) or in particle size distributions (caused during the introduction of the extra solids). This highlights the inherent problems of using refinery samples for flocculation studies.

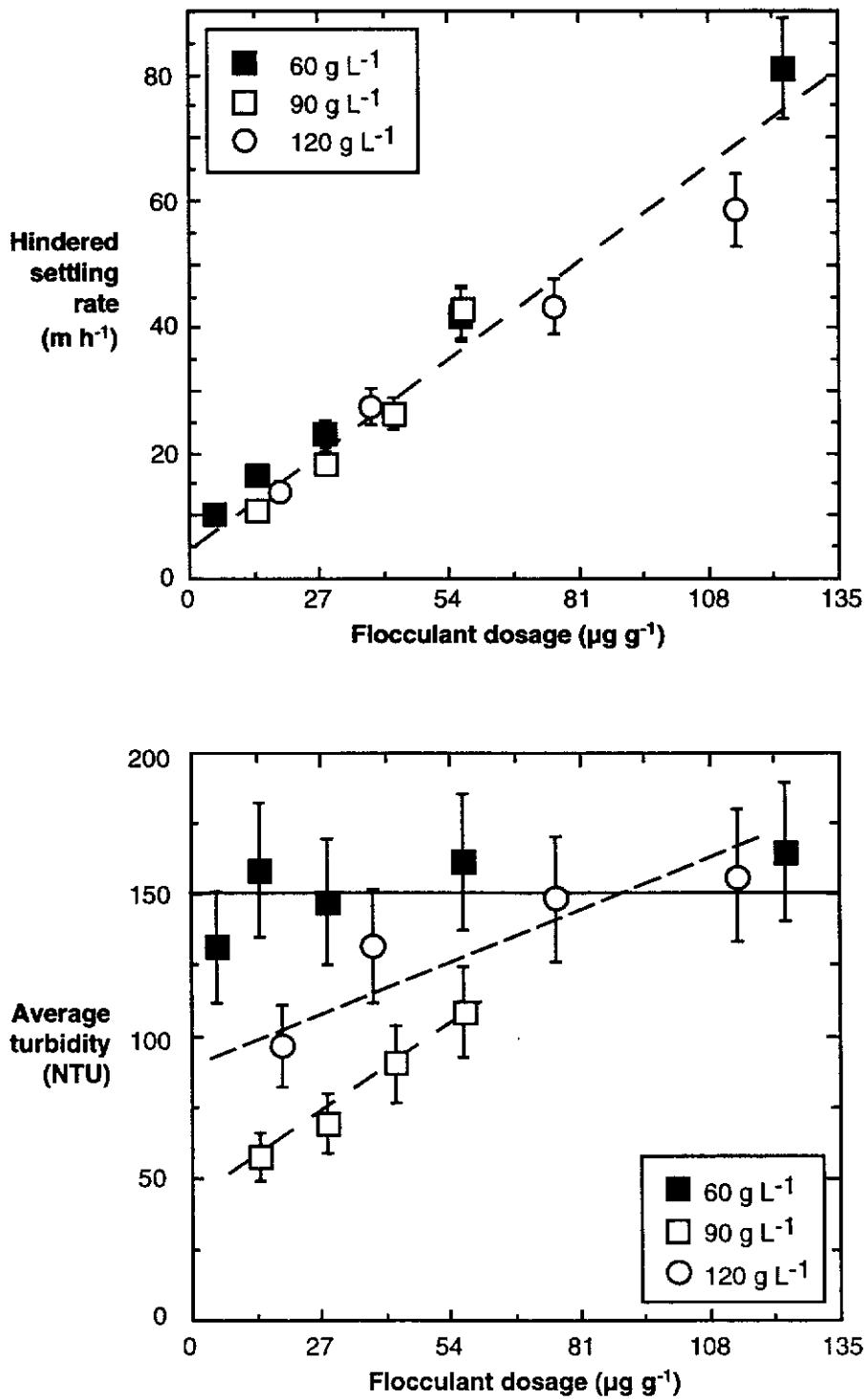

Figure 4.6 The sensitivity of flocculation to the solids concentration of the hematite slurry in synthetic Bayer liquors.

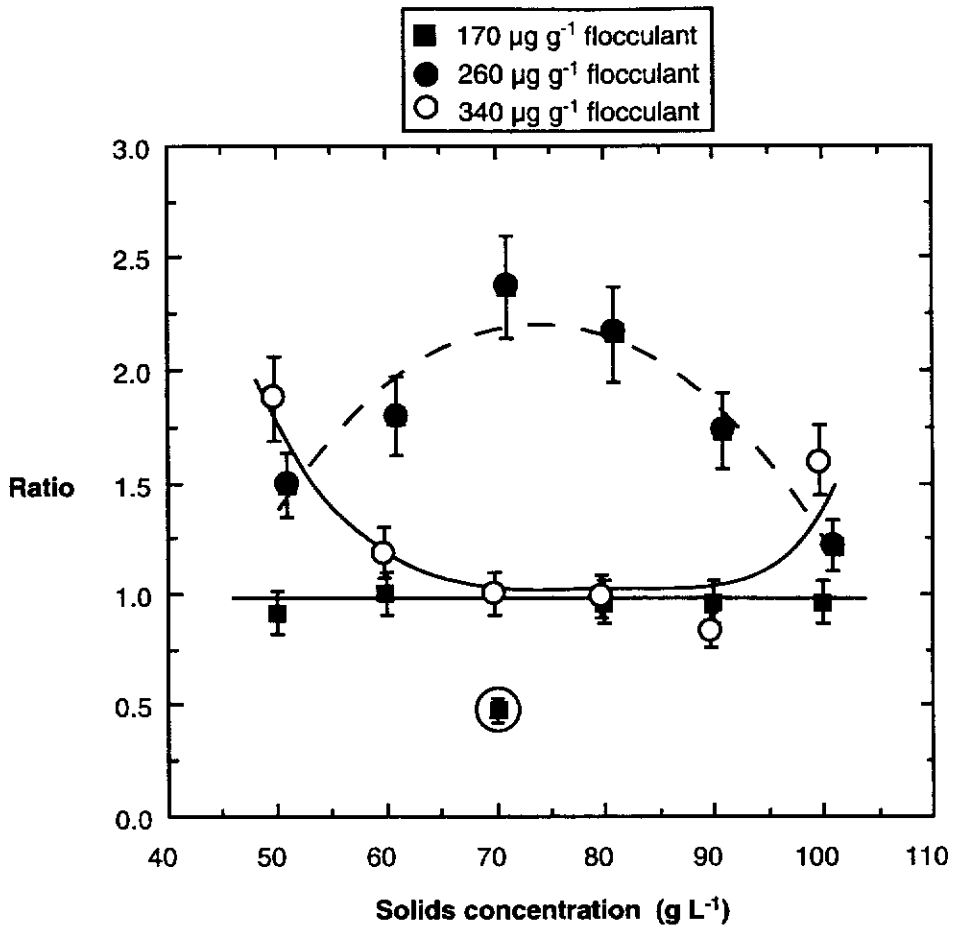

Figure 4.7 Settling rate ratio of refinery solids measured at different solids concentrations. (Ratio refers to performance compared to a standard test, see Section 3.3.4)

4.1.5 TEMPERATURE

Flocculation is thought to be sensitive to the kinetics of several processes such as adsorption of flocculant onto the particle, reconformation of the adsorbed flocculant, particle collisions, etc.. Temperature can also affect the thermodynamics of adsorption; if the adsorption of the flocculant on hematite were an endothermic process, increases in temperature should increase the quantity of flocculant adsorbed. The effect of temperature on aggregation and adsorption density of the flocculant was evaluated using liquors with a TC = 100, TA = 110 and A/TC = 0.3 at a flocculant dosage of 15 µg g^{-1}.

It can be seen in Figure 4.8 that the settling rate increases, while there is a corresponding decrease in turbidity with increasing temperature. An assessment was made as to whether this was a viscosity effect by determining the expected settling rates from the 25 °C experimental data point and the synthetic liquor viscosity values

derived from Ikkatai and Okada (1963). As the increased viscosity (with decreasing temperature) will slow the rate of particle settling, the effect of viscosity on turbidity was assessed by allowing the 25 °C experiment to stand proportionally longer according to the difference in viscosity compared to the 93 °C sample (3.5 hours).

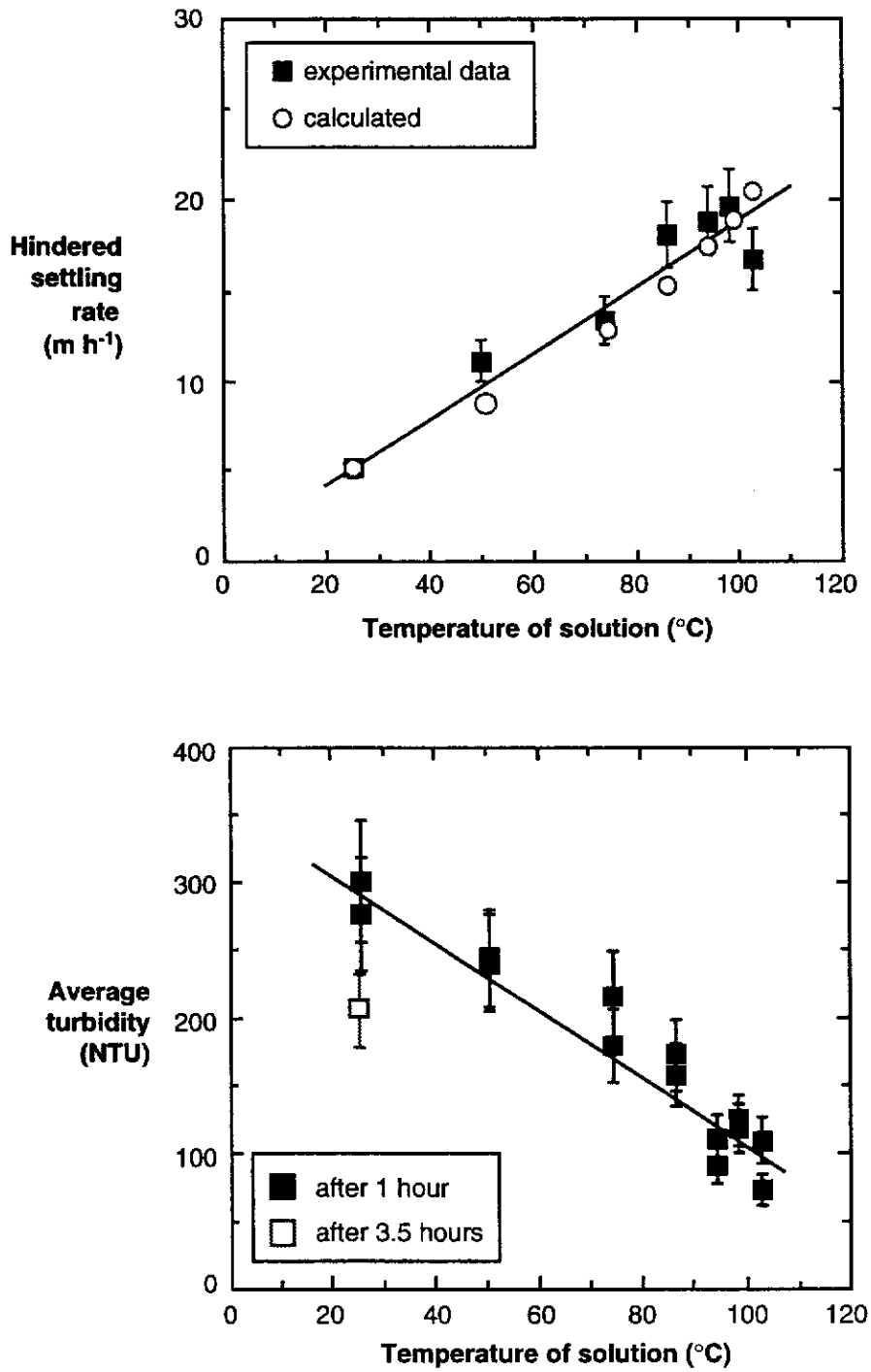

Figure 4.8 The sensitivity of flocculation to the temperature at which flocculation is performed.

It can be seen that settling rate is well predicted by the changes in liquor viscosity while the turbidity did not reduce to the extent expected. The calculated settling rate values account for the observed changes with temperature and suggest that, on the whole, the effect on flocculation performance is determined by the viscosity. The observation that the turbidity decreased by only 50 % of the expected change (200 NTU) with an extended standing time may be due to the particle size distribution of the residual solids. Also, the longer standing time to account for the increased viscosity was based on Stokes' settling which may only be an approximation. Most importantly, settling rate and turbidity show consistent behaviour (that is, increasing settling rate corresponds to decreasing turbidity) and both show a linear trend.

The adsorption of flocculant (Figure 4.9) was not affected significantly by changes in temperature, clear evidence that the improved settling and turbidity is not due to more flocculant being adsorbed. It can be concluded that flocculation is not an endothermic process and that flocculation performance is predominantly being altered by the viscosity of the system.

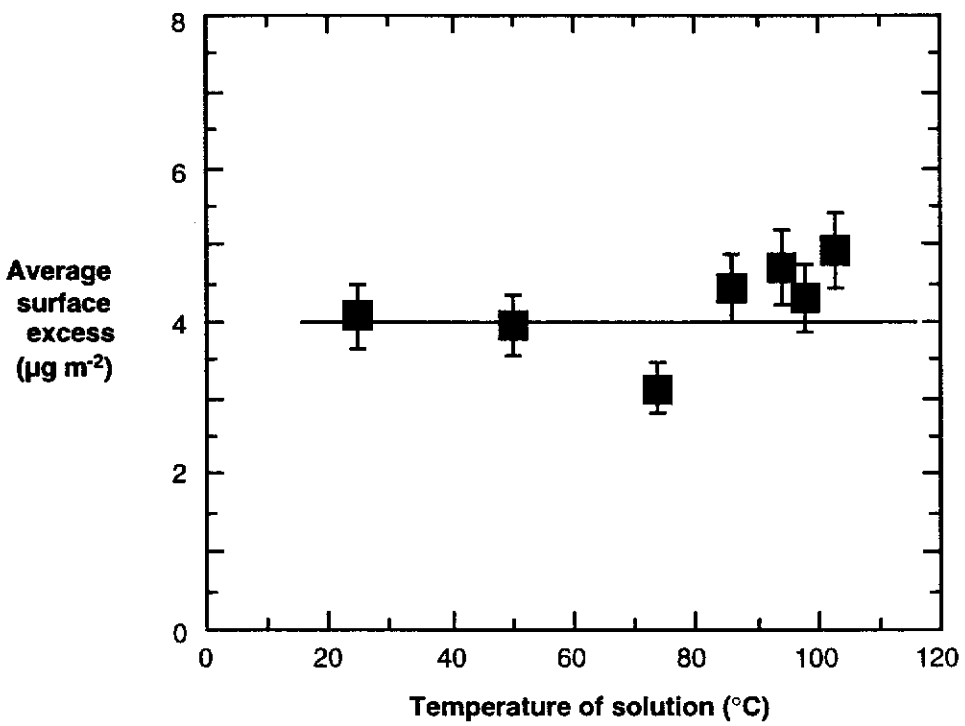

Figure 4.9 Effect of temperature on the adsorption of polyacrylate on hematite in synthetic Bayer liquor.

4.1.6 SUMMARY

Assessment of the effect of Bayer process parameters on flocculation performance established that:

- the surface of the hematite alters on contact with concentrated caustic solution. This is most likely due to solution hydroxide reacting with the surface. The surface formed in this process interacts less with the flocculant.
- aluminate ions do not interact with the hematite surface, nor do they affect flocculation performance in any way.
- solids concentration did not significantly impact on the aggregation state produced. This surprising outcome may only hold for the limited concentration range studied.
- increasing temperature improves settling but this is fully explained by the reduced liquor viscosity as temperature increases. The adsorption density of the flocculant did not alter with changes in temperature suggesting that flocculation is dominated by the kinetics of the system and that adsorption is not endothermic.

4.2 MECHANISM OF HEMATITE AGGREGATION

The natural aggregation state of hematite was assessed in a pure caustic system and the mechanism of flocculation determined based on the impact of flocculants with different molecular weights.

4.2.1 STABILITY OF HEMATITE SUSPENSIONS IN CAUSTIC LIQUOR

The stability of hematite suspensions, in the absence of flocculant, was examined as a function of the caustic concentration based upon room temperature measurements of the hindered settling rate. Hematite Sample B was used in these tests since it produced a more defined mudline than hematite Sample A.

Figure 4.10 shows that in the absence of flocculant, the hematite had a maximum hindered settling rate at ~pH 7.5 (i.e. $[OH^-]$ of $\sim 3\times10^{-7}$ M). This indicated that the hematite was coagulated (i.e. van der Waals attractive forces dominate over any electrostatic repulsive forces and hence the particles aggregate) achieving a maximum

hindered settling rate at pH 7.5. This is in agreement with the point of zero charge (pzc) for hematite of ~7.7 as reported by Ben-Taleb *et al.* (1994) and is indicative of a clean surface.

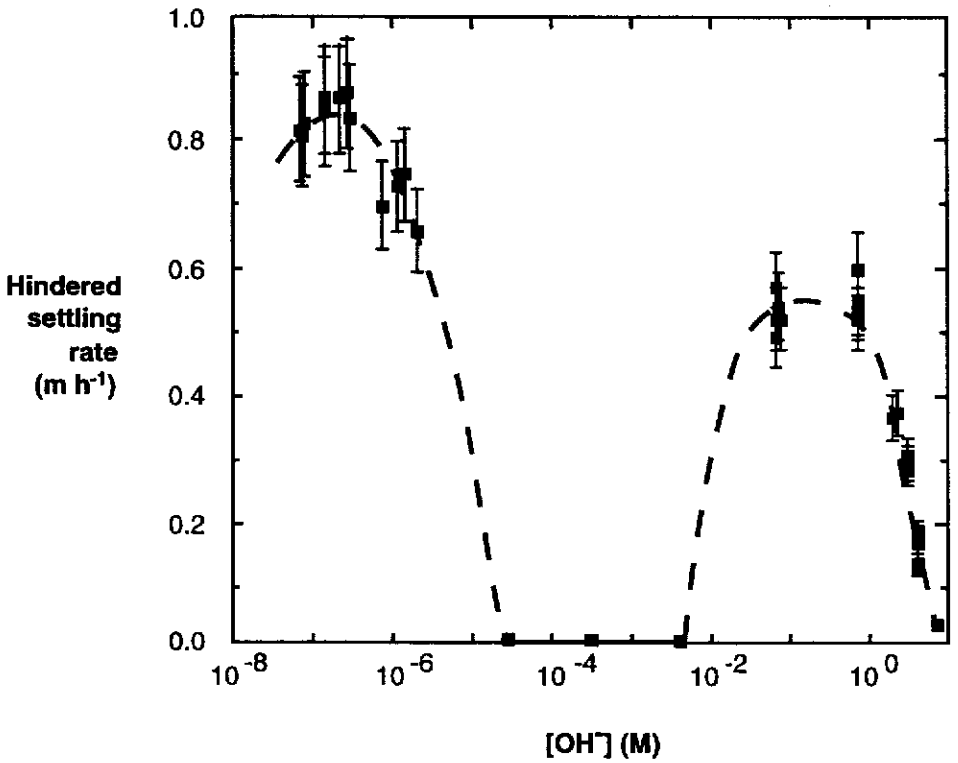

Figure 4.10 Natural settling rate of hematite in solutions with varying caustic concentration.

With [OH^-] between ~0.2×10^{-4} and 3×10^{-2} M, the hematite was fully dispersed and did not settle appreciably, reflecting a dominance of electrostatic repulsion over van der Waals attractive forces due to increased ionisation of surface hydroxyl groups with increasing caustic strength.

At higher caustic strengths, the hematite hindered settling rate increased to a maximum between 0.1 - 1 M, and then decreased. The initial increase in hindered settling rate at high caustic concentrations is due to sodium ions accumulating at the double layer which screen the negative surface and results in a reduction in the electrostatic repulsion between particles. The point is reached where van der Waals attractive forces dominate; coagulation of the hematite occurs leading to an enhanced hindered settling rate. The decrease in hindered settling rate seen above 1 M does not indicate a shift back towards a dispersed state, but reflects the effect of a significant increase in liquor viscosity as the concentration of caustic increases. The observed settling rates correspond with expected settling rate changes due to increased viscosity, as

determined from Ikkatai and Okada (1963).

Thus in high caustic strength synthetic Bayer liquor, prior to the addition of flocculant, the hematite surface is charged but this charge is screened and the solids would be expected to be weakly aggregated due to coagulation. This contrasts with the refinery situation where the residue solids are dispersed, presumably due to adsorbed organics and/or silica which stabilise the slurry by steric repulsion.

4.2.2 FLOCCULATION OF HEMATITE IN CAUSTIC LIQUOR

Proof that hematite flocculation in caustic liquor occurs by a bridging mechanism was obtained from settling tests conducted using two 100 % polyacrylate polymers with substantially different molecular weights (AN995SH, MW 1.4×10^7 g mol^{-1} and HP1, MW 1.5×10^4 g mol^{-1}). The results (Figure 4.11) show that only the high molecular weight polymer enhanced the hindered settling rate above that of hematite alone. Using the Hyamine method (for determination of flocculant concentration) it was found that the lower molecular weight flocculant adsorbed to the same extent as the higher molecular weight flocculant; for example at 0.1 M NaOH (~pH 13) the adsorption density was 4.0 ± 0.4 μg m^{-2} for both AN995SH and HP1 using a flocculant dosage of 118 μg g^{-1}. Clearly the key to flocculation is the molecular size, not the functional group nor the adsorption density, indicating that aggregation of the hematite occurs by the polymer bridging between particles and not by surface modification.

As caustic concentration increased, the hindered settling rate of hematite flocculated with the high molecular weight flocculant (AN995SH) decreased slightly more than predicted from viscosity changes. Nonetheless, the high molecular weight 100 % polyacrylate was still effective in enhancing the hindered settling rate at extreme caustic strengths (6 M NaOH). The effect of caustic strength on settling rate was investigated further and is discussed in Section 4.4. These results are contrary to previous reports that polyacrylates are only effective at high caustic strengths if Ca^{2+} is also present to provide a linkage between the flocculant and the hematite surface (Rothenberg *et al.*, 1989; Jin *et al.*, 1987; Khangoankar and Bala Subramani, 1993). Elemental analysis (ICP) showed that the liquors contained less than 1 μg g^{-1} Ca^{2+}. It could be suggested that the sodium ions in solution were playing the same role as calcium. The impact that sodium and calcium have on settling are discussed in more detail in Chapter 5.

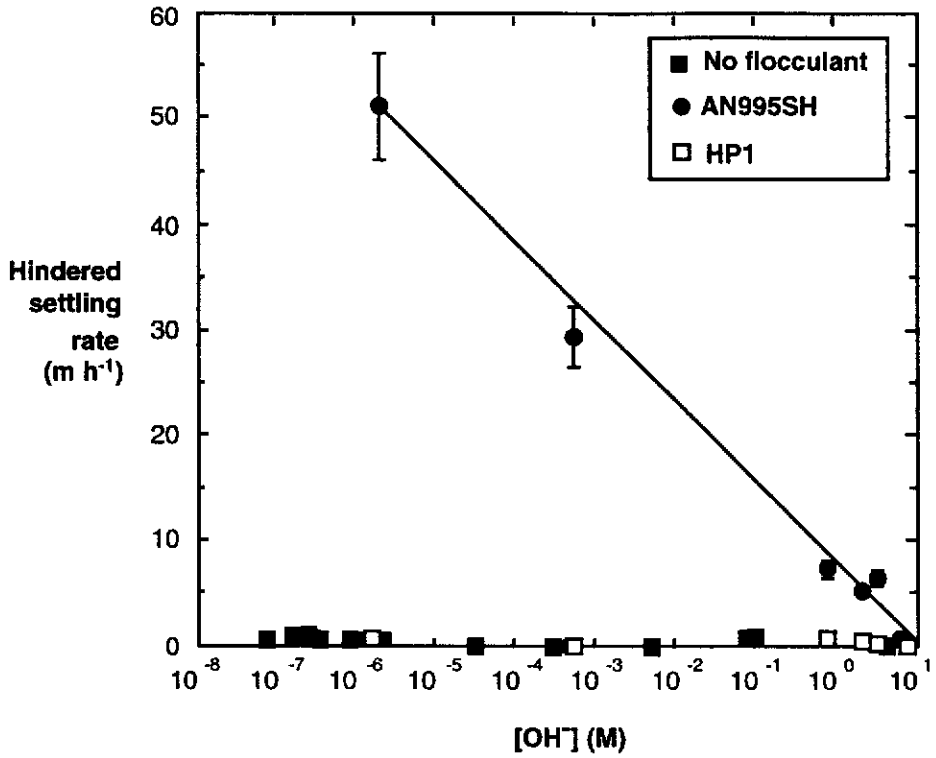

Figure 4.11 Effect of different polyacrylate flocculants (AN995SH, MW 1.4×10^7 g mol^{-1} and HP1, MW 1.5×10^4 g mol^{-1}) on the settling rate of hematite in solutions of varying caustic concentration.

4.3 ADSORPTION OF POLYACRYLATE

The effect of flocculant dosage on settling was investigated for both hematite and refinery solids. In the case of hematite, aliquots were analysed for residual flocculant concentration so that an adsorption isotherm could be obtained.

4.3.1 EFFECT OF FLOCCULANT DOSAGE

4.3.1.1 Hematite

Measurements of the hindered settling rate versus flocculant dosage (Figure 4.12) show a maximum at a dosage (AN995SH) of ~330 $\mu g\ g^{-1}$.

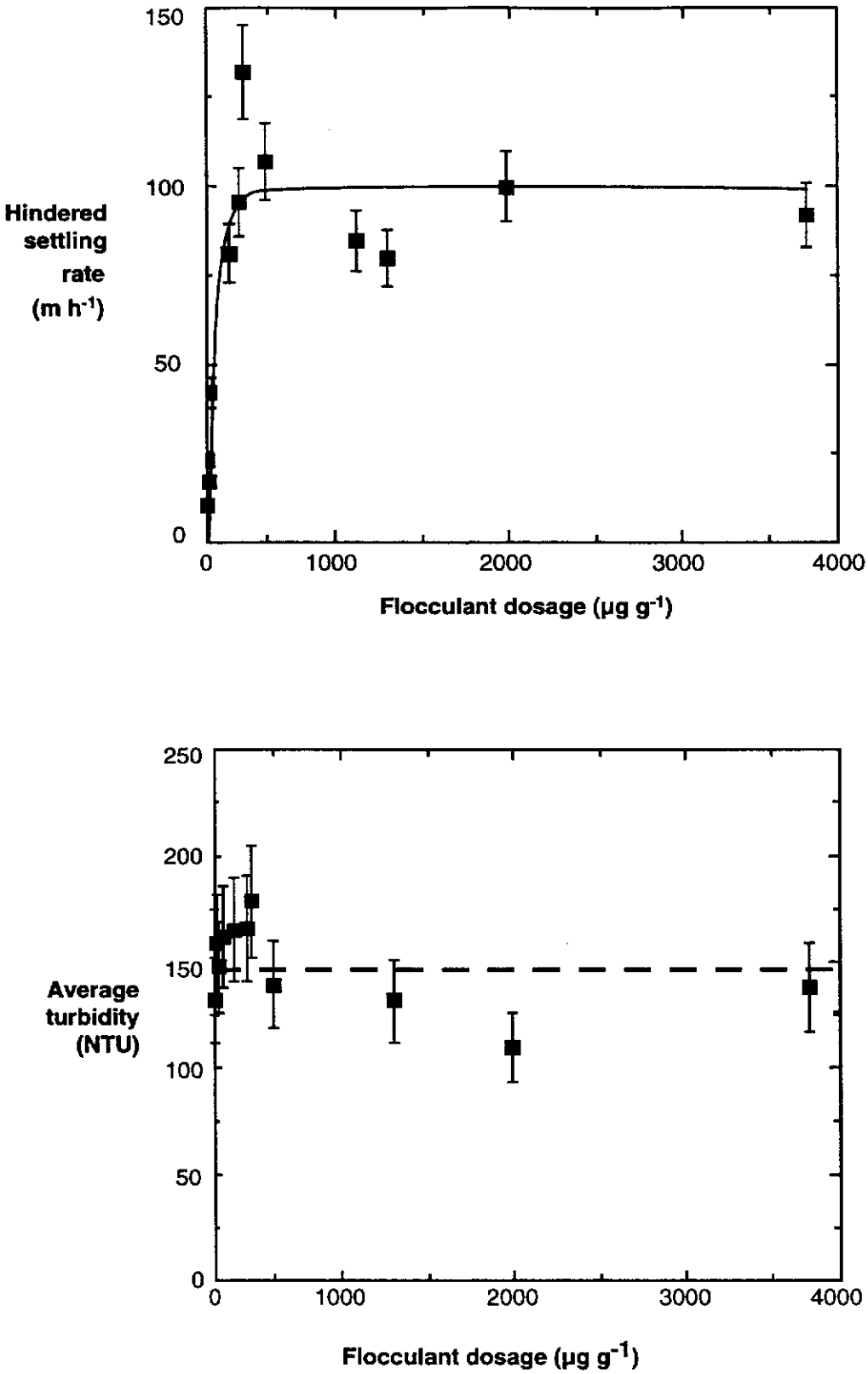

Figure 4.12. Settling rate and turbidity results of hematite in the synthetic Bayer liquor as a function of flocculant dosage.

With flocculant dosages above this optimum value there was no evidence of any significant re-dispersion of the hematite, even with 10 times the optimum dosage. This was supported by the residual turbidity measurements (Figure 4.12) which varied little over this range. If re-dispersion was occurring then the turbidity would have risen due to an increased number of discrete particles. Basu *et al.*'s (1986) investigation of the flocculation of goethite in synthetic Bayer liquor also found no evidence of re-dispersion, although the flocculant dosages they used did not extend significantly beyond that at which the maximum hindered settling rate occurred.

In systems where re-dispersion occurs, as the flocculant dosage increases, there is an increase in the proportion of molecules adsorbing onto single particles rather than bridging between two or more particles. This arises when the rate of flocculant adsorption dominates over the rate of effective particle-particle collisions. Since re-dispersion was not observed in these hematite measurements, despite using extreme flocculant dosages, it would appear that the rate of flocculant adsorption remained relatively low compared to the rate of effective particle-particle collisions. The turbidity is therefore low because the particles are able to aggregate before being stabilised by the flocculant.

4.3.1.2 Refinery solids

The results in Figure 4.13 show that, for refinery solids, some re-dispersion occurred beyond a dosage of ~1000 $\mu g\ g^{-1}$. However, even at extremely high dosages of flocculant, complete re-dispersion still did not occur; for example, at 4000 $\mu g\ g^{-1}$ the settling rate was only just below the standard settling rate. These results are similar to those for hematite, except that some re-dispersion is observed.

The turbidity was found to increase as the flocculant dosage increased, with no minimum observed. This could be related to the fact that the refinery solids are stable prior to flocculation, unlike hematite Sample A which was naturally coagulated. Thus, the rate of flocculant adsorption is still low compared to effective particle-particle collisions and so some bridging occurs (settling rate is still high) but those particles not bridged are either sterically stabilised by the flocculant or are in their original state (stable).

As the initial slurry is stable it would be expected that as flocculant is added the settling rate increases and that a corresponding decrease in turbidity should result. A minimum

in the turbidity result was not observed, however, this may be due to the flocculant dosage range used. The feed, as received, had a turbidity beyond the range of the meter (2000 NTU) and a minimum in the turbidity *might* have been observed had lower dosages had been used. The increasing turbidity does, however, also support the hypothesis of bridging as the flocculation mechanism (as increasing flocculant dosage stabilises more and more particles).

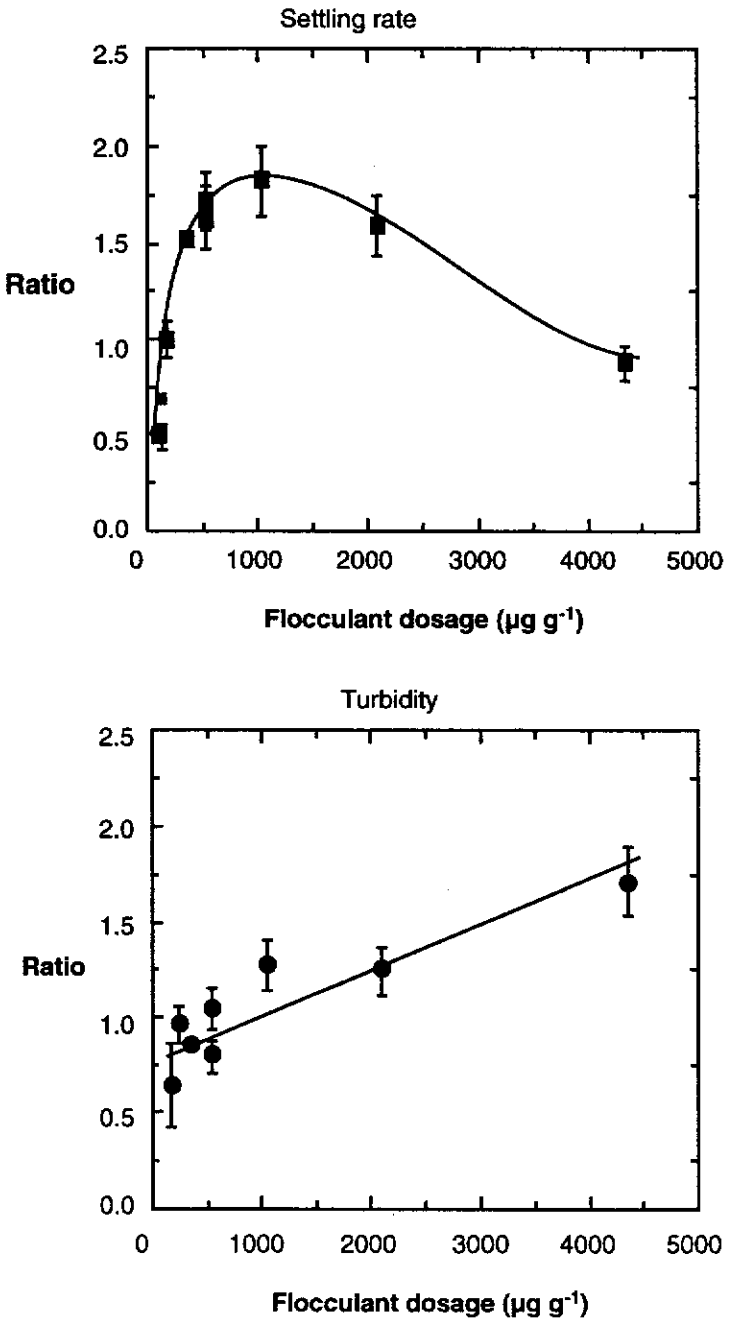

Figure 4.13 Flocculation performance as a function of flocculant dosage expressed as the ratio to the standard test for refinery solids. (Ratio refers to the performance compared to a standard test; see Section 3.3.4)

4.3.1.3 Adsorption isotherm of polyacrylate on hematite

Adsorption density measurements corresponding to the hematite flocculation settling tests are given in Figure 4.14. The amount of flocculant adsorbed on the hematite surface is shown as a function of the flocculant remaining in solution at equilibrium. The surface adsorption on hematite increased with increasing dosage to a plateau value of 164 ± 16 μg m^{-2} (dosage refers to the total quantity of flocculant added and the residual concentration refers to the quantity of flocculant remaining in solution after adsorption). This plateau is likely to reflect 'monolayer' coverage.

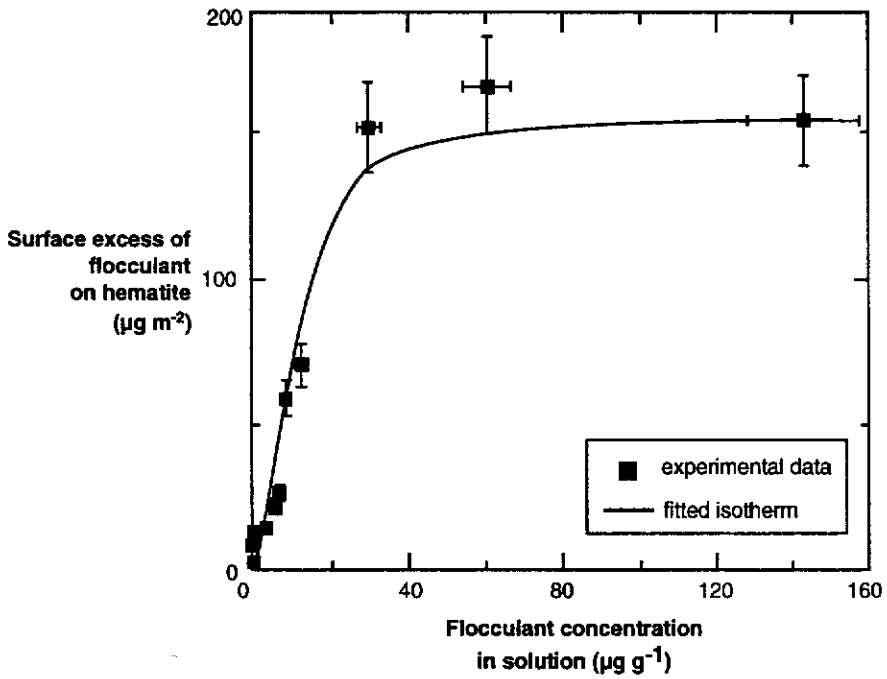

Figure 4.14 Adsorption isotherm of polyacrylate on hematite in synthetic Bayer liquor.

Analysis of the data found that the best fit was obtained with a Langmuir-Freundlich isotherm, of the form:

$$\Gamma = A\left(\frac{Bc^x}{1+Bc^x}\right) \qquad \text{(Eqn. 4.1)}$$

where Γ is the flocculant adsorption density (μg m^{-2})
c is the equilibrium solution flocculant concentration (μg g^{-1})
A=164 (plateau coverage, μg m^{-2})
B=0.01 and
x=1.90

While the constants B and x are sometimes given physical significance (B represents

the ratio of the forward and reverse reaction, x=1 means all the adsorption sites are thermodynamically equivalent), Lyklema (1995) suggests it is unwise to place too much meaning on these constants for adsorption from solution. This is especially true for flocculation where the equilibrium condition is not strictly satisfied, as discussed in Section 1.2.2. With a B value less than 1 it would be expected that the equilibrium of the adsorption reaction is towards the reactant side of the equation (that is, unadsorbed flocculant) while the x value clearly shows that surface sites of different enthalpies are being adsorbed and the surface is not homogenous with respect to the thermodynamics of the adsorption process.

The area occupied by the adsorbed flocculant can be estimated from the plateau coverage (164 $\mu g\ m^{-2}$) if it is assumed: i) that the flocculant lies completely flat on the hematite, ii) that the adsorption area of the carboxylate functional group is 0.15 nm^2 (Lyklema, 1995), iii) that all of the hematite surface is accessible to the flocculant and iv) that every second backbone carbon on the flocculant has a carboxylate functionality. A value of 0.158 m^2 of adsorbed flocculant per m^2 of hematite is obtained, that is, the flocculant covers only ~16 % of the hematite surface. The 'loops and trains' adsorption conformation associated with bridging flocculation (Fleer and Scheutgens 1993), instead of the flat conformation assumed for the above calculation, would mean the true surface coverage is even lower. This implies that a great deal of the hematite surface remains exposed or is sterically blocked by the adsorbed polymer. If the former is the case then it suggests there are a relatively small number of active sites onto which the flocculant adsorbs, which has been previously postulated (Hsu and Lin, 1996; Moudgil and Vasudevan, 1989).

The maximum hindered settling rate (Figure 4.12) occurred at a total flocculant dosage of 330 $\mu g\ g^{-1}$. This dosage corresponded to an adsorption density of ~35 $\mu g\ m^{-2}$, approximately 20% of the observed plateau coverage. It has been suggested by some authors that optimum flocculation should occur at about 50 % of the possible surface coverage (La Mer, 1964; Hogg, 1984). However, the present results are in accord with Hsu *et al.* (1995), who reported that optimum aggregation will occur at less than half monolayer coverage when the suspension is partially coagulated (as is the case with the hematite suspensions, see Figure 4.10) before the flocculant is added. This indicates that the aggregation state of the primary particles before the addition of flocculant is an important parameter affecting the subsequent flocculation behaviour.

4.4 THE EFFECT OF CAUSTIC CONCENTRATION ON FLOCCULATION PERFORMANCE

In determining the mode of polyacrylate adsorption on hematite, it was important to consider the impact of caustic concentration on flocculation performance. Also, the dependence of flocculant adsorption on caustic strength provides mechanistic information.

There are several possibilities by which caustic concentration could affect flocculation, such as a reduction in the flocculant adsorption density, a change in the flocculant conformation in solution or on the surface, solution viscosity and so on.

4.4.1 SETTLING CHARACTERISTICS

The flocculation characteristics of hematite were determined in synthetic Bayer liquor solutions having the same carbonate concentration (10 g L^{-1}) and aluminium concentration (A/TC = 0.3), but varying caustic concentrations (TC = 5 to 350) and a flocculant dosage of 15 μg g^{-1}.

As can be seen in Figure 4.15, it was found that the settling rate decreased with increasing caustic concentration while a corresponding increase in turbidity was observed. The decrease in settling is quite significant dropping from ~45 m h^{-1} at TC = 5 to ~4 m h^{-1} at a TC = 350.

Increasing the caustic concentration of the synthetic liquor from TC = 5 to 350 significantly increases the liquor viscosity from 0.972 to 3.663 centipoise, and slightly increases the liquor density (1071 to 1294 kg m^{-3}). The increase in liquor density would not be expected to greatly affect the settling rate, since it is likely there would be a corresponding increase in the aggregate density due to their highly porous nature (Farrow and Warren, 1989).

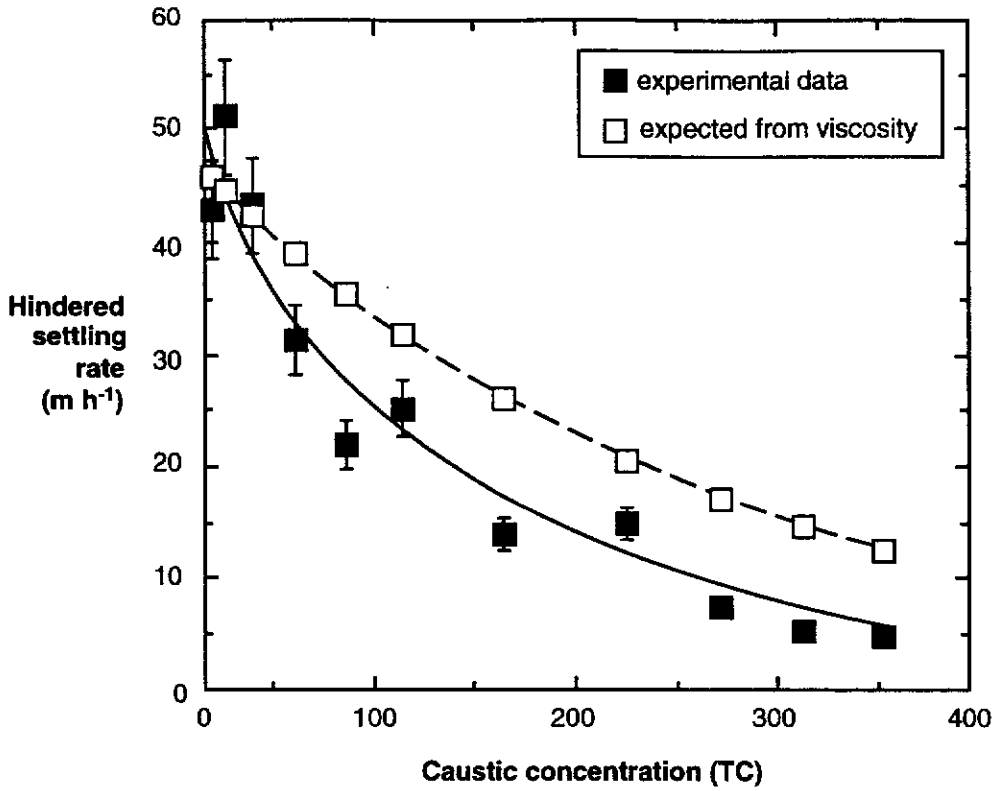

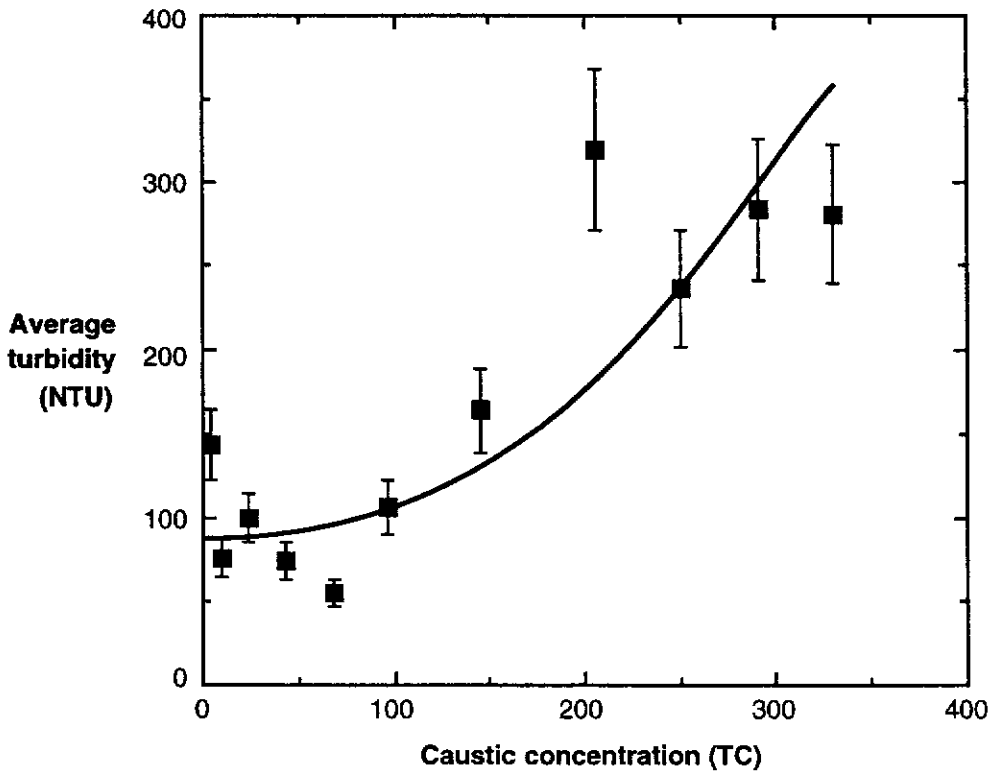

Figure 4.15 The observed flocculation performance at varying caustic concentration and the expected settling rate as calculated from viscosity changes (broken line).

An increase in the viscosity of the solution would certainly reduce the solids settling rate and lead to a higher residual turbidity. The significance of this was assessed in two ways. Firstly, based upon the settling rate observed at TC = 5, the expected change in settling rate at higher caustic concentrations due to the increased solution viscosity was calculated using Stokes' equation and a viscosity equation for caustic aluminate liquors at 95°C derived by Ikkatai and Okada (1963). The results are included in Figure 4.15 as the broken line, however, significant differences exist between the experimental data and the predicted data. For example at TC = 300, the measured settling rate was ~8 m h^{-1} compared to the predicted settling rate of 18 m h^{-1}. Furthermore, the standing time before the turbidity was measured at the higher caustic concentrations was increased to account for the increased viscosity, but this did not significantly change the turbidity value. Thus, although the change in viscosity does significantly contribute to the reduced settling rate at higher caustic concentrations, it is not the only factor involved.

While flocculation performance deteriorated with increasing caustic concentration the adsorption density of flocculant on hematite was relatively unchanged (Figure 4.16). Although there is considerable scatter in this data, there is no discernible decrease in the extent of adsorption as the caustic concentration is increased. Thus, the deterioration in settling is caused by effects other than flocculant adsorption density.

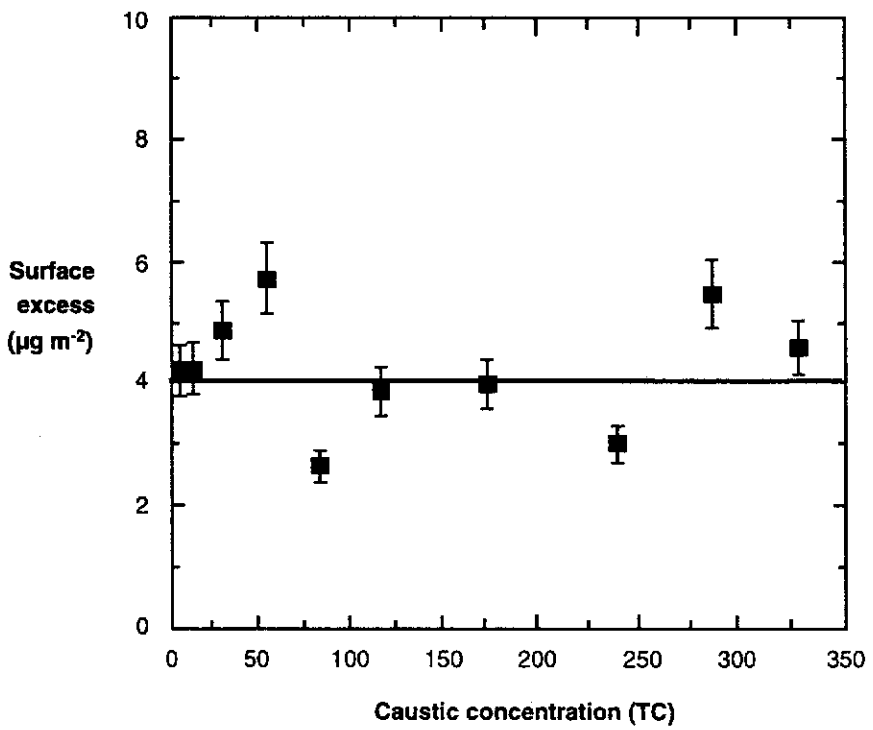

Figure 4.16 The adsorption density of polyacrylate on hematite at varying caustic concentration in synthetic Bayer liquor.

The consistent adsorption density also suggests that either the flocculant is chemisorbed to the surface (surface complexation) and is therefore not affected by ionic strength changes or that adsorption is via an electrostatic interaction for which even at the lowest TC investigated (TC = 5) there exist sufficient sodium ions in the double layer to allow the maximum possible electrostatic interaction with the flocculant.

4.4.2 POLYMER CONFORMATION

Changes in a flocculant's conformation can impact directly on its ability to form bridges between particles and hence affect flocculation performance. Such a conformational change in the flocculant may be caused by changes in the ionic strength, as the liquor concentration increases from TC = 5 to 330.

Multi angle laser light scattering (MALLS) was used to determine polymer hydrodynamic size (conformation) *in situ* by measuring the root mean squared (r.m.s.) radius of gyration (Section 2.2.2). MALLS was conducted on various solutions to determine the effect of increasing caustic concentration, increasing ionic strength and the difference between caustic solutions and synthetic liquors.

Figure 4.17 shows that the hydrodynamic size decreases (and hence the conformation becomes more coiled) with increasing caustic concentration, while Figure 4.18 shows a similar observation with increasing ionic strength of NaCl and Na_2CO_3 solutions.

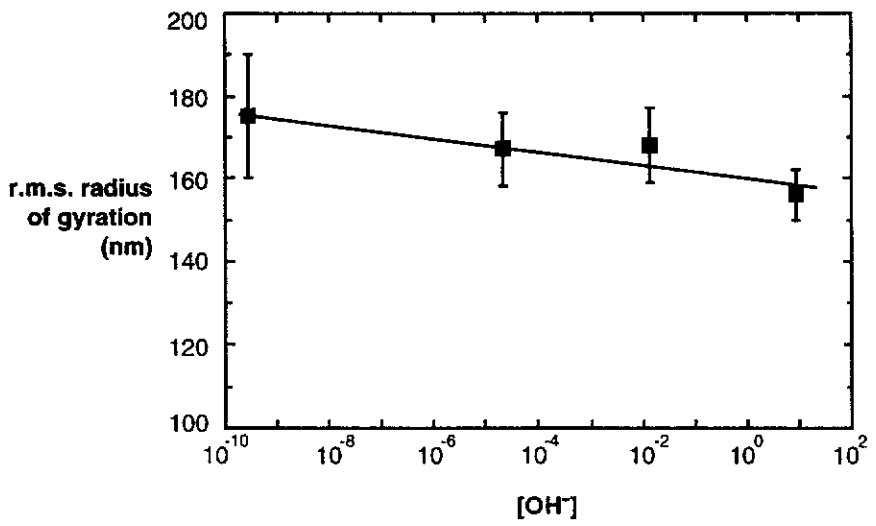

Figure 4.17 Root mean squared (r.m.s.) radius of gyration of a 100 % polyacrylate (50 μg g^{-1}) in aqueous solutions of differing caustic concentration.

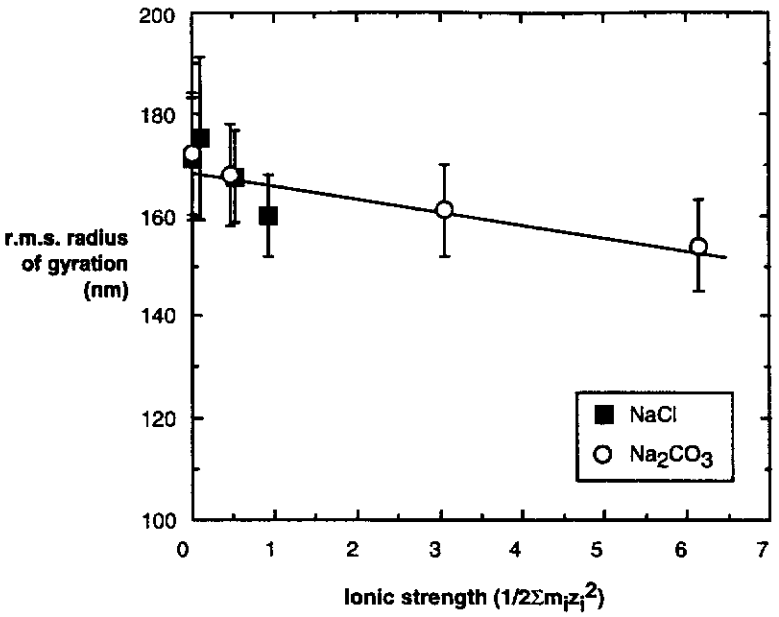

Figure 4.18 Root mean squared (r.m.s.) radius of gyration of a 100 % polyacrylate (50 μg g^{-1}) in salt solutions of differing concentration. Ionic strength is given by the molality, m_i of the ion and its charge, z_i, summed over all ions.

These results are in agreement with Rogan (1995) who found that the r.m.s. radius of gyration of low molecular weight polyacrylates decreases with increasing ionic strength in aqueous conditions due to greater charge shielding, leading to a more coiled configuration.

MALLS measurements of the flocculant hydrodynamic size (Figure 4.19) at Bayer strengths in caustic solutions were assessed in liquor solutions containing 0.094 M Na_2CO_3, while the synthetic liquor also contained aluminium a constant A/TC ratio of 0.3.

The results show that within experimental error:

- there is no difference in the hydrodynamic size between caustic solutions and synthetic liquors and
- the hydrodynamic size of the flocculant remained essentially constant as the caustic concentration increased from 1 M to 6 M (TC =50 to 330). For example, the average r.m.s. radius of gyration was ~139 nm for all caustic strengths ≥1 M.

This implies the functional charge was fully shielded above 1 M and that the flocculant molecule has a limiting size to which it can collapse.

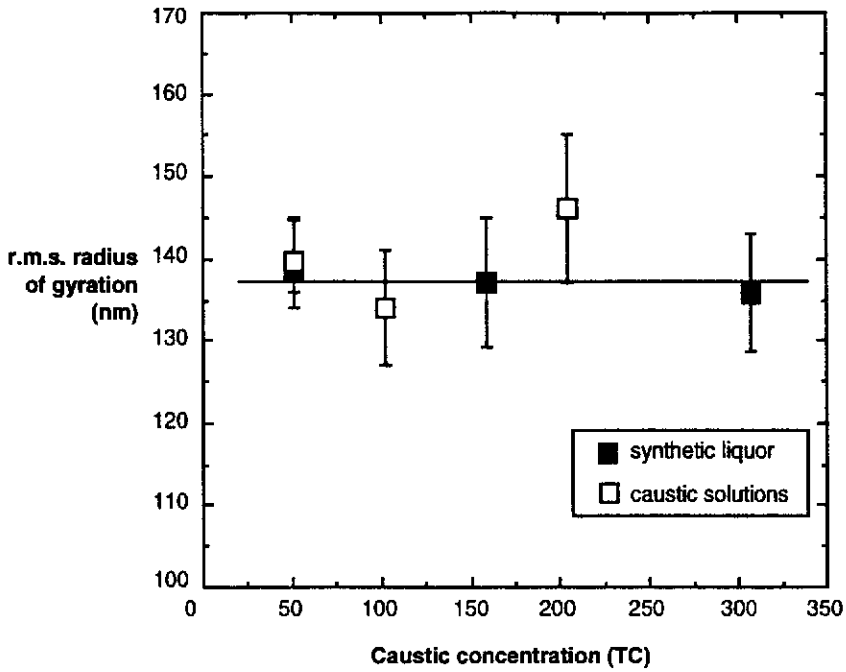

Figure 4.19 Root mean squared (r.m.s.) radius of gyration of 100 % polyacrylate flocculant (50 μg g^{-1}) in caustic solutions and synthetic liquor.

The difference between the r.m.s. radius of gyration found at high ionic strengths and that found in caustic solutions can be explained by the interaction of the flocculant with the positive ions in solution. That is, since the carboxylate is a negative ion only cations are able to screen its charge. Re-plotting of the data on a sodium basis (Figure 4.20) showed a large degree of scatter but a distinct trend of decreasing hydrodynamic size with increasing sodium ion content to a limiting value of ~140 nm is observed.

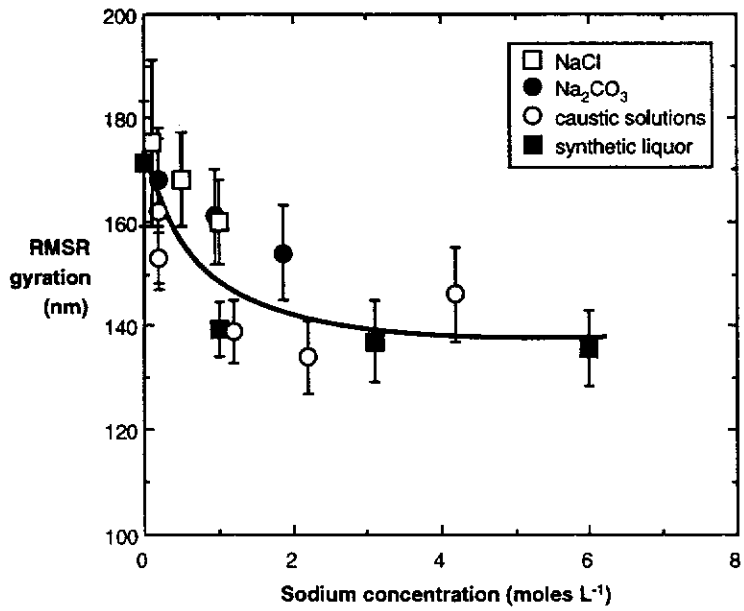

Figure 4.20 Root mean squared (r.m.s.) radius of gyration for the different flocculant solutions investigated plotted on a sodium concentration basis.

The results presented demonstrate that the loss in flocculation efficiency with increasing caustic strength is not fully accounted for by the increase in liquor viscosity, nor contributed to by a change in the flocculant adsorption density or a change in the flocculant conformation in solution. This suggests that the reduced flocculation efficiency is due to an increase in the proportion of flocculant molecules which adsorb only on single particles rather than bridging between two or more particles. This effect would arise when there is a change in the balance between the rate of flocculant adsorption and the particle-particle collision rate. Single particle adsorption is favoured when the rate of flocculant adsorption is much faster than the inter-particle collision rate. The inter-particle collision rate during flocculation would be expected to reduce as the caustic strength increased, since the higher viscosity would result in a lower shear rate (Levich, 1962). For the same reason, the higher viscosity would also reduce the flocculant adsorption rate since this depends essentially on 'collisions' between flocculant molecules and particles (Gregory, 1987).

4.5 INFRARED SPECTRA OF ADSORBED FLOCCULANT

The nature of the adsorbed flocculant carboxylate interaction with hematite was determined from the infrared spectra of flocculant adsorbed at pHs 7, 11, 13 and 14.

The hematite Fe-O bands are found at 470 and 540 cm^{-1} (Farmer, 1974) and are not observable with the mercury-cadmium-telluride (MCT) detector used, (cut-off of *ca.* 600 cm^{-1}). Thus, the hematite mineral surface spectra (Figure 4.21) is relatively featureless in the 2000 - 1000 cm^{-1} region where the significant flocculant peaks are found (Table 4.1).

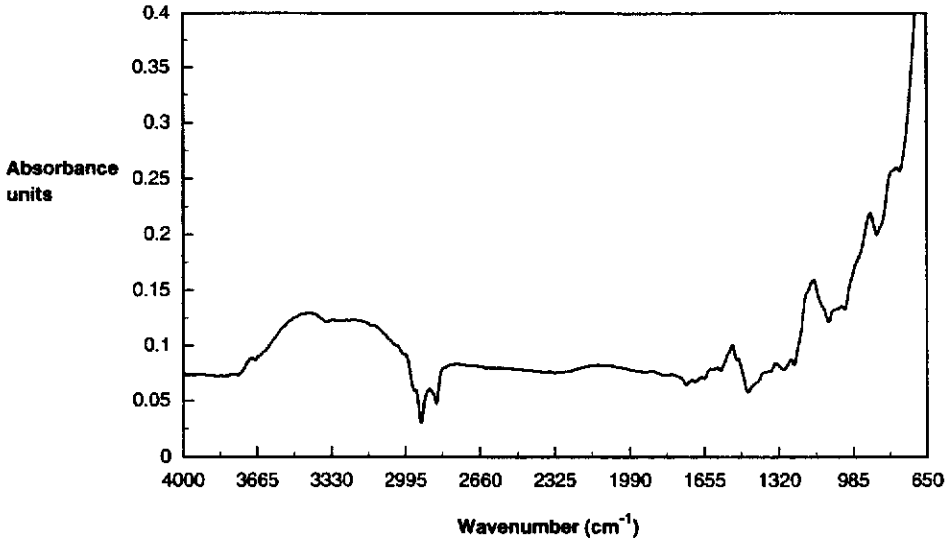

Figure 4.21 DRIFT spectrum of hematite Sample B at pH 7, no flocculant.

Table 4.1 Infrared band assignments for polyacrylates.

Assignment	Infrared bands for 100 % polyacrylate (cm^{-1})
OH stretch	3420 (very broad)
CH stretch	2940
C=O stretch	1650
COO^- asymmetric stretch	1560
CH bend	1450
COO^- symmetric stretch	1410

(Kulicke and Hörl, 1985; Tackett, 1990; McCluskey *et al.*, 1989).

Two adsorption mechanisms can be identified using infrared; hydrogen bonding and surface complexation. Hamilton and Ibers (1968) found that when hydrogen bonding is involved the O-H stretching frequency or bandwidth will change. Strong hydrogen bonds cause a frequency shift down while longer/weaker bonds have only a marginal effect (Ratajczak and Orville-Thomas, 1967, 1968). If complexation occurs the functional group frequencies of the polymer would be expected to shift significantly;

for example, the carboxylate frequencies of the polyacrylate.

Carboxylic acids have been shown to adsorb as carboxylates (Allara and Nuzzo, 1985; Lee *et al.*, 1996; Bournel *et al.*, 1996; Ishiduki and Esumi, 1997). When the carboxylate group is directly involved in adsorption it is possible to discriminate between monodentate (Figure 4.22, I), bidentate chelating (Figure 4.22, II) and bidentate bridging (Figure 4.22, III,) structures on the basis of the carboxylate asymmetric and symmetric stretches (Nakamoto 1986).

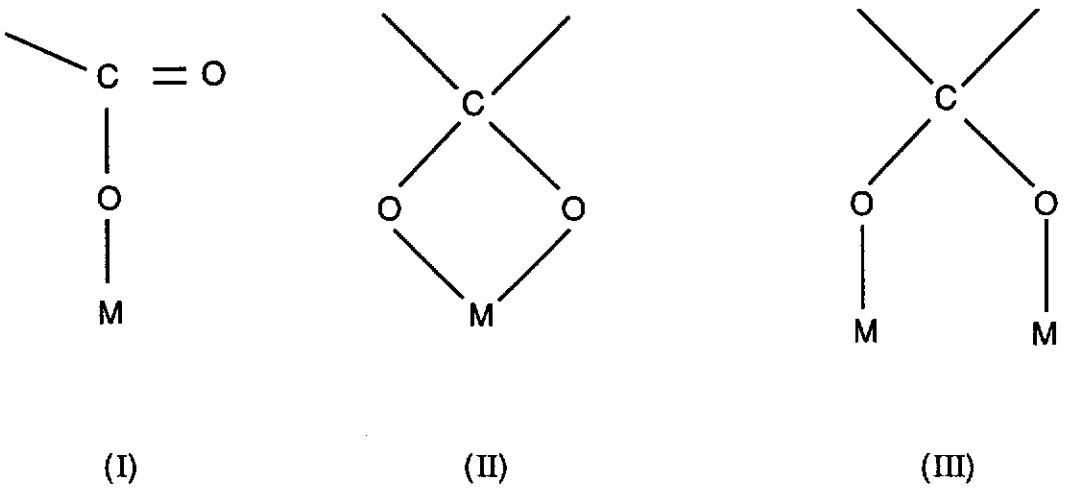

(I) (II) (III)

Figure 4.22 Modes of carboxylate adsorption onto a metal surface.

If the structure is monodentate (I) there must be a C=O stretch at ~1650 cm^{-1} and its absence is an indication of the bidentate structures. The separation of the symmetric and asymmetric stretches ($\Delta\nu = \nu_{asym} - \nu_{sym}$) of the carboxylate group can then be used to identify the bidentate adsorption conformations, as well as confirm the monodentate configuration, when it is compared to that of the carboxylate salt (Nakamoto, 1986):

i) If there is C=O character in the spectrum and $\Delta\nu_{(adsorbed)}$ is greater than $\Delta\nu_{(salt)}$, the adsorbed structure is monodentate (I).

ii) If there is no C=O character in the spectrum and $\Delta\nu_{(adsorbed)}$ is smaller than $\Delta\nu_{(salt)}$ the adsorbed structure is bidentate chelating (II).

iii) If there is no C=O character in the spectrum and $\Delta\nu_{(adsorbed)}$ is similar to $\Delta\nu_{(salt)}$ the adsorbed structure is bidentate bridging (III).

Allara and Nuzzo (1985) have made a detailed investigation on carboxylates adsorbed onto oxidised aluminium. They showed that n-alkanoic acids (monocarboxylates)

adsorb in a bridging bidentate (III) structure which is not completely symmetrical but tilted somewhat from the surface. Other studies (Buckland *et al.*, 1980; Parfitt *et al.*, 1977; Lee *et al.*, 1996) have compared the individual infrared band positions of the adsorbed species with those reported for non-adsorbed species. Using this approach, Lee *et al.* (1996) concluded a type II structure for polyacrylate adsorption onto alumina by comparing their spectra with those of aluminium complexes in solution. However, if the $\Delta\nu$ criteria were used, a conclusion of bridging bidentate (III) would result as $\Delta\nu_{(salt)}$=162 cm^{-1} and $\Delta\nu_{(adsorbed)}$=195 cm^{-1} and no C=O bond character was present. This would then be in agreement with Allara and Nuzzo (1985) and McCluskey *et al.* (1989) who found type III bonding. Comparison of band positions is not sufficient to determine structure as both the symmetric and asymmetric stretch can be shifted. It is the amount of strain in the carboxylate bonds (which determines the frequency difference $\Delta\nu$), and the presence or absence of C=O character which is a more accurate guide to the structure of adsorbed carboxylates.

4.5.1 ADSORPTION CONFORMATION

The position and separation of the symmetric and asymmetric carboxylate stretches of the flocculant and of the adsorbed flocculant on hematite are given in Table 4.2.

Table 4.2 Differences in the wavenumber between the symmetric and asymmetric COO^- stretch of the polyacrylate sodium salt and adsorbed polyacrylate.

Polyacrylate salt and adsorption conditions	ν_{asym} (cm^{-1})	ν_{sym} (cm^{-1})	separation $\Delta\nu$ (cm^{-1})
AN995SH (Na^+ polyacrylate)	1567±2	1407±2	160±4
pH 7	1731±4	-	-
	1674±4	1382±4	292±8
pH 11	1586±4	1412±4	174±8
pH 13	1589±6	1410±6	179±12
pH 14	1599±6	1411±6	188±12

At pH 7 there is definite C=O character (Figure 4.23) as evidenced by the bands at 1674 cm^{-1} and 1731 cm^{-1}, and a $\Delta\nu$ which is almost twice that observed for the sodium salt (292 and 160 cm^{-1} respectively). The 1674 band is due to free C=O and the 1731 cm^{-1} band can be attributed to a hydrogen bonded C=O species (Lee *et al.*, 1996). As the C=O group is in close proximity to the hydroxylated surface it is likely that the hydrogen bonding is to a surface hydroxyl proton, however, the OH stretches at ~3500 cm^{-1} are not sufficiently resolved to distinguish between this and the possibility of hydrogen bonding to adsorbed solvent (water). Thus, at pH 7, a monodentate structure with hydrogen bonding to some C=O groups appears to be the dominant mode of adsorption (structure I, Figure 4.22).

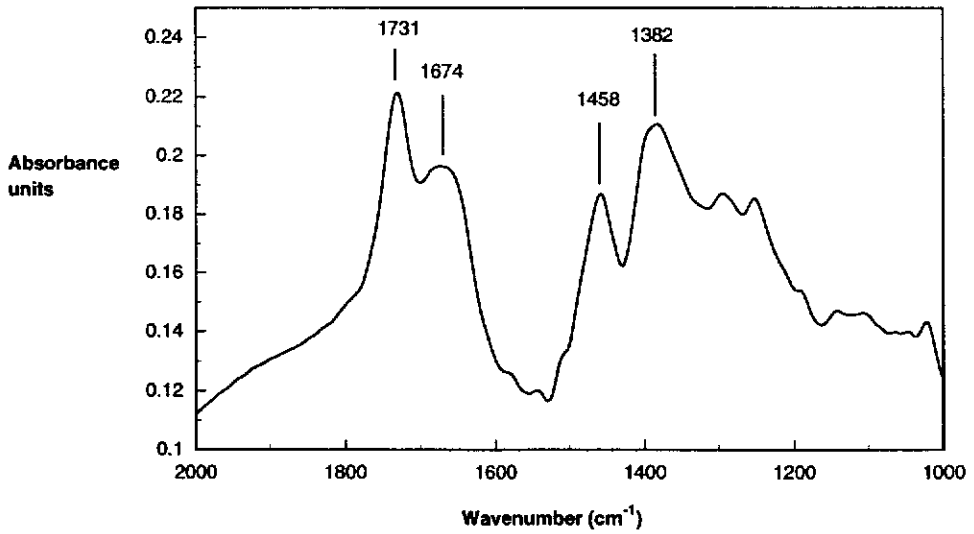

Figure 4.23 Spectrum of adsorbed polyacrylate on hematite at pH 7.

At pH 11 the monodentate character is reduced substantially (Figure 4.24) and the 1731 and 1674 cm^{-1} bands have almost disappeared. The separation of the symmetric and asymmetric stretch is reduced (Table 4.2) but is still larger than that found for the polyacrylate sodium salt (174 compared to 160 cm^{-1}). Thus, the adsorption conformation cannot be a bidentate chelating (II) structure as $\Delta\nu$ would have been <160 cm^{-1} and there is not enough C=O character to suggest a monodentate structure. A type III structure is therefore indicated.

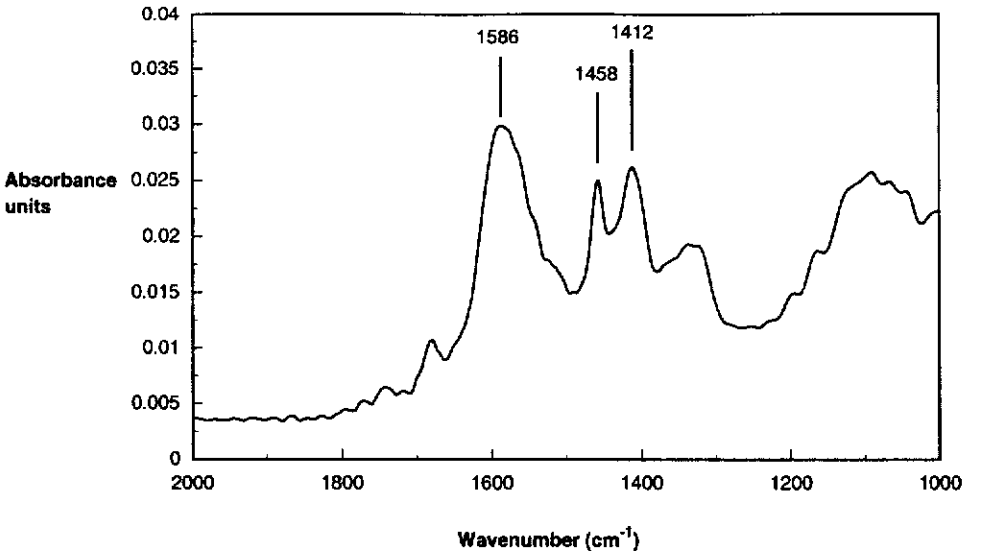

Figure 4.24 Spectrum of adsorbed polyacrylate on hematite at pH 11.

At pH 13 and 14 (Figure 4.25 and Figure 4.26) there is also little C=O character, although it appears to be greater than that at pH 11. An approximate calculation based on the area of the ~1650 cm^{-1} frequency suggests 5 and 20 % C=O character for pHs 11 and 14 (assuming quantitative spectra). There is no evidence for the hydrogen bonded C=O group in these spectra. The increase in $\Delta\nu$ as the pH increases from 11 to 14 could be attributed to the formation of a monodentate species but with the lack of substantial C=O character this is unlikely. It is more likely that the adsorbed configuration is a bridging bidentate structure (III, Figure 4.22) in which one C-O-M bond is longer than the other. This asymmetry imparts a degree of monodentate character which would increase $\Delta\nu$. This asymmetrical adsorption was also found by Allara and Nuzzo (1985) for n-alkanoic acids on oxidised alumina.

The infrared evidence thus clearly indicates that the AN995SH polyacrylate flocculant adsorbs onto hematite as a carboxylate and not as a carboxylic acid. This supports other studies that have shown that carboxylic acids adsorb as carboxylates (Allara and Nuzzo, 1985; Lee *et al.*, 1996; Bournel *et al.*, 1996; Ishiduki and Esumi, 1997; Papirer *et al.*, 1994).

The clearly defined shifts in frequencies for the flocculant on adsorption suggests a direct surface chemisorption mechanism in a bidentate bridging configuration and not electrostatic physisorption.

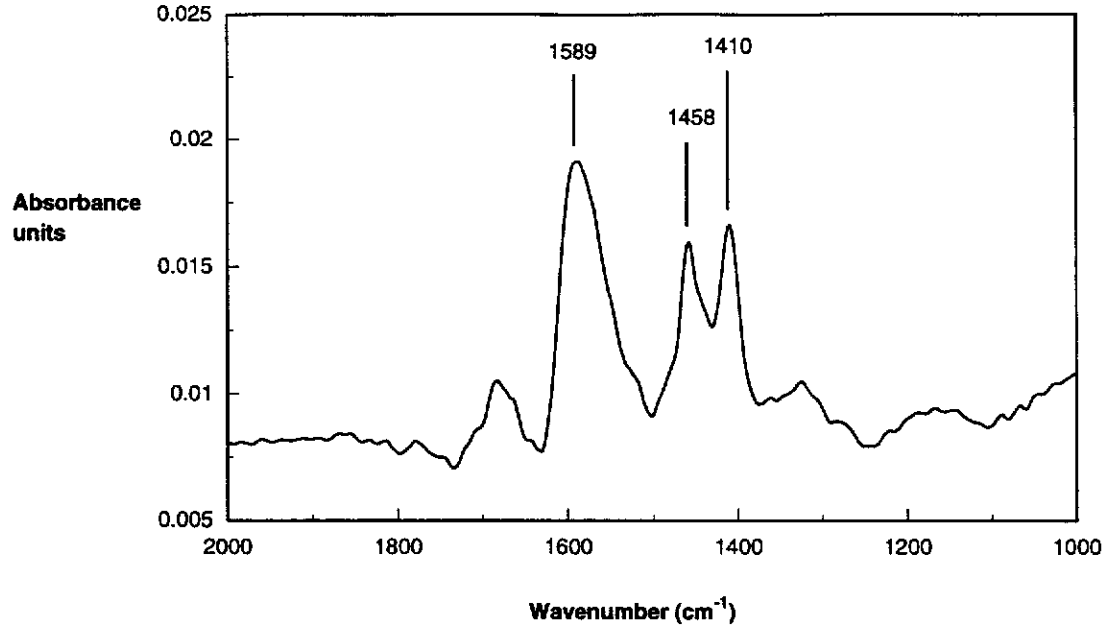

Figure 4.25 Spectrum of adsorbed polyacrylate on hematite at pH 13.

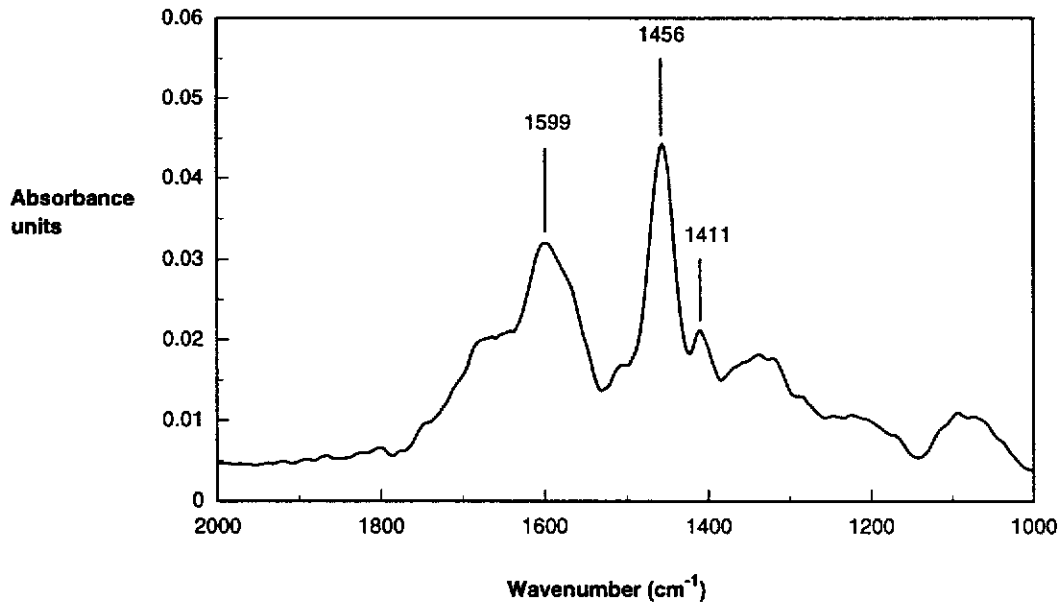

Figure 4.26 Spectrum of adsorbed polyacrylate on hematite at pH 14.

4.6 X-RAY PHOTOELECTRON SPECTROSCOPY (XPS) RESULTS

Due to problems associated with charging effects, polyacrylate adsorbed on hematite at pH 7 was the only sample assessed by XPS.

4.6.1 FLOCCULANT

The survey spectra for the AN995SH flocculant at a 50 eV pass energy is shown in Figure 4.27. The high resolution C 1s was found to split appropriately, but the primary C 1s shift for the acrylate group was not as high as would be expected, ~3.6 eV compared to 4.2 eV for acrylic acid (Beamson and Briggs, 1992). As the acidic proton is covalently bound, it is reasonable to assume that the ionic Na^+ actually causes less valence charge to be withdrawn from the associated oxygen atoms, the effect of which is a lower primary shift to higher binding energy for the 1s level of carbon atoms attached to the oxygen atoms.

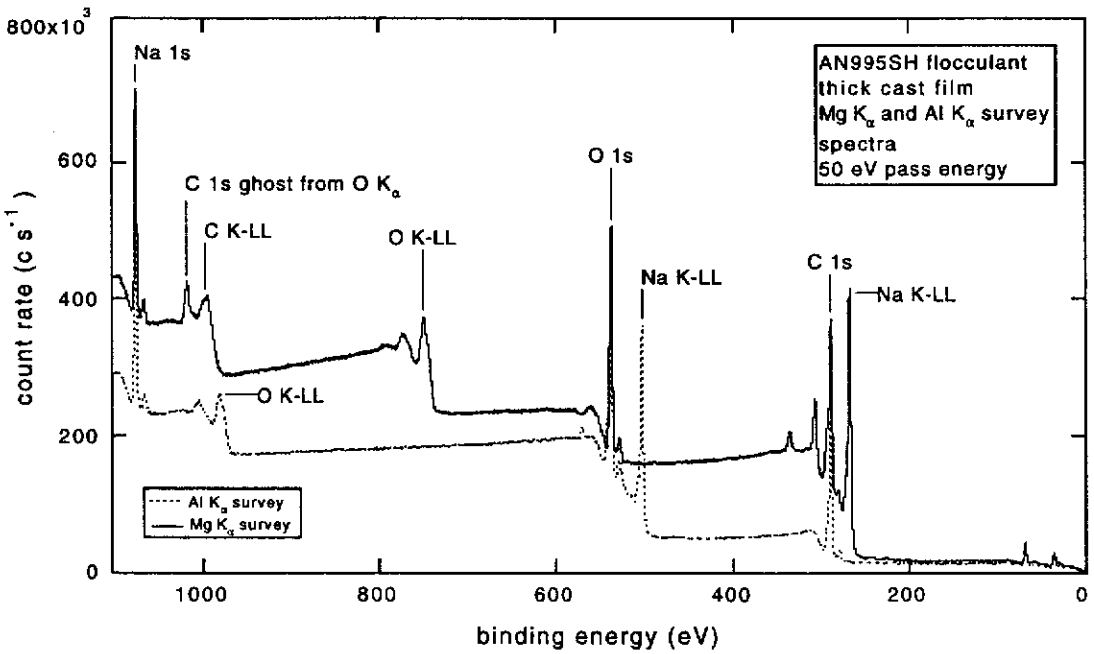

Figure 4.27 Survey XPS spectra of AN995SH at 50 eV using Al K_α and Mg K_α radiation.

Sodium complicates the stoichiometric analysis because of the C 1s and O 1s interference by the Na KLL Auger feature for the Mg K_α and Al K_α X-ray sources. However, the presence of Na^+ was used to advantage by normalising the survey spectra across both sources. When this was done, the cross-sections yield an acrylate

to sodium ratio of 1.1:1, which suggests a 1:1 ratio as that is well within the cross-section accuracy. A reasonable assumption is then that the flocculant is 100 % acrylate with no free acid present.

There was no specific evidence of any extensive radiation damage for the AN995SH flocculant. For $C_xH_yO_z$ polymers radiation damage is generally characterised by a loss of oxygen. There was some indication this could be happening for the 5 eV pass energy runs of the C 1s peak taken after both the survey spectra (50 eV pass energy) and the 20 eV pass spectra for the C 1s and the O 1s peaks. The C 1s at 5 eV showed what appeared as broadening of the primary C 1s shifted peak. This would be expected for removal of oxygen atoms from the acrylate group. Except in a general sense the 5 eV pass data were not used for polymer analysis and are not shown.

4.6.2 ADSORBED FLOCCULANT ON HEMATITE

The survey spectra for the AN995SH flocculant adsorbed on hematite is shown in Figure 4.28 at a 50 eV pass energy.

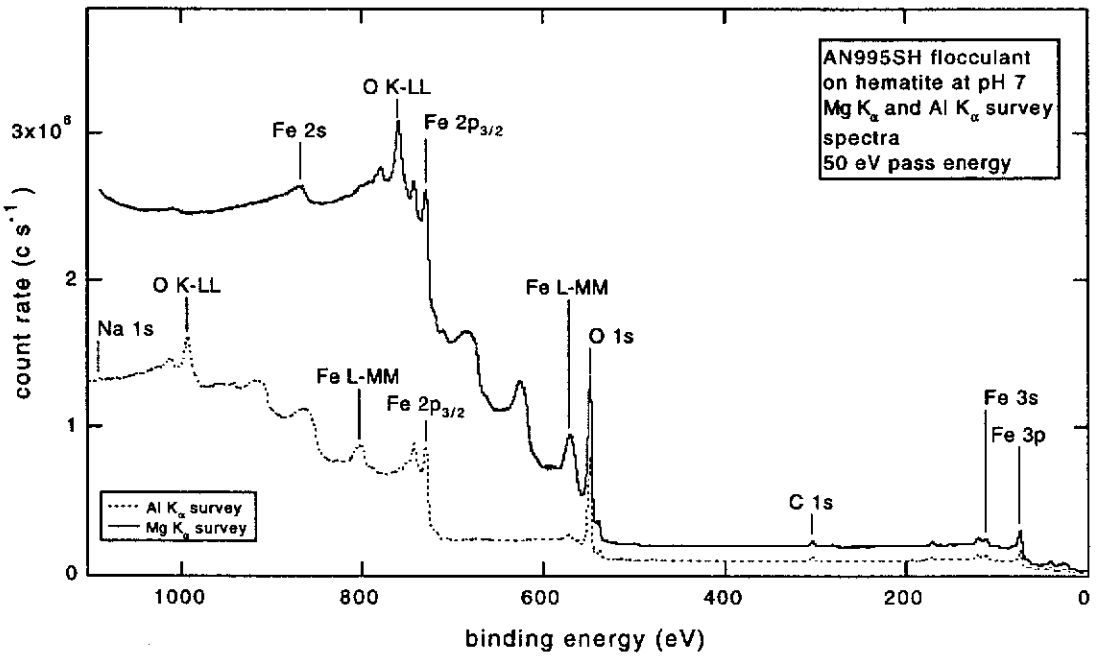

Figure 4.28 Survey XPS spectra of AN995SH adsorbed on hematite at 50 eV using Al K_α and Mg K_α radiation.

What is immediately obvious from the above spectra compared to that of the flocculant is that the amount of sodium present when the flocculant is adsorbed is greatly reduced to that from the standard. Based on the nett Na 1s to C 1s peak integrals from the respective survey spectra the surface sodium content drops to ~40 % of the level of sodium in the bulk flocculant. If all this sodium was initially associated with the flocculant carboxylate groups and ignoring any small level of acidification of the flocculant at pH 7 this indicates about 60 % of the flocculant groups could be attached to the hematite. This is a high level of adsorption showing that as most of the flocculant is attached it leaves only ~40 % of the flocculant to form 'loops and tails' for bridging. The results further suggest that sodium does not play a part in the adsorption configuration as it is lost on adsorption.

Figure 4.29 shows the raw C 1s data for two separate samples of AN995SH flocculant adsorbed on hematite at pH 7. Each curve is the summation of 60 sequential scans where the individual scans have been adjusted for any interim charging shift prior to summing. For the two hematite samples a free Voigt profile fit to minimise the residuals was evaluated, one of which is shown in Figure 4.30. Using the peak binding energy, the shift in binding energy between the backbone carbon and the carboxylate carbon is calculated.

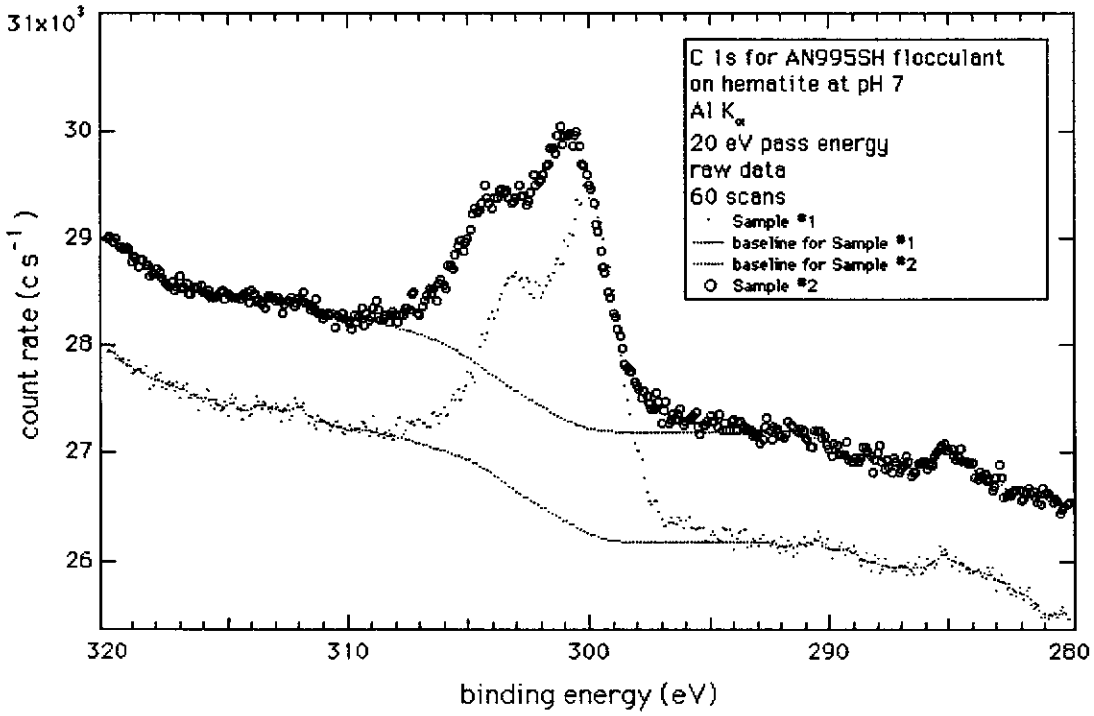

Figure 4.29 Raw C 1s data for two separate samples of AN995SH flocculant adsorbed on hematite at pH 7.

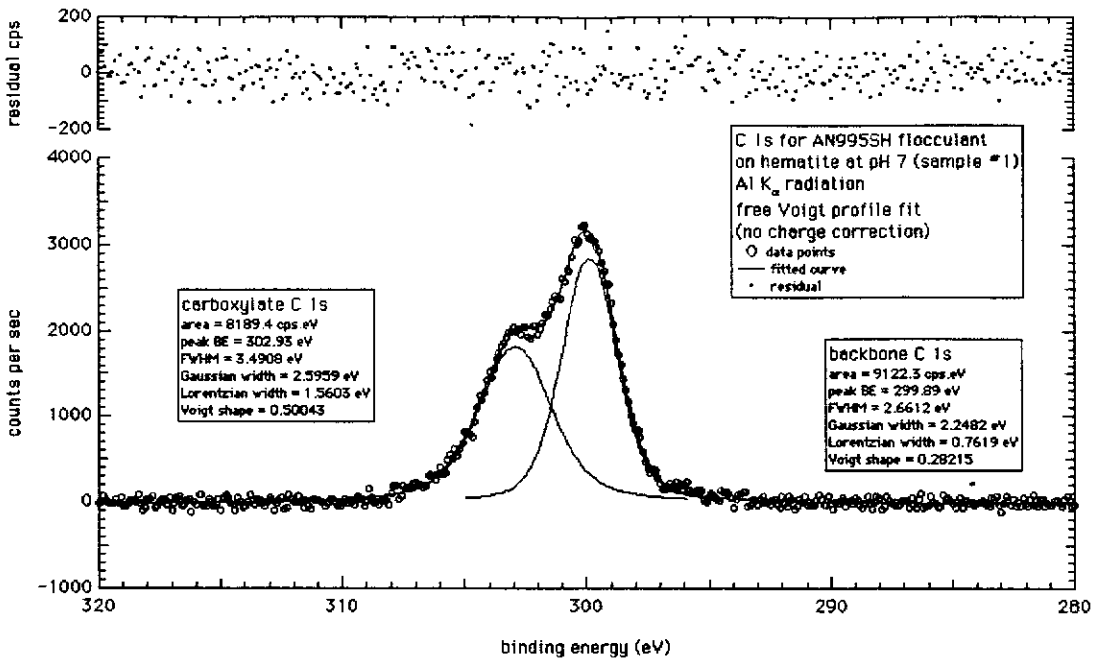

Figure 4.30 Fitted Voigt profile to XPS data for AN995SH flocculant adsorbed on hematite at pH 7 (where BE refers to binding energy, cps to counts per second and FWHM to full width at half maxima).

The primary shift of the carboxylate carbon C 1s feature for the two samples was 3.04 and 3.12 eV respectively with intensity fractions of 0.69 and 0.90; the average shift value being 3.08 eV with an average intensity ratio of 0.8 . The expected empirical values for polyacrylic acid (Beamson and Briggs, 1992) are 4.18 eV and 0.41 . The AN995SH flocculant indicated a shift for the carboxylate of ~3.6 eV. On simple charge transfer grounds the higher electronegative H atom, which is covalently bound to the carboxylate, allows more charge transfer away from the carboxylate carbon atom and hence a higher binding energy shift. When the H atom is replaced by Na^+ this formerly distributed charge relaxes back toward the carboxylate carbon atom and the binding energy shift diminishes. Hence, it can be concluded that the flocculant bonding to the hematite surface is ionic in nature (as opposed to a covalent bond) and to a cationic centre. Further, the indication is that this cationic centre has a positive charge influence less than that of Na^+ (less electronegative). This is because a lower negative charge is stabilised on the carboxylate oxygen atoms and the associated carbon atom displays a lowered shift. The most likely situation is that the carboxylate is directly bonded to surface iron atoms which have an effective charge less than +3.

The carboxylate to backbone carbon ratio of ~0.8 for the adsorbed flocculant is most likely a reflection of the free Voigt peak fit to two states without X-ray line width and satellite removal. This causes the backbone carbon concentration in this analysis to be underestimated. Due to the problems associated with sample charging the XPS spectra were not of a sufficient signal to noise ratio to determine the adsorbed

configuration. The finding of a weaker ionic coupling could be suggestive of some surface hydroxyl groups coupling with the carboxylate groups via hydrogen bonding, however, this cannot be determined conclusively from the data.

4.7 PROPOSED ADSORPTION MECHANISM

Increasing caustic concentration and ionic strength did not alter the flocculant adsorption density. This suggests that flocculant adsorption is not electrostatically determined.

The FTIR spectra of adsorbed flocculant supports this and suggests a bridging bidentate structure at high pHs.

From the XPS data it is clear that complexation occurs to a cation other than sodium, and that sodium is displaced. Once again, implying a direct chemisorption of carboxylate to iron.

The proposed mechanism of how polyacrylate is adsorbed at the different pHs is shown in Figure 4.31.

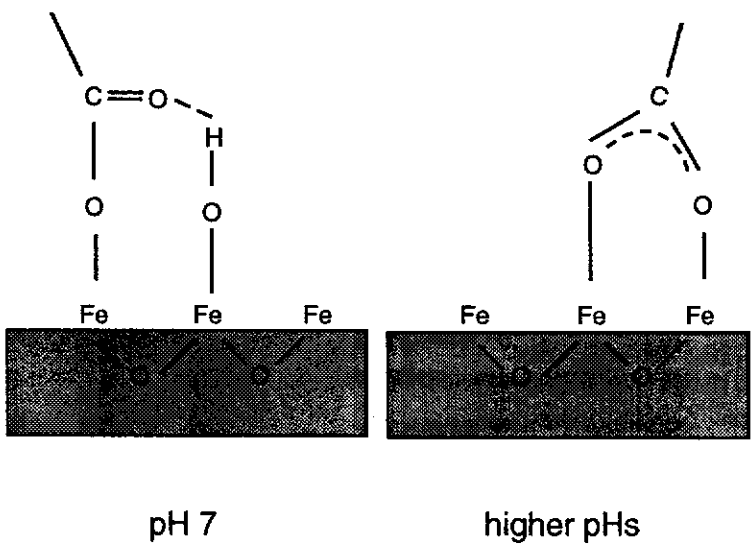

Figure 4.31 Proposed adsorption configuration for polyacrylate on the hematite surface at different pHs.

The aqueous slurry of hematite when contacted with hydroxide will cause the hydrated surface to deprotonate as is evidenced by the aggregation state of hematite before flocculant is added. It could then be argued that at higher pHs the increased number of $Fe\text{-}O^-$ groups then requires breaking the $Fe\text{-}O^-$ bond which may be less energetically favourable than breaking the Fe-OH bond. This would be one possible cause for the decreased settling observed on conditioning with hydroxide. If on the other hand, OH^- reacts to form additional Fe-OH groups it can be argued that this then blocks the flocculant's access to the surface irons with which it directly wishes to bond. The use of molecular modelling to determine which of these two mechanisms is predominant is discussed in Chapter 6.

4.8 SUMMARY

In working with hematite several important findings resulted and the following conclusions were drawn:

i) the hematite surface takes a long time to equilibrate in caustic solution (Figure 4.2) and this plays a role in how hematite flocculates, surface $Fe\text{-}O^-$ and/or Fe-OH groups may be formed during this process which results in a decrease in the flocculation efficiency.

ii) polyacrylate adsorption is not endothermic (Figure 4.9).

iii) the flocculation performance of hematite is kinetically controlled under Bayer conditions. Increased temperature improves flocculation performance because the liquor viscosity is reduced.

iv) in Bayer strength caustic solutions hematite is naturally coagulated (Figure 4.10).

v) the mechanism of aggregation is by flocculant bridging.

vi) polyacrylates are effective flocculants at very high caustic concentrations (Figure 4.11).

vii) optimum flocculation occurs at ~20 % of the monolayer coverage of flocculant

on the hematite surface.

viii) the initial aggregation state of the particles before flocculant addition is important (a flocculant adsorption density of 50 % monolayer coverage need not be optimal).

ix) although the polymer could adsorb in a flat conformation, as it does not occupy a great deal of surface area even at monolayer coverage, the extent of bridging flocculation suggests that only a small number of active surface sites exist on which the flocculant can adsorb.

x) caustic concentration does not affect the flocculant adsorption density on hematite (Figure 4.16).

xi) the decrease in flocculation performance with increasing caustic strength is partially explained by the increase in liquor viscosity but may also involve a lowering of the collision efficiency which lowers the bridging probability.

xii) the flocculant molecule conformation collapses to a limiting size in liquors of >1 M NaOH (Figure 4.19).

xiii) the bonding configuration of the polymer depends on the pH. At neutral pH a monodentate structure exists but at higher pHs a tilted bridging bidentate structure is formed (Figure 4.26).

xiv) the lack of an effect on polymer adsorption with increasing ionic strength, the shifts in peak positions in the infrared spectra and the XPS data showing displacement of sodium on flocculant adsorption all support a chemisorption mechanism of flocculation.

Settling of refinery residue solids gave inconsistent results and could not be used to obtain reliable data. The emulsion flocculant was found to show conformational readjustment over a 1-2 hour period (Figure 4.1) and the refinery solids showed a similar behaviour to pure hematite with increasing flocculant dosage in that the settling rate did not show complete re-dispersion.

5. THE EFFECT OF IMPURITIES ON HEMATITE FLOCCULATION

The difference observed between the settling characteristics of hematite and refinery residue solids are due to differences in mineralogy, physical properties and liquor composition. The waste solids in the refinery are a combination of several minerals, some of which are freshly precipitated after digestion. The solution species found in refinery Bayer liquors may also be important in determining settling characteristics. Known solution and solid species have been used to assess their impact on flocculation performance. Solid surface contaminants were studied to obtain information on the interaction occurring with the flocculant when DSPs precipitate from refinery liquors.

5.1 SOLUTION IMPURITIES

The effect that solution species have on flocculation was determined at 93 °C using a liquor that had a TC = 100, TA = 110, an A/TC = 0.3 with a flocculant dosage of 15 $\mu g\ g^{-1}$ and hematite Sample A, unless otherwise stated. The results were evaluated in light of the proposed mechanism of adsorption for polyacrylate on hematite.

5.1.1 SULPHATE, CHLORIDE AND PHOSPHATE

Sodium sulphate and chloride are two major salt species found in Bayer liquors. Phosphate is present in low levels, but Grubbs *et al.* (1980) found that the presence of small quantities of phosphate inhibits flocculation. The effect of these salts were investigated at concentrations which span the range found in normal refinery liquors.

The effect of sulphate (up to 50 $g\ L^{-1}$) on hematite flocculation is presented in Figure

5.1. Altering the sulphate concentration does not appear to affect the settling rate or turbidity. Both settling rate and turbidity vary within experimental error over the wide range of solution sulphate concentration studied.

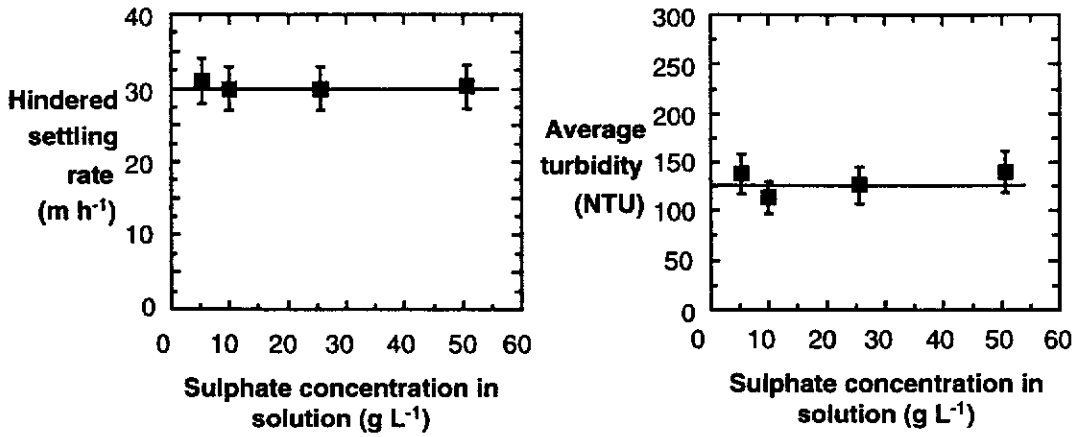

Figure 5.1 Flocculation performance of hematite in synthetic Bayer liquors at varying sodium sulphate concentration.

The adsorption density of polyacrylate on hematite was also not affected by the presence of sulphate in solution (Figure 5.2).

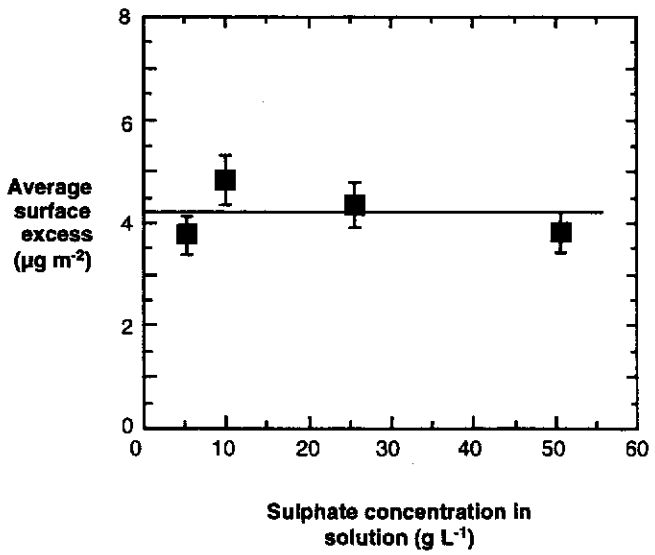

Figure 5.2 Adsorption of polyacrylate on hematite at varying sodium sulphate concentration.

The adsorption density of sulphate on hematite under synthetic Bayer conditions was not determined as the levels present in the liquor were so high as to cause excessive errors in the measurement of its loss from solution. Not withstanding this, it can be concluded that sulphate does not interfere with flocculant adsorption on hematite and therefore does not appear to interact with the hematite surface in a significant manner.

It is reasonable, therefore, to conclude that sulphate does not adsorb but is present as a 'screening' salt in the compressed double layer region and is readily displaced by the flocculant.

This result is in contrast to Basu *et al.* (1986) who stated that sulphate was beneficial to the settling of Bayer residue. As hematite was the only mineral phase investigated here, this may indicate a beneficial sulphate interaction with other mineral phases.

Chloride behaved similarly to sulphate with no effect on settling rate, flocculant adsorption density or turbidity being observed with increasing sodium chloride concentration (0 - 40 g L^{-1}). Determination of the adsorption density of chloride on hematite was also not undertaken due to the large excess in solution rendering meaningful results impossible to obtain. However, it can again be concluded that chloride is not detrimental to the amount of flocculant adsorbed.

Concentrations of 0 to 1200 mg L^{-1} phosphate were also found to have no effect on settling rate, turbidity or flocculant adsorption density. Chemical analysis (ICP) established that phosphate did not adsorb on the hematite surface over this concentration range. The latter result for phosphate is in agreement with literature reports indicating that increasing pH decreases phosphate adsorption (Parfitt *et al.*, 1977; White and Taylor, 1977) in aqueous systems.

While Grubbs *et al.*, (1980) have stated that phosphate inhibits flocculation of waste solids the results did not support this trend. This may be due to phosphate interacting with other minerals in the residue solids. However, the observations presented support O'Donnell and Martin (1976) who stated that phosphate consumed lime which is beneficial to flocculation performance but otherwise did not affect residue aggregation.

It can be concluded that the sodium salts of sulphate, chloride and phosphate do not adsorb on the hematite surface under Bayer conditions and at most form part of the compressed double layer. They do not inhibit flocculation and do not alter the quantity of flocculant adsorbed. Even increases in ionic strength due to their presence are not sufficient to alter the bridging efficiency of the polymer. It is also important to note that, once again, there was no evidence of increasing adsorption of polyacrylate with increasing ionic strength. This supports the proposed mechanism of chemisorption.

5.1.2 CARBONATE

Carbonate is present in all Bayer liquors due to the degradation of organics and the adsorption of CO_2 from the atmosphere. While it has been established that it is undesirable to have liquors containing high levels of carbonate, as aluminium extraction efficiency is lowered, the impact of carbonate on flocculation performance has yet to be quantitatively determined.

Increasing the amount of carbonate resulted in a steady, linear decrease of the settling rate and a simultaneous increase in turbidity (Figure 5.3). For example, the settling rate decreased from 23 m h^{-1} at 2 g L^{-1} to 14 m h^{-1} at 70 g L^{-1} carbonate, a 40 % reduction. The very minor change (2 %) in viscosity over this range of carbonate concentrations cannot account for this decrease. The distinction of the mudline also became more difficult as the carbonate concentration increased.

The decrease in flocculation performance cannot be due to changes in the flocculant conformation, as it has been shown (Section 4.4.2) that at 1 M NaOH the flocculant has already attained its limiting size and these experiments correspond to 1.89 M NaOH.

The adsorption density of the flocculant (at a fixed dosage of 15 $\mu g\ g^{-1}$) was found to decrease significantly with increasing carbonate concentration, from 5.0 to 1.5 $\mu g\ m^{-2}$ (Figure 5.4). Carbonate does not, therefore, behave in the same way as sulphate, chloride or phosphate.

The results show that carbonate competes with polyacrylate flocculants for surface adsorption sites on the hematite under Bayer liquor conditions. As the concentration of sodium carbonate increases, the driving force for its adsorption is also increased leading to fewer surface sites for the flocculant to adsorb. However, given the overall thermodynamics of the system, even at high concentrations of sodium carbonate some flocculant will also adsorb due to entropy effects (Lyklema, 1995).

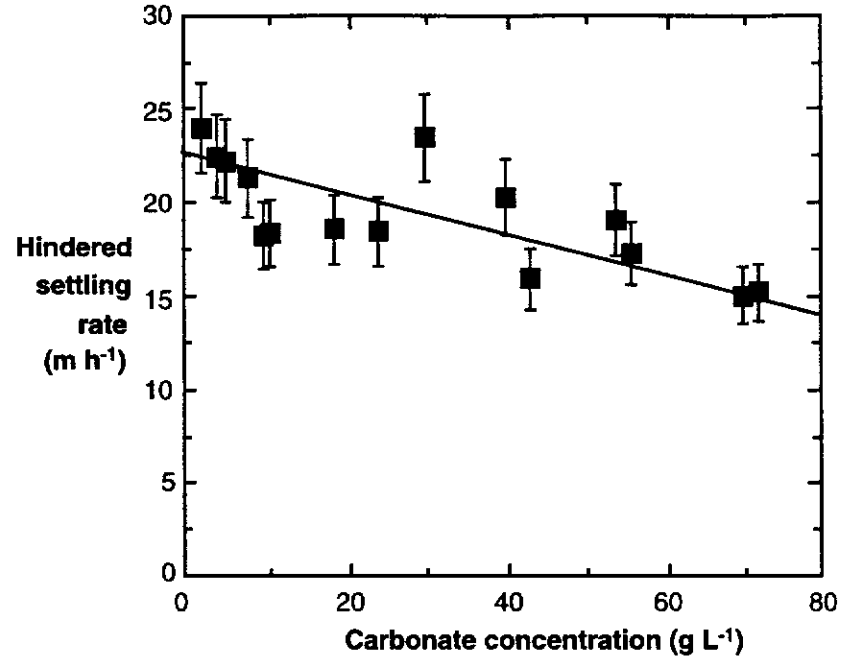

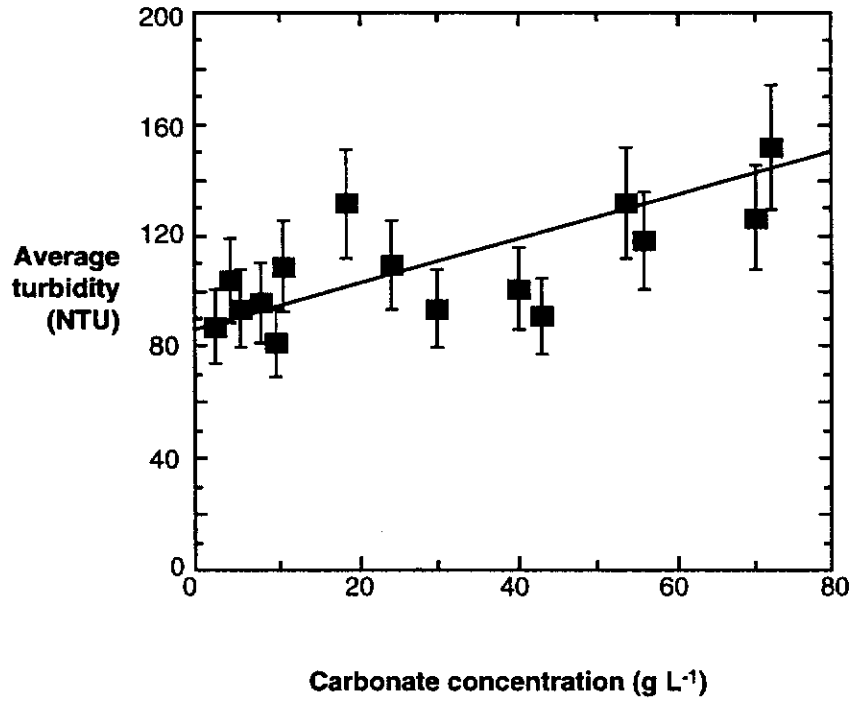

Figure 5.3 The observed flocculation performance as a function of increasing sodium carbonate concentration.

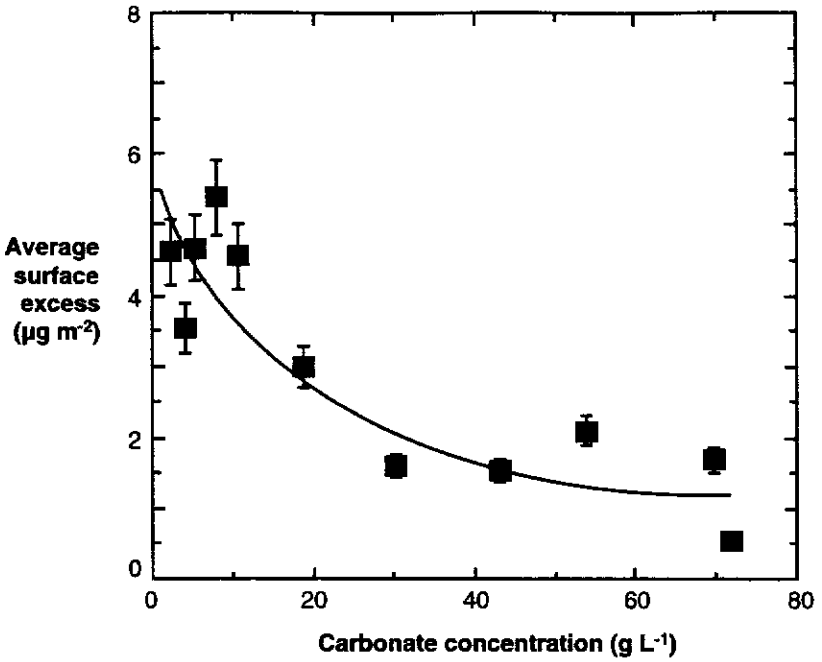

Figure 5.4 The adsorption density of polyacrylate flocculant with increasing sodium carbonate concentration.

The importance of entropy to the relative adsorption affinity of carbonate and polyacrylate was shown by conducting a batch settling test in the same manner as for the results in Figure 5.3 except that the flocculant was added prior to the sodium carbonate. After 1 h for equilibration, the residual flocculant concentration in the liquor was determined. It was found that no significant change in settling rate occurred while turbidity deteriorated slightly (Figure 5.5).

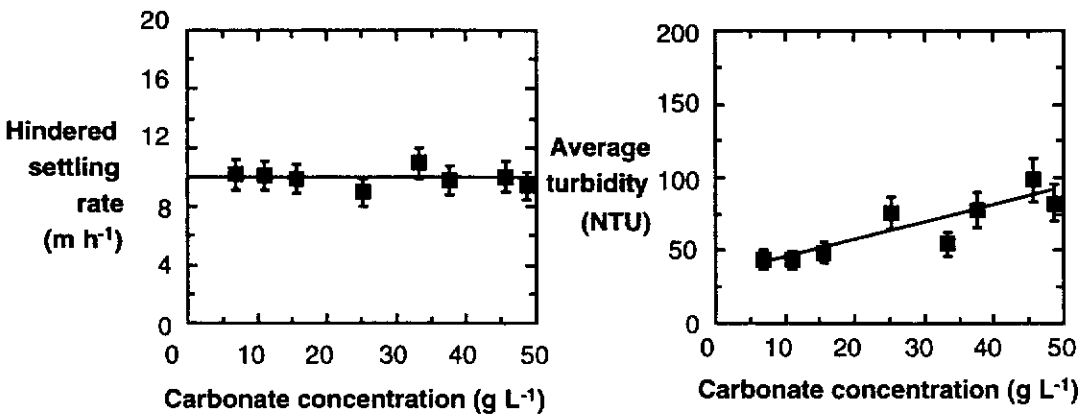

Figure 5.5 Flocculation performance results of hematite at varying sodium carbonate concentrations with flocculant addition prior to carbonate addition.

Notably, the adsorption density of the flocculant remained unchanged with increasing carbonate concentration (Figure 5.6), in contrast to the situation in Figure 5.4 when the carbonate was added prior to the flocculant. The adsorption density is similar to that when flocculant is added after carbonate at 10 g L^{-1}. This indicates that this polyacrylate flocculant is not displaced by the carbonate, while carbonate is displaced by the flocculant.

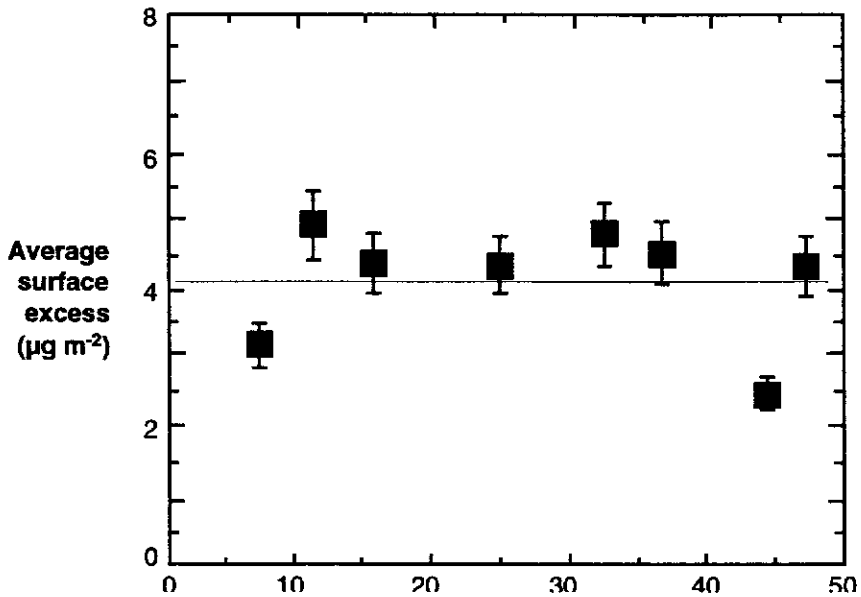

Figure 5.6 Flocculant adsorption density on hematite at varying sodium carbonate concentrations with flocculant addition prior to carbonate addition.

That both carbonate and polyacrylate are attracted to the hematite surface is not unexpected as both their functional groups are similar (Figure 5.7). The interaction of carbonate with hematite is thus postulated to be the same as the interaction of flocculant with hematite.

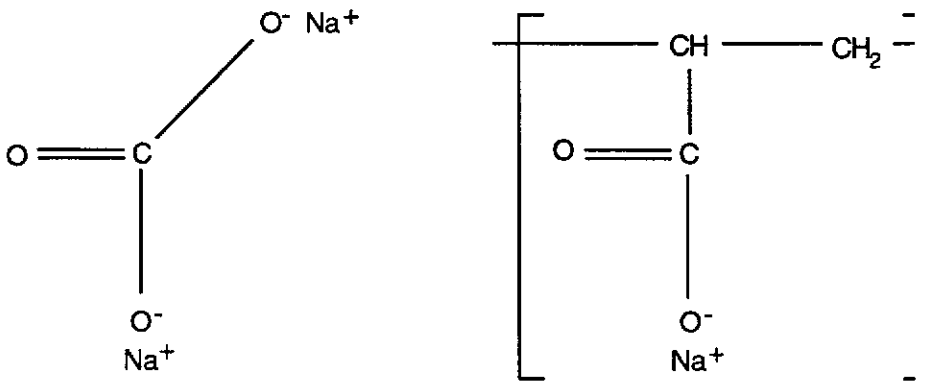

Figure 5.7 Schematic representation of a sodium carbonate molecule and a unit of sodium polyacrylate.

The observations presented here are analogous to when polydisperse flocculants adsorb. Lyklema (1995) showed that adsorption affinity of a flocculant increases with the chain length due to entropy effects. If carbonate can be considered to be a 'zero chain polyacrylate flocculant' then, based upon Lyklema's (1995) findings, it would be expected to have the observed lower adsorption affinity on hematite than the flocculant.

Hunter *et al.* (1990) stated that increasing carbonate levels deteriorated flocculation but did not provide evidence to support this. Thus, for the first time it has been clearly shown that if carbonate is present it will interfere and compete with polyacrylate for surface sites on hematite.

The increase in turbidity without a decrease in settling rate (Figure 5.5) is not due to conformational effects of the polymer (with increasing ionic strength) as the polymer is already at its limiting size as shown in Section 4.4.2. It may simply be due to aggregate rupture caused by the longer mixing regime (16 strokes) required to properly disperse this system.

5.1.3 CALCIUM

Many literature reports claim that calcium is beneficial to Bayer residue settling (Yamada *et al.*, 1980; Spitzer *et al.*, 1991; Rothenberg *et al*, 1989; Hunter *et al.*, 1990) and some postulate that the mechanism of adsorption for the flocculant is an electrostatic interaction via a calcium bridge to the surface (Rothenberg *et al*, 1989).

Calcium chloride was used as the source of calcium since chloride does not interact or interfere with flocculation (Section 5.1.1). Pure caustic solution rather than synthetic liquors were used in this study because C31 (the aluminium source in liquor preparation) contains entrained calcium (resulting in up to ~15 $\mu g\ g^{-1}$ dissolved Ca^{2+}). As it has been shown previously that the A/TC ratio did not affect flocculation performance or adsorption density, the results are applicable to the Bayer system.

The adsorption isotherm (Figure 5.8) of calcium on hematite shows Langmuir behaviour reaching a plateau at ~3 $\mu g\ g^{-1}$ Ca^{2+} in solution with a monolayer of 80±8 $\mu g\ m^{-2}$. This equates to approximately 2 μM calcium per m^2 of hematite. The levels of calcium investigated and the isotherm show that precipitation of calcium (as

the hydroxide) was not occurring (a further sharp increase in adsorption density at high calcium concentrations after the plateau would indicate precipitation). Thus, precipitation of a fresh surface could be excluded as a possibility.

The Langmuir-Freundlich curve which described the isotherm had the following parameters: A = 80 μg m^{-2}, B= 3.23, x = 1.00. Both x and B are higher than those found for flocculant on hematite previously (Section 4.3.1.1); firstly x = 1 shows the isotherm observed Langmuir behaviour and that all surface sites are equivalent thermodynamically and, secondly, B was ~3 which when compared to 0.01 for the flocculant shows that calcium has a much higher affinity for the surface under the same conditions than flocculant for the hematite surface. The equilibrium of the adsorption reaction favours the adsorption of calcium to the surface since B>1.

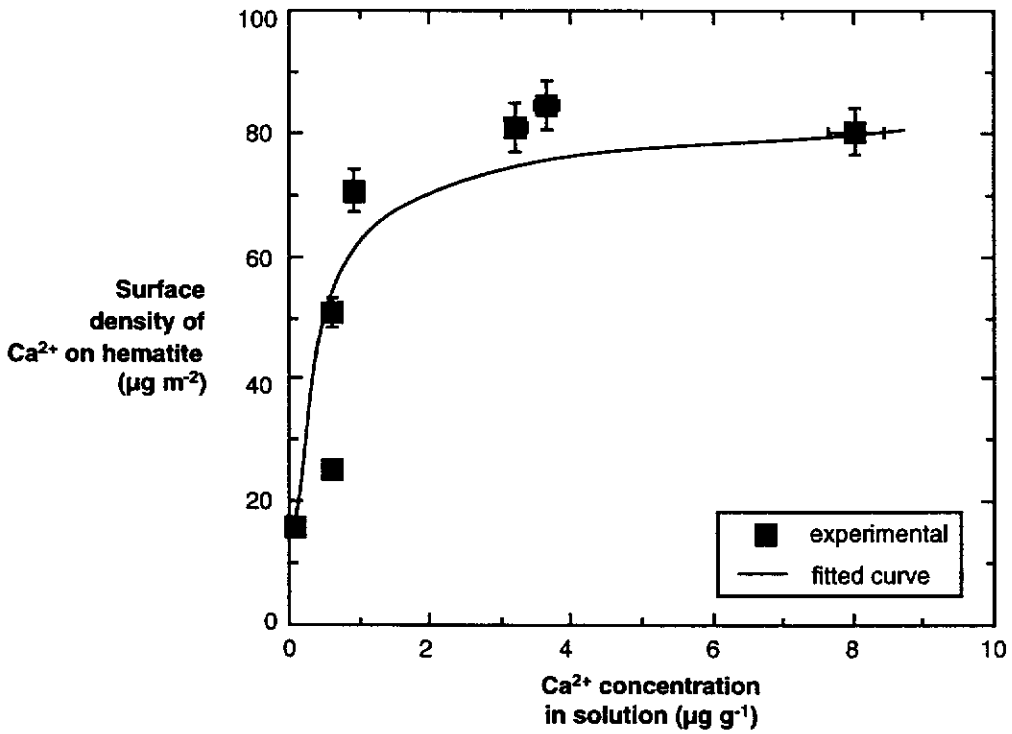

Figure 5.8 Adsorption isotherm of calcium on hematite under Bayer conditions.

The settling rate results with increasing calcium are surprising in that, although they show some scatter, they do not show any significant trend. That is, no increased or decreased settling rate is observed. However, the turbidity shows an improvement with increasing calcium in solution (Figure 5.9).

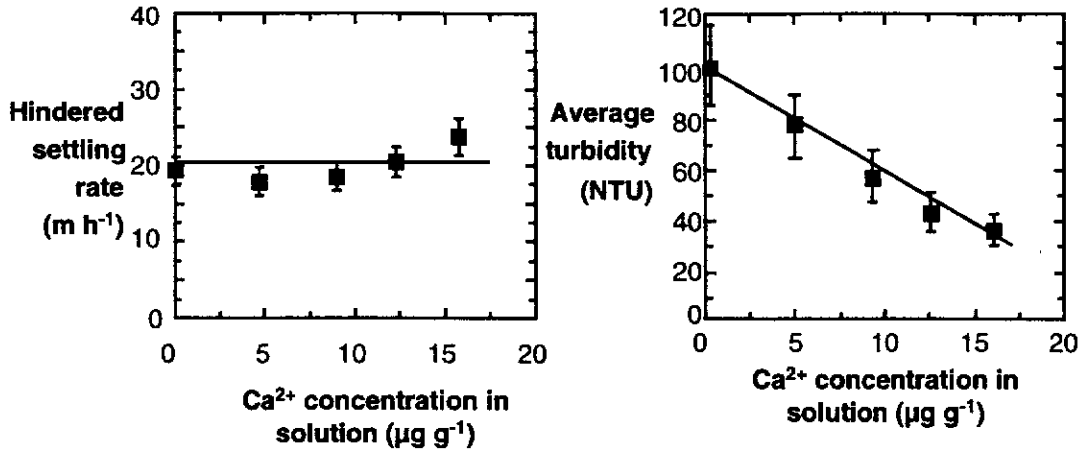

Figure 5.9 Flocculation performance of hematite in the presence of varying calcium concentration.

The settling results do not support most of the literature available on the effect of calcium (Yamada *et al.*, 1980; Spitzer *et al.*, 1991; Rothenberg *et al*, 1989; Hunter *et al.*, 1990), in that hematite settling was not improved. It cannot be concluded, however, that the results are in conflict. All previous data available on the effect of calcium has been obtained for residue solids which are of mixed mineral composition. It is quite possible that calcium does not improve hematite settling but does beneficially affect other minerals.

The adsorption of flocculant onto hematite in the presence of calcium is shown in Figure 5.10. No dependence of the adsorption density on the concentration of calcium in solution was observed. Thus, the improvement in turbidity can not be related to increased flocculant adsorption on hematite.

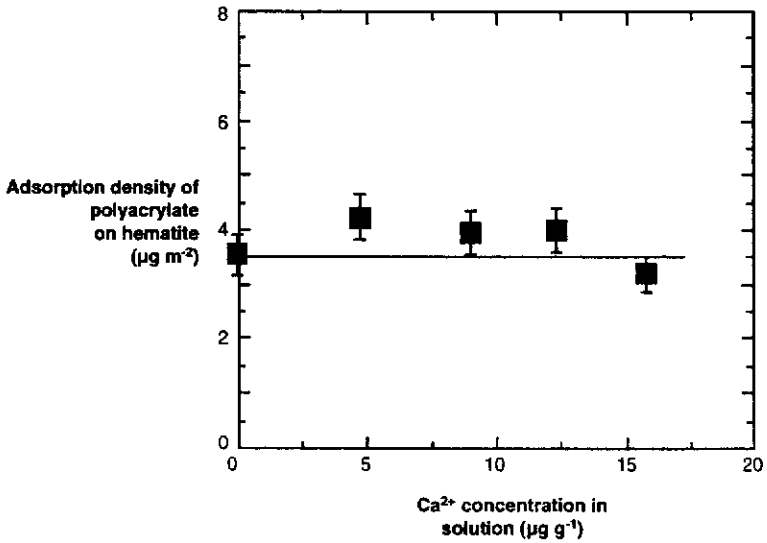

Figure 5.10 The adsorption density of polyacrylate on hematite in pure caustic in the presence of varying calcium concentration.

The electrostatic interaction proposed by Rothenberg *et al.* (1989), is not supported by these results, however, the mechanism derived in the previous chapter is further strengthened. The presence of a divalent cation on the hematite surface should have shown improved adsorption of flocculant if an electrostatic interaction was occurring. It appears that the only impact calcium has on flocculation of hematite is on turbidity.

Since no additional flocculant is adsorbed the improved clarity with increasing calcium in solution must be due to more bridging between particles which incorporates more fines within the aggregate structure. Perhaps, unadsorbed acrylate units within the adsorbed flocculant are electrostatically bound to residual particles containing adsorbed calcium. An approximate calculation, based on the values from the adsorption isotherm of calcium (Figure 5.8) and the present results for the flocculant (Figure 5.10), shows ~10 calcium atoms per flocculant molecule are present on the surface of the hematite. The presence of such calcium atoms has not induced more flocculant molecules to adsorb but may offer additional bridges between particles resulting in a lower turbidity (Figure 5.11).

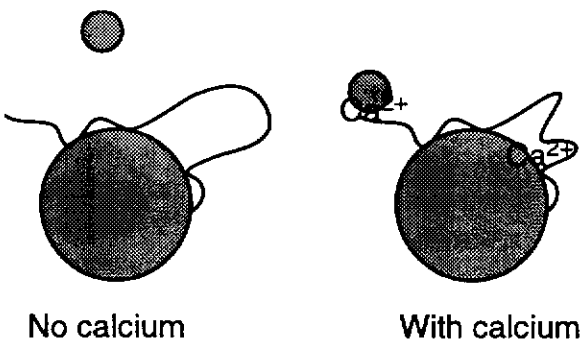

Figure 5.11 Schematic representation of the possible role of calcium.

5.1.3.1 Infrared spectra of polyacrylate adsorbed on hematite in the presence of calcium

DRIFT spectra of polyacrylate adsorbed in the presence of 20 $\mu g\ g^{-1}$ added calcium are summarised in Table 5.1. The results for pure caustic are included for comparison. The presence of 20 $\mu g\ g^{-1}$ calcium was chosen as this would guarantee a monolayer of adsorbed calcium on the hematite.

Table 5.1 Calculated Δν for the symmetric and asymmetric COO^- stretches of polyacrylate and adsorbed flocculant in the presence of 20 μg g^{-1} calcium.

Polyacrylate salts and adsorption conditions	ν_{asym} COO^- (cm^{-1})	ν_{sym} COO^- (cm^{-1})	separation Δν (cm^{-1})
AN995SH, Na^+ salt	1567±2	1407±2	160±4
AN995SH, Ca^{2+} salt	1552±2	1411±2	141±4
pH 7	1731±4	-	-
	1674±4	1382±4	292±8
pH 11	1586±4	1412±4	174±8
pH 13	1589±6	1410±6	179±8
pH 14	1599±6	1411±6	188±12
pH 7, Ca^{2+}	1725±4	-	-
(20 μg g^{-1})	1652±4	1410±4	242±8
	1546±4	1410±4	136±8
pH 13, Ca^{2+} (20 μg g^{-1})	1594±6	1411±6	182±12
pH 14, Ca^{2+} (20 μg g^{-1})	1585±6	1406±6	179±12

The results shows that in the presence of calcium at pHs>11 there are no significant differences in the conformation of adsorbed polyacrylate (Figure 5.12), the spectra show similar peak positions and separations as to when calcium is absent. A bridging bidentate structure (III) is indicated as was found in the absence of calcium (Figure 4.22).

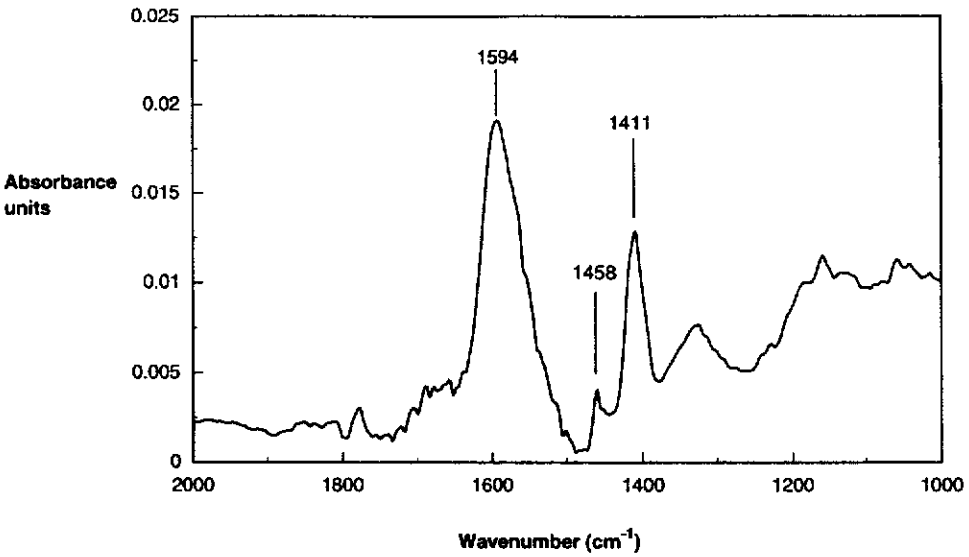

Figure 5.12 DRIFT spectra of adsorbed flocculant on hematite at pH 13 in caustic containing 20 μg g^{-1} calcium.

At pH 7 (Figure 5.13), the 1725 and 1625 cm^{-1} bands indicate the same hydrogen bonded C=O, monodentate structure found in the absence of calcium. The bands at 1546 and 1410 cm^{-1} suggest that a bidentate structure is also formed. As Δν (136 cm^{-1}) is slightly smaller than for the flocculant salts (Na^+ 160 cm^{-1}, Ca^{2+} 141 cm^{-1}) and calcium is known to complex polyacrylate in solution (Miyajima *et al.*, 1996; 1997) a bidentate chelating structure (II) is indicated. Having already determined that the calcium adsorbs on the hematite surface it can be concluded that the flocculant is both monodentate chemisorbed to the hematite and electrostatically complexed to calcium. The proposed structures are shown in Figure 5.14.

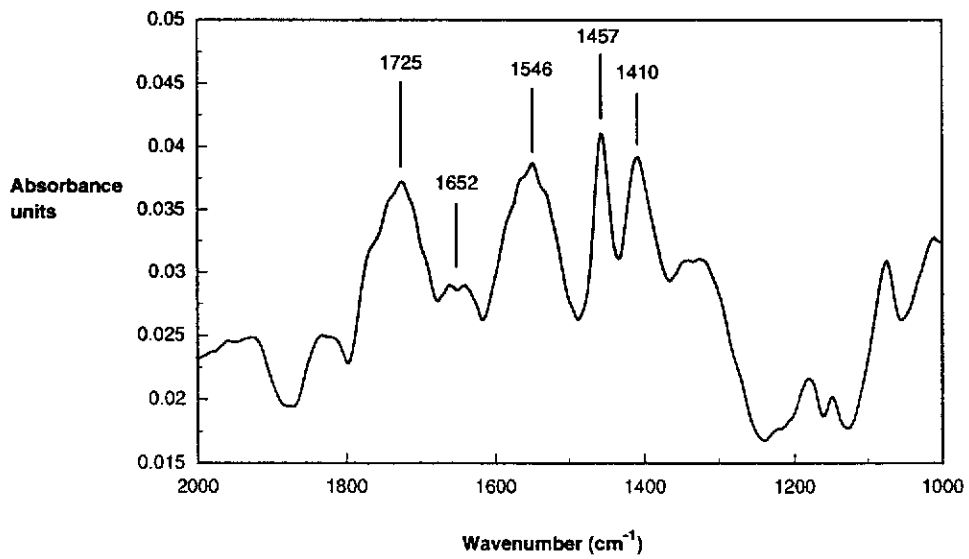

Figure 5.13 DRIFT spectra of adsorbed flocculant on hematite at pH 7 in caustic containing 20 μg g^{-1} calcium.

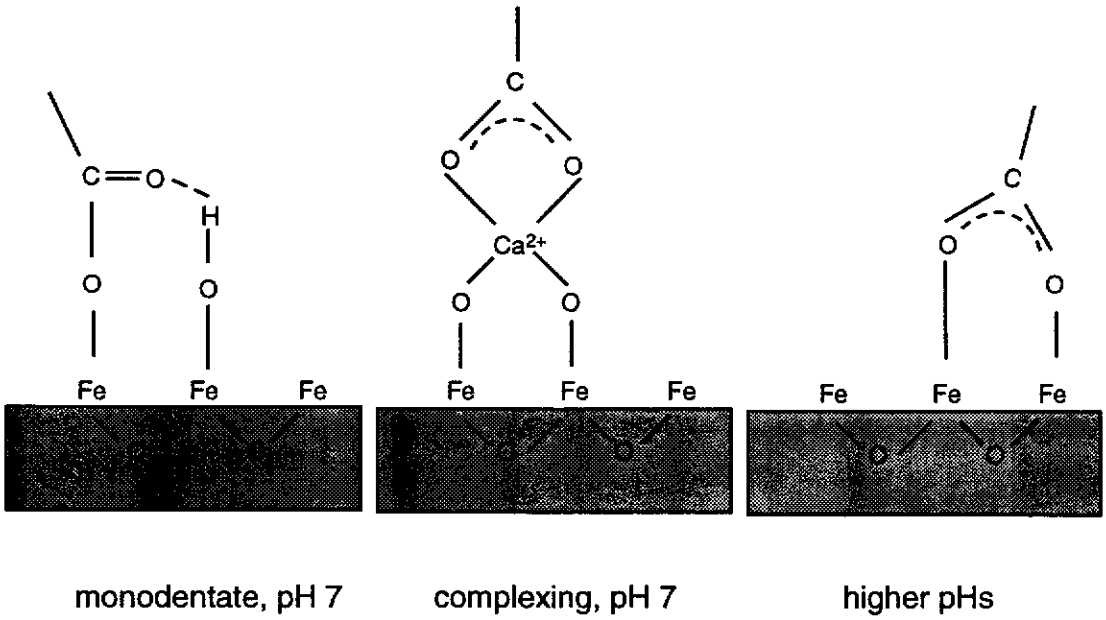

Figure 5.14 Proposed adsorption mechanism in the presence of calcium.

The additional mechanism of electrostatic complexation of the flocculant by the calcium supports the turbidity results in Bayer liquor. That is, more carboxylate units may have adsorbed on the particle surfaces, but the mass of the adsorbed flocculant as whole is unaltered (4 $\mu g\ m^{-2}$). The complexed flocculant however, can not be the dominant mode of flocculation at pHs >7 as it is not observed in the infrared spectra of flocculated hematite in the presence of calcium at pHs ≥13.

The hypothesis put by Rothenberg *et al.* (1989) that the calcium electrostatically binds the flocculant to the mineral surface is only partially correct for the case of hematite. If calcium is present some carboxylate units will electrostatically adsorb, but the dominant mode of adsorption is still direct chemical interaction with the surface of the hematite.

5.1.4 SILICATE

Low levels of silicate are normally found in alumina refineries as most reactive silica has been reacted to form DSPs. However, like calcium, these low levels may be sufficient to impact on flocculation behaviour.

Silicate was added to synthetic liquors as sodium metasilicate and the Si levels measured before and after flocculation. Results showed that as for calcium, the silicate had adsorbed on the surface of the hematite (Figure 5.15), but unlike calcium a

monolayer had not been reached even at the highest level added (1000 μg g^{-1}). Thus, it appears that silicate adsorbs strongly on the hematite surface (adsorbing ~70 % of the added silicate).

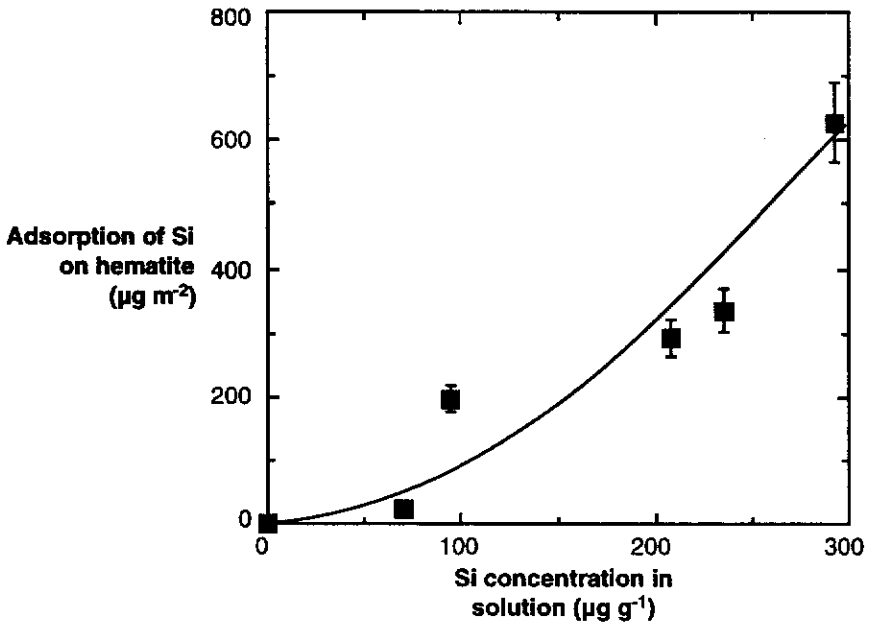

Figure 5.15 Adsorption density of Si on hematite under Bayer conditions.

Due to the high concentration of aluminium in solution it could not be determined whether the adsorption was of a pure silicate or of an aluminosilicate species (which would involve the loss of aluminium from solution).

Settling rates were found to decrease significantly and turbidity increased with increasing silicate in solution (Figure 5.16). The settling rate decreased from ~39 m h^{-1} to 20 m h^{-1} with just 200 μg g^{-1} Si in solution. As was found for carbonate, the distinction of the mudline also deteriorated with increasing silicate addition.

The adsorption of polyacrylate decreases markedly with increasing silicate adsorption (Figure 5.17) from ~6 μg m^{-2} to ~2 μg m^{-2} at 350 μg m^{-2} Si on hematite. This suggests that silicate, like carbonate, competes for adsorption sites with the flocculant.

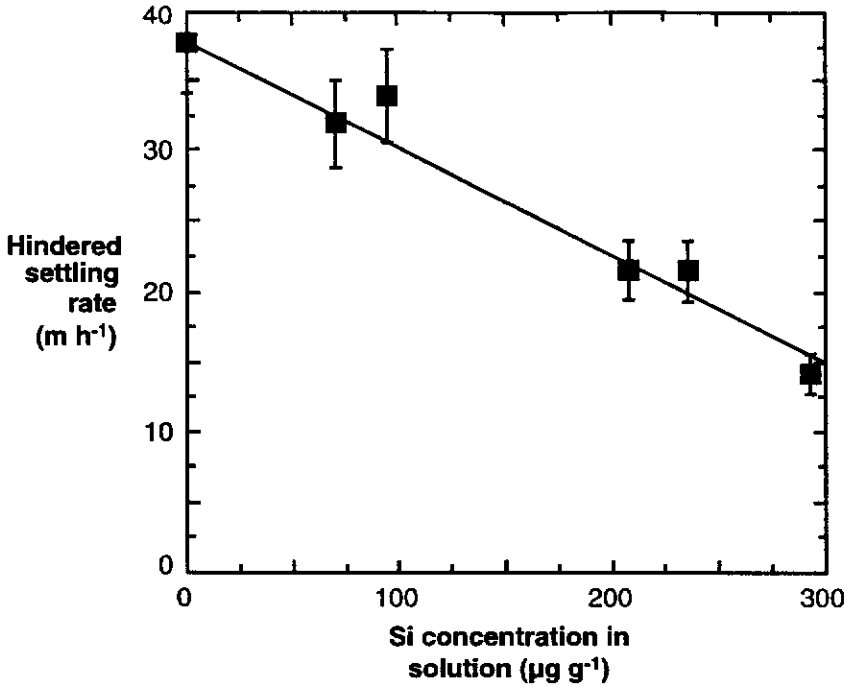

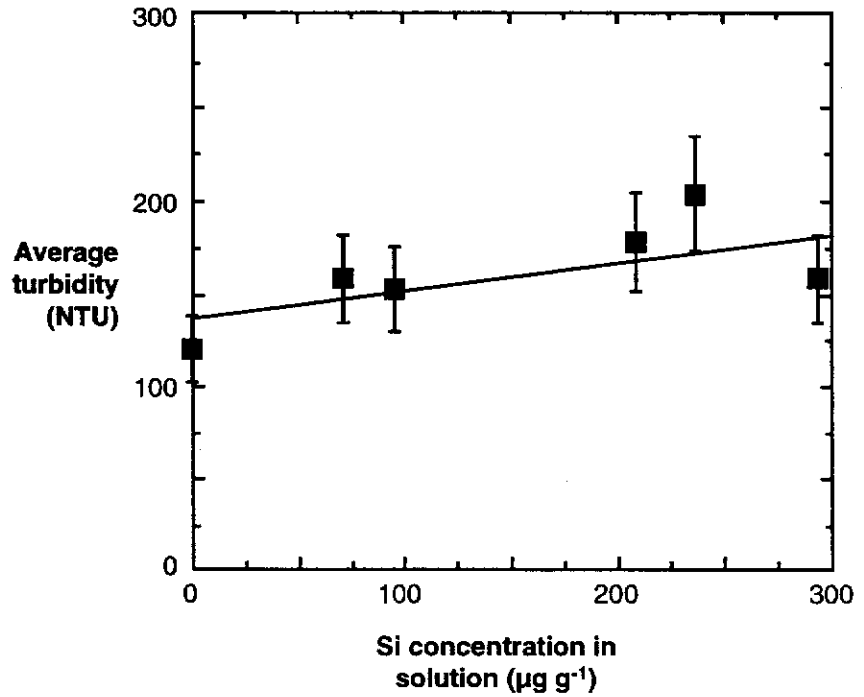

Figure 5.16 Flocculation performance of hematite in synthetic liquor at varying Si solution concentration.

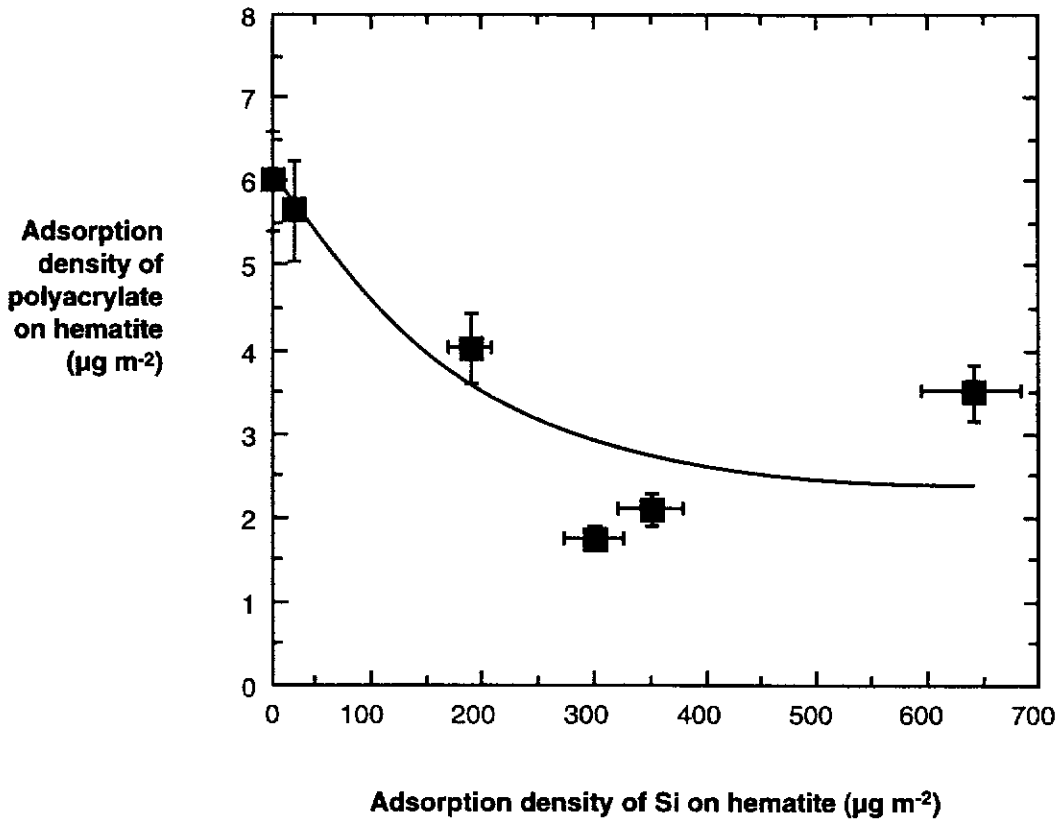

Figure 5.17 The adsorption density of polyacrylate on hematite as a function of the adsorption of Si on hematite under Bayer conditions.

The DRIFT spectrum of hematite flocculated in the presence of silicate (Figure 5.18) confirms that the silicate was indeed adsorbing. Broad bands in the 1200-900 cm^{-1} region are characteristic of (alumino)silicate species (Farmer, 1974; Wada, 1989; Drees, 1989). The other bands in the spectrum appear to be those of the flocculant, and a bridging bidentate structure for the polyacrylate flocculant would be predicted from their positions.

Of major significance is that silicate is competing effectively with the flocculant at µg g^{-1} levels whereas carbonate begins to compete at g kg^{-1} concentrations. The silicate concentrations causing deterioration in settling and turbidity are only an order of magnitude greater than the flocculant concentrations used to aggregate the system.

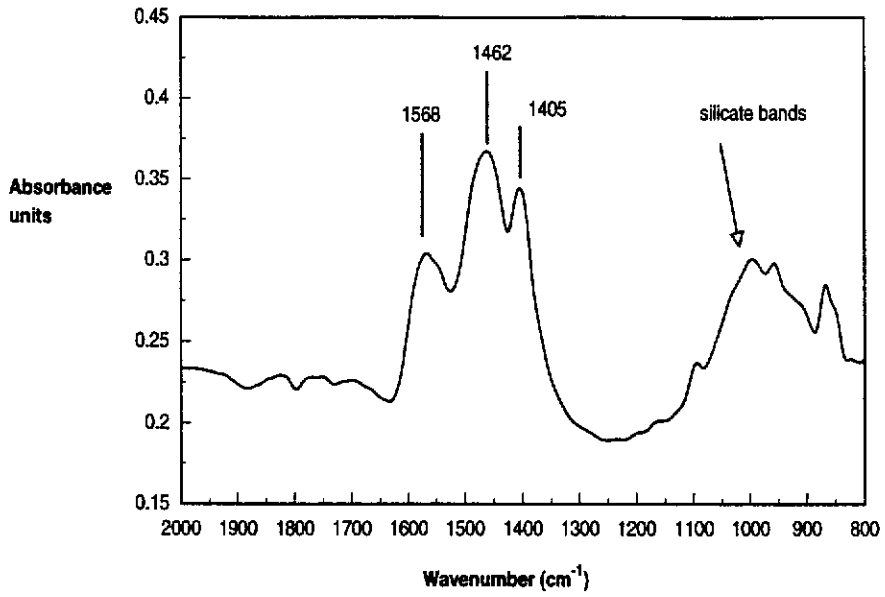

Figure 5.18 DRIFT spectrum of silicate adsorbed on hematite.

It is evident that the silicate has a strong affinity for the hematite surface and that, hence, it is the adsorption of silicate on hematite blocking active sites (Figure 5.19) rather than solution complexation of the flocculant which is the cause of the reduced flocculant performance. Also, it should be noted that the adsorbed silicate may be part of a alumino-silicate structure as they are known to form under these conditions (Section 1.1.3.2).

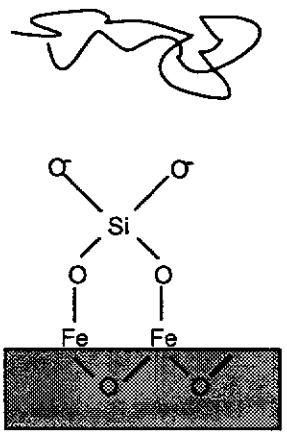

Figure 5.19 Schematic of silicate adsorption on hematite blocking flocculant adsorption.

5.2 SOLID IMPURITIES

Hematite Sample C contains a natural, homogenous surface impurity of an amorphous (alumino)silicate (Section 3.1.1) composition and this was utilised to assess the impact of surface impurities on aggregation. The results were compared with hematite Sample A, subjected to digestion in the presence of kaolin in order to mimic desilication, as a means of determining the importance of silicate reprecipitation on flocculation behaviour.

The settling tests for hematite Sample C and the digested samples were conducted in liquors comprising TC = 100, TA = 110 and A/TC = 0.3 unless otherwise stated.

The effect of altering the physical properties of refinery solids was also investigated by adding different sand fractions to refinery solids and then determining the settling characteristics. The refinery solids were tested in refinery liquor whose composition was given in Section 3.3.4.

5.2.1 THE EFFECT OF A HOMOGENOUS SURFACE CONTAMINANT

SEM did not show that the natural amorphous silicate impurity on hematite Sample C consisted of individual particles and FTIR analysis suggested that it was a surface contaminant. It was therefore concluded that the impurity was a homogenous layer; that is, a precipitated surface coating. Hematite Sample C, thus provided an opportunity to further test silicate surface contaminants and their effect on flocculation.

5.2.1.1 Contacting the solids with caustic

As the contaminant on hematite Sample C is a silicate, contact with strong caustic could alter the surface. Batch settling tests were conducted with 200 $\mu g\ g^{-1}$ AN995SH flocculant after the hematite was conditioned with caustic having a TC = 200.

Flocculation tests indicate that the surface characteristics were changing during the first 24 - 48 hours, as the settling rate and turbidity did not alter significantly if the hematite had been contacted with caustic for longer than this period (Figure 5.20).

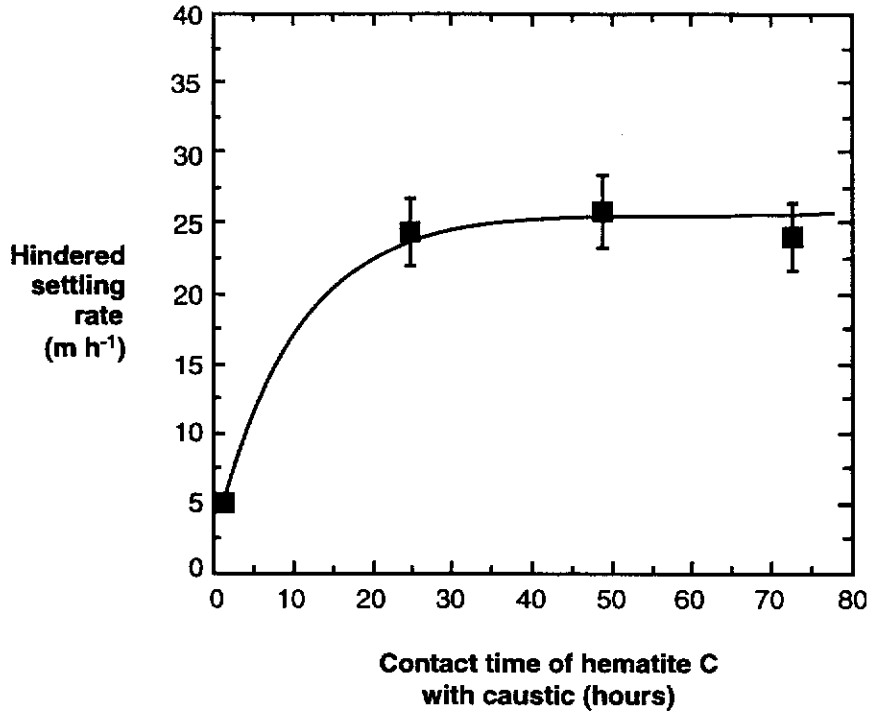

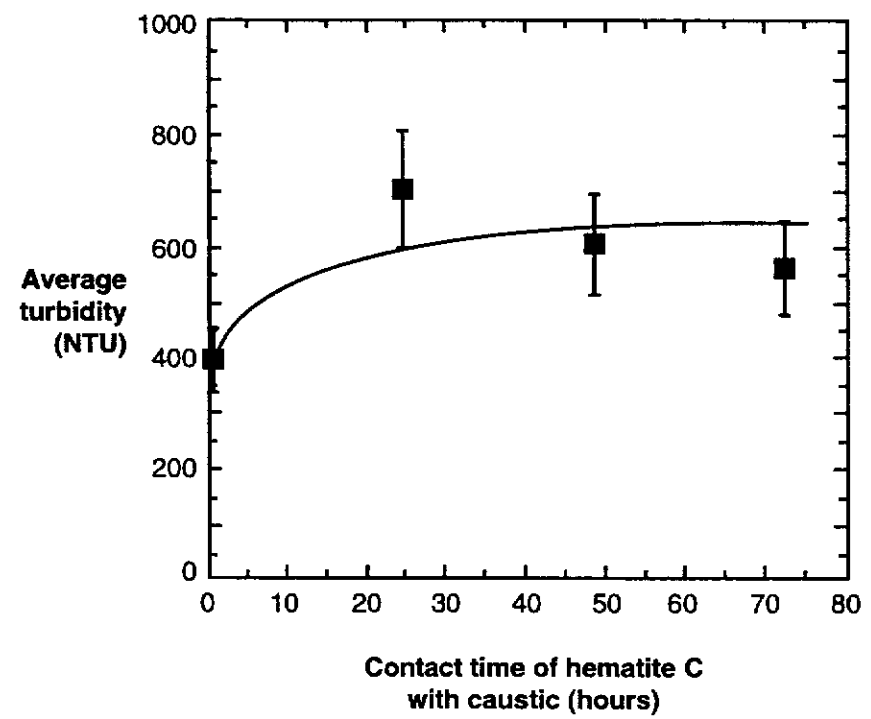

Figure 5.20 Flocculation performance for hematite Sample C after different contact times with caustic solution (TC = 200).

Flocculation was found to be very inefficient in the early stages (0 - 20 hours) which suggests that the surface contaminant limits flocculant adsorption and that flocculation only occurs after it has been, at least partially, removed. The trend in flocculation for this hematite sample is rather different to the case with hematite Sample A where contact with caustic resulted in a decreased settling rate. The increase in turbidity observed over this time is probably due to dissolution of the amorphous silicate and the consequent release of small particles (particle number effect resulting in higher turbidity).

The dissolution of the silicate was confirmed from DRIFT spectra (Figure 5.21) which showed a decrease in the Si-O stretch region after the hematite had been treated with TC = 200 caustic for 24 hours.

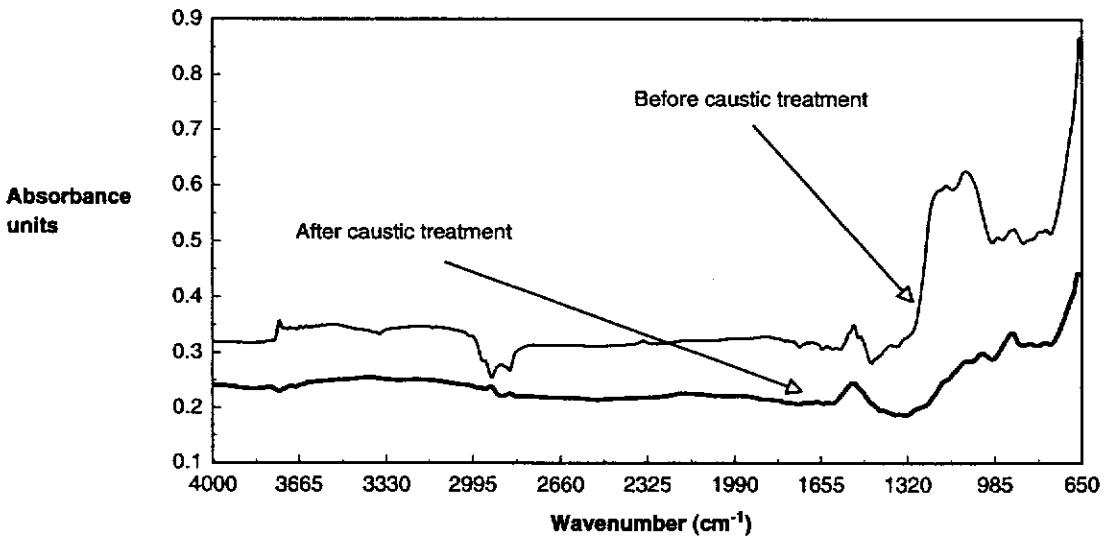

Figure 5.21 DRIFT spectra of Sample C before and after contact with caustic, TC = 200, 24 hours.

Seen in conjunction with the results obtained for dissolved silicate (Figure 5.16), it is clear that silicate inhibits flocculation of hematite regardless of whether it is already deposited on the surface or whether it is adsorbed from solution during processing.

As both settling rate and turbidity had stabilised after a 48 hour contact time with caustic solution, a conditioning period of 48 hours in caustic solution was maintained throughout all subsequent experiments with hematite Sample C.

5.2.1.2 Effect of flocculant dosage

The effect of flocculant dosage was studied and an adsorption isotherm constructed simultaneously for hematite Sample C (after conditioning with caustic for 48 hours) in the following liquor; TC = 100, TA =110, A/TC =0.3 at 95 °C.

The settling rate data (Figure 5.22) for hematite Sample C generally supports the results obtained for hematite Sample A. However, for this sample a slight drop in settling is evident at the higher flocculant dosages (and thus some re-dispersion is occurring), as was found for the refinery solids. The turbidity increases to a plateau as flocculant dosage increases (Figure 5.22). In the case of hematite Sample A, the residual turbidity was relatively stable, for hematite Sample C there is an initial rise but a steady residual turbidity eventually results. The similarity between the refinery settling results and this sample, both of which show some redispersion, may be indicative of an effect of silicate. That is, the presence of adsorbed silicate on residue solids could cause some dispersion, particularly as it is evident silicate does not interact with the flocculant.

The eventual plateau seen in the turbidity measurements is probably a result of the rate of particle-particle collisions compared to the rate of flocculant adsorption, as found for hematite Sample A.

The adsorption isotherm for hematite Sample C shows a lower plateau value under identical liquor conditions as those for which the isotherm was obtained for Sample A, clearly an effect of the surface contaminant (Figure 5.23). For hematite Sample A the plateau value was 164 ± 16 μg m^{-2} while for Sample C it is 63 ± 6 μg m^{-2}.

The adsorption isotherm was able to be fitted using a Langmuir-Freundlich equation with the following parameters: A = 63 μg m^{-2}, B = 0.01 and x = 1.90. That is, the B and x values are equivalent to the hematite Sample A results and only the monolayer coverage differs. This is further evidence that the affinity of the flocculant to the surface has not altered and that the silicate is merely blocking available adsorption sites.

The low plateau value observed could be caused by two mechanisms:

- the dissolved silicate readsorbs and hinders flocculation
- the amorphous silicate is not fully removed

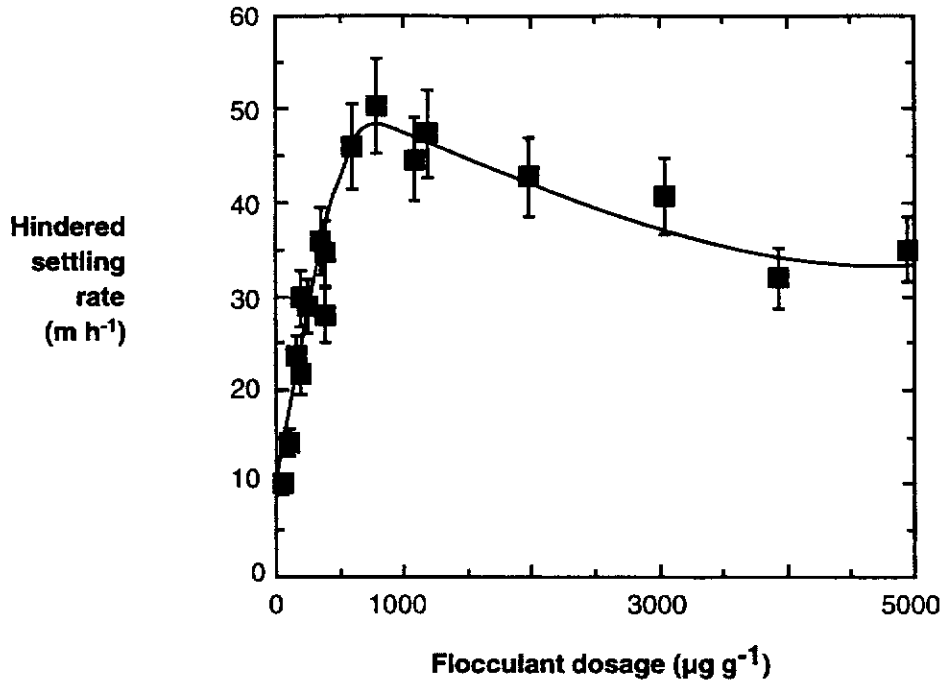

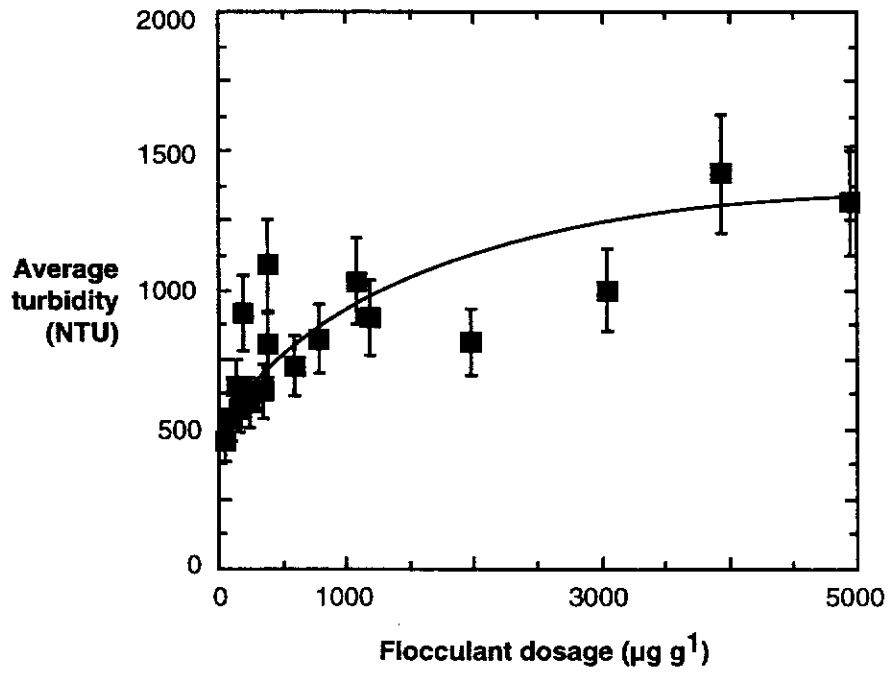

Figure 5.22 The flocculation performance of hematite Sample C with increasing flocculant dosage.

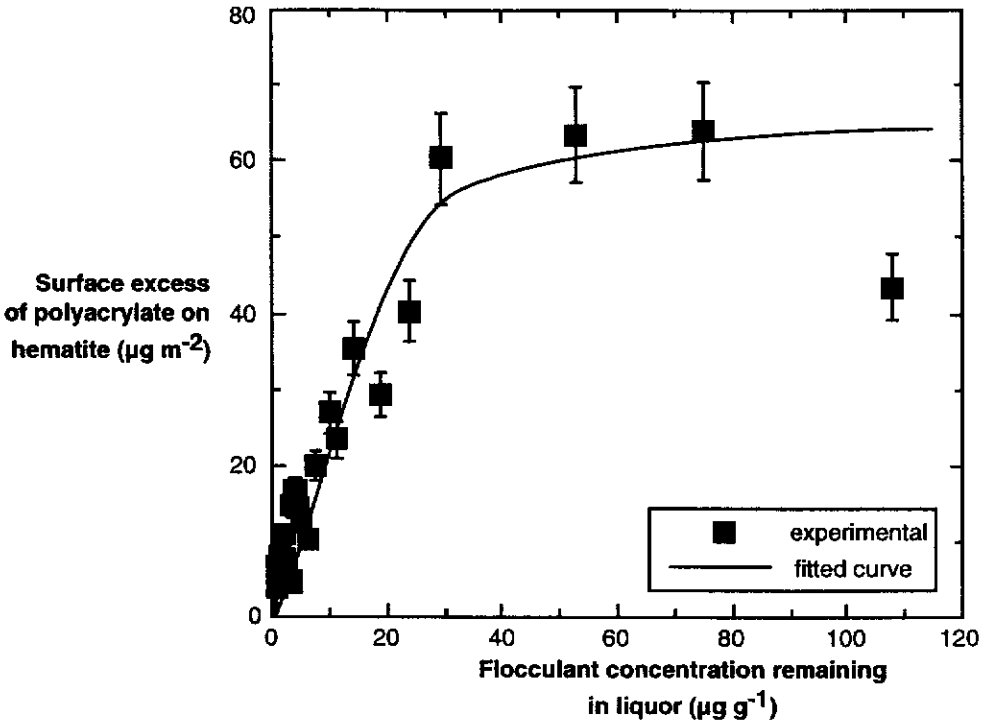

Figure 5.23 Adsorption density of polyacrylate adsorbed on hematite Sample C.

Readsorption of the silicate has already been shown to be possible from the solution silicate results (Section 5.1.4). However, it is just as likely that the surface contaminant is not completely removed on contact with caustic and this stops flocculant adsorption. Either mechanism limits flocculant interaction with the surface. This agrees with Bell's (1976) finding that DSPs hindered starch adsorption. Thus, both polyacrylate and starch do not interact with amorphous silicates.

5.2.1.3 Effect of caustic

In view of earlier results which showed that caustic altered the surface characteristics of hematite Sample C and Sample A, the effect of caustic was assessed to determine if there were any differences in flocculation behaviour between Sample C and Sample A after conditioning both samples with caustic. The flocculation tests were conducted at 93 °C under varying caustic concentrations with a constant carbonate concentration of 10 g L^{-1}, A/TC = 0.3 and 200 μg g^{-1} AN995SH flocculant.

For hematite Sample C the settling rate decreased (as was observed for Sample A in Figure 4.15) with increasing caustic concentration, however, no flocculation was observed beyond a TC of 200 (Figure 5.24). This 'shut-down' point for flocculation is extremely low in process terms, as refineries routinely operate at TC ≥ 200.

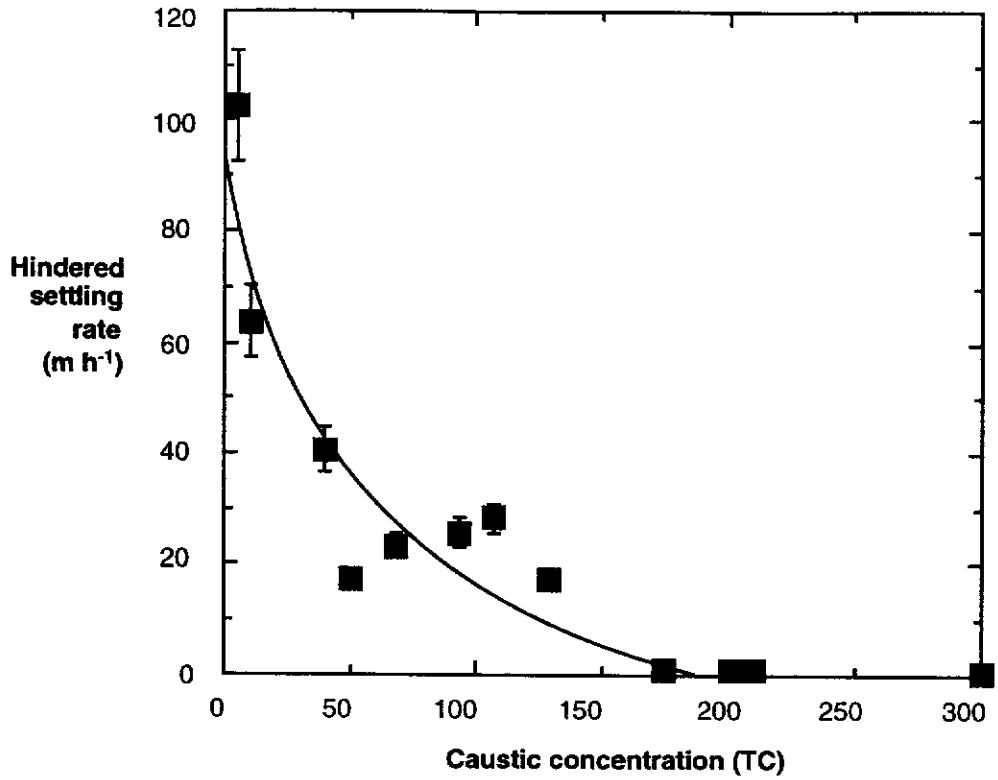

Figure 5.24 The observed settling rate of Sample C in synthetic Bayer liquors of varying TC after contact with pure caustic solution for 48 hours.

In comparison Cleaned Sample C was found to still flocculate at TC = 200 and at a TC = 100 the settling increased from 22 to 60 m h^{-1} after removal of the impurity. Also, pure hematite (Sample A) did not show any flocculation hindrance even at TCs > 300. This reinforces the link between the surface silicate contaminant and flocculation already established; that is, that flocculation is inhibited by the presence of silicate irrespective of its origins.

Investigation of the flocculation hindrance

The settling rate and turbidity measurements are batch techniques which give bulk information. The Lasentec® probe offered the opportunity to investigate flocculation at a more in-depth level as it provides aggregate chord length (which, in turn, depends on aggregate size) information.

It was found that in pure caustic solution, hematite Sample C always showed aggregation in the presence of flocculant (Figure 5.25). The average chord lengths observed in the presence of caustic at TC = 50 and 100 show the expected trend of increasing chord length with time after flocculant is added and then breakage to a limiting value caused by the shear conditions of the system. The limiting aggregate size is determined by both the aggregate strength and the shear conditions encountered.

At TC = 200 the behaviour was different in that the size increased slowly but continuously.

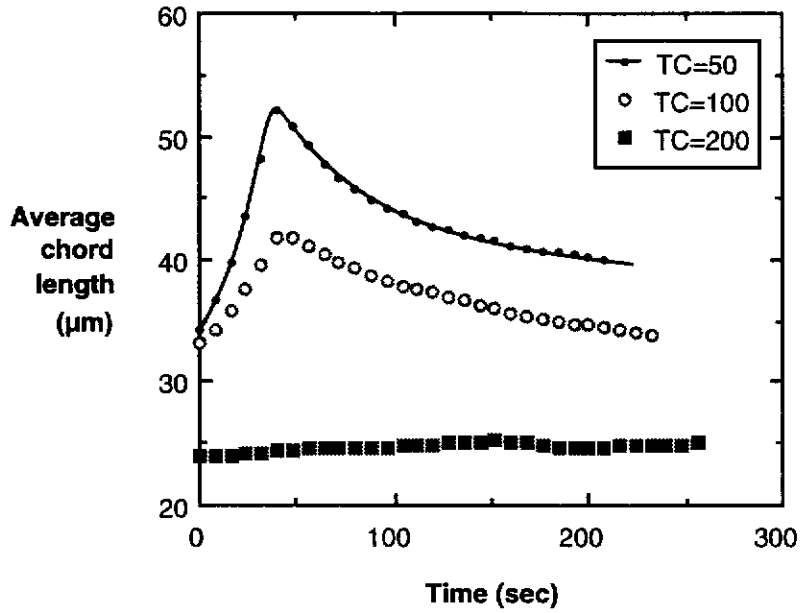

Figure 5.25 Average chord length of hematite Sample C observed by the Lasentec® as a function of time and caustic strength.

In synthetic liquor, the increase in aggregate size, particularly for TC = 200, is smaller (0.59 µm compared to 1.20 µm in caustic, Figure 5.26). The small increase in average chord length for the TC = 200 liquor was not enough to be reflected in the settling rate of batch settling tests. This highlights the sensitivity of the probe to observe size changes, and its ability to produce information relevant to changes in the aggregate state.

The effect of increasing caustic on hematite Sample C can be explained by superimposing the effect of caustic seen for hematite Sample A with the effect of the surface contaminant.

As caustic is increased, although the silicate should dissolve to a greater extent, (alumino)silicate will readsorb onto the hematite surface. As shown in the adsorption isotherm results (Figure 5.23), this limits the adsorption of flocculant. The dominant effect is still the same as that found for hematite Sample A. However, the additional burden of silicate species adsorbing on the hematite results in severely reduced flocculation. The larger chord length change observed in the pure caustic experiment compared to the synthetic liquor suggests that aluminium may form part of the readsorbed species.

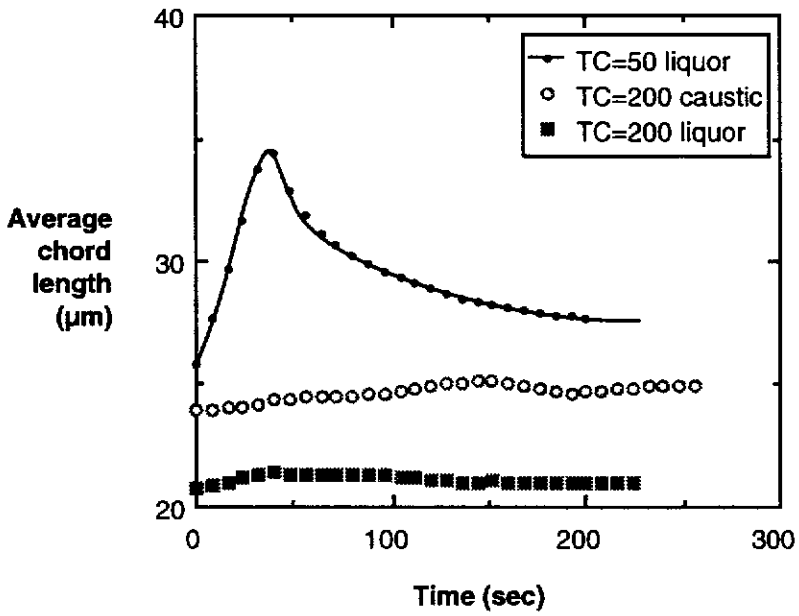

Figure 5.26 Average chord length of hematite Sample C observed by the Lasentec® as a function of time and liquor strength. The TC = 200 caustic result is included for comparison.

5.2.2 PRECIPITATION OF A DSP ON HEMATITE

A DSP contaminated hematite was produced by digesting Sample A in the presence of kaolin for 1 hour in a liquor of composition TC = 180, A/TC = 0.3 and TA = 190 as discussed in Section 2.4.7. It showed both muscovite ($KAl_2(Si_3Al)O_{10}(OH)_2$) and an aluminium silicate being formed by the digestion procedure (as assessed by XRD).

The hematite digested without kaolin showed that trace quantities of magnetite (by XRD) formed, which were not present prior to digestion. The formation of magnetite by dissolution of hematite in caustic liquors has been previously reported by Ishikawa *et al.* (1997).

SEM of the both samples showed fines were produced by the digestion process while in the absence of kaolin clear evidence of hematite dissolution was observed (Figure 5.27). Also, the DSP material formed was not a homogenous coating but was precipitated randomly over the hematite surface. The DRIFT spectrum showed a strong peak in the expected Al/Si-O region (Figure 5.28) for the sample digested in the presence of kaolin, confirming the presence of silicate or aluminosilicate.

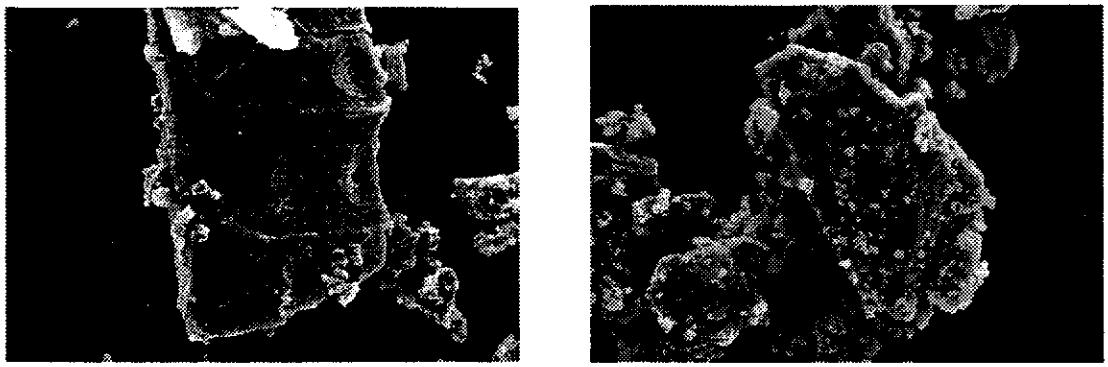

a b

Figure 5.27 SEM images of hematite Sample A digested a) without kaolin (showing dissolution of the hematite) and b) with kaolin (showing the precipitated DSP).

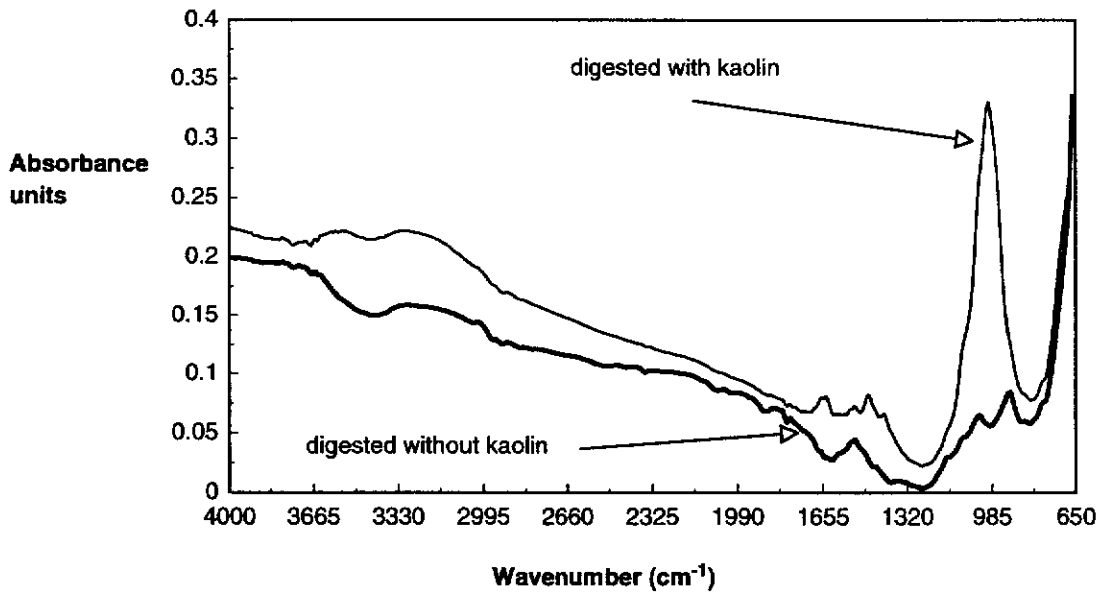

Figure 5.28 DRIFT spectra of hematite digested with and without kaolin present.

Duplicate settling tests performed for both samples at a TC = 100, TA = 110, A/TC = 0.3 at 93 °C using 15 μg g^{-1} AN995SH flocculant showed that there is a slightly higher settling rate in the presence of the DSP, while the turbidity also increased and the quantity of flocculant adsorbed showed a slight decrease (Table 5.2). These values are, however, not sufficiently different to make definitive conclusions. It tentatively suggests that DSPs increase turbidity and block adsorption of the flocculant on hematite. What is clear is that the presence of this DSP does not significantly enhance flocculation.

Table 5.2 Flocculation behaviour of digested hematite samples.

	Digested without kaolin	Digested with kaolin
Settling rate (m h^{-1})	22±2	26±3
Turbidity (NTU)	211±32	279±42
Flocculant adsorption density (μg m^{-2})	3.8±0.4	2.9±0.3

The lack of a significant difference between the hematite with DSP and that without is probably a result of the inhomogenous nature of the DSP formed on digestion. The results for hematite Sample C reflect the presence of a uniform surface coating of impurity. As bare hematite surface was still available for interaction in the DSP experiments with hematite Sample A, the latter data does not wholly reflect the interaction of the flocculant with a surface coating of DSPs.

5.2.3 CHANGING THE PARTICLE SIZE DISTRIBUTION OF REFINERY SOLIDS

Handling of waste solids in the alumina process requires the separation of the sand fraction (Glenister and Thornber, 1985) and the cut-off size is set by process parameters. The effect of altering this cut-off point on the settling of residue was determined by the addition of different sand fractions to the fine waste mud, thereby altering its particle size distribution.

Within the hindered settling regime, any increase in the Stokes' settling rate will also increase the hindered settling rate. Thus the addition of sand, based on size considerations, would be expected to increase the settling rate, although, this may be offset somewhat by the effect of higher solids concentration. As the experiments were conducted on refinery solids the results are expressed as a ratio to the standard result (as described in Section 3.3.4).

Addition of the 185 - 315 μm sand fraction (Figure 5.29) increased the settling rate to a greater extent than addition of the 38 - 185 μm fraction. At 10 % w/w sand added the ratio in settling was 1.25 and 1.45 for the 38 - 185 μm and the

185 - 315 μm sand fraction respectively. The turbidity was not significantly affected, appearing unaltered (within experimental error) by the addition of sand. The addition of the 400 - 800 μm sand fraction (Figure 5.30) did not further improve the settling rate above that of the 183 - 315 μm sand fraction. The settling ratio being 1.4 at 10 % w/w added sand. However, the turbidity in this case appeared to be constant but lower than at the standard conditions.

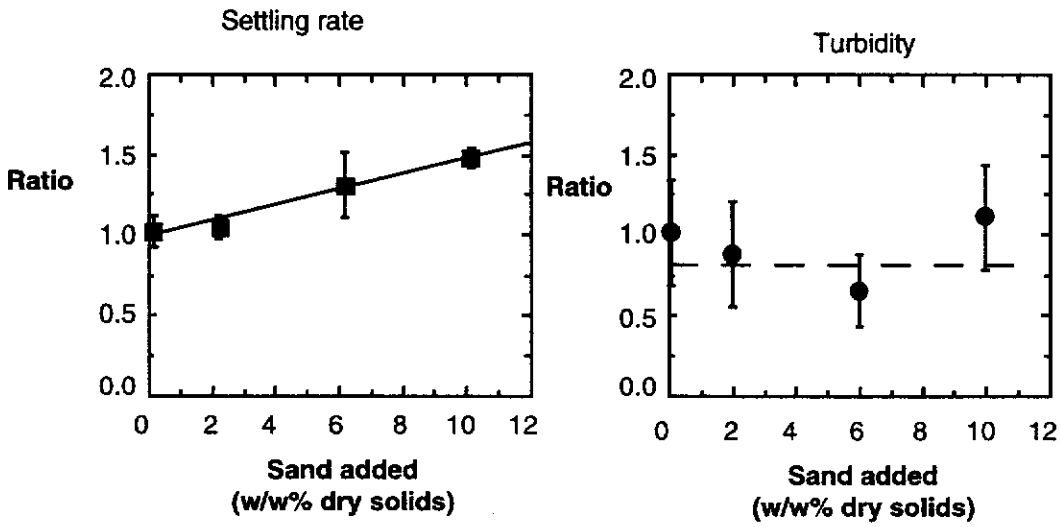

Figure 5.29 The resultant ratio to the standard test on addition of sand (185 - 315 μm fraction). (Ratio refers to the performance compared to a standard test; see Section 3.3.4)

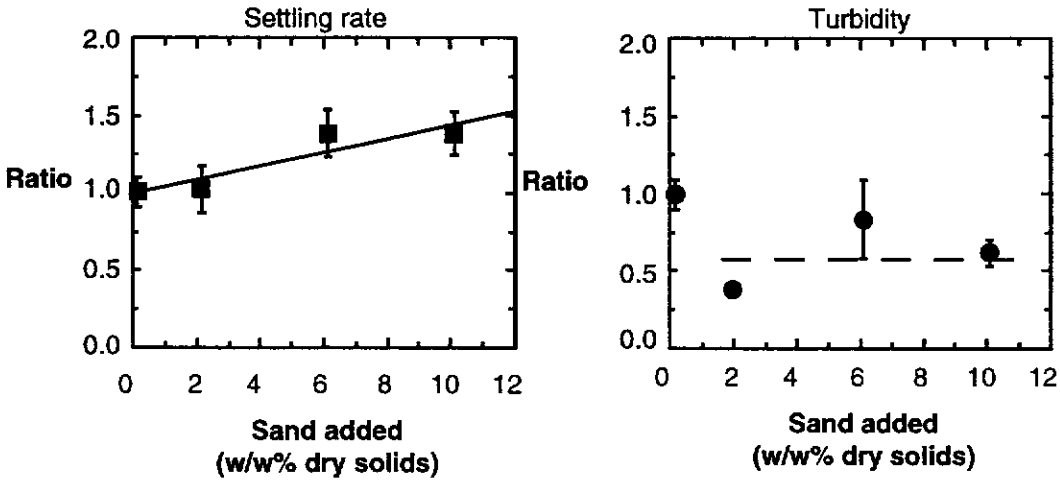

Figure 5.30 The resultant ratio to the standard test on addition of sand (400 - 800 μm fraction). (Ratio refers to the performance compared to a standard test; see Section 3.3.4)

The d_{50} of the refinery solids was 10 μm and the d_{50} of the sand fractions added to the feed were 148, 214 and 402 μm for the 38 - 185, 185 - 315 and 400 - 800 μm

fractions respectively. This gives a new d_{50} at 10 % w/w addition of the three fractions of 23.8, 30.4, and 49.2 μm respectively. The new Stokes' settling rate can be determined (excluding the broadness of the particle size distribution) by assuming that the density of the aggregates is unaltered by the addition of sand. The predicted ratio of the Stokes' settling rate was calculated to be 5.66, 9.24 and 24.21 for the three sand fractions. Much lower ratios were obtained experimentally indicating increased hindered settling caused by higher solids concentration or changes in the aggregate structures when sand is present.

The results demonstrate that the size distribution and/or density of the aggregates has a large impact on the settling rate, supporting the results of Parekh and Goldberger (1976) and Buravlev *et. al.* (1972).

It does not appear that there is an appreciable gain in removing the >150 μm sand fraction from the waste residue as making the residue solids more coarse (as shown above) may improve settling. Industry separates the sand for clarification and, sometimes, re-mixes the two slurries for disposal and consolidation (Section 1.1.1.5). Thus, a fraction of the sand could be included with the residue solids to produce a faster settling aggregate provided there was no detrimental impact on the process overall.

5.3 SUMMARY

For solution impurities it has been found that:

- Sodium sulphate, chloride and phosphate do not effect the flocculation behaviour or adsorption of flocculant on hematite.

- Carbonate and silicate compete for adsorption sites with the flocculant. Silicate is effective in competing with the flocculant at relatively low levels (0.2 mg g^{-1} added) while carbonate requires >10 mg g^{-1} before the adsorption of flocculant is affected. The effect observed with silicate and carbonate is associated with adsorption of solution species at active sites which block the adsorption of flocculant and not with solution complexation of the flocculant.

- Calcium does not increase the amount of flocculant adsorbed but does improve the residual turbidity; suggesting more particles are incorporated into the aggregated

structures. The adsorption of polyacrylate on hematite in the presence of calcium at pH 7 is both of a chelating bidentate (II) and a monodentate (I) structure. The mass of flocculant adsorbed is unaltered with increasing calcium concentration but the number of carboxylate units per molecule bonding with the surface is increased thereby resulting in reduced residual turbidity.

- No effect was observed either with increasing ionic strength or in changing the charge of the cation (Na^+ versus Ca^{2+}), therefore, it must be concluded that the adsorption of flocculant is not electrostatically determined. This supports the proposed chemisorption mechanism.

In the case of surface impurities the following conclusions can be drawn:

- The homogenous surface contaminant on hematite Sample C results in a conditioning effect when contacted with caustic. Flocculation is improved with contact due to dissolution of the impurity. This removes surface silicate which blocks active sites on which the flocculant adsorbs.

- The adsorption isotherm of hematite Sample C showed the same affinity of flocculant for the hematite surface but a lower monolayer coverage. This confirms that the action of silicate is to block active sites on which the flocculant adsorbs.

- Increasing caustic (>TC = 100) lowers the settling rate significantly for Sample C, apparently totally hindering flocculation at TC = 200. This is caused by a combination of effects. The main causes are the increased viscosity of the liquor and the readsorption of silicate onto hematite which hinders the adsorption of flocculant. The readsorbed silicate may be an aluminosilicate species as flocculation is more hindered in synthetic liquors than in pure caustic.

- Studies using a DSP precipitated on pure hematite were inconclusive. The adsorption of flocculant appeared to decrease and the turbidity increase, however, the values were within experimental error. This was probably due to the random precipitation of DSP on the hematite surface which left exposed pure hematite to interact with the flocculant.

- Changing the physical properties of refinery solids can have a significant impact on settling. If the remainder of the refining process remains unaffected, increasing the residue component up to a size of 315 μm may be beneficial.

6. MOLECULAR MODELLING OF FLOCCULANT ADSORPTION ON HEMATITE

The hydrated surface structure of iron oxides is of great importance in understanding surface reactions in many systems; for example selective flocculation of hematite from gangue minerals (Bagster, 1985; Weissenborn, 1993) and the leaching and adsorption of ions in geochemical processes, which impacts on contaminant mobility in the environment (Brown Jnr., 1990). As these reactions occur in aqueous solution, surface hydration configurations for iron oxides have been postulated in the literature (Parfitt *et al.*, 1978; Rochester and Topham, 1979; Barrón and Torrent, 1996). Infrared spectroscopy has been used in attempts to elucidate surface hydroxyl configurations (Parfitt *et al.*, 1978; Rochester and Topham, 1979) but it is not a good tool for this, given the wide distribution of hydrogen bonding configurations which could exist in these systems. Furthermore, infrared cannot give information regarding the strength of adsorption of the flocculant on a particular face. As Brown Jnr. (1990) points out, macroscopic techniques do not provide information on the microscopic mechanisms underlying fundamental processes.

In Bayer liquors, hematite is undoubtedly hydrated though to what extent is unknown. Molecular modelling is a powerful tool in developing an understanding of, firstly, the hydration of the hematite in an aqueous environment and, secondly, the interaction of this hydrated surface with the flocculant. The methodology adopted in this study was discussed in Section 2.7.

6.1 INTRODUCTION

The {111}, {011} and {210} planes (in rhombohedral coordinates) of hematite were chosen for hydration studies as these faces are found in >60 % of all naturally occurring samples of hematite (Hartman, 1989).

Before the modelling of any surface is undertaken, it is necessary to determine which cut of the plane is the most stable. Any crystal when cleaved will separate such that the configuration with the lowest surface energy is exposed and no dipole is formed perpendicular to the surface. For the hematite {111} plane this is an Fe-terminated surface. Hartree-Fock calculations by Becker *et al.* (1996) found that if the hematite {111} plane is cleaved to leave an iron terminated surface, the iron atoms relax towards the bulk by about 0.5 Å and this predicted behaviour has been observed experimentally by Henderwerk (1986) under vacuum conditions. Similarly large surface relaxations have been calculated for the basal plane of the isostructural corundum (Nygren *et al.*, 1997; Gale *et al.*, 1992; Gay and Rohl, 1995).

Rustad *et al.* (1996), have used molecular mechanics to model goethite, lepidocrocite and hematite structures to within 4 % of their known values. The surface interaction of water with the goethite {001}, {021}, {100} and {110} planes was shown to be via the oxygen atom of the water molecules interacting with the surface iron atoms whilst the water hydrogen atoms interacted with surface oxygen atoms.

Recently, a combined scanning tunnelling microscopy (STM) and computational study investigated the {111} basal plane of hematite (Becker *et al.*, 1996). They found that the physisorbed water was only very weakly bound to the surface and that the STM tip could shear the physisorbed water away, making it impossible to image. This work did not address the dissociation of water and only physisorption was considered.

Surface hydroxyl configurations have been calculated for the corundum {111} plane by Nygren *et al.* (1997). The water in that study was adsorbed onto an O-terminated surface. They chose this surface to hydrate as experimental results suggested that the {111} surface was not aluminium but oxygen terminated. The surface hydroxyl configuration on corundum was shown to be a series of hydrogen bonded OH groups in a triangular configuration keeping the symmetry of the crystal intact. They found that only for the {111} plane can a fully close packed oxide surface be formed with no net dipole on hydration. As hematite is isostructural, the only oxide layer investigated in this study was the {111} plane.

As Bayer liquors are a highly caustic environment where water should be predominantly dissociated and infrared shows hematite is hydrated even in aqueous solutions, physisorption was not investigated.

The simulation cell thicknesses for Region I (the surface) and Region II (the bulk) found to satisfy the criteria for MARVIN are given in Table 6.1.

Table 6.1 Simulation cell thickness for the different faces studied.

	Region I	Region II	
{111}	6	6	Fe layers deep
{011}	8	12	Fe layers deep
{210}	6	17	Fe layers deep

6.2 POTENTIALS

The potentials used in this work are given in Table 6.2. They enabled the structures of hematite, goethite and lepidocrocite to be calculated to within 2 % of their known structures (Table 6.3) compared to within 4 % that Rustad *et al.*, (1996) achieved. These potentials were then used to hydrate hematite and to adsorb the organic molecules.

6.3 SURFACE HYDRATION OF HEMATITE

For the pure hematite {111} plane (no water) *in vacuo* the surface iron atoms were found to relax inwards by ~0.72 Å for the Fe-terminated plane. This supports the trend of Becker *et al.* (1996), who used Hartree-Fock calculations and found the movement towards the bulk at a slightly smaller distance of 0.48 Å. The difference in magnitude of the iron atom movement after relaxation between the two studies probably reflects the greater layer thickness of the simulation cell used in this study rather than the computational models used. Similar discrepancies have been reported previously for corundum (Gay and Rohl, 1996). The thickness used by Becker *et al.* (1996) was only 3 Fe layers deep whereas in this work Region I alone was 6 Fe layers thick.

Table 6.2 Potentials used for modelling adsorption of water on hematite and adsorption of organic molecules on the hydrated hematite surface.

Buckingham potentials for hematite

Interactions	A	r	c
$^{\#}O_{lattice}$-$O_{lattice}$	22764.3	0.14900	27.879
Fe-$O_{lattice}$	1102.4	0.32990	0.000

Buckingham potentials for surface OH

$O_{hydroxide}$-$O_{hydroxide}$	22764.3	0.14900	7.840
Fe-$O_{hydroxide}$	965.0067	0.32990	0.000
$H_{hydroxide}$-$O_{lattice}$	701.0801	0.22278	0.000
$H_{hydroxide}$-$O_{hydroxide}$	109.0888	0.25547	0.000

Harmonic potentials for organic molecules

	k	bond length cut-off
C-C	28.007506	1.5260
$H_{organic}$-C	29.561139	1.1050
$C_{carboxy}$-C	24.568714	1.5200
C-$O_{carboxy}$	46.864929	1.2500

Three body potentials for organic molecules

	k	θ_o
$H_{organic}$-C-$H_{organic}$	3.428083	106.400
$H_{organic}$-C-C	3.853339	110.000
C-C-C	4.044270	110.500
$C_{carboxy}$-C-$H_{organic}$	3.905411	109.500
C-C-$C_{carboxy}$	4.044270	110.500
$O_{carboxy}$-$C_{carboxy}$-$O_{carboxy}$	12.584101	123.000
C-$C_{carboxy}$-$O_{carboxy}$	5.90151	120.000

four body potential for organic molecule

k	S	P
0.006859	1	3

Intermolecular Morse potential†

D_e	α	r_o
7.0525	2.1986	0.9485

Charges

Atom	Core charge	Shell charge
Fe	-1.7654	4.7654
$O_{lattice}$	0.86902	-2.86902
$O_{hydroxide}$	0.69187	-2.11787
$H_{hydroxide}$	0.4260	
$H_{organic}$	0.1000	
$C_{carboxylate}$	0.1400	
$C_{backbone}$	-0.200 (-0.3 end of chain carbon)	
$O_{carboxylate}$ -0.570		

Table 6.2 continued

k value in spring potential		
$O_{lattice}$ = 26.499		
$O_{hydroxide}$ = 40.385		
Fe = 173.192		
Lennard-Jones potentials for organic molecules		
	A	C
$C\text{-}C_{carboxy}$	1157.474	26.693
$H_{organic}\text{-}C_{carboxy}$	187.149	6.787
$C_{carboxy}\text{-}O_{carboxy}$	837.004	22.167
$H_{organic}\text{-}C$	205.718	7.360
$C\text{-}O_{carboxy}$	920.053	24.036
$H_{organic}\text{-}O_{carboxy}$	148.761	6.112
C-C	1052.995	24.618
$C_{carboxy}\text{-}C_{carboxy}$	1272.320	28.943
$H_{organic}\text{-}H_{organic}$	33.262	1.872
$O_{carboxy}\text{-}O_{carboxy}$	665.318	19.961
for hematite-organic interactions		
$H_{hydroxide}\text{-}C$	10.346	0.943
$H_{hydroxide}\text{-}C_{carboxy}$	11.372	1.023
$H_{hydroxide}\text{-}H_{organic}$	1.839	0.260
$H_{hydroxide}\text{-}O_{carboxy}$	8.224	0.850
$C_{carboxy}\text{-}O_{hydroxide}$	896.194	21.564
$C\text{-}O_{hydroxide}$	985.115	23.382
$H_{organic}\text{-}O_{hydroxide}$	159.281	5.945
$O_{carboxy}\text{-}O_{hydroxide}$	712.367	19.418
$C_{carboxy}\text{-}O_{lattice}$	880.508	23.867
$C\text{-}O_{lattice}$	967.872	25.879
$H_{organic}\text{-}O_{lattice}$	156.493	6.581
$O_{carboxy}\text{-}O_{lattice}$	699.898	21.492
$C_{carboxy}$-Fe	416.558	23.440
C-Fe	457.889	25.416
$H_{organic}$-Fe	74.035	6.463
$O_{carboxy}$-Fe	331.113	21.107

Lewis and Catlow (1985), † Schröder *et al.*, (1992)

Table 6.3 Calculated and experimental unit cell dimensions (Å) for hematite, goethite and lepidocrocite.

cell axis	Hematite		Goethite		Lepidocrocite	
	Calculated	Experimental*	Calculated	Experimental†	Calculated	Experimental#
a	5.035	5.038	4.57	4.62	3.94	3.87
b	5.035	5.038	10.11	9.95	12.51	12.50
c	13.733	13.772	3.02	3.01	3.09	3.08

* Blake *et al.*, (1966), † Szytuta *et al.*, (1968), # Christensen and Christensen (1978)

When the minimum energy configuration had been obtained, the surface energy of the hydrated plane was calculated according to Nygren *et al.* (1997):

$$E_{surf} = \frac{E_{regl} - mE_{bulk} + 0.5nE_{corr}}{A} \qquad \text{(Eqn. 6.1)}$$

as defined in Section 2.7.2.

To obtain a surface energy using Equation 6.1 for the different hydration configurations of the different hematite surfaces E_{corr} is required. There are several ways of estimating the value of E_{corr}, but the approach of de Leeuw *et al.* (1995, 1996) was adopted. Firstly, a value for the enthalpy of reaction of water with an oxide ion was obtained using the following cycle:

			ΔH
$2Fe^{3+} + 3O^{2-}$	----->	Fe_2O_3	-14516.066†
Fe_2O_3	----->	$2Fe + 3/2O_2$	823.411*
2FeOOH	----->	$2Fe^{3+} + 2O^{2-} + 2OH^-$	13400.448†
$2Fe + 2O_2 + H_2$	----->	2FeOOH	-1116.290*
H_2O	----->	$H_2 + 1/2O_2$	285.830^
$H_2O + O^{2-}$	----->	$2OH^-$	-1122.667 kJ mol^{-1}

*Experimental formation energies from Knacke *et al.* (1991)
†Calculated lattice energies, ^from de Leeuw *et al.* (1995, 1996)

To then determine E_{corr}, the internal energy of two free hydroxide ions was subtracted from the water dissociation energy. The value of E_{corr} obtained using the above data is E_{corr} = 2.475 eV. Surface energies and the difference in energy between the relaxed surface with and without hydration were calculated for each plane studied with different amounts of chemisorbed water and are shown in Table 6.4.

Table 6.4 Calculated surface energy (in J m^{-2}) for hydrated hematite planes.

Surface Plane	% water coverage	Surface Energy	$\Delta E = E_{hydrated} - E_{unhydrated}$
{011}	100	0.670	-0.484
	83	0.971	-0.183
	67	1.246	0.093
	50	1.422	0.269
	33	1.734	0.580
	17	1.922	0.769
	0	1.153	0.000
{210}	100	1.275	0.251
	80	1.651	0.627
	60	1.218	0.194
	40	1.421	0.397
	20	1.221	0.197
	13	1.386	0.362
	7	1.472	0.448
	0	1.024	0.000
{111}	100	1.421	0.667
	67	0.824	0.070
	33	0.898	0.144
	25	0.879	0.124
	17	0.943	0.188
	8	0.826	0.072
	0	0.754	0.000

There are two ways of interpreting the results, either by looking at the surface energy alone (the lowest surface energy is the most stable surface) or by looking at the difference in energy once the surface becomes hydrated (the more negative change means the most stabilised surface on hydration).

6.3.1 {011} AND {210} SURFACES

On the most stable cut of the {011} plane all the iron atoms are five-coordinate. Thus, each adsorbed water molecule produces a fully coordinated iron atom. Each surface cell has 3 surface iron atoms, thus a 2x1 cell has 6 possible sites for adsorption to occur. The surface energy calculated using Equation 6.1 increases as the number of water atoms decreases to 17 % coverage (Table 6.4). At 100 and 83 % coverage the surface energy is less than the relaxed unhydrated surface energy, leading to a negative ΔE value. This suggests that monolayer coverage is the most energetically stable of the hydrated surfaces on the {011}. The surface iron atoms were found to undergo relaxations depending on the water coverage. Small relaxations of ~0.03 Å towards the bulk are observed at 100 % coverage while at 50 % coverage the iron atoms relax (again towards the bulk) by 0.70 Å. This further supports the finding that the 100 % hydrated {011} is the most energetically favoured, as it is also the most stable with respect to atomic movements.

The 2x1 cell at 100 and 17 % water coverage is shown in Figure 6.1. Some interaction can be seen to exist between the OH groups. There is hydrogen bonding between those OH groups within the surface and those at the top of the figures but the top OH groups are almost perpendicular and do not interact with each other.

On the {210} plane there are both five and three coordinated surface irons prior to adsorption of water. The surface energies do not show a distinct trend with water coverage (Table 6.4). What is clear is that the surface energies are all higher than the relaxed unhydrated surface. Thus, hydration of this plane does not lead to stabilisation. Furthermore, the values are higher for the {210} than they are for the {011} at high water coverages suggesting that in excess water conditions, the {011} preferentially hydrates.

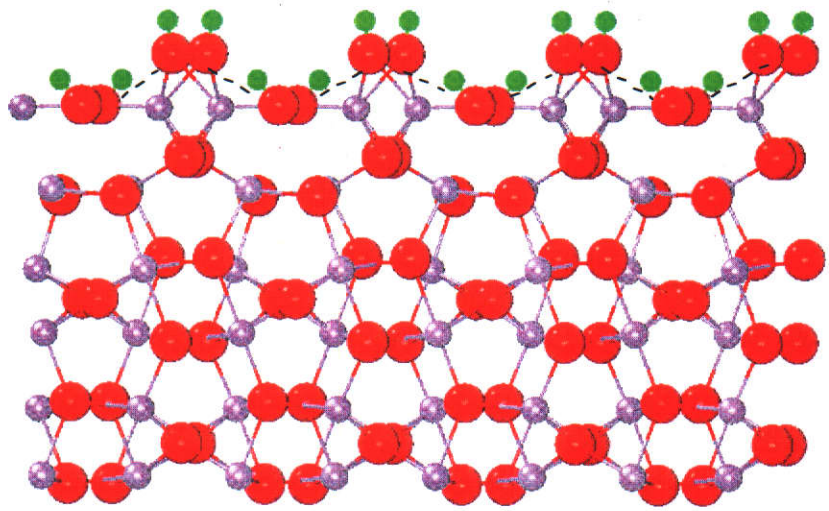

100 % coverage

Oxygen

Hydrogen

Iron

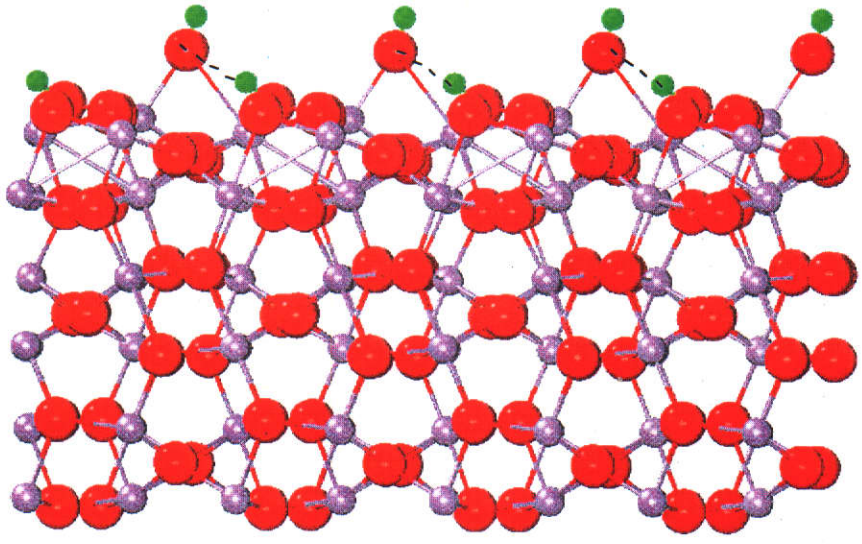

17 % coverage

Figure 6.1 Side view of chemisorbed water at 100 and 17 % coverage for the {011} plane. Hydrogen bonding is shown as broken lines.

The movement of the surface iron atoms on this face is also very dependent on the numbers of water adsorbed. To accommodate all the water, the surface iron atoms move up and out of the surface by 0.80 Å for 100 % coverage. As the numbers of waters decrease, the movement of the uppermost iron atoms lessens reversing direction at 60 % (that is, the iron then relaxes towards the bulk) until finally at the lowest coverage studied the iron has relaxed by 0.50 Å into the surface.

Figure 6.2 shows the {210} plane hydrated at 100 and 7 %. Once again, the OH configuration at low surface coverage consists of surface OH groups almost perpendicular to the surface with the other OH groups in the surface showing some hydrogen bonding.

6.3.2 {111} Fe-terminated surface at monolayer coverage

The Fe-terminated surface is the plane obtained when hematite is cleaved *in vacuo* and all iron atoms are only three-coordinate before the adsorption of water. When water is chemisorbed to this surface at 100 % coverage the iron atoms move away from the bulk crystal (Figure 6.3) by about 1.7 Å. This is a large movement which shows that there is a strong desire for the iron atoms to separate from the surface. This is in contrast to the pure surface and the {011} and {210} planes where relaxations less than 0.8 Å are observed. A clear indication of this surface's instability is the relatively large surface energy value. It is the highest surface energy for the {111} face and is of the same order as the least energetically favourable hydrated faces for the {011} and {210} hydrated planes.

The instability of this hydrated surface was further supported by calculations where the $Fe(OH)_3$ units were dissociated from the surface and moved 10 Å away. This cell had a lower surface energy of 0.820 J m^{-2} compared to when the $Fe(OH)_3$ units were still attached (1.421 J m^{-2}, Table 6.4); the relaxed structure had the subunits at a distance of ~21 Å from the surface (Figure 6.4) where they are too far apart to have any detectable interaction.

The surface left behind by the 'dissolution' of the iron atoms is an O-terminated surface and contains OH groups which interact with each other via hydrogen bonding.

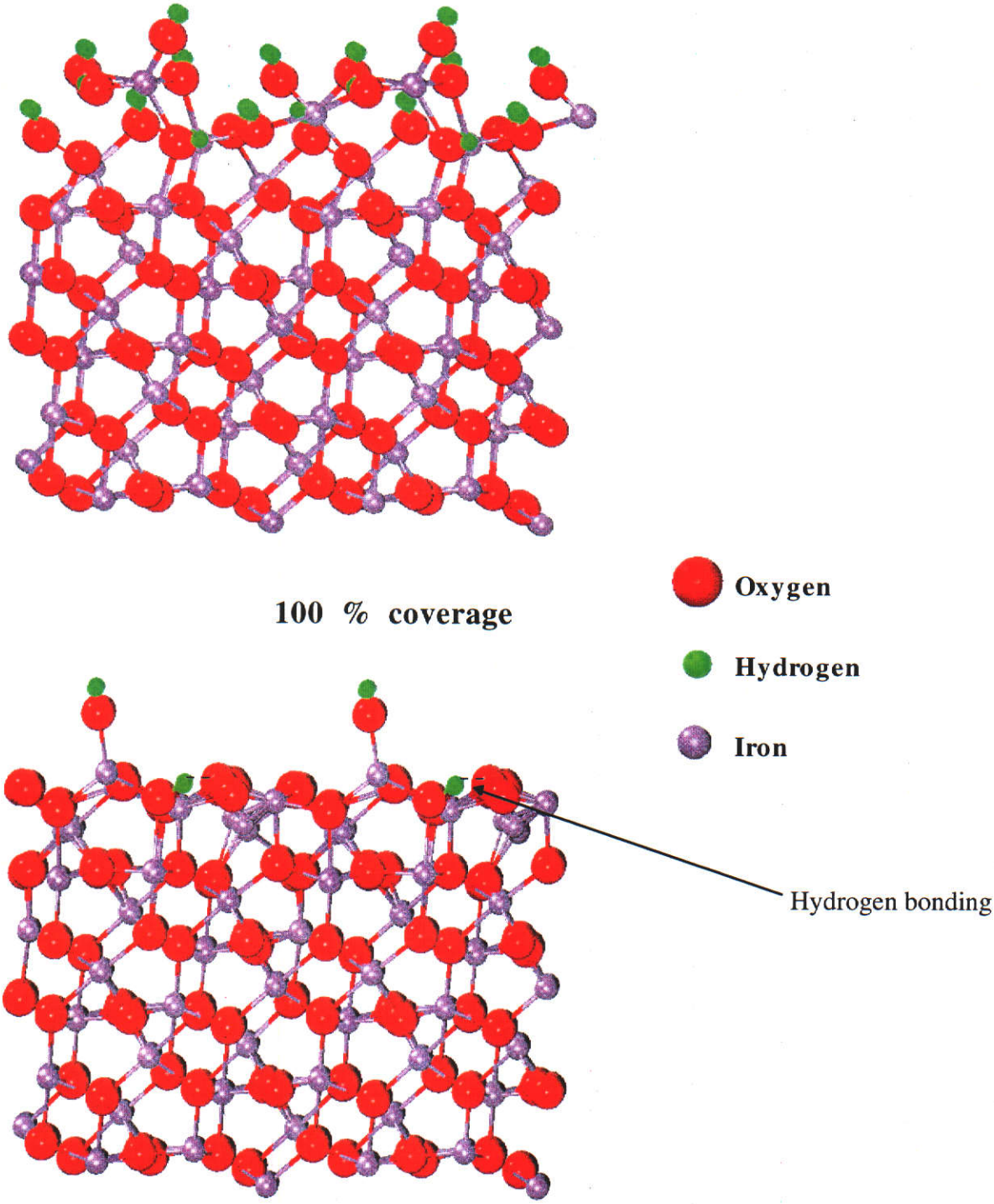

Figure 6.2 Side view of chemisorbed water on the {210} plane at 100 and 7 % coverage. Hydrogen bonding shown by broken line.

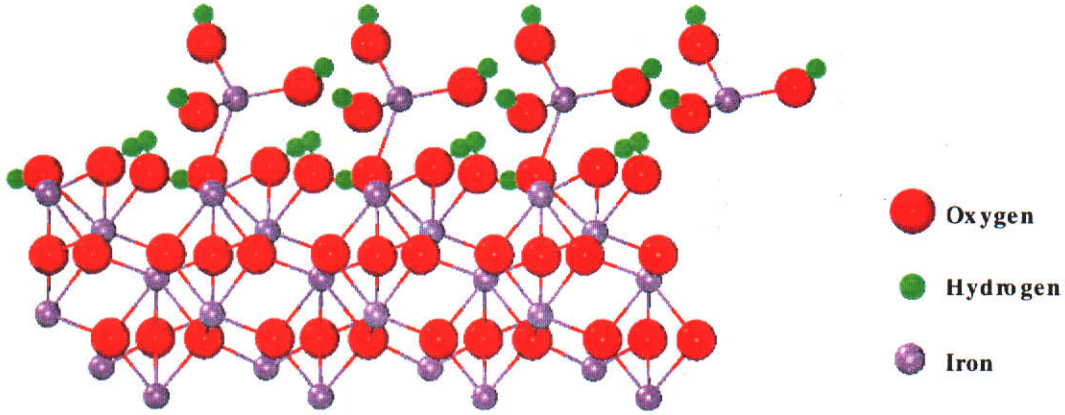

Figure 6.3 Side view of chemisorbed water on the Fe-terminated {111} plane at 100 % coverage.

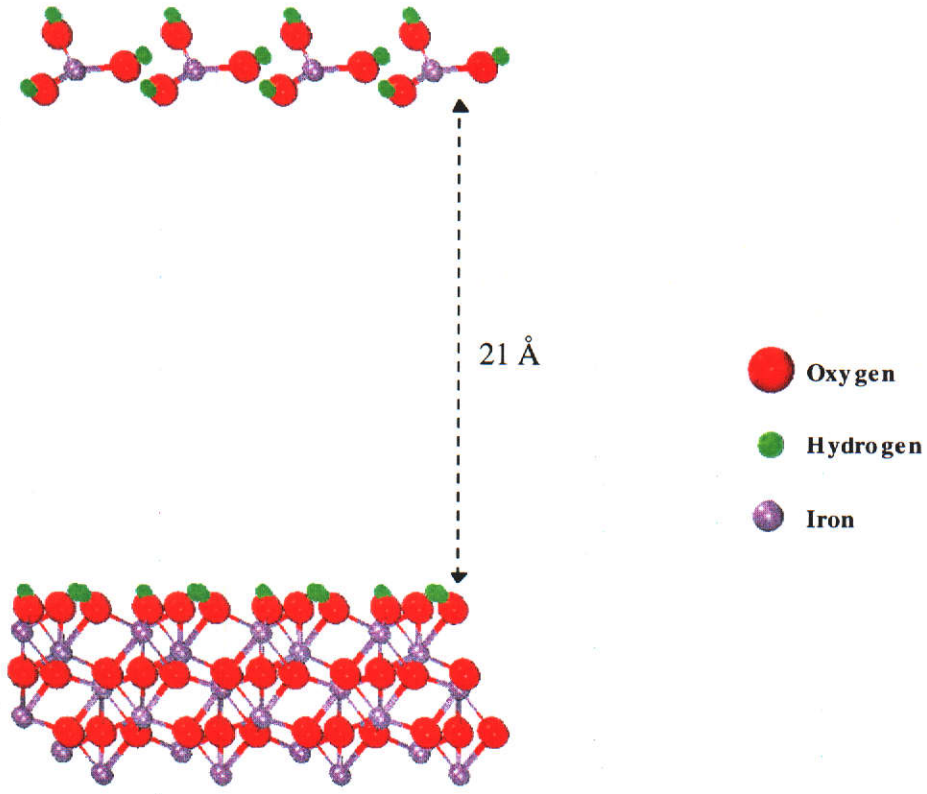

Figure 6.4 Side view of the relaxed surface after the $Fe(OH)_3$ subunits have been 'unbonded' to the surface.

The high surface energy for the Fe-terminated {111} also indicated that this plane was not stabilised by hydration, thus it would be expected to be unstable. It is predicted, therefore, that the instability of this hydrated surface is the route by which a freshly cleaved (Fe-terminated) hematite plane would form the hydrated oxide in the presence of excess water. Furthermore, if the Fe-terminated {111} plane were reacted with water, the surface hydroxyl configuration would be equivalent to that formed on an O-terminated surface due to dissolution of the top $Fe(OH)_3$ units.

6.3.3 {111} Fe-terminated surface at less than monolayer coverage

For less than full coordination of iron on the surface, the surface energies are relatively stable at coverages between 33 and 17 % (Table 6.4). At the lowest water coverage of 8 % the surface energy is only 0.072 J m^{-2} less stable than the bare surface thus, at this very low coverage some hydration of the Fe-terminated {111} may occur. The iron atoms still relax by about 1.7 Å away from the surface at 67 % coverage though this reduces dramatically to 0.005 Å for coverages <33 %.

6.3.4 {111} O-terminated surface

With the {111} plane cleaved such that oxygen is uppermost, a dipole results. To remove this dipole, half the oxygen atoms are moved to the bottom of the simulation cell, as per Nygren *et al.* (1977). Water dissociation is modelled by replacing the empty sites with hydroxide ions and hydrogen is bonded to the remaining oxygen atoms. The structure is then minimised to obtain the most energetically favourable configuration.

When water is chemisorbed on the O-terminated {111} plane, the restructuring of the surface is significantly less, the iron atoms below the oxygen layer move by only 0.02 Å. There is certainly no movement away from the surface by either the iron or oxygen atoms, indicating a stable configuration (Figure 6.5).

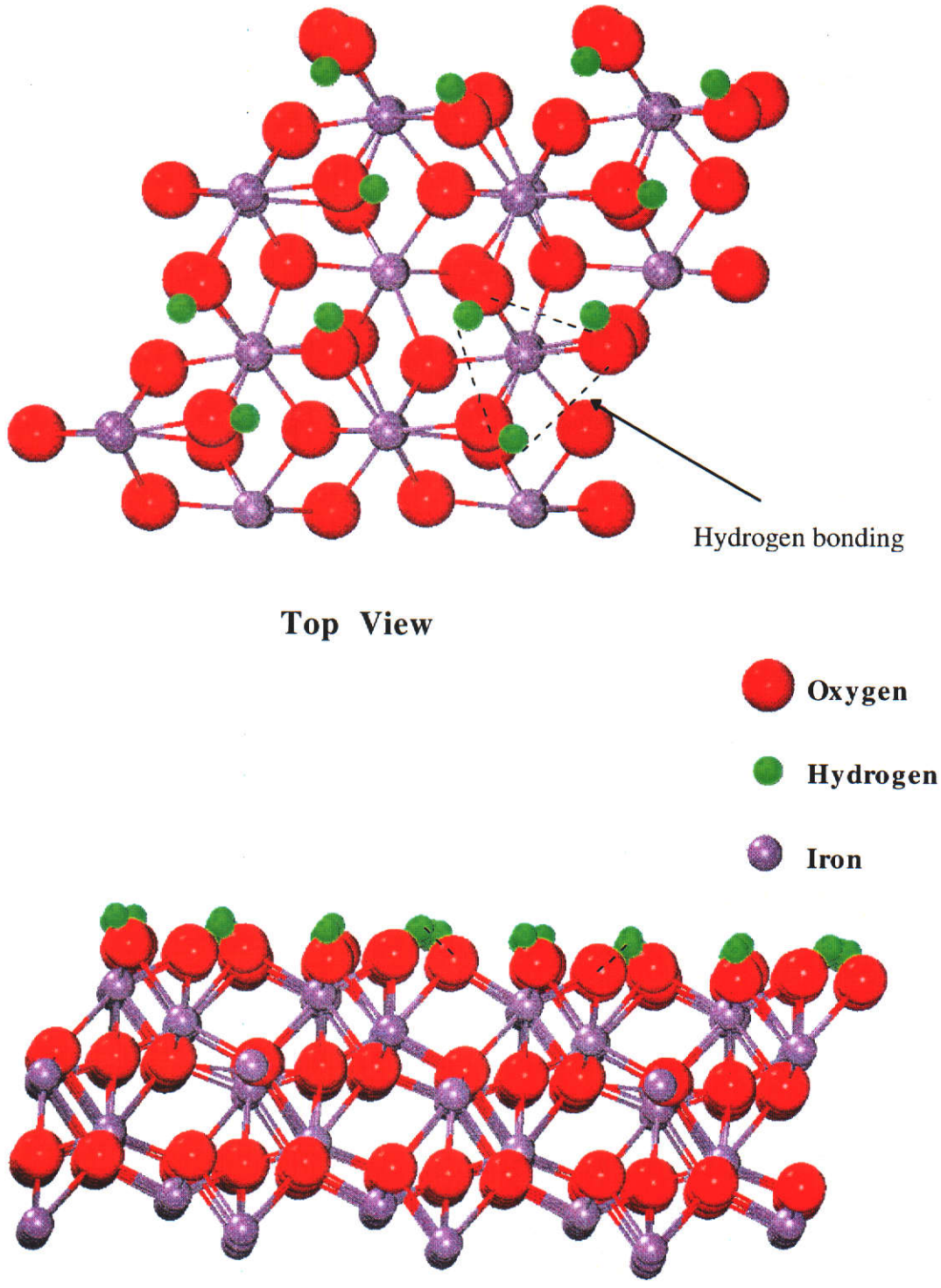

Figure 6.5 Side and top view of chemisorbed water on the O-terminated {111} plane at 100 %. Hydrogen bonding shown as broken line.

The minimum energy configuration is very similar to that found for corundum (Nygren *et al.*, 1997) with triangular hydrogen bonds. Most importantly this surface is identical to the {111} surface obtained when the $Fe(OH)_3$ units were detached in the Fe-terminated case.

The surface energy for the O-terminated {111} hydrated plane was found to be 0.6170 J m^{-2}. The surface energy calculated for this face is the lowest energy of all the faces at all coverages (Table 6.4). The change in energy between the unhydrated and hydrated surface is -0.9660 J m^{-2} and is also the largest difference, implying that this surface is not only the most energetically favourable but that the bare oxide surface is the most stabilised by its reaction with water.

Thus, clearly, it would be expected that the {111} hydrates in preference to either the {011} or the {210} planes. However, the {011} plane could also hydrate under favourable conditions which produced a monolayer.

6.4 Adsorption of Carboxylate Groups onto Hydrated Hematite

The adsorption of organics (decanoate and decandioate) was investigated for the O-terminated {111} hydrated plane (most energetically stable hydration configuration) and the {011} plane at 17 % water coverage (the least stable configuration) using the method described in Section 2.7.3. As the adsorption of the flocculant could either be preferred on a hydrated plane or the presence of surface hydroxyls may interfere with the interaction of the carboxylate with the surface, a 'water rich' and a 'water poor' surface was studied.

The lowest energy configuration of the adsorbed carboxylate group on both surfaces was always found to be the same, regardless of the plane or the organic species (monocarboxylate or dicarboxylate).

Qualitatively, the adsorption configuration of the two organics agreed remarkably well with the DRIFT results at high pH. That is, the carboxylate bonded directly to iron such that a non-symmetric, bridging bidentate structure was formed (Figure 6.6). The reproduction of the high pH results rather than the pH 7 adsorption results is a consequence of the way in which the organic was modelled. The carboxylate moiety

was constructed such that both oxygen atoms were equivalent. No attempt was made to reproduce the hydrogen bonded carboxylate adsorption mechanism found at pH 7 as this was not relevant to Bayer conditions.

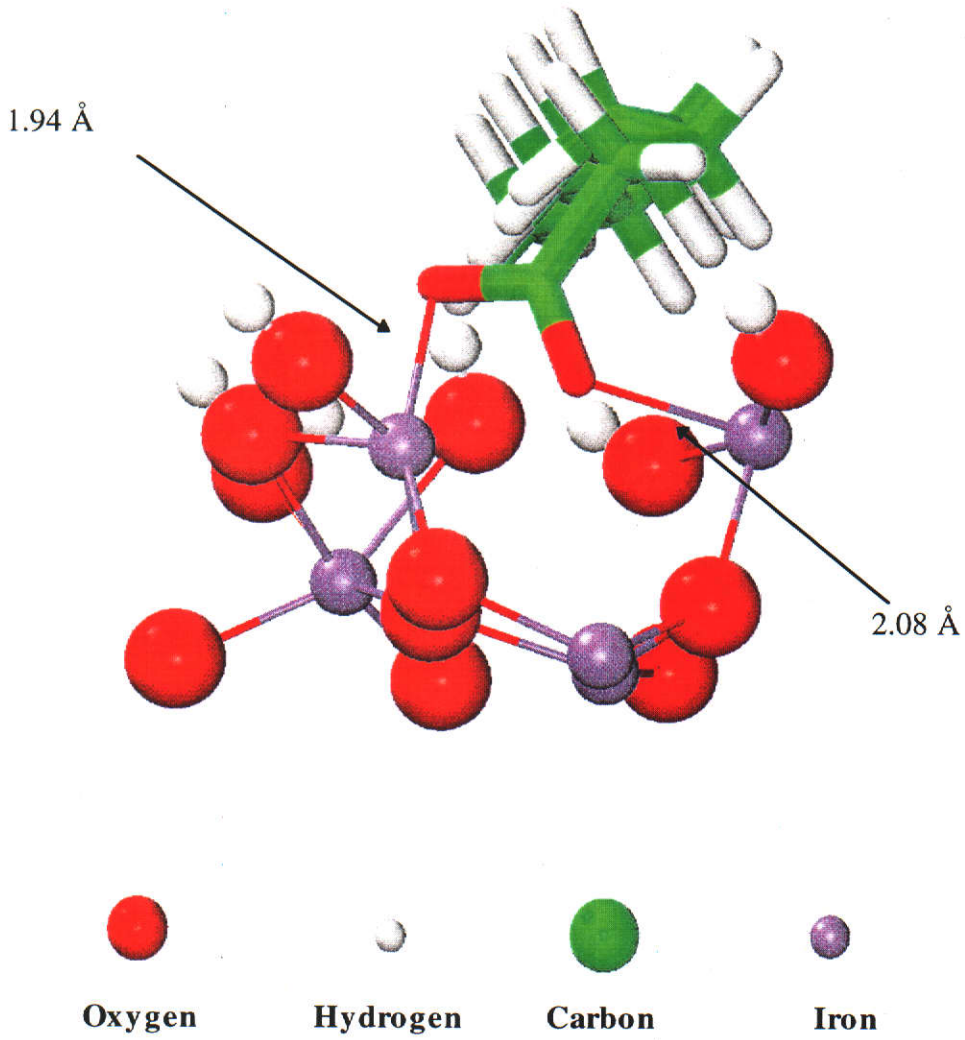

Figure 6.6 Close-up view of the adsorption of the carboxylate group with surface irons on the O-terminated {111} hydrated surface.

On the {111} O-terminated face, the decanoate formed an asymmetric structure with one Fe-OC bond at 1.94 Å and the other at 2.08 Å. The carboxylate backbone was found not to be completely repelled by the surface, particularly on the water rich plane ({111}) where the hydrocarbon hydrogens showed some interaction with surface oxygen atoms. However, on this surface, adsorption of the organic molecules was accompanied by large movements in surface iron atoms (1.1 - 1.5 Å) to accommodate the bonding. This was even more pronounced for the dicarboxylate which involved both surface restructuring and carboxylate restructuring (Figure 6.7).

The movement of surface iron atoms was up to 2.5 Å in this instance. Hydrogen bonding does not appear to be occurring between the carboxylic oxygen atoms and the surface hydrogen atoms. Most surface protons appear to point away from the carboxylates to make room for its bonding.

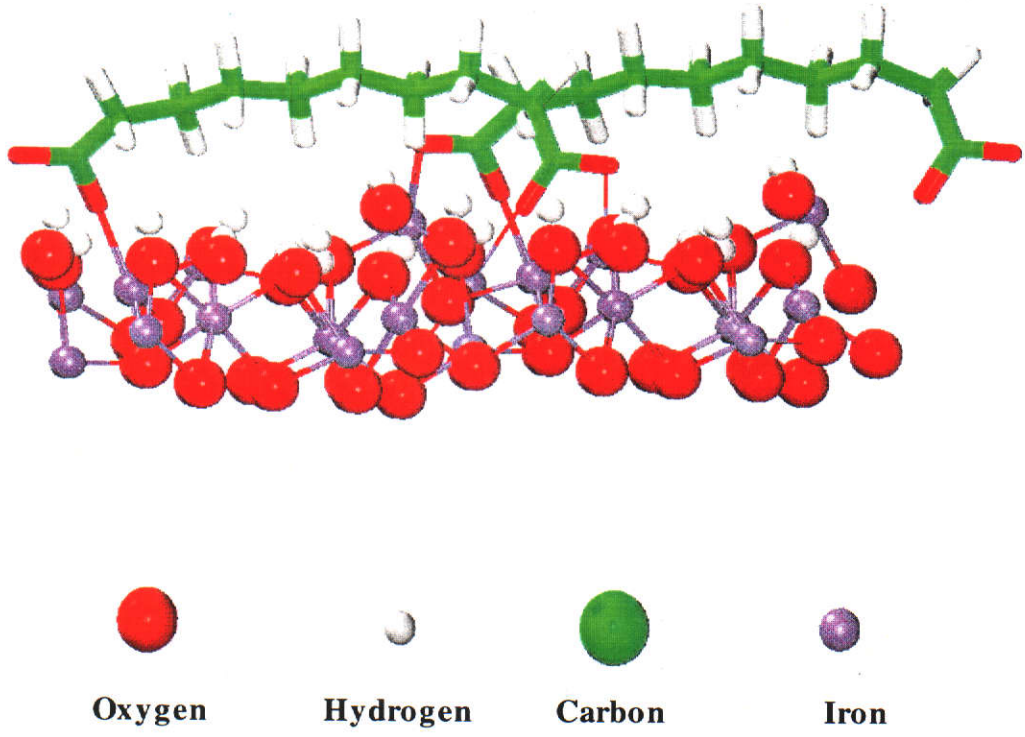

Figure 6.7 Side view of the decandioate molecule adsorbed on the O-terminated {111} hydrated surface. A 4x4 simulation cell is shown so that the mode of attachment at both ends of the molecule is shown.

The surface restructuring was much less on the {011} plane for both organic molecules where there was little water to interfere with the carboxylate-iron interaction (Figure 6.8). The maximum movement of surface irons for the decanoate was less than 0.40 Å, while for the decandioate it was 1.20 Å. The carboxylate bonding to iron was also more symmetrical with Fe-OC bonds of 1.84 and 1.90 Å in length. The adsorption configuration was the same as that for the {111} plane thus the carboxylate interaction with all the hematite surfaces appears to be by direct bonding to Fe. It is also clear that while bidentate chelating is a possible adsorption mechanism, it is more energetically favourable to interact with two irons rather than just the one.

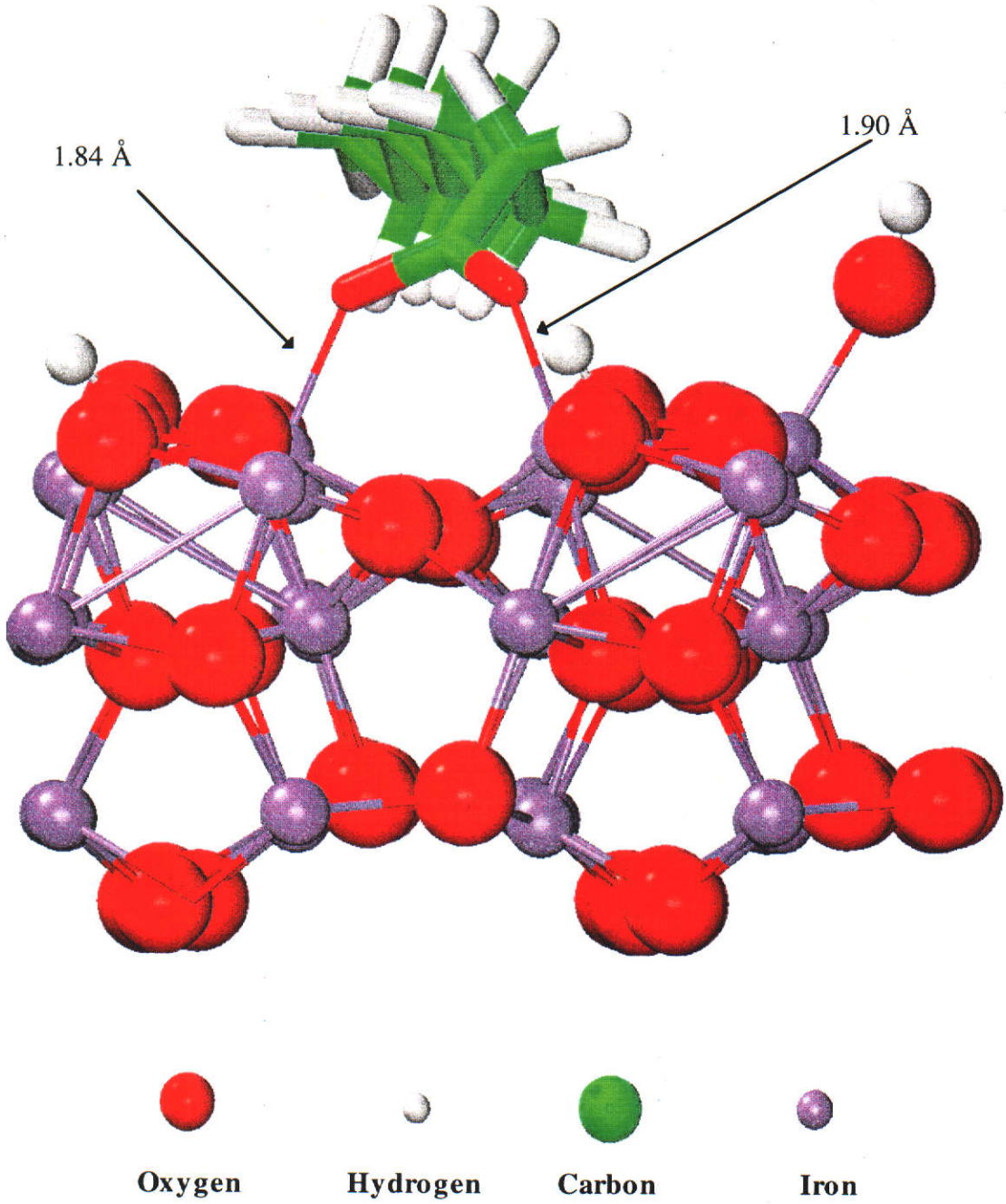

Figure 6.8 Adsorption configuration of decanoate on the 17 % chemisorbed water hydrated {011} plane.

The replacement energy given by:

$$\Delta E_{rep} = (E_{org+surf} + nE_{OH}) - (E_{surf} + E_{org}) \qquad \text{(Eqn. 6.2)}$$

as defined in Section 2.7.3 was calculated to determine whether the adsorption of the organic molecule is favoured. The values for ΔE_{rep} are given in Table 6.5. The lower the ΔE_{rep} value, the more favoured the adsorption reaction.

Table 6.5 ΔE_{rep} values (J) for the different organics adsorbed on the two planes investigated.

	{111} O-terminated plane	{011} plane
decanoate	9.92	0.385
decandioate	17.8	-2.40

Of particular note is the fact that the replacement energy is actually negative for one of the structures on the {011} plane while it is always positive for the {111} plane. This suggests that the restructuring involved in adsorbing the organic on the {111} hydrated surface is large and thus, the organic would prefer to adsorb onto the {011} plane.

It is also interesting to note that the di-carboxylic acid gives a lower replacement energy on the {011} while it is higher on the {111}. This probably reflects the greater surface restructuring required to accommodate the additional carboxylate on the {111} hydrated surface. Thus, there is a higher steric energy component in the dicarboxylate than in the monocarboxylate. As the organic molecule is somewhat constrained in its geometry the surface modifies itself to a greater degree to actually bond with any additional groups. The results presented here show a very high energy on replacement of ~-1.2 J per carboxylate segment for the dicarboxylate on the {011} surface.

It is significant that the preferred adsorption site for these organics is not the hydrated surface, however, these results ultimately support the experimental data. If adsorption is indeed favoured on the almost bare hematite surface, this would explain the low adsorption area found even at monolayer coverage of the flocculant. This is because the hematite (and corundum) crystal morphology is dominated by the {111} basal plane (Figure 6.9). Preferential adsorption onto faces other than the basal plane has been previously shown for organic molecules on gibbsite (M. Lee *et al.*, 1996).

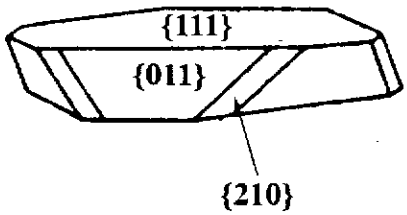

Figure 6.9 Morphology of hematite showing the dominant {111} basal plane (modified from Tröger, 1979).

The configuration inferred from the infrared spectra at pH 7 could not be investigated with the carboxylate model used in this study. However, it is possible that the difference in the adsorption at pH 7 is caused by some of the carboxylate groups adsorbing on the hydrated surface which, due to the 'crowded' nature of this surface, prefers a monodentate configuration. Or it may be due to an exceptionally long Fe-OC bond which imparts monodentate character (as seen by infrared) into the bond.

Finally, the lowered settling of hematite after ageing with hydroxide could be due to the hydroxide ion aggressively hydrating surfaces other than the {111} which under aqueous conditions is not energetically favourable. As the hematite surface should already be hydrated on the {111} under aqueous conditions and contain a negative surface charge by deprotonation of these surface hydroxyls by pH 14, it is likely that ageing the hematite solids in caustic may attack the {011} plane (which is stabilised by hydration at high surface coverages). This then lowers the probability of carboxylate adsorption as hydrated surfaces require greater surface restructuring to allow the carboxylate to interact directly with the surface iron atoms. It also suggests that the proton of the Fe-OH on the hydrated basal plane is not as acidic as that on the near unhydrated {011} plane. As the replacement energy becomes negative for dicarboxylic acids, the surface OH is more likely to be replaced on this ({011}) plane than on the {111} plane where the replacement energy is positive.

6.5 SUMMARY

The molecular modelling work presented in this chapter suggests that the hydration of the hematite surface may well be limited to the O-terminated {111} plane. The {011} plane may interact with water at high coverages while the {210} plane is not stabilised by reaction with water.

When a 'water-rich' and a 'water-poor' hydrated surface are used to investigate the adsorption of decanoate and decandioate on hematite, the adsorption configuration of the carboxylate group is the same as that found by DRIFT at high pH. Qualitatively, the adsorption of carboxylate is independent of the hematite surface it is adsorbed onto, and the chain length of the organic molecule in which the carboxylate functional group is imbedded.

Adsorption of carboxylate is more energetically favourable on the almost unhydrated surface. This may have far reaching ramifications as to the preferred adsorption faces on iron oxides in aqueous systems. For the Bayer system, this may explain the low adsorption area for the flocculant even at the plateau level. If hydroxide ions were more aggressive at hydrating other hematite surfaces this may also explain the decreased settling when hematite is contacted with caustic solution.

7. SUMMARY AND CONCLUSIONS

A number of different strands of information have been gathered together to give a coherent picture of how a polyacrylate flocculant interacts with hematite in synthetic Bayer liquors. Settling tests were able to show the mechanism of flocculation and the Hyamine test allows the adsorption density of the polyacrylate flocculant to be determined in synthetic Bayer liquors for the first time. DRIFT was successfully applied to show the adsorption bonding configuration and molecular modelling was able to independently confirm this configuration. The proposed mechanism is supported by several different techniques ranging from batch settling tests to molecular modelling.

In summary, electrostatic interactions appear to have little impact on flocculation performance due to the high ionic strength nature of Bayer liquors. The adsorption of polyacrylate flocculant onto hematite is by a chemisorption mechanism. The 'active sites' are those containing low numbers of surface hydroxyls, for example the {011} plane, where the carboxylate can directly interact with surface iron atoms. Species such as hydroxide and silicate can also react with these faces lowering the number of 'active sites' for the flocculant to adsorb on.

7.1 HEMATITE

7.1.1 THE HEMATITE SURFACE

Molecular modelling showed that when hematite is contacted with water the oxygen terminated basal {111} plane will hydrate. If the {111} plane was originally iron terminated, $Fe(OH)_3$ units will dissolve to leave behind the oxygen terminated {111} hydrated plane. Under more extreme conditions which were able to produce a monolayer coverage of surface hydroxyls, the {011} plane might also hydroxylate but the {210} plane was not stabilised by reaction with water at any coverage and is not expected to hydroxylate.

Experimentally, it has been shown that the hematite alters its surface characteristics when contacted with hydroxide. A loss of caustic from solution is observed with time (Section 4.1.2) and settling rates decrease to a steady state value during this period. This involves some deprotonation of the surface hydroxyls, however, as the caustic concentration is increased further the modelling results suggest that hydroxide ions may then begin to hydrate non basal planes (for example, the {011} to monolayer coverage).

The deprotonation of surface hydroxyls gives the hematite surface a charge which is then screened by the abundance of counter ions in solution, leading to the observed coagulation of hematite in high caustic environments.

7.1.2 THE FLOCCULATION MECHANISM OF HEMATITE IN SYNTHETIC BAYER LIQUORS

It was shown conclusively that polyacrylate flocculants can adsorb onto hematite in high caustic environments without the presence of calcium, contrary to previous reports (Rothenberg *et al.*, 1989; Jin *et al.*, 1987; Khangoankar and Bala Subramani, 1993). The flocculation mechanism of hematite in Bayer liquors was shown to be bridging. The adsorption of the flocculant produced a monolayer coverage of ~160 $\mu m\ m^{-2}$, best described by a combined Langmuir-Freundlich isotherm. However, the monolayer corresponded to a low adsorbed area (~16 % of the total available area) suggesting that there are few 'active' sites on which the polymer can attach (Section 4.3.1).

Adsorption was found not to be endothermic as the adsorption density remained unaltered with changes in temperature. The synthetic Bayer liquor components of sodium hydroxide and aluminium also did not alter the flocculant adsorption density on hematite.

Flocculation performance was found to be kinetically controlled under Bayer conditions. Factors which affect the kinetics, particularly temperature and viscosity, significantly affect flocculation performance. However, the flocculant conformation, which impacts on the bridging efficiency, does not affect performance as the limiting coiled size of the flocculant is achieved at TCs $\geq$ 50. The optimal settling rate occurred at ~20 % of the monolayer coverage which confirmed that the original

aggregation state played an important role in determining the optimum flocculant dosage.

7.1.3 THE ADSORPTION MECHANISM

XPS showed that sodium was lost from the flocculant on adsorption, suggesting that it did not take part in any adsorption interaction between the flocculant and the hematite surface. Furthermore, results at varying caustic and ionic strengths did not show any change in flocculant adsorption density on hematite. Infrared spectra indicated that the bonding configuration was dependant on the pH of the solution from which adsorption took place. In neutral solutions a monodentate structure was formed while at higher pHs an asymmetric bridging bidentate structure resulted. The shifts in the flocculant infrared band positions on adsorption and the lack of a correlation between ionic strength and flocculant adsorption density suggests a chemisorption mechanism. This was confirmed by the molecular modelling results which were able to reproduce the high pH adsorption configuration.

Molecular modelling also predicted that the most likely plane of adsorption was a near unhydrated (almost bare) hematite surface where direct binding of the carboxylate to the surface iron atoms is easier. Thus, the low monolayer coverage observed is due to the preference of the flocculant to adsorb on almost bare hematite surfaces rather than the hydrated basal plane which dominates the hematite morphology.

7.1.4 PROCESS PARAMETERS' IMPACT ON HEMATITE FLOCCULATION

Aluminium supersaturation did not appear to affect flocculation performance. This suggests that the aluminium is strongly held within the aluminate structure and that the OH ions are not labile. The aluminium thus appears to have no interaction either with the hematite surface or with the flocculant in solution (Section 4.1.3).

Increasing temperature improved flocculation performance, but this is due to the reduction in liquor viscosity (Section 4.1.5) rather than changes in flocculant adsorption density.

Caustic concentration changes do not alter the quantity of flocculant adsorbed but result in decreasing flocculation performance with increasing caustic concentration. The dominant cause of this is due to the increased viscosity of the liquor, however, it may additionally be linked to changes in the kinetics of particle-particle and particle-flocculant collisions resulting in a less efficient aggregation process (Section 4.4).

No impact on flocculation performance was observed with changes in solids concentration, within the solids concentration range studied.

7.2 IMPURITIES

Having established the mechanism of hematite flocculation in synthetic Bayer liquors, a further understanding of the interactions occurring under real refinery conditions was obtained by the investigation of impurities.

7.2.1 SOLUTION IMPURITIES

Some salts were found not to interfere with aggregation; for example, sulphate, chloride and phosphate (Section 5.1.1). The result with phosphate was interesting in that previous work has suggested that it inhibits flocculation (Grubbs *et al.*, 1980). If phosphate does have an effect it must be limited to removal of beneficial species such as calcium as proposed by O'Donnell and Martin (1976).

Other important impurities had significant effects:

i) Carbonate competed with flocculant for surface sites. This is due to the similarity of the carbonate structure to the carboxylate group on the polyacrylate flocculant. However, because of entropy effects large quantities of carbonate (>10 mg g^{-1}) are required before the adsorption of flocculant is significantly affected (Section 5.1.2).

i) Calcium adsorbed on hematite but its presence did not alter the quantity of flocculant adsorbed on the hematite surface, further supporting the chemisorption

hypothesis (Section 5.1.3). However, the observed improvement in turbidity suggested that more flocculant linkages are being made when calcium is present.

ii) FTIR of adsorbed flocculant in the presence of calcium at pH 7 showed carboxylate adsorption in both a monodentate and bidentate configuration. The monodentate configuration was the same as when calcium was absent while the bidentate configuration is most likely to be a chelating structure. It is known that calcium can complex polyacrylate (Miyajima *et al.*, 1996) and therefore it is likely that the adsorbed calcium on hematite complexes additional carboxylate units to the surface without increasing the number of flocculant molecules adsorbed at a given dosage.

iv) Silicate competed for surface adsorption sites (Section 5.1.4). With 0.2 mg g^{-1} sodium silicate in Bayer liquors, aggregation was significantly affected. The silicate was found to have a high affinity for the hematite surface (adsorbing ~70 % of the added silicate). The decrease in settling rate and increase in turbidity is thus thought to be due to readsorption of (alumino)silicate species on the hematite surface which block the 'active' sites for the flocculant.

7.2.2 SOLID IMPURITIES

A hematite sample containing a uniform surface contaminant of an (alumino)silicate composition was found to show distinct flocculation behaviour:

i) The sample showed improved, rather than deteriorating, flocculation with conditioning in caustic (Section 5.2.1.1). This is due to the amorphous silicate contaminant dissolving in the caustic and leaving behind vacant sites for the flocculant to adsorb.

ii) The effect observed with increasing flocculant dosage was similar to that found for refinery materials (Section 5.2.1.2) in that some re-dispersion is observed at high flocculant dosages. The adsorption isotherm for hematite Sample C was similar to pure hematite except that the monolayer coverage was lower even after the standard contact time with caustic (which should have removed the surface impurity). Thus, caustic may dissolve the amorphous impurity which then establishes an equilibrium between adsorbed and solution species. The

readsorption of these species onto 'active sites' blocks flocculant adsorption. Alternatively, not all of the surface silicate may have been removed.

iii) Flocculation was very sensitive to caustic strength. Flocculation was not observed in batch settling tests (Section 5.2.1.3) at TCs > 200. Aggregate size data, obtained with a Lasentec® probe, showed flocculation did occur but only to a very low extent. It is speculated that the readsorption of silicate (from the liquor) hinders aggregation at the higher caustic strengths. This is supported by the observation of flocculation for this sample when the hematite surface was cleaned by dialysis, by the lack of similar behaviour with the pure hematite and by the solution silicate results. The lower chord length change observed by the Lasentec® probe in synthetic liquor as compared to pure caustic lends weight to the notion that the readsorbing species could be both a silicate or an aluminosilicate.

Precipitation of a surface contaminant by digestion with kaolin resulted in an inhomogenous surface impurity (Section 5.2.2). This was shown to have a lower flocculant adsorption density, however, the difference was small as a large part of the hematite surface was not affected by the DSP precipitation. Clearly, however, the presence of both solution and surface silicates is detrimental to flocculation of hematite by polyacrylates.

7.3 REFINERY SOLIDS

Refinery solids were found to vary substantially from batch to batch and clear trends were difficult to extract. However, the major findings from the refinery samples are:

i) The refinery flocculant (H-199B) does not degrade over a 24 hour period but does show a conformational adjustment over a 1-2 hour period (Section 4.1.1). This is due to the flocculant being in an elongated conformation in the original emulsion which then coils when it comes into contact with the high ionic strength Bayer liquors. This results in a decrease to a steady state value once the equilibrium conformation has been obtained.

ii) Refinery solids, like hematite, do not show complete re-dispersion at high dosages of flocculant (Section 4.3.1.2). This is thought to be due to the fact that

adsorption and particle collisions occur simultaneously. The kinetics of adsorption is similar to the kinetics of collisions so the particles are able to flocculate even when the concentration of polymer exceeds monolayer coverage.

The presence of coarser sand fractions was found to be beneficial to both settling and turbidity (Section 5.2.3). If not detrimental to the industrial process, the cut-off for the sand fraction need not be as low as 150 μm, as is commonly used and could be set at ~300 μm.

From the pure hematite data it would be recommended that, for optimal flocculation, improving kinetic factors would result in improved refinery solids flocculation. If not detrimental to other unit operations in the refining process, an increase in temperature could be an easy and cost-efficient means of achieving better waste solids flocculation due to the decrease in viscosity which results.

Factors which affect polymer conformation are not expected to impact on the clarification stage as the polymer should be at its limiting size, but they may significantly affect flocculation in the washer trains at lower caustic concentrations.

Refineries routinely operate at high carbonate concentrations, however the presence of both carbonate and silicate in solution is to be avoided as these species compete with the flocculant. While polyacrylate flocculation performance is not significantly reduced until carbonate concentrations of >10 mg g^{-1} are reached, silicate will impact on flocculation at levels of 0.2 mg g^{-1}. The addition of lime in the refinery may improve the flocculation of other minerals, however, even if its action were only to improve clarity as was observed for hematite in this work, its addition would be of benefit as clarity impacts on product purity.

7.4 FUTURE WORK

While a clear picture of polyacrylate flocculation of hematite has been gained, the settling of other Bayer minerals such as goethite and quartz and the formation of both amorphous and crystalline DSPs may have very a significant effect on the overall settling process. The adsorption of other flocculants used in the Bayer process (such as starch, polyacrylamides and polyhydroxamates) is of interest. Finally, the effect (if

any) of minerals acting synergistically (as suggested by Yamada *et al.*, 1980) needs to be addressed.

On the modelling front many avenues are open to future work. For example:

i) the investigation of other organics species to determine whether there are organics which prefer water rich surfaces

ii) the modelling of the carboxylate with non equivalent oxygen atoms so that the pH 7 results could be tested.

Charging problems with the samples prevented much useful information from being obtained from XPS analysis. Investigation of ways to overcome the sample charging problems may allow higher pH samples and conformational information on the adsorbed flocculant to be obtained. Also, the flocculant XPS characteristics when sodium is exchanged with lithium, potassium and other cations would remove the interference found and make the spectra more quantitative.

Bibliography

Allara, D. L. and Nuzzo, R. G. (1985) 'Spontaneously organized molecular assemblies. 2. Quantitative infrared spectroscopic determination of equilibrium structures of solution-adsorbed n-alkanoic acids on an oxidised aluminum surface', *Langmuir*, **1**, 52-66.

Allen, T. (1990) *Particle Size Measurement*, Chapman and Hall, Cornwall.

Allison, J. D., Wimberly, J. W. and Ely, T. L. (1987) 'Automated and manual methods for the determination of polyacrylamide and other anionic polymers', *SPE Resevoir Engineering*, **2(2)**, 184-188.

Anthony, M. T. and Seah, M. P. (1984) 'XPS: Energy calibration of electron spectrometers', *Surf. Interface Anal.*, **6(3)**, 95-106.

Armstrong, G. H., Johnson, L. and Parker, A. A. (1994) 'Effect of polymeric steric stabilizers on the settling of alumina', *J. Applied Polym. Sci.*, **52**, 997-1004.

Bagster, D. F. (1985) 'Studies in the selective flocculation of hematite from gangue using high molecular weight polymers. Part 1 Chemical Factors. Part 2. Physical Factors', *Int. J. Miner. Processing*, **14**, 1-32.

Bajpai, A. K. and Bajpai, S. K. (1996) 'Kinetics of flocculation of iron oxide particles by polyacrylamide', *Indian Journal of Chemical Technology*, **3**, 219-223.

Barrón, V. and Torrent, J. (1996) 'Surface hydroxyl configuration of various crystal faces of hematite and goethite', *J. Colloid and Interface Sci.*, **177**, 407-410.

Basu, P. (1983) 'Reactions of iron minerals in sodium aluminate solutions', *Light Metals*, 83-97.

Basu, P., Nitowski, G. A. and The, P. J. (1986), 'Chemical interactions of iron minerals during Bayer digest and clarification', *Proceedings of Iron Control in Hydrometallurgy*, 223-244.

Bayer, K. J. (1888), Patent 43977, Germany.

Beamson, G. and Briggs, D. (1992) *High resolution XPS of organic polymers, the Scienta ESCA 300 Database*, J. Wiley and sons, Chichester.

Becker, U., Hochella Jnr., M. F. and Aprà, E. (1996) 'The electronic structure of hematite {001} surfaces: Applications to the interpretation of STM images and heterogenous surface reactions', *Am. Mineralogist*, **81**, 1301-1314.

Bell, G. M. (1976) 'The partition of starch between Bayer plant liquor and red mud', *Light Metals*, **2** 99-113.

Ben-Taleb, A., Vera, P., Delgado, A. V. and Gallardo, V. (1994) 'Electrokinetic studies of monodisperse hematite particles: effects of inorganic electrolytes and amino acids', *Mater. Chem. Phys.*, **37**, 68-75.

Bergström, L., Schilling, C. H. and Aksy, I. A. (1992) 'Consolidation behaviour of flocculated alumina suspensions', *J. Am. Ceramic Soc.*, **75(12)**, 3305-3314.

Bhatty, J. I., Davies, L., Dollimore, D. and Zahedi, A. H. (1982) 'The use of hindered settling data to evaluate particle size or floc size and the effect of particle-liquid association on such sizes', *Surf. Techn.*, **15**, 323-344.

Blake, R. L., Hessevick, R. E., Zoltai, T. and Finger, L. W. (1996), 'Refinement of the hematite structure', *Am. Mineralogist*, **51**, 123-129.

Blecic, D. and Adzic, M. (1990), 'Analysis of the results obtained by experimental investigation of aluminate solution separation from red mud', *6th Yugoslav International Symposium on Aluminium. I. Bauxites and Extractive Metallurgy*, Yugoslavia, 113-123.

Bloys van Treslong, C. J. and Staverman, A. J. (1974) 'Poly(ethylenimine) II Potentiometric titration behaviour in comparison with other weak polyelectrolytes', *Recueil, Journal of the Royal Netherlands Chemical Society*, **93(6)**, 171-178.

Bournel, F., Laffon, C., Parent, P. and Tourillon, G. (1996) 'Adsorption of acrylic acid on aluminium at 300K: a multi-spectroscopic study', *Surface Sci.*, **352-354**, 228-231.

Bremer, L. G. B., Walstra, P. and van Vliet, T. (1995) 'Estimations of the aggregation time of various colloidal systems', *Colloids Surfaces*, **99**, 121-127.

Brown Jnr., G. E. (1990) In *Mineral-Water Interface Geochemistry*, Reviews in Mineralogy, Mineralogical Society of America, Chapter 8.

Brown, R. W. (1942), Aluminium Company of America, Patent 2,280,998, USA.

Buckland, A. D., Rochester, C. H. and Topham, S. A. (1980) 'Infrared study of the adsorption of carboxylic acids on haematite and goethite immersed in carbon tetrachloride', *J. Chem. Soc. Faraday Trans. 1*, **76**, 302-313.

Buravlev, T. T., Slyusarov, I. T., Lyashenko, A. A. and Plyushkin, M. Z. (1972) 'Investigation of certain factors influencing the rate of settling of muds during alumina production from Yugoslav bauxite by the Bayer process', *J. Appl. Chem. USSR*, **45(1)**, 25-30.

Buscall, R. and White, L. R. (1987) 'The consolidation of concentrated suspensions. Part 1. The theory of sedimentation', *J. Chem. Soc. Faraday Trans. 1*, **83**, 873-891.

Bush, T. S., Gale, J. D., Catlow, R. A. and Battle, P. D. (1994) 'Self-consistent interatomic potentials for the simulation of binary and ternary oxides', *J. Mater. Chem.*, **4(6)**, 831-837.

Cambridge Crystallographic Database; Allen, F. H. and Kennard, O. (1993) *Chemical Design Automation News*, **8(1)**, 31-37.

Cardile, C. (1992), 'Removal and conversion of DSP in red mud into type 4A zeolite', *International Bauxite Tailings Workshop*, Perth, Western Australia, 399-408.

Chandler, J. L. (1976) 'Advances in the use of synthetic polymers', *Light Metals*, **2**, 163-171.

Chapman, D. D. (1913) *Phil. Mag.*, **25(6)**, 457.

Childers, J. W., Röhl, R. and Palmer, R. A. (1986) 'Direct comparison of the capabilities of photoacoustic and diffuse reflectance spectroscopies in the ultraviolet, visible and near-infrared regions', *Anal. Chem.*, **58**, 2629-2636.

Chmelir, M., Kurscher, A. and Bathell, E. (1980) 'Water soluble acrylamide polymers 2. Aging and viscous flow of aqueous solutions of polyacrylamide and hydrolysed polyacrylamide.', *Angew. Makromol. Chem.*, **89**, 145-165.

Christensen, H. and Christensen, A. N. (1978) *Acta Chem. Scand.*, **A32**, 87-88.

Connelly, L. J., Owen, D. O. and Richardson, P. F. (1986) 'Synthetic flocculant technology in the Bayer process', *Light Metals*, 61-98.

Crees, O. L., Senogles, E. and Whayman, E. (1991) 'The flocculation of cane sugar muds with acrylamide-sodium acrylate copolymers', *J. Appl. Polym. Sci.*, **42**, 837-844.

Crummett, W. B. and Hummel, R. A. (1963) 'The determination of traces of polyacrylamides in water', *J. Am. Wat. Wks Ass.*, **55** 209-219.

de Leeuw, N. H., Watson, G. W. and Parker, S. C. (1995) 'Atomistic simulation of the effect of dissociative adsorption of water on the surface structure and stability of calcium and magnesium oxide', *J. Phys. Chem.*, **99**, 17219-17225.

de Leeuw, N. H., Watson, G. W. and Parker, S. C. (1996) 'Atomistic simulation of adsorption of water on three-, four- and five-coordinated surface sites of magnesium oxide', *J. Chem. Soc. Faraday Trans.*, **92(12)**, 2081-2091.

Department of Resources Development (1997) In *Prospect. Western Australia's international magazine of resources development*, pp. 30-31.

Derjaguin, B. V. and Landau, L. D. (1941) *Acta Physiochim URSS*, **14**, 633.

Dick, B. G. and Overhauser, A. W. (1958) *Phys. Rev.*, **112**, 90.

Drees, L. R., Wilding, L. P., Smeck, N. E. and Senkayi, A. L. (1989) In *Minerals in soil environments*, (Eds, Dixon, J. B. and Weed, S. B.) Soil Science Society of America, Madison, pp. 916.

Dryzmala, J. and Fuerstenau, D. W. (1987) In *Flocculation in Biotechnology and Separation Systems*, (Ed, Attia, Y. A.) Elsevier Science Publishers B.V. Amsterdam, , pp. 45-60.

Evans, S. J. (1992), 'Flocculation and viscosity modification of red mud as an aid to dry disposal of tailings', *International Bauxite Tailings Workshop*, Perth, Western Australia, 70 -83.

Farmer, V. C. (1974) *The infrared spectra of minerals*, Mineralogical Society, London.

Farrow, J. B., Gong, W.-Q. and Warren, L. J. (1985), 'Floc size and floc density by the hindered settling method', *The Thirteenth Australian Chemical Engineering Conference, Chemeca 85*, Perth, Australia, 211-216.

Farrow, J. B. and Swift, J. D. (1996) 'A new procedure for assessing the performance of flocculants', *Int. J. Miner. Process.*, **46**, 263-275.

Farrow, J. B. and Warren, L. J. (1989) In *Flocculation and Dewatering*, (Eds, Moudgil, B. M. and Scheiner, B. J.) Engineering Foundation, New York, pp. 153-165.

Farrow, J. B. and Warren, L. J. (1993) In *Coagulation and Flocculation: Theory and Applications*, (Ed, Dobias, B.) Marcell Dekker, New York, pp. 391-426.

Fawell, P., Richmond, W., Jones, L. and Collisson, M. (1997) 'Focused beam reflectance measurement in the study of mineral suspensions', *Chemistry in Australia*, **4(2)**, 4-6.

Fleer, G. J. and Schuetgens, J. M. H. M. (1993) In *Coagulation and Flocculation: Theory and Applications*, (Ed, Dobias, B.) Marcell Dekker, New York, pp. 209-263.

Fripiat, J. G., Lucas, A. A., André, J. M. and Derouane, E. G. (1977) 'On the stability of polar surface planes of macroscopic crystals', *J. Chem. Phys.*, **21**, 101.

Gale, J. D. (1992-96), General Utility Lattice Program (GULP), Royal Institute of Great Britain, Imperial College.

Gale, J. D. (1996) 'Empirical potential derivation for ionic materials', *Philosophical Magazine B*, **73(1)**, 3-19.

Gale, J. D., Catlow, C. R. A. and Mackrodt, W. C. (1992) 'Periodic *ab initio* determination of interatomic potentials for alumina', *Modelling Simul. Mater. Sci. Eng.*, **1**, 73-81.

Gay, D. H. and Rohl, A. L. (1995) 'MARVIN: A new computer code for studying surfaces and interfaces and its application to calculating the crystal morphologies of corundum and zircon', *J. Chem. Soc. Faraday Trans.*, **91**, 925-936 and references there in.

Glenister, D. J. (1992), Preface to the *International Bauxite Tailings Workshop*, Perth, Western Australia.

Glenister, D. J. and Thornber, M. R. (1985), 'Alkalinity of red mud and its application for the management of acid wastes', *The Thirteenth Australian Chemical Engineering Conference, Chemeca 85*, Perth, Australia, 109-113.

Gong, W. Q., Parentich, A., Little, L. H. and Warren, L. J. (1991) 'Diffuse reflectance infrared Fourier transform spectroscopic study of the adsorption mechanism of oleate on haematite', *Colloids Surfaces*, **60**, 325-339.

Goüy, G. (1910) *J. Phys.*, **9(4)**, 457.

Gregory, J. (1987) In *Flocculation in Biotechnology and Separation Systems*, (Ed, Attia, Y. A.) Elsevier Science Publishers B. V., Amsterdam, pp. 31-44.

Gregory, J. (1989) 'Fundamentals of flocculation', *CRC Critical Reviews in Environmental Control*, **19(3)**, 185-230.

Grubbs, D. K., Rodenburg, J. K. and Wefers, K. A. (1980), 'The geology, mineralogy and clarification properties of red and yellow Jamaican bauxites', *Proceedings of Bauxite Symposium IV*, 176-186.

Haas, H. C. and MacDonald, R. L. (1972a) 'Dichotomies in the viscosity stability of polyacrylamide solutions. I', *J. Appl. Polym. Sci.*, **10**, 461-467.

Haas, H. C. and MacDonald, R. L. (1972b) 'Dichotomies in the viscosity stability of polyacrylamide solutions. II', *J. Appl. Polym. Sci.*, **16**, 2709-2713.

Hamilton, W. C. and Ibers, J. A. (1968) *Hydrogen Bonding in Solids: Methods of Molecular Structure Determination*, Benjamin, New York.

Han, K. N., Healy, T. W. and Fuerstenau, D. W. (1973) 'The mechanism of adsorption of fatty acids and other surfactants at the oxide-water interface', *J. Colloid Interface Sci.*, **44(3)**, 407-414.

Hartman, P. (1989) 'The effect of surface relaxation on crystal habit: cases of corundum (α-Al_2O_3) and hematite (α-Fe_2O_3)', *J. Crystal Growth*, **96**, 667-672.

Hashiba, M., Sakurada, O., Itho, M., Takagi, T., Hiramatsu, K. and Nurishi, Y. (1993) 'Effectiveness of a dispersant for the thickening of alumina slurries whilst retaining the fluidity', *J. Mater. Sci.*, **28**, 4456-4460.

Healy, T. W. (1961) 'Flocculation-dispersion behaviour of quartz in the presence of a polyacrylamide flocculant', *J. Colloid Sci.*, **16**, 609-617.

Henderson, J. M. and Wheatley, A. D. (1987) 'Factors affecting the efficient flocculation of tailings by polyacrylamides', *Coal Preparation*, **4**, 1-49.

Hendewerk, M., Salmeron, M. and Somorjai, G. A. (1986) 'Water adsorption on the (001) plane of Fe_2O_3: An XPS, UPS, Auger, and TPD study', *Surf. Sci.*, **172**, 544-556.

Hogg, R. (1984) 'Collision efficiency factors for polymer flocculation', *J. Colloid Interface Sci.*, **102(1)**, 232-236.

Hogg, R., Bunnaul, P. and Suharyono, H. (1993) 'Chemical and physical variables in polymer-induced flocculation', *Minerals and Metallurgical Processing*, **10(2)**, 81-85.

Hogg, R., Kimpel, R. C. and Ray, D. T. (1987) 'Agglomerate structure in flocculated suspensions and its effect on sedimentation and dewatering', *Minerals and Metallurgical Processing*, **4(2)**, 108-114.

Hsu, J.-P. and Lin, D.-P. (1996) 'Flocculation by very high molecular weight polymers', *Colloid Polym. Sci.*, **274**, 172-177.

Hsu, J.-P., Lin, D.-P. and Tseng, S. (1995) 'The sticking probability of colloidal particles in polymer-induced flocculation', *Colloid Polym. Science*, **273** 271-278.

Hunter, J. R. (1987) *Foundations of Colloid Science*, Clarendon Press, Oxford.

Hunter, T. K., Moody, G. M. and Tran, C. A. (1990), 'Advances in liquor clarification and mud flocculation in the Bayer process alumina industry', *International Alumina Quality Workshop*, Perth, Australia, 395-404.

Ikkatai, T. and Okada, N. (1963), 'Viscosity, specific gravity and equilibrium concentration of sodium aluminate solutions', *The Extractive Metallurgy of Aluminium*, 159-174.

Ishiduki, K. and Esumi, K. (1997a) 'Adsorption characteristics of poly(acrylic acid) and poly(vinylpyrrolidone) on alumina from their mixtures in aqueous solution', *J. Colloid Interface Sci.*, **185**, 274-277.

Ishiduki, K. and Esumi, K. (1997b) 'The effect of pH on adsorption of poly(acrylic acid) and poly(vinylpyrrolidone) on alumina from their binary mixtures', *Langmuir*, **13**, 1587-1591.

Ishikawa, K., Yoshioka, T., Sato, T. and Okuwaki, A. (1997) 'Solubility of hematite in LiOH, NaOH and KOH solutions', *Hydrometallurgy*, **45**, 129-135.

Jin, R., Hu, W. and Hou, X. (1987) 'Mechanism of selective flocculation of hematite from quartz with hydrolyzed polyacrylamide', *Colloids Surfaces*, **26**, 317-331.

Kahane, R. B. (1992), 'Effective flocculation in a counter current decantation circuit', *International Bauxite Tailings Workshop*, Perth, Western Australia, 14-23.

Khangoankar, P. R. and Bala Subramani, K. J. (1993) 'Flocculation of hematite fines by anionic polyacrylamide polymers', *Miner. Eng.*, **6(7)**, 765-774.

Klauber, C. (1993) 'Refinement of magnesium and aluminium K_α X-ray source functions', *Surf. Interface Anal.*, **20**, 703-715.

Knacke, O., Kubaschewski, O. and Hesselmann, K. (1991) *Thermochemical properties of inorganic substances I*, Springer-Verlag, Berlin.

Kolb, M., Botet, R. and Jullien, R. (1983) 'Scaling of kinetically growing clusters', *Phys. Rev. Lett.*, **51(13)**, 1123.

Kontopoulos, A., Marinos-Kouris, D. and Vassiliou, P. (1981) 'Effect of flocculants on settling and filtration of red mud in the alumina industry', *Filtration and Separation*, **18(4)**, 321-322.

Koopal, L. K. (1992) In *Colloid Chemistry in Mineral Processing*, (Eds, Laskowski, J. S. and Ralston, J.) Elsevier, Amsterdam, pp. 37-96.

Kretzschmar, R., Robarge, W. P. and Weed, S. B. (1993) 'Flocculation of kaolinitic soil clays: effects of humic substances and iron oxides', *Soil Sci. Soc. Am. J.*, **57(5)**, 1277-1283.

Kulicke, W., Otto, M. and Baar, A. (1993) 'Improved NMR characterization of high-molecular-weight polymers and polyelectrolytes through the use of preliminary ultrasonic degradation', *Makromol. Chem.*, **194**, 751-765.

Kulicke, W.-M. and Hörl, H.-H. (1985) 'Preparation and characterisation of a series of poly(acrylamide-co-acrylates), with a copolymer composition between 0-96.3 mol%

acrylate units with the same degree and distribution of polymerisation', *Colloid Polym. Sci.*, **263**, 530-540.

Kulicke, W.-M. and Kniewske, R. (1981) 'Long term change in conformation of macromolecules in solution', *Makromol. Chem.*, **182**, 2277-2287.

La Mer, V. K. (1964) 'Coagulation Symposium Introduction', *J. Colloid Sci.*, **19**, 291-293.

Lee, D. H., Condrate Snr., R. A. and Reed, J. S. (1996) 'Infrared spectral investigation of polyacrylate adsorption on alumina', *J. Mater. Sci.*, **31**, 471-478.

Lee, L. T. and Somasundaran, P. (1989) 'Adsorption of polyacrylamide on oxide minerals', *Langmuir*, **5**, 854-860.

Lee, M., Rohl, A. L., Gale, J. D., Parkinson, G. M. and Lincoln, F. J. (1996b) 'The influence of metal ion inclusion on the morphology of gibbsite', *Trans. IChemE*, **74(A)**, 739-743.

Leontaridis, N. and Marinos-Kouris, D. (1992) 'Grecian red mud - thickening and filtration parameters and process design', *Filtration and Separation*, **29(1)**, 51-56.

Levich, V. G. (1962) *Physiochemical Hydrodynamics*, Prentice-Hall, Englewood Cliffs (USA).

Lewis, G. V. and Catlow, C. R. A. (1985) 'Potential models for ionic oxides', *J. Phys. C: Solid State Phys.*, **18**, 1149-1161.

Li, L. Y. and Rutherford, G. K. (1996) 'Effect of bauxite properties on the settling of red mud', *Int. J. Miner. Process.*, **48**, 169-182.

Lyklema, J. (1989) In *Flocculation and Dewatering*, Engineering Foundation, New York, USA, pp. 1-20.

Lyklema, J. (1995) *Fundamentals of Interface and Colloid Science*, Academic Press Limited, London.

McCluskey, P. H., Snyder, R. L. and Condrate Snr, R. A. (1989) 'Infrared spectral studies of various metal polyacrylates', *J. Solid State Chem.*, **83**, 332-339.

Meakin, P. (1983) 'Formation of fractal clusters and networks by irreversible diffusion-limited aggregation', *Physical Rev. Lett.*, **51(13)**, 1119.

Michaels, A. S. and Bolger, J. C. (1962) 'Settling rates and sediment volumes of flocculated kaolin suspensions', *Ind. Eng. Chem. Fundam.*, **1**, 24-33.

Michaels, A. S. and Morelos, O. (1955) 'Polyelectrolyte adsorption by kaolinite', *Indust. Eng. Chem.*, **47**, 1801-1809.

Miyajima, T., Mori, M. and Ishiguro, S. (1997) 'Analysis of complexation equilibria of polyacrylic acid by a Donnan-based concept', *J. Colloid Interface Sci.*, **187**, 259-266.

Miyajima, T., Mori, M., Ishiguro, S., Chung, K. H. and Moon, C. H. (1996) 'On the complexation of Cd(II) ions with polyacrylic acid', *J. Colloid Interface Sci.*, **184**, 279-288.

Morrison, R. T. and Boyd, R. N. (1977) *Organic Chemistry*, Allyn and Bacon, USA.

Molecular Simulations Incorporated, Biosym Technologies, San Diego.

Moudgil, B. M. and Vasudevan, T. V. (1989) 'Role of active sites in selective flocculation', *J. Colloid Interface Sci.*, **127(1)**, 239-243.

Nakamoto, K. (1986) *Infrared and Raman spectra of inorganic and coordination compounds*, John Wiley & Sons, New York and references there in.

Narkis, N. and Rebhun, M. (1966) 'Ageing effects in measurements of polyacrylamide solution viscosities', *Polymer*, **7**, 507-512.

Ni, L. P., Bunchuk, L. V., Kopylova, E. A., Goldman, M. M., Ponomarev, V. D. and Kushinkov, Y. A. (1968) 'A study of hydrogarnets formed in the Al_2O_3-CaO-Fe_2O_3-Na_2O-SiO_2-H_2O system', *Russian Journal of Inorganic Chemistry*, **13(11)**, 1585-1587.

Nygren, M. A., Gay, D. H. and Catlow, C. R. A. (1997) 'Hydroxylation of the surface of the corundum basal plane', *Surf. Sci.*, **380**, 113-123.

O'Donnell, N. B. and Martin, W. (1976) 'The commercial processing of goethitic bauxites from Western Jamaica', *Light Metals*, 135-146.

Orban, F., Pinter, T., Sigmond, G., Siklosi, P., Solymar, K., Tóth, P. and Zambo, J. (1973) 'Processing of bauxites containing goethite', *Hung. Teljes.*, **6**, 758.

Panzer, H. P. and Halverson, F. (1989) In *Flocculation and Dewatering*, (Eds, Moudgil, B. M. and Scheiner, B. J.) Engineering Foundation, New York, pp. 239-249.

Papirer, E., Perrin, J.-M., Nanse, G. and Fioux, P. (1994) 'Adsorption of poly(methylmethacrylate) on an alpha alumina: Evidence of formation of surface carboxylate bonds', *Eur. Polym. J.*, **30(8)**, 985-991.

Parekh, B. K. and Goldberger, W. M. (1976), 'An assessment of technology for possible utilization of Bayer process muds', 600/2-76-301 US EPA Report.

Parfitt, R. L., Farmer, V. C. and Russell, J. D. (1977) 'Adsorption on hydrous oxides. I. Oxalate and benzoate on goethite. II. Oxalate, benzoate and phosphate on gibbsite', *J. Soil Sci.*, **28**, 29-47.

Parfitt, R. L. and Smart, R. S. C. (1978) 'The mechanism of sulphate adsorption on iron oxides', *Soil Sci. Soc. Am. J.*, **42**, 48-50.

Pavez, O., Brandao, P. R. G. and Peres, A. E. C. (1996) 'Technical note: Adsorption of oleate and octyl-hydroxamate on to rare-earths minerals', *Miner. Eng.*, **9(3)**, 357-366.

Pawlek, R. (1995) *Alumina refineries and producers of the world*, Aluminiums - Verlag, Düsseldorf.

Pearse, M. J. and Sartowski, Z. (1984), 'Application of special chemicals (flocculants and dewatering aids) for red mud separation and hydrate filtration', *1984 Bauxite Symposium*, Los Angeles, California, USA, 788-810.

Prakash, S. and Horváth, Z. (1981) 'Effect of titanium dioxide content of the bauxite charge on the settling properties of the red mud', *Publ. Techn. Univ. Heavy Industry, Series B. Metallurgy*, **34**, 69-89.

Pugh, R. J. and Lundström, H. (1987) In *Flocculation in Biotechnology and Separation Systems*, (Ed, Attia, Y. A.) Elsevier Science Publishers B. V., Amsterdam, pp. 673-694.

Ratajczak, H. and Orville-Thomas, W. J. (1967-68) 'Hydrogen bond studies. Part 1: The relationship between vibrational frequencies and bond length in the O-H···O hydrogen bonded systems', *J. Molecular Struct.*, **1**, 449-461.

Richardson, J. F. and Zaki, W. N. (1954) 'Sedimentation and fluidisation: Part I', *Trans. Instn. Chem. Engrs.*, **32**, 35-52.

Ringenbach, E., Chauveteau, G. and Pefferkorn, E. (1993) 'Adsorption of polyelectrolytes on soluble oxides induced by polyion complexation with dissolution species', *J. Colloid Interface Sci.*, **161**, 223-231.

Roach, G. I. D. (1992), 'Recovering value from bauxite tailings', *International Bauxite Tailings Workshop*, Perth, Western Australia, 409-418.

Rochester, C. H. and Topham, S. A. (1979a) 'Infrared study of surface hydroxyl groups on goethite', *J. Chem. Soc. Faraday Trans.*, **75**, 591-602.

Rochester, C. H. and Topham, S. A. (1979b) 'Infrared study of surface hydroxyl groups on hematite', *J. Chem. Soc. Faraday Trans.*, **75**, 1073-1088.

Rogan, K. R. (1995) 'The variations of the configurational and solvency properties of low molecular weight sodium polyacrylate with ionic strength', *Colloid Polym. Sci.*, **273**, 364-369.

Rohl, A. L., Gay, D. H., Davey, R. J. and Catlow, C. R. A. (1996) 'Interactions at the organic/inorganic interface: Molecular modeling of the interaction between diphosphonates and the surfaces of barite crystals', *J. Am. Chem Soc.*, **118(3)**, 642-648.

Rothenberg, A. S., Spitzer, D. P., Lewellyn, M. E. and Heitner, H. I. (1989) 'New reagents for alumina processing', *Light Metals,* 91-96.

Ruehrwein, R. A. and Ward, D. W. (1952) 'Mechanism of clay aggregation by polyelectrolytes', *Soil Sci.*, **73**, 485-492.

Rustad, J. R., Felmy, A. R. and Hay, B. P. (1996a) 'Molecular statics calculations of proton binding to goethite surfaces: A new approach to estimation of stability constants for multisite surface complexation models', *Geochimica et Cosmochimica Acta*, **60(9)**, 1563-1576.

Rustad, J. R., Felmy, A. R. and Hay, B. P. (1996b) 'Molecular statics calculations for iron oxide and oxyhydroxide minerals: Toward a flexible model of the reactive mineral-water interface', *Geochimica et Cosmochimica Acta*, **60(9)**, 1553-1562.

Ryles, R. G. and Avotins, P. V. (1996), 'Superfloc® HX, a new technology for the alumina industry', *Fourth International Alumina Quality Workshop*, Darwin, Australia, 205-215.

Sankey, S. E. and Schwarz, R. J. (1984) 'The use of synthetic flocculant polymers in settling red muds derived from high goethitic bauxite ores', *Light Metals,* 1653-1667.

Sarmiento, G. and Uhlherr, P. H. T. (1979) 'The effect of temperature on the sedimentation parameters of flocculated suspensions', *Powder Techn.*, **22**, 139-142.

Schrader, B. (1995) *Infrared and Raman Spectroscopy*, VCH Verlagsgesellschaft mbH, Weinheim.

Schröder, K., Sauer, J., Leslie, M., Richard, C., Catlow, A. and Thomas, J. M. (1992) 'Bridging hydroxyl groups in zeolitic catalysts: a computer simulation of their structure, vibrational properties and acidity in protonated faujasites (H-Y zeolites)', *Chem. Phys. Lett.*, **188(3,4)**, 320-325.

Schwertmann, U. and Cornell, R. M. (1991) *Iron oxides in the laboratory. Preparation and Characterization*, VCH Verlagsgesellschaft mbH, Weinheim.

Scott, J. P., Fawell, P. D., Ralph, D. E. and Farrow, J. B. (1996) 'The shear degradation of high-molecular-weight flocculant solutions', *J. Appl. Polym. Sci.*, **62**, 2097-2106.

Shirley, D. A. (1972) 'High-resolution X-ray photoemission spectrum of the valence bands of gold', *Phys. Rev. B.*, **5(12)**, 4709-4714.

Shyluk, W. P. and Stow, F. S. (1969) 'Ageing and loss of flocculation activity of aqueous polyacrylamide solutions', *J. Appl. Polym. Sci.*, **13**, 1023-1036.

Silbert, F. J. (1968), Nalco Chemical Company, Patent 3,390,959, USA.

Smellie Jnr., R. H. and La Mer, V. K. (1958) 'Flocculation, subsidence and filtration of phosphate slimes. VI. A quantitative theory of filtration of flocculated suspensions', *J. Colloid Sci.*, **23**, 589-599.

Song, Q. Y., Xu, F. and Tsai, S. C. (1992) 'Magnetic seeding flocculation of weakly magnetic iron materials', *Int. J. Min. Process.*, **34**, 219-229.

Spitzer, D. P., Rothenberg, A. S., Heitner, H. I., Lewellyn, M. E., Laviolette, L. H., Foster, T. and Avotins, P. V. (1991) 'Development of new Bayer process flocculants', *Light Metals*, 167-171.

Stern, O. (1924) *Z. Elektrochem.*, **30**, 508.

Swingle, R. S. and Riggs, W. M. (1975) 'ESCA', *Critical Reviews in Analytical Chemistry*, **5(3)**, 267-321.

Szytuta, A., Burewicz, A., Dimitrijevic, Z., Krasnicki, S., Rzany, H., Todorovic, J., Wanic, A. and Wokki, W. (1968) *Physica Status Solidi*, **26**, 429-434.

Tackett, J. E. (1990) 'Determination of low amounts of carboxylate in polyacrylamide using FT-IR', *Appl. Spectroscopy*, **44(9)**, 1581-1583.

The, P. J. and Sivakumar, T. J. (1985) 'The effect of impurities on calcium in Bayer liquor', *Light Metals*, 209-222.

Tóth, L. and Zöldi, J. (1982) 'Intensifying of the red mud thickening', *Publ. Techn. Univ. Heavy Industry, Miskolc, Series B. Metallurgy*, **35**, 69-82.

Tröger, W. E. (1979) *Optical determination of rock-forming minerals*, 4th Edition (Ed, Bambauer, H. U., Taborszky, F., and Trochim, H. D.), Schweizerbartsche Verlagsbuchhandlung, Stuttgart.

van Bronswijk, W. (1997), personal communication.

Verwey, E. J. W. and Overbeek, J. T. G. (1948) *Theory of the stability of hydrophobic colloids*, Elsevier, Amsterdam.

von Smoluchowski, M. (1916) *Phys. Z.*, **17**, 557.

von Smoluchowski, M. (1917) *Z. Phys. Chem.*, **92**, 129.

Wada, K. (1989) In *Minerals in Soil Environments*, (Eds, Dixon, J. B. and Weed, S. B.) Soil Science Society of America, Madison, pp. 1051-1088.

Watts, H. L. and Utley, D. W. (1953) 'Volumetric analysis of sodium aluminate solutions: Determination of carbonate, hydroxide and alumina', *Anal. Chem.*, **25**, 864-867.

Watts, H. L. and Utley, D. W. (1956) 'Sodium gluconate as a complexing agent in the volumetric analysis of aluminium compounds', *Anal. Chem.*, **28**, 1731-1735.

Weissenborn, P. K. (1993), 'Selective flocculation of ultrafine iron ore', PhD Thesis, Curtin University of Technology.

White, R. E. and Taylor, A. W. (1977) 'Effect of pH on phosphate adsorption and isotopic exchange in acid soils at low and high additions of soluble phosphate', *J. Soil Sci.*, **28**, 48-61.

Whittington, B. I. (1996) 'The chemistry of CaO and $Ca(OH)_2$ relating to the Bayer industry', *Hydrometallurgy*, **43**, 13-35.

Witten, T. A. and Sander, L. M. (1981) 'Diffusion-limited aggregation, a kinetic critical phenomenon', *Phys. Rev. Lett.*, **47(19)**, 1400.

Wyatt, P. J. (1993) 'Light scattering and the absolute characterization of macromolecules', *Analytica Chimica Acta*, **272**, 1-40.

Yamada, K., Harato, T. and Shiozaki, Y. (1980) 'Flocculation and sedimentation of red mud', *Light Metals*, 39-50.

Yong, R. N. and Ludwig, R. D. (1986), 'Process technology and properties of red mud', *International Conference on Bauxite Tailings*, Kingston, Jamaica, 31-35.

Yu, X. and Somasundaran, P. (1996) 'Kinetics of polymer conformational changes and its role in flocculation', *J. Colloid Interface Sci.*, **178(2)**, 770-774.

Zrinyi, M., Kabai-Faix, M. and Horkay, F. (1988) 'On the sediment volume of colloidal aggregates. I A fractal approach to the problem', *Progr. Colloid Polymer Sci.*, **77**, 165.

Zurimendi, J. A., Guerrero, S. J. and Leon, V. (1984) 'The determination of the degree of hydrolysis in poly(acrylamides): simple methods using ^{13}C NMR, and elementary analysis', *Polymer*, **25**, 1314-1316.

Appendix:

Publications from this thesis

"Flocculation of hematite in synthetic Bayer liquors"
F Jones, JB Farrow and W van Bronswijk
Colloids and Surfaces, **135,** 183-192 (1998)

"Effect of caustic and carbonate on the flocculation of hematite in synthetic Bayer liquors"
F Jones, JB Farrow and W van Bronswijk
Colloids and Surfaces (in press)

"An infrared study of a polyacrylate flocculant adsorbed on hematite"
F Jones, JB Farrow and W van Bronswijk
Submitted to Langmuir

"Molecular modeling of water adsorption on hematite"
F Jones, AL Rohl, JB Farrow, W van Bronswijk
Submitted to Journal of the Chemical Society, Faraday Transactions